Steam Gasification of Rice Husk Pellets in a Dual Fluidized-Bed Gasifier for Hydrogen-Rich Producer Gas

A thesis submitted for a Master of Engineering degree

in Chemical and Reaction Engineering

By Rahman Jinar Hadi

University of Canterbury

2018

Supervised by: Prof. Shusheng Pang

Dedicated to my wife, Nida, and my daughter, Yasmin Salsabila Firdaus, who have been the most of motivation to accomplish this thesis.

Summary

Experiments were conducted in this study on steam gasification of rice husk pellets (RHP) at a 100 kW_{th} dual fluidized bed (DFB) gasifier, which consists of a circulating fluidized bed (CFB) column and a bubbling fluidized bed (BFB) column. Effect of operation conditions including gasification temperature, steam to biomass (S/B) ratio and catalytic bed material on yield and composition of producer gas (gas product) and condensable gas compounds (tars) has been investigated in this study. Prior to running the hot experiment at high temperatures, cold runs on the gasifier system were performed to experimentally examine the behaviour of bed material fluidisation and to compare the results with those obtained from theoretical calculations.

The experimental results from the cold runs, in which the operation temperature was assumed to be 25^{o}C, show that appreciable circulation was obtained for both silica and olivine, which had a mean particle size of 227 μm and 256 μm, respectively. While the theoretical terminal velocity (u_t) was 2.07 m s^{-1}, the required superficial gas velocity (u_{sf}) was found to be 3.43 m s^{-1} to achieve fast fluidisation of silica with air as the fluidisation agent in the CFB column. In the BFB column, meanwhile, the fluidisation behaviour was found to be in the bubbling fluidisation regime, obtained when the air velocity (u_{sf}) was 0.12 m s^{-1}, falling in between the calculated u_{mf} and u_t. The theoretical terminal gas velocity of olivine sand (u_t) was 2.40 m s^{-1}, which was slightly higher than that of silica sand. In order to achieve the desirable fluidisation in both CFB and BFB columns using olivine sand as the bed material, the air superficial velocities (u_{sf}) in the two columns were found to 3.77 m s^{-1} and 0.12 m s^{-1}, respectively.

In hot test runs with RHP, gasification temperature was the first parameter to be investigated which was found to significantly influence the composition and yield of the producer gas and tars. With increase in temperature from 650 to 800^{o}C, both yield and quality

of the producer gas were improved with significant increase in producer gas LHV largely due to the increase in H_2 concentration in the producer gas. Over the range of temperatures tested from 650 to 800°, the highest LHV of 13.06 MJ Nm^{-3} was achieved at 750°C, where the producer gas yield was 0.53 Nm^3 kg^{-1}_{od} and the concentrations of H_2, CO, CO_2 and CH_4 in the produce gas were, respectively, 24.44 vol. % , 35.34 vol.%, 20.27 vol.% and 11.92 vol.%. At this gasification temperature, tar yield and its concentration in the producer gas were also reduced. Under the optimum gasification temperature of 750°C and S/B ratio of 0.7, the total yield of GC-detectable tars was 0.53 g kg^{-1}_{od}, with a concentration of 9.23 g Nm^{-3}. The tar concentration was 9.42% lower than that measured at 650°C, but slightly higher than that obtained at 800°C (7.53 g Nm^{-3}). Over the temperature range examined, class 2 and class 3 tars was found to be dominant with phenol and benzene becoming the majority for each tar class. The heavy tar compounds in class 4 and class 5 tars were found to be less influenced with the temperature increase, leading to minimal change in their overall tar concentration.

For the second part of experiments, S/B ratio was varied by decreasing the feed rate of biomass (RHP) from 17.5 to 10.7 kg_{od} h^{-1} while holding the rate of steam injection constant at 10.5 kg h^{-1}. The gasification temperature was controlled at 750°C. The experimental results show inconsistent trend of producer gas yield and composition when the S/B ratio was increased from 0.7 to 1.1 with 0.1 ratio increments. The highest gas yield (0.57 Nm^3 kg^{-1}_{od}) was detected at S/B ratio of 1.0, in which CO was the most dominant gas species with concentration of 33.89%, followed by H_2 (25.10%), CO_2 (21.07%) and CH_4 (11.94%), while the other 7.99% was made up of C_2H_4, C_2H_6 and N_2. The gas LHV was 13.08 MJ Nm^{-3} in this case. Furthermore, at an S/B ratio of 0.8 the lowest yield of gas (0.44 Nm^3 kg^{-1}_{od}) was observed where the concentrations of H_2, CO, CO_2, CH_4, C_2H_4, C_2H_6 and N_2 were measured to be 26.61%, 32.57%, 21.43%, 11.82%, 4.42%, 0.70% and 2.29%, respectively, with gas LHV of 12.90 MJ Nm^{-3}.

Further experiments were conducted with higher biomass feed rate of 14.5 kg_{od} h^{-1} whereas the steam injection rate was varied from 19.2 to 18.4 kg h^{-1}, giving the range of S/B ratio from 0.7 to 1.3 with 0.3 increments. With a constant gasification temperature of 750^{o}C, the S/B ratio of 0.7 demonstrated the highest gas LHV reaching 12.95 MJ Nm^{-3}, while the gas yield was found to be 0.54 Nm^3 kg^{-1}_{od}. In this case, a consistent trend was observed within the given range of S/B ratio, in which the H_2 concentration was decreased with increasing S/B ratio, leading to the highest H_2 concentration of 25.01% at S/B ratio of 0.7. Meanwhile, CO, CO_2 and CH_4 concentrations were 33.46%, 21.03% and 12.01%, respectively. The remaining gas species accounted for 8.4% of the producer gas.

The tar yield and tar composition were found to be influenced by the S/B ratio. In a general trend, the tar yield was observed to decrease with increase in the S/B ratio, which could be correlated with the transformation of tar classes. The lowest tar yield (3.73 g kg^{-1}_{od}) was obtained at S/B ratio of 0.8 where class 2 and class 3 tars were found to be the majority components and these together accounted for 82.5% of the overall tar existing in the producer gas.

Olivine sand was found to be a catalytically active bed material, which improved the producer gas yield and quality in gasification of RHP. At the optimum operation condition of operation temperature of 750^{o}C and S/B ratio of 0.7, producer gas yield was 0.60 Nm^3 kg^{-1}_{od} producer gas with application of olivine sand, which was about 10% higher than that obtained with silica sand (0.54 Nm^3 kg^{-1}_{od}) at the same operation condition. The olivine sand also favoured the water-gas shift reaction, enhancing the formation of H_2 and CO_2. As a result, less CO and CH_4 were formed, having concentrations of 32.08% and 11.50%, respectively, with olivine; while the corresponding values with silica sand were 35.34% for CO and 11.92% for CH_4. However, the gas LHV was slightly lower with the olivine sand (12.72 MJ Nm^{-3}) than that produced with silica (13.06 MJ Nm^{-3}).

Lower tar yield and concentration could also be seen from the use of olivine, showing its catalytic effect on the tar conversion. Apart from that of class 2 tars, the concentrations of other classes showed significant reduction with the overall tar concentration (6.15 g Nm^{-3}) being much lower than that(9.96 g Nm^{-3}) with silica.

To sum up, this study has successfully examined the impacts of important parameters in steam gasification of RHP. The experimental results are expected to provide important information for operation optimisation steam gasification of RHP to produce a gas product (producer gas) which is used as a fuel for internal combustion engine.

Acknowledgement

I am really grateful and want to express lots of thanks to my supervisor, Prof. Shusheng Pang, who has been really helpful and provided me with a financial aid in addition to valuable practical and theoretical advices. His exceptional knowledge and expertise in biomass gasification have been highly insightful to broaden my horizon, shaping a comprehensive understanding about the gasification process. Your encouragement and patience whenever we had a meeting have made it seemed easier and strengthened my belief to complete this research appropriately.

Thanks also to all of the technical staff, Tim Moore, Leigh Richardson, Michael Sandridge and Glenn Wilson, for fabricating my experimental apparatus, troubleshooting the equipment and helping me to order the research materials. Their practical guidance and training have helped me extensively to operate micro gas-chromatography and other equipment for laboratory analysis.

Sincere thanks are extended to all of the members of research group under the supervision of Prof. Shusheng Pang. Through a routine knowledgeable sharing and discussion with them, it has been lot easier for me to run the gasifier, perform the gas sampling and conduct the gas and tar analysis.

Special note of appreciation comes to my lovely wife, Nida, and my little girl, Yasmin Salsabila Firdaus, for being always cheerful and delivering limitless care and attention at all the time. They have always got involved in every stage of important progress over my Master's study, especially in this research.

I would like to highly appreciate my adorable parents, Jinar Hadi and Hosiah, who have provided me with a lot of positive moral support. Their good wishes upon prayers are such priceless spiritual motivation to boost my motivation when times were getting hard.

To my beloved mother in law, Djamilah Abdullah Martak, I would like to present immensely big thanks for your never ending affection. Your constant endorsement has given me a lot of joy, making this academic journey very pleasant.

Thanks to all of my brothers, for always sparking my spirit so I can acquire my Master's degree in a timely manner.

Last but not least, my thanks go to Indonesia Endowment Fund for Education (Lembaga Pengelola Dana Pendidikan), for providing me the tuition aids financially.

Table of Contents

List of Figures

List of Tables

Nomenclature

Symbols

A	cross sectional area of gasification column, (m^2)
Ar	Archimedes number, dimensionless
$\mathbf{A_{r,C}}$	atomic weight of carbon, dimensionless (A_r carbon=12)
$\mathbf{c_{H2O}}$	mass fraction of moisture in the fuel (%wt., a.r.)
$\mathbf{c_s}$	specific heat of steam (2.09 J g^{-1} $^oC^{-1}$)
$\mathbf{c_w}$	specific heat of water (4.18 J g^{-1} $^oC^{-1}$)
d	diameter of BFB or CFB columns, (m)
$\mathbf{d_p^*}$	dimensionless particle size
$\mathbf{d_p}$	mean particle size, (m)
$\mathbf{d_{sv}}$	sauter diameter, (μm)
g	gravity, (m s^{-2})
$\mathbf{\Delta H_{LPG}}$	heating value of LPG, (~87.50 MJ m^{-3})
$\mathbf{\Delta H_s}$	total heat energy for steam generation, (J)
$\mathbf{\Delta H_v}$	heat of water vaporation, (2,257 J g^{-1})
$\mathbf{\Delta H_1}$	heat required to raise the temperature of 25^{o}C water to 100^{o}C water, (J)
$\mathbf{\Delta H_2}$	heat required to convert 100^{o}C water to 100^{o}C steam, (J)
$\mathbf{\Delta H_3}$	heat required to increase the temperature of steam from 100^{o}C to 170^{o}C, (J)
$\mathbf{LHV_{dry\text{-}pg}}$	lower heating value of dry producer gas, (MJ Nm^{-3})
$\mathbf{LHV_i}$	lower heating value of individual compound of combustible gas, (MJ Nm^{-3})

$\mathbf{MC_{wet}}$	wet-based moisture content of biomass, (%)
$\mathbf{MC_{od}}$	oven-dry-based moisture content of biomass, (%)
$\mathbf{\dot{m}_{C,pg}}$	the mass flow rate of carbon leaving the reactor, (kg h^{-1})
$\mathbf{\dot{m}_{f,od}}$	mass feed rate of oven-dry biomass, (kg h^{-1}, d.b.)
$\mathbf{\dot{m}_{f,wet}}$	mass feed rate of wet biomass, (kg h^{-1}, w.b.)
$\mathbf{M_{r,Ci}}$	relative molecular mass of carbon-containing molecules including CH_4, CO, CO_2, C_2H_4 and C_2H_6, dimensionless
$\mathbf{\dot{m}_s}$	total mass flux rate of steam in the BFB column, chute and syphon, (kg h^{-1})
$\mathbf{m_w}$	mass of water used for steam production, (g or kg)
n	number of moles, (mol)
P	gas pressure, (Pa)
$\mathbf{q_b}$	chemical energy of RHP in gasification column, (kW)
$\mathbf{q_{dry\text{-}pg}}$	chemical energy of producer gas combustion, (kW)
$\mathbf{q_{LPG}}$	chemical energy of supplementary LPG in combustion column, (kW)
$\mathbf{q_s}$	energy consumed for steam generation, (kW)
r	radius of BFB or CFB columns, (m)
R	universal gas constant, (8.314 Pa m^3 mol^{-1} K^{-1})
R1, R2, R3	repeat 1, repeat 2, repeat 3, etc.
$\mathbf{Re_p}$	Reynold number of particle, dimensionless
T	Temperature, (K)
$\Delta\mathbf{T}$	temperature difference, (^oC)

$\mathbf{T_g}$	temperature of gasification, (^oC)
$\mathbf{T_{D0}}$	mass of tar from extraction with DCM, (μg)
$\mathbf{T_{D1}}$	mass of tar from extraction with DCM-IPA, (μg)
$\mathbf{T_{TCP}}$	total GC-detectable tar concentration, (μg ml^{-1})
$\mathbf{T_{TY}}$	total GC-detectable tar yield, (g kg^{-1}_{od})
$\mathbf{U^*}$	dimensionless gas velocity
$\mathbf{u_{mf}}$	minimum fluidisation velocity, (m s^{-1})
$\mathbf{u_{se}}$	superficial velocity, in which the solids begin to be significantly entrained, (m s^{-1})
$\mathbf{u_{sf}}$	superficial velocity, (m s^{-1})
$\mathbf{u_t}$	terminal velocity, (m s^{-1})
$\mathbf{V_{dry\text{-}pg}}$	volume of producer gas drawn for tar sample analysis, (ml)
$\mathbf{\dot{v}_{dry\text{-}pg}}$	volumetric flow rate (yield) of dry producer gas, (Nm^3 kg^{-1}_{od})
$\mathbf{\dot{v}_f}$	volumetric flux rate of fluids including steam or air, (m^3 s^{-1})
$\mathbf{\dot{v}_{He,out}}$	volumetric flux rate of He exiting the BFB column, (L min^{-1})
$\mathbf{\dot{v}_{LPG}}$	volumetric flow rate of LPG, (L.min^{-1})
$\mathbf{x}$	mass fraction of sand particle, (mass. %)
$\mathbf{x_C}$	carbon conversion, (%)
$\mathbf{x_{C,f}}$	carbon fraction in the solid feedstock, (wt.%, d.b.)
$\mathbf{x_{He}}$	concentration of He flowing out of the BFB column, (mol.% = vol.%)
$\mathbf{y_{C,f}}$	mole fraction of carbon-containing molecules in oven-dry feedstock, (%)

$y_{Ci,pg}$ mole fraction of carbon in producer gas mixture, (%)

y_{Ci} He-free mole fraction of carbon-containing molecules in producer gas mixture, including CH_4, CO, CO_2, C_2H_4 and C_2H_6, (%).

y_i mole fraction of each combustible gas component, (%)

$y_{i,He\text{-}free}$ the fraction of individual and He-free combustible producer gas compound, (mol.% = vol.%)

Greek Letters

$Ø_{SB}$ S/B ratio, dimensionless

Ω_A rotation speed of auger, (r.p.m.)

ρ_g fluid (gas) density, (kg m^{-3})

ρ_s solid (particle) density, (kg m^{-3})

μ dynamic viscosity, (kg m^{-1} s^{-1})

η_c cold gas efficiency, (%)

Abbreviations and subscripts

a.r. as received

Avg average

BFB bubbling fluidized bed

Btu British thermal unit

CFB circulating fluidized bed

db (d.b.)	dry-basis
DFB	dual fluidized bed
EF	entrained flow
f	feedstock, fluids (air or steam)
GC	gas chromatography
GHGs	greenhouse gases
HHV	higher heating value
HTM	heavy tar method
LHV	lower heating value
LPG	liquefied petroleum gas
LTM	light tar method
MSW	municipal solid waste
Mtoe	million tone oil equivalent
NCV	net calorific value
od	oven-dry
pg	producer gas
PV	photovoltaic
RHP	rice husk pellets
wb (w.b)	wet-basis

1. Introduction

The rising world energy demand coupled with efforts to mitigate global warming has necessitated the exploration of using environmentally friendly energy resources which are termed as renewable energy or sustainable energy. Renewable energy has been the focus of research and development in recently years because it is the potential alternative energy in the future as it is reproducible in relatively short period of time and has much less carbon emission to the atmosphere. Biomass, which is defined as organic-based material, is a promising source of renewable energy because, in addition to being abundantly available, the biomass is naturally replenished and carbon neutral.

To produce energy from biomass resources, there are a number of conversion paths that have been used or developed in recent years. Combustion as one of the thermochemical conversion technologies has been widely used to transform agricultural and forestry residues into useful energy of heat and electricity. Gasification technology, another thermochemical conversion technology, has been used to convert the carbonaceous feedstock into a gaseous product, producer gas or product gas, which can then be used directly as engine fuel for power generation (Susastriawana et al. 2017). The gaseous product can also be further transformed into other valuable chemical substances such as methanol, dimethyl ether (DME) and Fischer-Tropsch liquid fuel (Venvika and Yang 2017).

In Indonesia, electricity is vitally needed for industrial purposes, transportation, lighting and household appliances. In 2013, households had a significant demand for electric power of 9,293 MW, representing approximately 14% of the total power generation and 4% of the overall energy supply (Indonesia 2014). However, not all households in Indonesia have equal access to electricity. For example, people living in isolated areas have been suffering from the lack of adequate electricity supply. With an electrification ratio of 88.3% in 2016 in Indonesia, there are still approximately 7.6 million households living without electricity.

As far as electricity production in Indonesia is concerned, the majority of resources used for this purpose come from fossil fuels including oil (30%), natural gas (30%) and coal (30%). Renewable resources only account for 10% of electricity production, primarily supplied from hydropower (Indonesia 2014). More effort is therefore required to utilize sustainable energy resources such as biomass, solar photovoltaic and geothermal, all of which are widely available in Indonesia.

Rice husk is a type of biomass generated from agricultural sector that has been traditionally used as organic fertilizer. The advancement of bioenergy technology would make it possible to transform this biomass resource into electric power, for example through gasification process and gas turbine or gas engine. In Indonesia, a huge amount of rice husk is produced annually in villages, as well as in isolated regions with no power distribution. In 2015, it was estimated that 75.4 million tonnes of rice was produced in Indonesia (Indonesia 2017). With a ratio of 0.2 (Shafie et al. 2012), Indonesia produced approximately 15 million tonnes of rice husk in 2015. Assuming rice husk heating values range from 13,158 to 15,217 kJ kg^{-1} on a dry basis (Yadav and Singh 2011), this corresponds to as much as 22,825 TJ of the potential energy source. Therefore, the gasification of rice husk for electricity production would be an attractive option for reducing Indonesia's dependence on fossil fuels while increasing electricity generation for rural areas.

It has been reported that the gasification of rice husk generates a combustible gas (producer gas) that can be used in an internal combustion engine to produce electricity (Yoon et al. 2012). However, there are still a number of challenges related to the operation of the gasifier and the maintenance of the combustion engine. The quality of the producer gas from the gasification is influenced by physical and chemical characteristics of the biomass. The better quality of producer gas generally refers to higher calorific values, lower tar concentration and marginal amounts of particulate residue. In order for the producer gas to be acceptable for

use in an internal combustion engine, a certain gas quality standard must be complied with, such as tar content ranging between 50 and 100 mg Nm^{-3} (Baratieri et al. 2009) and particle content less than 50 mg Nm^{-3} (Hasler and Nussbaumer 1999). Although there is a lack of information about acceptable calorific value for the combustible engine from literature, high heating value of the producer gas is preferable so as to provide a more reliable process and a longer plant lifetime (Baratieri et al. 2009).

Dual Fluidized Bed (DFB) gasifiers have received more attention in recent years. Depending on the gasification agents introduced into the system, the calorific value of producer gas generated using the DFB gasifier varies between 4 and 16 MJ Nm^{-3} (Saw et al. 2012). In practice, the typical operation temperature ranges from 700 to 900^{o}C. The increase of the gasification temperature tends to result in higher calorific value and lower tar content. To further improve producer gas quality, another treatment involving catalytic bed materials can be applied in the DFB gasifier. A research study conducted by (Koppatz et al. 2011) showed that the presence of olivine sand in the gasification process with a DFB reactor is favourable for the increase of hydrogen content and a decrease of tar concentration.

The objectives of this study are:

- To investigate the gasification performance of Indonesian rice husk pellets (RHP) in a 100 kW DFB gasifier;
- To examine the effects of gasification operation parameters including temperature and steam to biomass (S/B) ratio.
- To investigate effect of various bed materials on producer gas composition and tar concentration in the producer gas from the steam gasification of rice husk.

2. Literature Review

2.1. At a glance: International energy overview

The worldwide primary energy consumption has shown a significant increase and resource change since 1990. Between 1990 and 2015, as shown in Figure 2.1, there was an upward trend in the world's primary energy consumption for six different resources which include coal, renewables, hydroelectricity, nuclear energy, natural gas and oil. It was reported that the worldwide energy demand in 2015 was about 13,000 Mtoe (BP 2016).

The data presented in Figure 2.1 revealed the growth of the energy demand that was dominated by the fossil fuels. A significant amount of coal, natural gas and oil were used in 2015, with a total consumption of approximately 11,000 Mtoe. This value represents around 84.6% of the total primary energy consumption, with a growth of around 62.5% from 1990. Following this, hydroelectricity and nuclear power collectively took the remaining share (13.1%) of the 2015 energy usage which accounted for about 1,000 and 700 Mtoe, respectively. In the same year, the use of energy from renewables category experienced a slight increase when it reached approximately 2.3% of the global energy consumption.

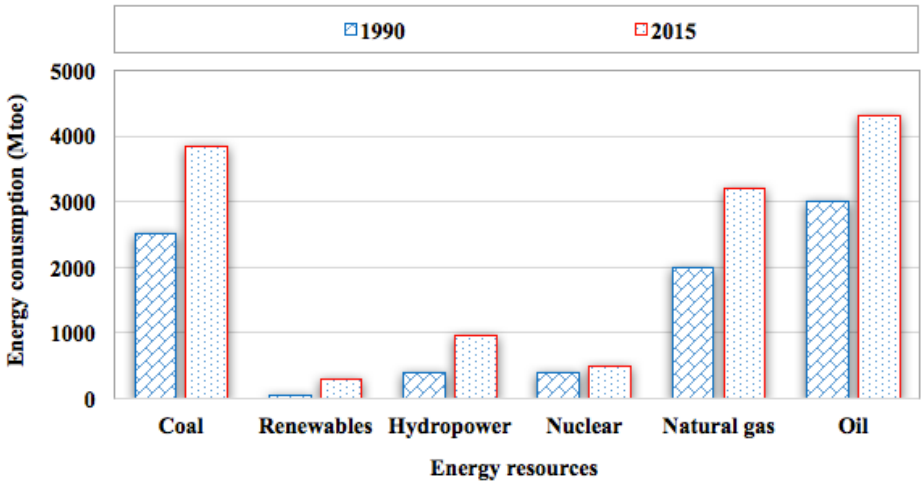

Figure 2.1. World primary energy consumption by fuel in Mtoe (BP 2016).

According to Annual Energy Outlook 2016 (Administration 2016), the energy consumption in 2030 is projected to increase up to 717.7 quadrillion Btu (equal to 18,086 Mtoe) by 2030, with fossil fuels remaining the major contributor of 221.8 quadrillion Btu (equal to 5,589 Mtoe). In 2040, furthermore, the projection shows the need for global energy demand to be as much as 815 quadrillion Btu.

On the other hand, based on IEA data from the World Energy Balances © OECD/IEA 2016, www.iea.org/statistics. Licence: www.iea.org/t&c; as modified by Rahman Jinar Hadi, there has been a significant increase in global energy production between 1971 and 2014. As depicted in Figure 2.2, the total primary energy production rose dramatically by 148%, from 5,523 Mtoe in 1971 to 13,700 Mtoe in 2014 (Agency 2016). Like in energy demand, the fossil fuels particularly remained the greatest contributors to the energy production with a share of 81% within the time frame concerned.

From the non-fossil category, a total increase of 4% share occurred in 43 years (from 1971 to 2014). Biofuels experienced 1% decrease in 2014 in which their share was 10% while nuclear owned 4% more share than in 1971 when its proportion was only 1%. Interestingly, the contribution of energy generated from hydro remained unchanged at 2% in the 43-year period. Eventually, newly emerging energy resources which consist of wind, solar photovoltaic (PV) and geothermal, collectively accounted for 1% share under the "other" fuel category.

Furthermore, the proportion of the primary energy production in continental scope follows the same pattern as that in global energy production. Asia (China and non-OECD Asian countries), for example, is a region where the non-renewables had a dominant share of 83% from the total production of 4,085 Mtoe in 2014 (exclude electricity trade), followed by natural gas (8%), hydropower (2%), nuclear (1%) and other type of energy (2%) (Agency 2016).

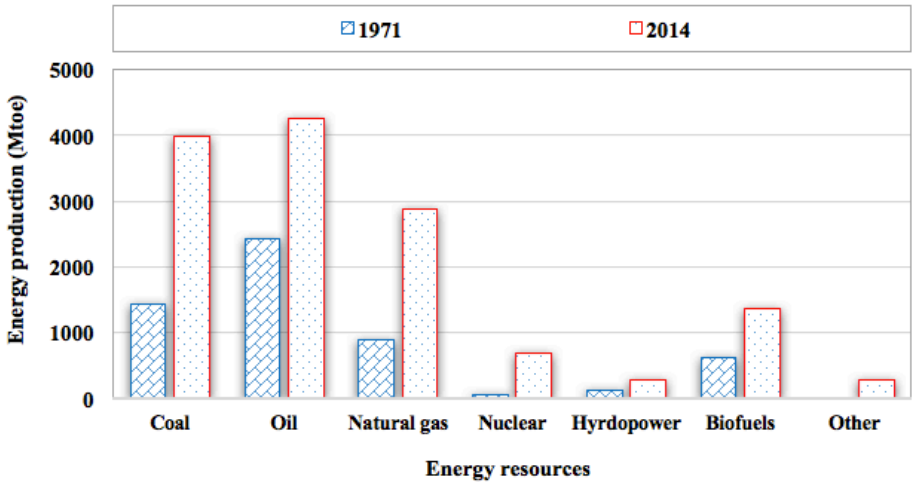

Figure 2.2. World primary energy production by fuel (Agency 2016).

2.2. The need of renewable energy development

As is discussed in Section 2.1, the world's population have been heavily dependent on fossil fuels since 1970s. Consequently, huge amount of CO_2 and other greenhouse gases (GHGs) have been emitted to the atmosphere since the beginning of industrial revolution due to the usage of non-renewable fuels (Chiari and Zecca 2011). Therefore, there has been a growing concern about the likely impacts of the anthropogenic GHGs in the climate system (Zecca and Chiari 2010).

To reduce or at least maintain the rate of the fast-growing level of carbon emission in the air, a number of possible efforts are available (Al-Amin et al. 2015). Firstly, the introduction of a carbon tax would enable the use of environmentally friendly and more efficient technologies due to the higher cost of energy production using the conventional method. Secondly, government should play important role to encourage both energy producers and consumers to raise awareness upon the debilitating impacts of the climate change. It can be done by, for instance, making an improvement on the efficiency of the carbon tax collection system and supporting research and development of clean technology. Finally, governments

should promote the use of renewable energy sources which has advantages including mitigating the future depletion of non-renewable category of energy resources, securing future increased energy supply, meeting the need to achieve the sustainable development goals, and benefiting people's health (Amri 2017).

2.3. Energy generation development in Indonesia

Indonesia is the biggest developing country in South East Asia with a projected total population of 255 million in 2015 (Indonesia 2014). By 2040, this number is estimated to grow by more than 23%, reaching approximately 314 million. To supply its national energy demand, Indonesia still heavily relies on non-renewable resources such as coal, natural gas and oil. As depicted in Figure 2.3, there was a considerable change in the energy supply between 2003 and 2013, in which the upward trend followed a similar pattern with the major growth centralized in fossil-based resources.

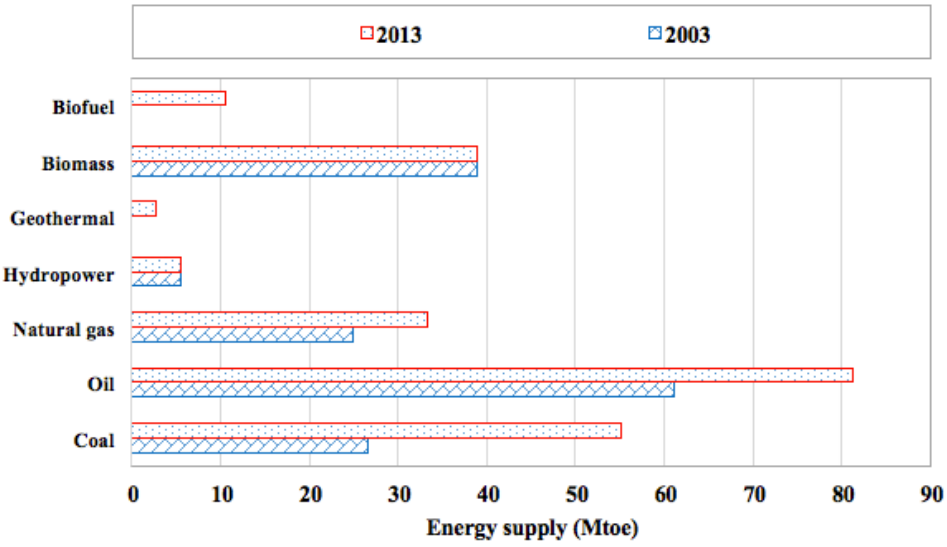

Figure 2.3. The change in primary energy supply in Indonesia (Indonesia 2014).

Between 2003 and 2013, there was a total increase of 45% in energy supply, from 157.08 to 228.22 Mtoe. Oil had been the biggest resource supplying approximately 81 Mtoe in 2013,

followed by coal (55 Mtoe) and natural gas (33 Mtoe), while their corresponding values in 2003 were just about 61, 26 and 25 Mtoe, respectively. Interestingly, hydro and biomass made no difference in terms of energy supply contribution remaining at around 6 Mtoe (hydro) and 39 Mtoe (biomass) during this period. Geothermal and biofuel as the newly developed energy resources experienced a significant increase in 10 years. In 2013, the former accounted for about 3 Mtoe and the latter contribution was 25.1 Mtoe.

Figure 2.4 highlights the total energy consumption in Indonesia from 2003 to 2013, grouped in six different sectors. In general, there was an average annual growing rate of 4.87% in the energy demand, with demand growing up from 117 Mtoe in 2003 to 174 Mtoe in 2013 (Indonesia 2014). The increased national energy demand is linked with further development in several sectors including industry, domestic, commercial, transport, non-energy and others categories such as mining, construction, fishery, agriculture and farming. The proportion of each sector is presented in Figure 2.4 (A), in which industry, domestic and transport were the big three energy consumers, with share of 33%, 27% and 27%, respectively. In addition, commercial, non-energy and others collectively accounted for only 13%.

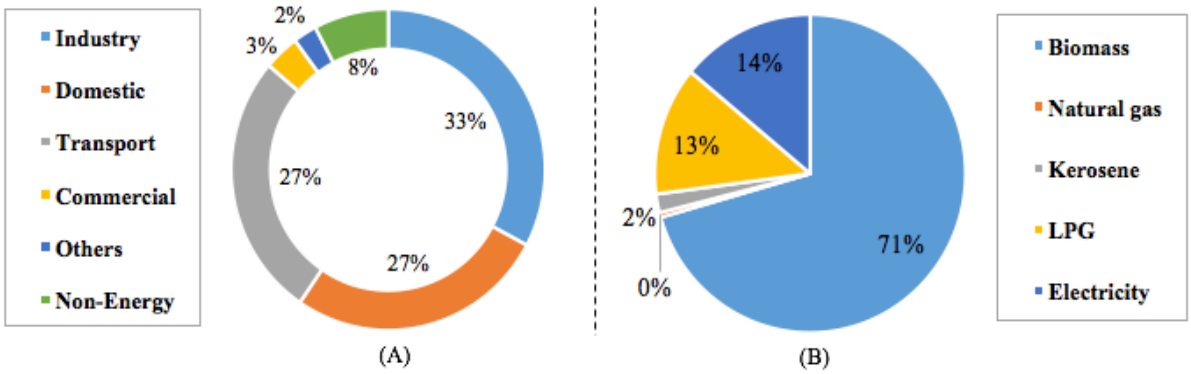

Figure 2.4. The distribution of energy demand in Indonesia (A) and the percentage of energy resources for domestic usage (B) (Indonesia 2014).

The energy demand for the domestic use can be further classified with respect to the resources from which the energy was produced, as presented in Figure 2.4 (B). Within a-10 year period, there was 9.7% increase in the energy consumption for domestic use, rising from 42.96 Mtoe in 2003 to 47.11 Mtoe in 2013 (Indonesia 2014). Biomass has been the most popular energy source used in rural households for traditional applications like cooking and heating. In urban areas, however, the energy need for the domestic activities are heavily relied on natural gas, liquefied petroleum gas (LPG) and kerosene for cooking, while electricity is used for lighting and home appliances (Indonesia 2014).

Table 2.1. The ratio of installed capacity vs. potential resources of renewable energy for electricity generation in Indonesia (Indonesia 2014).

No	Type	Potential Resources for Electricity Generation	Installed Electricity Generation Capacity (MW)	Ratio of Installed to Potential Renewable Electricity Generation (%)
1	Hydropower	75,000 MW	7,573	10.10
2	Geothermal	28,910 MW	1,344	4.65
3	Biomass	32,654 MW	1,717	5.26
4	Solar PV	4.80 $kWh.m^{-2}.day^{-1}$	48	-
5	Wind	3-6 $m.s^{-1}$	1.87	-
6	Tide	49 GW	0.01	-
7	Uranium	3,000 GW	30	-

Indonesia has a good potential of utilisation of renewable energy resources for electricity generation, as presented in Table 2.1. However, the ratio of installed power capacity relative to the potential resources was still very low. Amongst the seven renewable resources listed in Table 2.1, hydro was the largest energy resource with an installation ratio of 10.1% in 2013. Biomass, as the second biggest installed capacity, had a ratio of 5.25%, followed by geothermal with a ratio of 4.65%. Compared to the installed capacity of these three major renewable resources, solar PV, wind, tide and uranium were not really significant, and therefore their ratios were negligible.

Biomass, in particular, is an important renewable energy source but needs research and development for increasing its utilisation. Since biomass gasification is the focus of this study, the succeeding sections are aimed to explain the biomass-related topic in terms of biomass characteristics and conversion technologies.

2.4. Bioenergy: Characteristics and technologies

Bioenergy can be defined as energy extracted from biological waste and organic raw material sources such as forestry, agriculture, food, fisheries and municipalities (Alsaleh et al. 2017). Bauen et al. (2009) reported that many technologies can be used to convert a range of raw biomass feedstocks into a final energy product. In its various forms, the biomass-based energy can meet diverse energy demands and play a unique role in promoting rural development (Shu et al. 2017). Amri (2017) identified four reasons motivating countries to promote renewable energy resources which include the increased energy demand, the depletion of non-renewable energy, the need to achieve the sustainable development goals and the consideration of health benefits.

As far as environment and economic sustainability are concerned, the use of biomass fuels may provide two essential benefits. Firstly, it includes so-called "zero-emission" of CO_2 by looking at the big picture including biomass growth and bioenergy processing or direct combustion (Wielgosinski et al. 2017). As a result, biomass helps the atmospheric carbon dioxide recycling and does not contribute to the GHGs effect (Demirbas 2004). Secondly, the development of biomass energy infrastructure can help strengthen agricultural economies or improve living standard of rural communities (Paine et al. 1995).

Biomass can be used to meet a variety of energy needs, including generating electricity, heating homes, fuelling vehicles using biomass derived fuels and providing process heat for

industrial facilities (Demirbas 2001). For the energy production, biomass feedstock can be converted into solid, liquid and gaseous fuels through two general paths, thermochemical processes and biological processes. Conversion technologies play an essential role to facilitate the process of biomass-to-energy transformation. The thermochemical processes, which are the centre of discussed topic in this study, involve thermal decomposition reactions such as combustion, pyrolysis and gasification, whereas biochemical processes comprise anaerobic digestion and alcoholic fermentation.

Combustion is a complex phenomenon involving simultaneous coupled heat and mass transfer with chemical reaction and fluid flow (Demirbas 2004). As much as 97% of the worldwide bioenergy is estimated coming from the combustion route (Demirbas 2004), and thus it is most common form of biomass-derived power generation (Agency 2012). The power generation through direct combustion is a mature technology that has been commercially available and applied on various scales from 1 to 100 MW.

Gasification is a partial oxidation conversion process in which carbonaceous materials such as biomass, coal and plastics are turned into gaseous products in the presence of a gasification medium (Ruiz et al. 2013). Commonly termed as producer gas or product gas, the gaseous product consists mainly of combustible elements such as H_2, CO, and CH_4 as well as non-combustible gas compounds (CO_2 and N_2). As undesirable side products, small particles of char, ashes, tars and oil are also produced. The producer gas can then be applied for gas burner or internal combustion engine (Susastriawana et al. 2017), or be further converted into methanol, dimethyl ether (DME) and Fischer-Tropsch liquid fuels (Venvika and Yang 2017). Meanwhile, the gasification mediums are used in the gasification process which can be air, steam, oxygen, CO_2 or the mixture of these substances.

Pyrolysis is process occurring in the absence of oxygen, through which lignocellulosic biomass is converted into carbon-rich solids, liquids and gas (Roy and Dias 2017). Since no

oxygen is present, the organic material is not combusted, instead, the biomass is decomposed into three forms, a liquid called bio-oil, a solid termed as bio-char, and non-condensable gas which is also combustible. Pyrolysis is also the initial stage the gasification process, but the pyrolysis process is limited to between 300 and 600^{o}C (Agency 2012).

Anaerobic digestion, furthermore, is a bacterial biomass decomposition in no oxygen environment (Demirbas 2001), generating two main products, called biogas and digestate (Agency 2012). The biogas is primarily a mixture of methane (CH_4) and carbon dioxide (CO_2), as well as some other minor constituent such as sulphur dioxide (SO_2), hydrogen sulphide (H_2S), nitrogen, ammonia (NH_3), and hydrogen. The methane can be used for transportation fuels, whereas digestate can be transformed into a bio-fertilizer after appropriate treatment. Anaerobic digestion is commonly operated as a continuous process and thus needs a steady supply of feedstock. To maximise methane production and to minimise the possibility of killing the natural digestion process, pre-treatment of the feedstock sometimes might be required (Agency 2012).

Alcoholic fermentation, eventually, is the process of converting glucose derived from biomass into alcohol, or ethanol, through the use of yeast (Agency 2012). As a liquid fuel, ethanol can be used as a supplement or substitute for an automotive fuel (Demirbas 2001).

2.5. Biomass for power generation

Electricity generation from biomass has been the centre of attention in recent years in Indonesia. This section is focused on the biomass contribution to the electricity generation, highlighting its ratio to the total energy consumption starting from the global perspective and then with more details on Indonesia.

As mentioned in Section 2.1, bioenergy still contributes a minor fraction to the energy consumption. With an annual production of approximately 1,370 Mtoe in 2014, it accounted for nearly 10% share in the total global production of primary energy (Agency 2016). On the other hand, 14% of global energy consumption was claimed to be from biomass, of which 0.4% was allocated for electricity generation, as shown in Figure 2.5 (Century 2016). Meanwhile, there was a significant proportion of the biomass usage for heating purposes (10.4% in total). However, transport and industry sectors only gained shares of 0.8% and 2.2%, respectively.

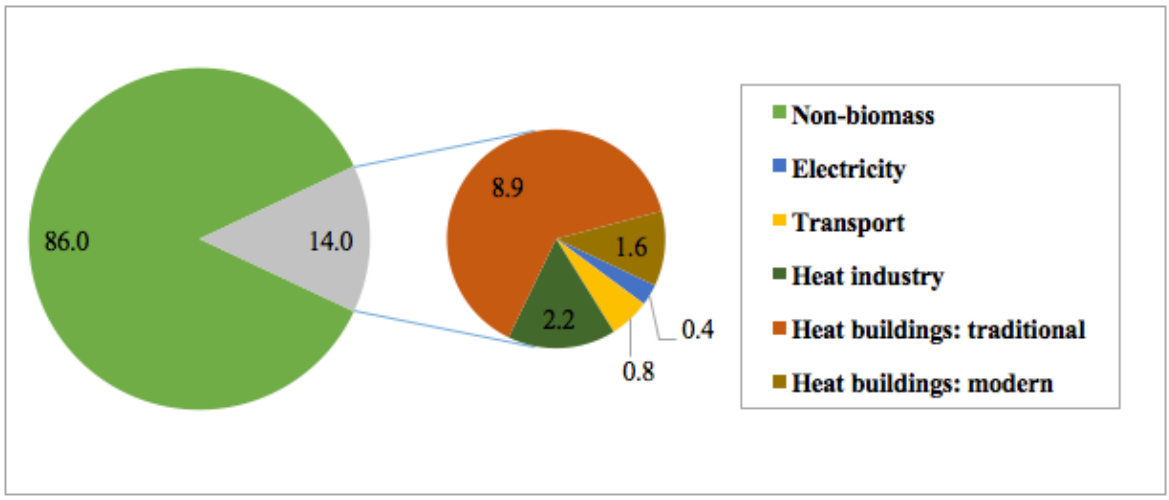

Figure 2.5. The distribution of energy demand in Indonesia (A) and the percentage of energy resources for domestic usage (B) (Century 2016).

In global application, biomass resources are utilised in four different forms of fuels including dry solid biomass, dry municipal solid waste (MSW), biogas and biofuel (Century 2016). Under these categories, the dry biomass resources are used largely for heating and power generation, with their proportions being highlighted in Figure 2.6. In general, solid biomass was the most consumed feedstock compared with the other types of biomass resources. In 2015, approximately 77% of the total biomass-based power generation was derived from solid biomass while the proportion of that for the heat heating generation was about 71%. In comparison with the solid biomass, MSW was the second largest feedstock used for the heat

generation (18%), followed by biogas (4%) and biofuels (1%). In the same year, the corresponding proportions of those biomass resources for the electricity generation were 8%, 20% and 1%.

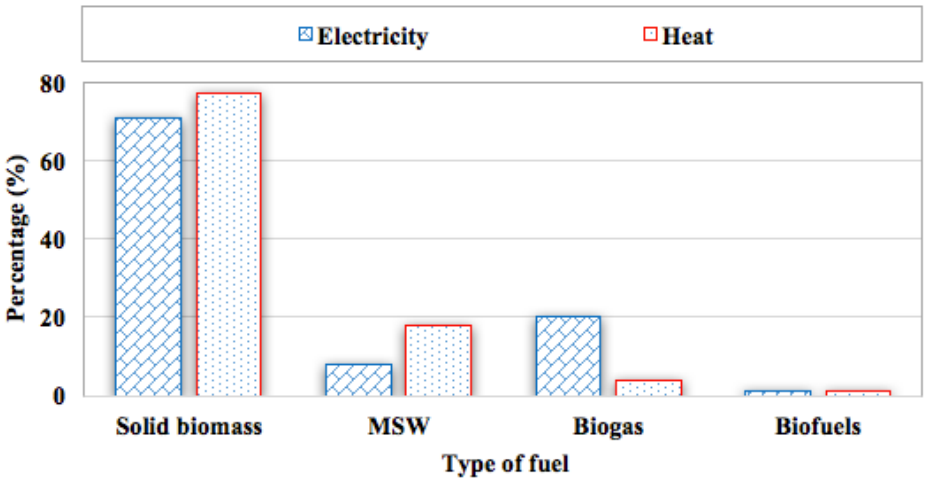

Figure 2.6. The proportion of biomass-derived fuel types for global generation of heat and electricity (Century 2016).

Figure 2.7 further illustrates data on global electricity production in six regions from 2005 to 2015. The amount of electricity produced in all regions followed an upward trend, in general, with European Union (EU-28) having the largest share. In addition, at the start of the period, the world's electricity generation from biomass was just under 200 TWh (approximately 17.20 Mtoe) per year, of which a half was produced in EU-28 and North America. However, the annual production of biomass-based electricity in the North America remained at around 60 TWh (approximately 5.16 Mtoe) in 2015, whereas those in EU-28 almost tripled to reach just about 180 TWh (approximately 15.48 Mtoe).

The overall power generation in Asia, South America and China was approximately 50 TWh in 2005. In Asia, this increased significantly by more than 200% from 2005 with generation rate of about 80 TWh in 2015. Likewise, South America and China experienced gradual increase with a similar pattern, with both countries consuming the bio-electricity

in 2015 of around 50 TWh. Eventually, a small number of the electric power was produced in rest of the world, with 6 TWh in 2005 and 19 TWh in 2015.

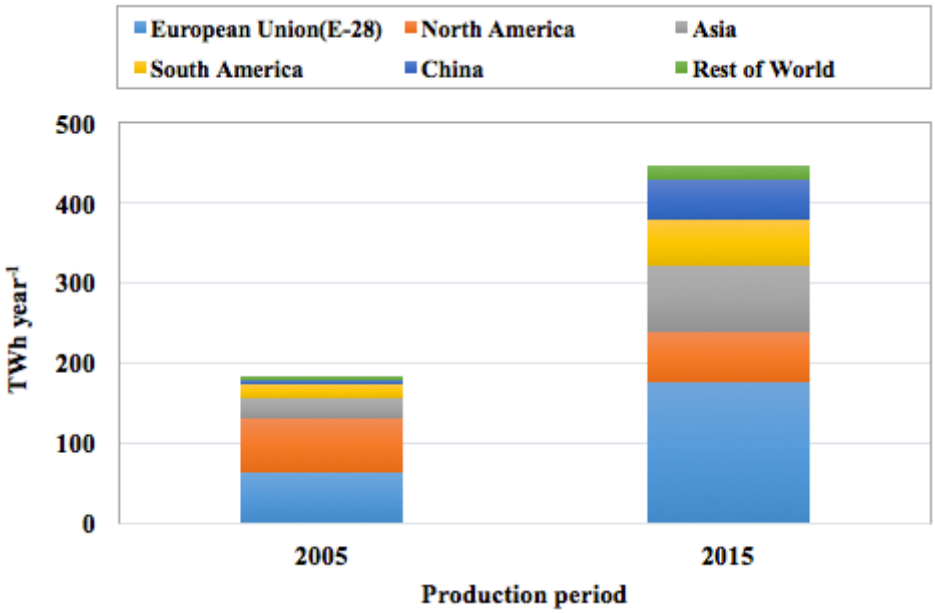

Figure 2.7. World's electricity production based on biomass resource (Century 2016).

In Indonesia, the installed capacity of power plants has gradually developed since 2003. In 2013, the electricity generating stations had a total capacity of approximately 51,000 MW (Ketenagalistrikan 2016), with the electricity production increasing by around 70% from 2003 (Indonesia 2014). Produced from seven different types of power plants, the distribution of the electricity generation for each electricity producing station can be seen in Figure 2.8.

Overall, steam-driven generation remained the most popular method, for which fossil fuels (oil, coal and natural gas) were used to produce steam that was then used to drive the steam turbine to produce electricity, with 47% of the total electricity generation in 2013. Diesel engine, hydropower and gas-fired power stations shared relatively similar proportions of 12%, 10% and 9%, respectively. Meanwhile, 19% of electricity was from the gas-steam combined power plant, while steam engine gained only 1% share. 2% of electricity was contributed from geothermal (Indonesia 2014).

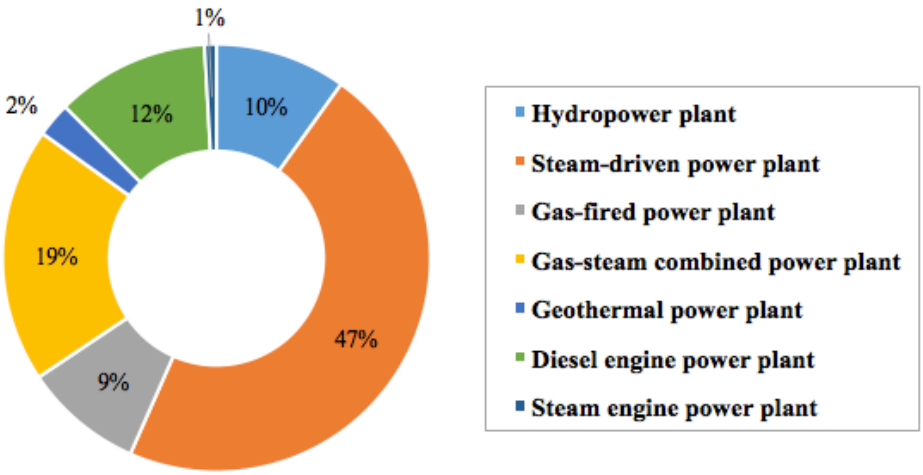

Figure 2.8. The distribution of installed power capacity in Indonesia in 2013 (Indonesia 2014).

Although the installed power capacity has been developed significantly, the power distribution remains a challenging issue in Indonesia. In terms of electrification ratio, for instance, 11.7% of the total households in Indonesia (65,669,197) in 2015 lived with no electricity, most of which were situated in rural areas (Ketenagalistrikan 2016). To solve this problem, however, Indonesian government has been providing massive supports to the implementation of renewable energy technologies, in order to increase the current electrification ratio up to 100%. By 2025, it is expected that 22.5% of the total national electricity supply are generated from biomass resources (Wicaksono 2017). In other words, this implies that a lot of attentions are paid to bioenergy development in Indonesia, especially for the power generation in isolated regions.

Meanwhile, rice husk has recently gained more attention as a bioenergy resource for power generation. According to (Akgün and Luukkanen 2012), rice husk gasification systems can be considered as a novel and promising way to utilize rice residues which otherwise would just cause waste disposal and breathing problems. In succeeding sections, the discussion will be given on details of rice husk in terms of its global production, characteristics and potential use for electricity generation.

2.6. Rice husks: Global availability

Rice husk is the hard outer layer covering the paddy grain that is separated from the rice grains during the milling process (Pode 2016). As a major by-product generated from rice milling process, the availability of rice husk depends on the amount of rice production. Rice husk is one of the major biomass resources in the world. In 2016, global paddy grain production was estimated to reach 753 million tonnes and is estimated to increase by 0.8% in 2017 (Organization 2017). Asian countries remain the dominant rice producers in which the total production is expected to reach 686.1 million tonnes by the end of 2017. China, India and Indonesia are the top three countries in Asia and together their production accounts for more than 50% of the total 2017 paddy production in Asia.

Paddy is commonly composed of 20-33% husk (Lim et al. 2012). However, in other literature the rice husk proportion is considered to be 20% (Shafie et al. 2012). Based on the total paddy grain production, the rice husk availability was estimated to be approximately 151 million tonnes in 2016 and this value is expected to increase up to 163 million tonnes in 2017, provided the rice husk ratio is 0.2. Moreover, Indonesia had approximately 15 million tonnes of rice husks in 2015, with a paddy production of around 75.4 million tonnes (Indonesia 2017).

As a residue from agricultural product processing, rice husk has been utilised in a number of applications. Patel et al. (2015) reviewed the properties and industrial applications of rice husk. They found the rice husk has been used either in its original or in the ash form. The ash from the rice husk has been used as a value added construction material, feedstock for new materials or a low cost substitute material to modify the properties of existing products. Silica derived from rice husk ash has been further used for production of zeolite (Mohamed et al. 2015), refractory ceramics (Sobrosa et al. 2017), electronic packaging material (Hsieh et al. 2017), and thermal insulation (Sembiring et al. 2016). A separate study has shown that the rice

husk ash can also be used for production of activated carbon and fertilizer (Ding et al. 2014). Recently, the expansion of rice husk usage have been directed to the production of energy in various forms such as heat (Kwofie et al. 2017) and electricity (Akgün and Luukkanen 2012).

2.7. Rice husk pellet for power generation

For many biomass resources, pre-treatment processes are required before they can be converted into energy. To use biomass such as wood, drying and grinding are two essential pre-treatment processes, but they are not necessary for another type of biomass such as rice husks (Yoon et al. 2012). However, the low energy density and complexity of material handling remain the major issues for the rice husk use. In this case, densification process as a physical pre-treatment is often needed, reshaping the rice husk into the forms of briquette or pellets in order to solve the aforementioned problems.

In this research, the term pellet denotes a densified biomass fuel with a tubular shape having uniformity in length, diameter and energy density. The use of rice husk pellet for gasification process has been discussed in a study performed by Yoon et al. (2012). It was found that pelletisation could improve the quality of the solid fuel in terms of higher energy density per unit volume and promotes less biomass bridging in a downdraft gasifier. In addition, (Yank et al. 2016) studied the rice husk briquette for rural application such as cooking and concluded that the densified biomass has improved its properties such as physical integrity (durability and compressive strength), low moisture content (less than 7.5%) and higher calorific value (16 MJ kg^{-1}_{db}). Furthermore, Uslu et al. (2008) studied the techno-economic aspect of torrefaction, pyrolysis and pelletisation of the rice husk, and concluded that pre-treatment processes are able to convert biomass at modest scales into dense energy carriers that ease handling and transportation.

The use of pelletised biomass is becoming popular for thermal energy use both in industrial sector and in space heating in a household, especially for those living in four-season countries. For quality control and processing control, standards have been established on physical and chemical properties of the rice husk pellet, which are given in Table 2.2 (Obernberger and Thek 2010). The standards have specified the pellet diameter (4-10 mm), length (3.15-50 mm), bulk density (600-720 kg m^{-3}) and particle density (1-1.4 kg dm^{-3}). In these standards, the highest value for the moisture content is 12 wt.% (w.b.), while those for ash content range between 0.5-3.5 wt.% (d.b.). The nett calorific value (NCV) varies in a range from 16.5 to 19.5 MJ kg^{-1} (w.b.).

Moreover, standards in Table 2.2 also highlights the ranges of variations in the chemical composition of the pellet standard. Sulphur content, for instance, has a value ranging between 0.03 and 0.08 wt.% (d.b.), whereas those for nitrogen and chlorine are from 0.3 to 1.0 wt.% (d.b.) and from 0.02 to 0.03 wt.% (d.b.), respectively. In terms of mechanical durability, the minimum value is set at 96.5 wt.% (d.b.). Interestingly, the values for fines and additives are the same across the standards, with the former having a value of 1.0 wt.% (d.b.) and the latter being set at 2%.

A proper understanding of the feedstock properties is necessary prior to conducting any further conversion processes such as combustion, pyrolysis or gasification. The chemical composition and elemental composition of biomass as a solid fuel can be determined from the proximate and ultimate analyses. Moisture or water content is the amount of water present in the material which is expressed as a percentage of the material's weight. According to (Knoef 2005), low moisture content is more preferable for thermal conversion of biomass to produce gaseous products with a better quality such as greater heating value, higher efficiency and lower tar levels.

Table 2.2. The comparison of pellets standard properties in some European countries (Obernberger and Thek 2010).

Parameter	Unit	Final draft prEN 14961-2			ONÖRM	SS 187 120	DIN 51731	DIN_{plus}	CTI
		Class A1	Class A2	Class B	M 7173				
Diameter	mm	6 or 8	6 or 8	6 or 8	4-10		4-10	4-10	6
Length	mm	3.15-40	3.15-40	3.15-40	5 x D	4 x D	50	5 x D	D – 4 x D
Bulk density	kg m^{-3}	≥ 600	≥ 600	≥ 600		≥ 600			620-720
Particle density	kg dm^{-3}				≥ 1.12		1-1.4	≥ 1.12	
Moisture content	wt.% (w.b.)	≤ 10	≤ 10	≤ 10	≤ 10	≤ 10	≤ 12	≤ 10	≤ 10
Ash content	wt.% (d.b.)	0.7	1.5	3.5	0.5	0.7	1.5	0.5	0.7
NCV	MJ kg^{-1} (w.b.)	16.5-19.0	16.3-19.0	16.0-19.0	≥ 18.0	≥ 16.9	17.5-19.5	≥ 18.0	≥ 16.9
Sulphur content	wt.% (d.b.)	0.03	0.03	0.04	0.04	0.08	0.08	0.04	0.05
Nitrogen content	wt.% (d.b.)	0.30	0.50	1.0	0.30		0.30	0.30	0.30
Chlorine content	wt.% (d.b.)	0.02	0.02	0.03	0.02	0.03	0.03	0.02	0.03
Mechanical durability	wt.% (d.b.)	≥ 97.5	≥ 97.5	≥ 96.5	≥ 97.7	≥ 99.2		≥ 99.7	≥ 99.5
Fines	wt.% (d.b.)	1.0	1.0	1.0	1				1.0
Additives	%	2.0	2.0	2.0	2			2.0	

Inorganic or mineral components of biomass which remain after complete combustion of the feedstock is called ash (Knoef 2005). High ash content in a feedstock is the main drawback of using rice husks, that may lead to some problems to the combustion chamber (Caneghem et al. 2012) by forming deposits and slags which are not desired during the thermal conversion (Lim et al. 2012). Fouling, agglomeration and corrosion on heat transfer units are amongst the serious issues resulting from the melting of the rice husk ashes (Armesto et al. 2002). Volatile matters are defined as all substances in a feedstock, except for moisture, released as gas and vapour during combustion (Knoef 2005). In a gasifier, the amount of volatiles affects the levels of tar production. Fixed carbon, in addition, is the solid combustible residue remaining after the feedstock is heated and the volatile matter is expelled.

Table 2.3 give results of proximate and ultimate analyses for the rice husk pellets which show variations in different studies. In the table, moisture content varies from 3.60-9.80%,

while ash content ranges from 11.36-20.60%. The volatile matter content ranges from 58.40% to 69.83%, and the fraction of fixed carbon is between 10.65% and 20.10%. Additionally, the data from ultimate analysis shows carbon content ranging from 37.6 to 42.3% and oxygen content from 35.70 to 55.13%. Minor elements include hydrogen, nitrogen, and sulphur with corresponding contents in ranges of 1.90-6.43%, 0.01-4.6% and 0.00-0.20%, respectively. The higher heating value (HHV) ranges from 13.20 to 16.57 MJ kg^{-1} and the low heating value (LHV) was slightly lower than the upper limit of HHV in a range of 14.31-16.08 MJ kg^{-1}.

Table 2.3. The proximate and ultimate analyses of rice husk in various studies.

Reference	**Kook et al. (2016)**	**Zhai et al. (2015)**	**Srinath and Reddy (2011)**	**Yoon et al. (2012)**	**Thakkara et al. (2016)**
Proximate analysis	(wt% d.b.)	(wt% d.b.)	(wt% a.r.)	(wt% a.r.)	(wt% a.r.)
Moisture	9.96	5.08	6.10	3.60	9.80
Ash	11.36	14.98	20.60	16.30	19.52
Volatile matter	66.39	63.05	58.40	60	69.83
Fixed carbon	11.96	16.89	14.90	20.10	10.65
Ultimate analysis	(wt% d.b.)	(wt% d.a.f.)	(wt% a.r.)	(wt% a.r.)	(wt% a.r.)
Carbon (C)	55.13	46.18	36.4	38.50	35.70
Sulphur (S)	0.00	0.10	0.17	0.20	-
Nitrogen (N)	0.01	2.62	0.44	0.40	4.60
Hydrogen (H)	6.43	6.08	4.84	5.50	1.90
Oxygen (O)	38.43	45.02	25.11	36.60	38.20
LHV (MJ kg^{-1})	16.08	-	14.31	-	-
HHV (MJ kg^{-1})	-	-	-	16.57	13.20

Biomass pellets have been used in gasification for production of producer gas. Alamsyah et al. (2015) investigated gasification of Indonesian biomass pellets to produce the producer gas which is then combusted for heat. They found that the emissions from combustion of the gasification producer gas comply with the required standard. Simone et al. (2012) conducted a separate study on feasibility and reliability of gasification of pelletised biomass using a downdraft gasifier. They found that the biomass pellet is not an ideal feedstock for the

downdraft gasifiers due to high pressure drop, complexity of controlling the gasifier and fragmentation of the gasification residue.

However, other studies have shown that the rice husks can be a promising feedstock for gasification for electricity generation, and this has become an attractive area for further research and development. For example, Affendi et al. (2010) conducted a study on rice husk gasification and the producer gas is then applied in a 100 kW dual fuel generator engine. It was found that gasification technology was potentially able to offer economical solution in providing electricity for isolated remote areas. In another study by Fatimah et al. (2016), a bench-scale downdraft gasifier was used for gasification of Indonesian rice husk in which the producer gas was used in a gas engine for electricity generation. From the literature review, reports on gasification of RHP is scarce and only two references have been found so far. Firstly, Manatura et al. (2017) performed a study of exergy analysis on torrefied rice husk pellet. This study has shown that at the proper torrefaction temperature of 250^{o}C, the properties of RHP were improved, leading to enhanced gasification performance and energy efficiency. Secondly, Yoon et al. (2012) reported a study of gasification of both pelletized rice husk and un-pelletized rice husk particles in a bench-scale downdraft fixed-bed gasifier with air as the gasification agent. In this study, the high heating value of the producer gas obtained from gasification of the pelletised rice husk was 21% higher than those from gasification of rice husk particles. From the above discussion, it is apparent that there are uncertainties on gasification of rice husk pellets regarding gasification performance, gas composition and effects of operation parameters. Further investigation, therefore, is needed in order to provide more fundamental information related to the gasification of RHP.

2.8. Gasification: Concept and technologies

2.8.1. Typical reactions associated with biomass gasification

Gasification is defined as a conversion process of solid or liquid feedstock to produce useful and combustible gaseous fuel that can be burned to release energy or can be used as a chemical feedstock for production of value-added chemicals or liquid fuel. The gasification process consists of three stages starting with drying, followed by pyrolysis (devolatilization), char gasification and partial combustion (Basu 2010).

In biomass gasification, drying is an initial step before the biomass decomposition to release the moisture from the feedstock when the feedstock is heated up above 100°C. With further increase in the biomass temperature above 250-300°C, the remaining components of the solid fuel start to volatilize to release volatiles, and this process is the pyrolysis stage.

At the biomass pyrolysis stage, the large hydrocarbon molecules of biomass are transformed into both condensable and non-condensable gas molecules as well as char. When the condensable gas experiences a temperature decrease to a certain point, liquid is formed and tar refers to liquids formed at high temperatures. In the final stage and most important gasification stage, numerous reactions may occur both among gases and between char and gases. The exact number of reactions and reaction kinetics are dependent on the biomass type, gasification agent and gasification temperature (Basu 2010). Some of these reactions in the pyrolysis and gasification processes are given as follows for illustration (Moghadam et al. 2014):

Pyrolysis stage: Biomass → Gas (condensable and non-condensable) + Tars + Chars

Pyrolysis and gasification: Tars → Light and Heavy hydrocarbons + CO + CO_2 + H_2

Pyrolysis and gasification: Heavy hydrocarbons → Light hydrocarbons + H_2

Gasification: Char → CO + CO_2 H_2 + Solid residue

Typical chemical reactions taking place during the gasification include those for formation and consumption of the gaseous elements such as CO, CO_2, CH_4, H_2 and steam, and more details are given in Table 2.4 (Moghadam et al. 2014). In a gasifier, some of those reactions are possible to occur regardless of gasifier type and operation conditions, but others are dependent on operation conditions, gasification agent and use of catalytic bed material (Kern et al. 2013).

In these reactions, combustion reactions with carbon, either complete or incomplete, energy is releases to form CO_2 (complete) or CO (incomplete). These reactions significantly affect the level of calorific value and chemical composition of the producer gases. For a biomass feedstock with high moisture content, pre-drying is necessary to reduce the moisture content as low as 10 to 20% to achieve a reasonably high heating value if a fuel gas is the desired end product. When air or oxygen is used as the gasification agent, the combustion reactions occur at very fast rates thus CO_2 and CO are quickly produced. Following this, the water-gas reaction is likely the next fast reaction that converts char and moisture (H_2O) into CO and H_2.

The next slower reaction is the char gasification reaction between char and carbon dioxide, well known as Boudouard reaction, which produces carbon monoxide (CO). Further down on the list with reaction rate decreasing is the hydrogasification between char and H_2 which produces methane (CH_4). When steam is used as gasification agent or sufficient steam is generated from drying, water-gas shift reaction is significant in which CO and steam react to form CO_2 and H_2. The homogeneous gas-gas reaction is desirable as it enriches the hydrogen content in the producer gas (Basu 2010).

Table 2.4. Typical equilibrium reactions in biomass gasification (Moghadam et al. 2014).

No	Chemical equation	ΔH (kJ.mol^{-1})	Name of reaction
1	$C + 0.5\ O_2 \rightarrow CO$	- 111	Combustion
2	$C + O_2 \rightarrow CO_2$	-283	Combustion
3	$C + CO_2 \leftrightarrow 2CO$	+ 172	Boudouard
4	$C + 2H_2 \leftrightarrow CH_4$	- 75	Methanation
5	$C + H_2O \leftrightarrow CO + H_2$	+ 131	Water-gas
6	$CO + H_2O \leftrightarrow CO_2 + H_2$	- 41	Water-gas shift
7	$CH_4 + H_2O \leftrightarrow CO + 3H_2$	+ 206	Steam-methane reforming
8	$CH_4 + CO_2 \leftrightarrow CO + H_2$	+ 260	Dry reforming
9	$C + 2H_2O \leftrightarrow CH_4 + CO_2$	+103	Methanation

2.8.2. Structure and operation of gasification reactors

Gasification technology has been used for coal gasification for many year, and the gasifier can be classified based on different criteria as discussed by Knoef (2005) as presented in Table 2.5. In practice, however, a gasifier may be named under a combination of these classification criteria.

Table 2.5. Classification of gasifiers (Knoef 2005).

Classification reference	Gasifier
Gasification agent	Air-blown, oxygen and steam gasifiers
Heat for gasification	Auto-thermal and allo-thermal gasifiers
Pressure in the gasifier	Atmospheric and pressurised gasifiers
Structural design	Fixed-bed, fluidized bed, entrained flow and twin-bed gasifiers

Air is a common fluid used as gasification agent due to its low cost and the auto-thermal process (Kern et al. 2013). However, the high nitrogen content dilutes the producer gas, leading to a reduction of the producer gas heating value as low as 3 to 6 MJ Nm^{-3}_{db}. (Zainal et al. 2002). The use of oxygen as a gasification agent, on the other hand, results in the higher gas calorific

value, yet it is not economically attractive as purification process to get pure oxygen is expensive (Pang 2016). Additionally, steam can be used for gasification in order to generate N_2-free producer gas with a greater LHV, ranging from 10 to 18 MJ Nm^{-3}_{db} (Rapagnà et al. 2000).

Moreover, auto-thermal or direct gasifier is a gasification reactor in which heat is provided from the combustion of biomass (Knoef 2005), while allo-thermal gasifier requires external heat for the endothermal gasification (Kern et al. 2013). In the pressurised gasifier, the gasification process can be under pressure up to 62 bar. This process condition suits the application of integrated gasification combined cycle (IGCC) since the producer gas can be directly injected into the gas turbine, which otherwise needs a gas compressor if atmospheric (low-pressure) gasifier is used (Phillips 2017). In the following sections, various types of gasifiers are described and their characteristics are discussed.

2.8.2.1. Fixed-bed gasifier

Fix bed gasifiers are the summary of three distinctive types, updraft, downdraft and cross-draft reactors, whose schematic diagrams are depicted in Figure 2.9(A), 2.9(B) and 2.9(C), respectively (Knoef 2005). Basically, these gasifiers are identical in their physical designs, but different in flow directions of the gasification agent and the producer gas.

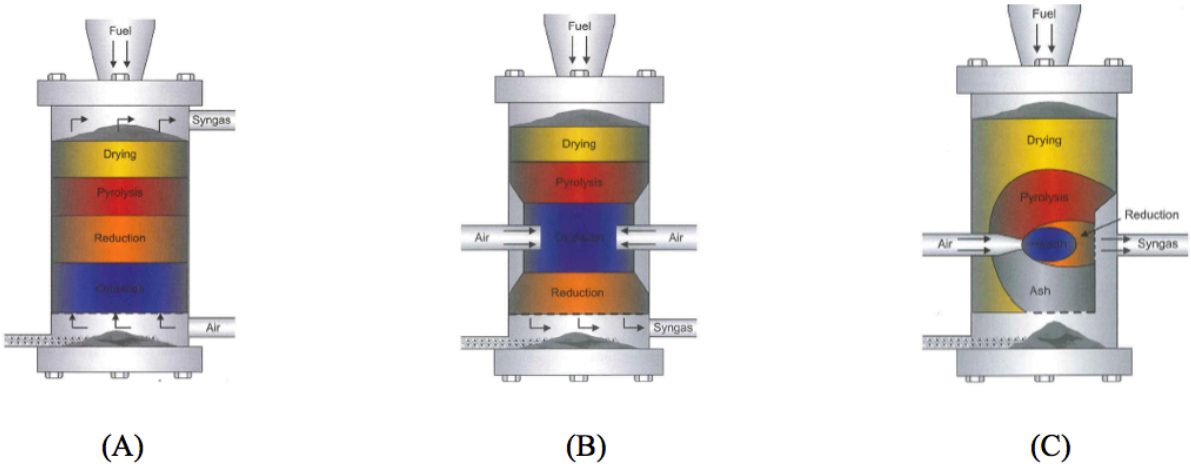

(A) (B) (C)

Figure 2.9. Fixed-bed gasifier; (A) updraft gasifier, (B) downdraft gasifier, (C) cross-draft gasifier (Knoef 2005).

In the fixed-bed gasifiers, biomass is fed at the top, whereas ash disposal is designed at the base. For the updraft gasifier, in particular, gasification agent enters the system from the bottom and the producer gas exits at the upper part. The biomass flows downward counter-currently to the gas flow, entering the drying zone, pyrolysis zone, reduction zone and oxidation zone. In contrast, the biomass in downdraft gasifier goes down co-currently with gasification agent and producer gas, passing through drying zone, pyrolysis zone, oxidation zone and reduction zone, with the gasification agent intake being normally located at the middle part of the gasifier. Cross-draft gasifier, finally, has about similar location of the gasification agent intake to that in the downdraft gasifier, which is also placed at the middle. Nevertheless, the producer gas stream comes out of the system from about the same height level as the gasification agent intake.

In most applications, downdraft gasifiers are used for power generation with plant scale ranging between 80 and 500 kW_e. On the other hand, 10 kW_e shaft power is generally coupled with the cross-draft gasifier (Knoef 2005). For each type of fixed-bed gasifier, several benefits and drawbacks associated with the operation simplicity, gasification efficiency, biomass size

requirement, producer gas quality and scaling up possibility are presented in the following table.

Table 2.6. Advantages and disadvantages of fixed-bed gasifier (Knoef 2005).

Fixed-bed gasifier	Advantages	Disadvantages
Updraft	• Simple operation • High gasification efficiency • Able to be operated for biomass with various size and high moisture content	• Great amount of tar and pyrolysis products • For power generation purposes, extensive gas cleaning is required
Downdraft	• Producer gas production with low tar concentration • Application scale in a range between 80 and 500 kW_e	• Limited scaling up possibility • High concentration of ash and dust particles • Lower gasification efficiency • Pelletization or briquetting is often required
Cross-draft	• Small scale operation is acceptable ($10kW_e$)	• Low tar conversion

2.8.2.2. Fluidized-bed gasifier

Fluidized bed gasifier refers to the gasification reactors in which solid particles behave like a fluid by contacting with a gas phase agent like air, oxygen or steam (Knoef 2005). The fluidized bed gasifiers cover three distinctive designs, which have different characteristics from each other: (1) bubbling fluidized bed gasifier, (2) circulating fluidized bed gasifier, (3) dual fluidized bed gasifier. Normally the fluidized bed gasifiers use bed materials to enhance heat and mass transfer rates between gases and solid biomass.

In a fluidized bed gasifier, the biomass feedstock fed into the system is quickly heated up by the bed material that results in subsequent thermal reactions including rapid drying and pyrolysis, producing char and gaseous products (Basu 2010). Winkler initially introduced this old technology in 1926 for massive-scale coal gasification. In 1970s, a significant improvement on the thermal process took place to increase the carbon conversion and to improve the quality of producer gas by operation the gasifier at higher temperatures (Laboratory 2017).

The working principle behind the fluidized bed gasifier is based on the fluidising bed material, for instance sand, by injecting the gas phase substance at the bottom of a vertical reactor vessel. The gaseous agent is passed upwards through the bed at a gradually increased velocity. As the pressure drop of the gasification agent reaches the same point as those of gravity force of the sand, the particles are suspended, at which the minimum fluidisation velocity (u_{mf}) is reached. The higher gas velocity allows the bed to expand and creates gas bubbles like boiling liquid. After the gas passes the bed, the velocity is much lower in the freeboard, majority of the coarse bed material and the biomass or char stay in the gasifier. This type of gasifiers is termed as bubbling fluidized bed gasifier. When the gas velocity is further increased to sufficiently high, the entire particles including bed materials are entrained out of the reactor, resulting in a simultaneous gas-solid flow (Knoef 2005). In order to maintain steady operation of the gasifier, the bed materials return back to the gasifier after separating from the producer gas, and thus this type of gasifiers is called circulating fluidized bed gasifier.

The fluidized bed gasifier has operational advantages over the fixed bed gasifiers in terms of fuel flexibility, uniform distribution of temperature and enhanced transfer rates over the fixed bed gasifiers. However, the producer gas contains more fine particles in comparison with the down draft fixed bed gasifier. The fluidized bed gasifiers has the capability to gasify a wide range of feedstock, including more reactive low-class coals and various forms of biomass with relatively high ash and moisture contents (Laboratory 2017). In addition, due to the rapid heat exchange and reaction rate inside the reactor, the fluidized bed gasifier has compact construction and uniform temperature profile that can be controlled, normally between 700 to 900^{o}C (Knoef 2005). It is reported that at very high gasification temperatures, the produced gas tends to contain more dust and alkali metal in the vapour state. Incomplete carbon reaction may also occur in the fluidized bed gasifiers although this can be minimised with optimum gas flow

velocity (Knoef 2005). In the subsequent sub-sections, each type of fluidized bed gasifier are described and discussed.

Bubbling fluidized bed gasifier

Bubbling fluidized bed (BFB) gasifier has been used for a thermal decomposition of coals and biomass. Pang (2016) noted that BFB gasifier could proceed various properties of solid fuel with a good temperature control. In 1997, a power plant, called Enamora, with the electricity generation capacity of 750 kW_e was successfully established in Spain by coupling a BFB gasifier with dual fuel engine, in which almond shell was used as the biomass feedstock. The physical structure of the BFB gasifier is presented in Figure 2.10.

In most designs of the BFB gasifiers, the feedstock is fed from the lower side of the gasifier into a bed of hot material, which can be inert medium or a catalytic solid material (Pang 2016). To fluidize the bed materials, the gasification agent enters the system through the bottom. After the thermochemical conversion takes place inside the reactor, the producer gas generated flows out from the top of the gasifier. In the meantime, fly ash and any fine particles are entrained in the producer gas which are separated by a cyclone and trapped into a container, which can be emptied, if required.

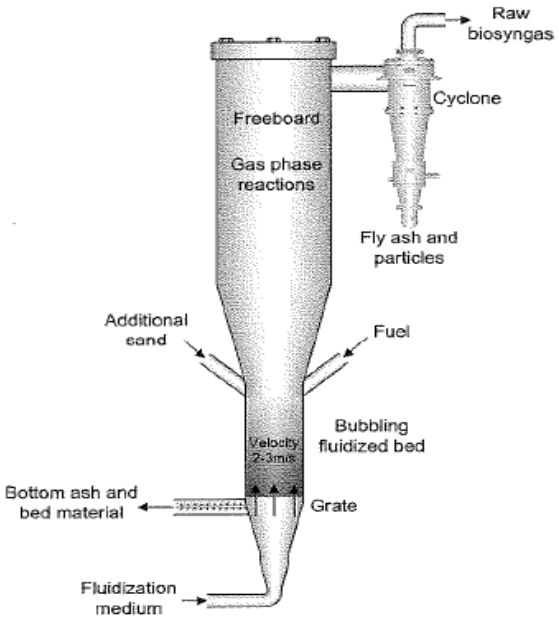

Figure 2.10. Structural design of the BFB gasifier (Knoef 2005).

In operation the BFB gasifier, bed temperature during the biomass gasification is normally maintained at around 900^{o}C (Basu 2010), resulting in considerably high fine particles concentration of the producer gas (Pang 2016). Nevertheless, a unique characteristic of the BFB gasifier is that it has a uniform temperature profile and relatively high rate of reaction as well as good efficiency of carbon conversion. Thus, the zone of thermochemical reactions such as drying, pyrolysis, oxidation, and reduction is difficult to be distinguished (Knoef 2005).

Circulating fluidized bed gasifier

Circulating fluidized bed (CFB) gasifier shares a lot in common with the BFB, particularly in terms of operation conditions and the flow directions of the gasification agent and producer gas. However, the gas velocity in the CFB gasifier is significantly higher to entrain the solid particles (bed material) out of the reactor, therefore, CFB reactor has notably smaller diameter than that of BFB (Pang 2016).

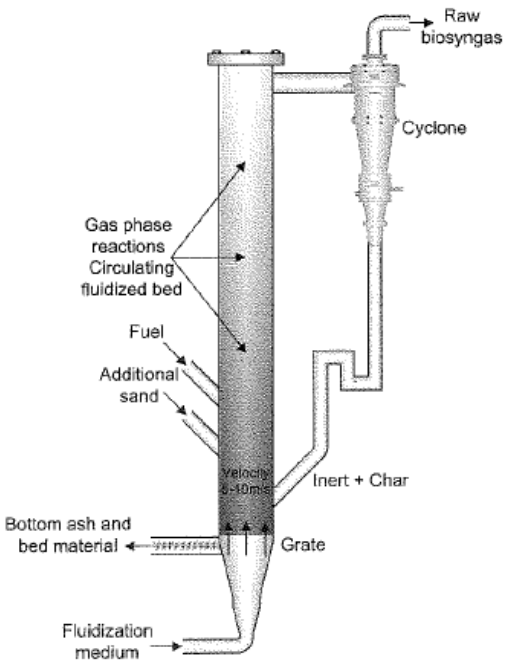

Figure 2.11. Schematic diagram of CFB gasifier (Knoef 2005).

As depicted on Figure 2.11, the schematic diagram shows the main components of the CFB gasifier with the flow directions of materials entering and exiting the system. Fluidisation gas agent comes into the reactor from the lower part below the grate, which is comparable to those in the BFB gasifier. The producer gas at high temperatures flows out of the gasifier to pass through a cyclone for a separation process. The solid particles including ash, char and solid bed material entrained in the producer gas first flow out of the gasifier together with the producer gas and are then separated from the gas. The bed material and char are finally recycled back to the gasifier through a syphon while the ash and char are further carried away by the producer gas for separation below the standpipe. The ash in the gasifier is collected from the disposal channel just under the grate.

Dual fluidized bed gasifier

Dual fluidized bed (DFB) gasifier is a gasification reactor that consists two separated columns as an interconnected thermal system. When steam is used as the gasification agent,

production gas with moderate to high calorific value is the unique feature of this type of reactor (Bridgwater 1995). The current development of this new technology has enabled to the conversion of biomass into valuable gaseous products for a wide range of application, including power generation with a gas engine or a gas turbine, synthesis of liquid fuel (Fischer-Tropsch) and fuel cell (Saw and Pang 2013).

Figure 2.12. conceptualizes the design of DFB gasifier, developed in Vienna University of Technology (Kern et al. 2013). Some typical components of the pilot scale rig include combustion reactor, gasification reactor, upper and lower loop seals, and feedstock hoppers located at three different levels.

In the DFB gasification system, the gasification occurs in a BFB reactor. Steam as the gasification agent is injected from the base of the BFB reactor while the solid fuel (biomass) is fed into the bed position of the BFB reactor. The location in which feedstock is admitted into the system significantly affect the amount, composition and quality of the produced gas (Kern et al. 2013). At the bottom position, the bed material and char flow through a loop seal to another reactor, termed as combustion reactor, in which the char is combusted by injected air and the bed material is heated up. This combustion reactor is a fast fluidized bed (FFB) or circulating fluidized bed (CFB) reactor with small reactor this high velocity of flue gas can be achieved. For complete combustion of the char and for achieving target temperature, an excessive fuel (LPG) can be supplied, if needed, from the bottom of the combustion reactor. The flue gas and heated bed material flow up to the top of the CFB reactor and then the bed material is separated from the flue gas. The heated bed material falls into a channel by gravity flowing into the BFB gasification reactor to supply needed heat for steam gasification of biomass.

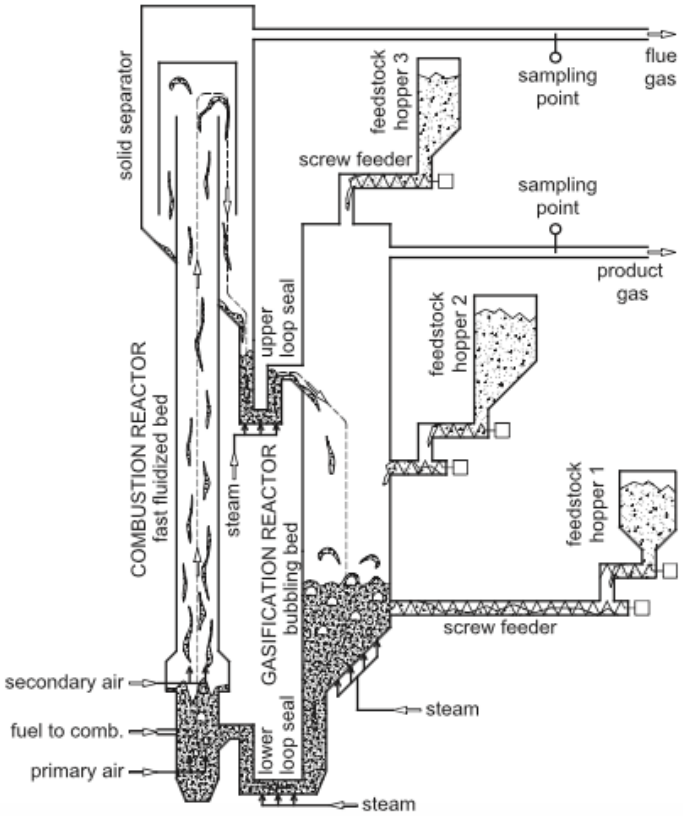

Figure 2.12. Schematic design of DFB gasifier at Vienna University of Technology (Kern et al. 2013).

A slightly variation was made in the University of Canterbury's 100 kW DFB gasifier in which the bottom loop seal was replaced by an inclined chute and a cyclone at the CFB reactor was added for separation of heated bed material and flue gas (Bull 2008). During the gasification process on this DFB gasifier, the bed materials (silica sand or olivine sand) and the solid char at the BFB reactor base were hydraulically transferred through the inclined chute to the CFB, where the char was combusted with air. The bed material was then fluidized upwards and passed to the CFB cyclone separating the heated bed material from the flow of the flue gas. After that, the solid carrying heat from the combustion column was delivered back to the BFB column through a siphon, providing heat required for the endothermic gasification reactions.

2.8.2.3. Entrained flow gasifier

Entrained flow (EF) gasifier is another type of gasifier for gasification of pulverised fine particles and slurry type of fuels, in which a spray of fuel is generated at the top part of the reactor. Then gasification agent is injected at high pressure for uniform mixing and reaction with the sprayed fuel. In then EF gasifier, thermal conversion occurs in much higher temperature than in either BFB or CFB gasifier. EF gasifier has made it possible to obtain constant temperature in the reactor, higher heating rate, and short but narrowly distributed residence time at which the producer gas produced normally has low tar concentration (Knoef 2005).

Hernández et al. (2010) performed study on the EF gasifier and they concluded that fuel size reduction and longer residence time are possible to improve the produced gas quality, meaning that higher values were achieved at all operation parameters such as CO and H_2 content, LHV, cold efficiency and fuel conversion. Nonetheless, finely reduced feedstock or liquid fuel is required in order to achieve high level of fuel conversion (Drift et al. 2004), resulting in a high cost of the feedstock pre-treatment, and hence economically unattractive (Knoef 2005).

2.8.3. Producer gas application for internal combustion engine

From above discussion, the producer gas generated from biomass gasification can be used for in gas engine or gas turbine for power generation which offers a possibility to produce electricity from the rice husk biomass. One possible schematic diagram describing the integration of a DFB gasifier and gas engine is provided in Figure 2.13 (Baratieri et al. 2009), in which the producer gas was first cleaned in a scrubber to remove tars and fine particles before being fed into a gas engine. It was reported that this system can achieve electrical and

thermal efficiencies of 35% and 40%, respectively. In addition, this technology was considered to be suitable for a combined heat and power (CHP) plant with a scale range of between 100 and 1000 kW_{el}. However, typical impurities produced along with producer gas such as tar and fine particles remain the major area of concern, leading to a number of operational problems such as sintering, agglomeration and coking (Baratieri et al. 2009).

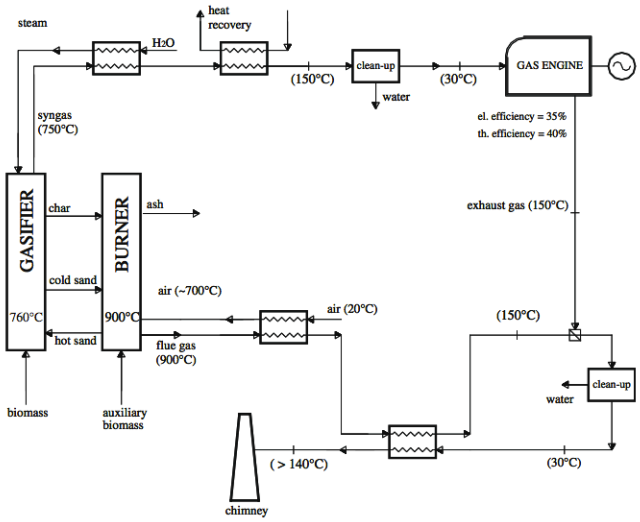

Figure 2.13. Schematic diagram of producer gas-fuelled gas engine (Baratieri et al. 2009).

In many applications, the tar concentration in the product gas needs to be removed to meet a particular standard as these contaminants would cause operation problems such as blocking and corrosion of the downstream pipes and equipment of the system (Basu 2010). In terms of electricity generation, the use of producer gas in the gas engines requires considerably low levels of tar and particulate content for the engine operation to be reliable and to maintain the durability of the engine's component for a long period. It is suggested that the concentration of tar must be between 50 and 100 mg Nm^{-3} (Baratieri et al. 2009) and the maximum particulate content be 50 mg Nm^{-3} (Hasler and Nussbaumer 1999). However, care is needed when accepting these gas quality requirements as there may be differences between the engine used in the experiment and that to be used in a commercial plant.

2.8.4. Tar aspects: Definition and classification

In order to develop efficient and cost-effective tar removal technology, understanding of tar composition and properties is important. Milne and Evans (1998) reported a comprehensive definition of tar as "organics produced under thermal or partial-oxidation regimes (gasification) of any organic material, which are generally assumed to be largely aromatic". Another definition of tar is proposed to be hydrocarbons with a complex mixture including single ring and multiple ring aromatic compounds in addition to other oxygen containing hydrocarbons and complex polycyclic aromatic hydrocarbons (Devi et al. 2005). Based on molecular weight, tar is considered to be all organic impurities whose molecular weights are more than 78 (Neeft et al. 1999).

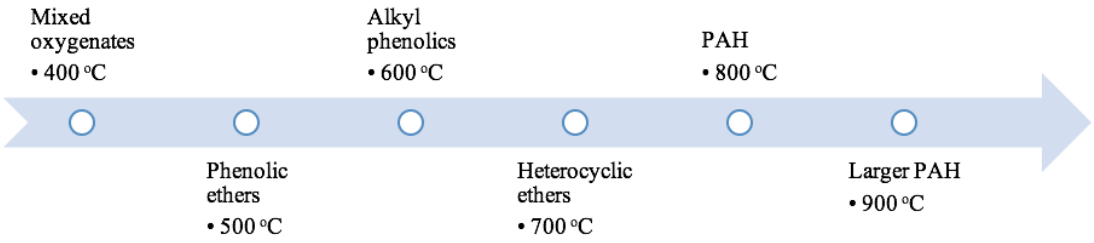

Figure 2.14. Schematic diagram of tar maturation proposed by Elliot (1988) as cited in Milne and Evans (1998).

The tar in the producer gas is formed in the biomass gasification through a series of complex reactions, which are strongly dependent on the reaction conditions (Li and Suzuki 2009). Milne and Evans (1998) proposed the scheme of tar maturation as is presented in Figure 2.14. It shows the transformation of tar compounds as a function of process temperature from primary products to phenolic compounds and then to aromatic hydrocarbons.

In some literatures, two types of tar classification have been proposed. In a report published by Milne and Evans (1998), tar was classified into four categories including primary products, secondary products, alkyl tertiary products and condensed tertiary products. In a

separate report by Kiel et al. (2004), tar components can be grouped into five classes based on the chemical, solubility and condensability of different tar compounds and this method is known as "ECN (Energy research Centre of the Netherlands) class". In this classification method, tar compounds can be divided into class 1 (GC-undetectable), class 2 (heterocyclic), class 3 (aromatic), class 4 (light polycyclic aromatic hydrocarbons) and class 5 (heavy polycyclic aromatic hydrocarbons). The comparison of these classification methods are given in Table 2.7.

Table 2.7. Tar classification and the associated compounds.

Tar classification proposed by Kiel et al. (2004) (ECN class)	**Class name**	**Representative tar compounds**	**Tar classification proposed by Milne and Evans (1998)**	**Tar compounds**
Class 1	GC-undetectable	Very heavy tars, cannot be detected by GC	Primary products	Cellulose-derived products (levoglucosan, hydroxyacetaldehyde and furfurals), analogous hemicellulose-derived products and lignin-derived methoxyphenols
Class 2	Heterocyclic	Pyridine, phenol, cresols, quinoline and isoquinoline	Secondary products	Phenolics and olefins
Class 3	Light aromatic	Toluene, xylenes, ethylbenzene and styrene	Alkyl tertiary products	Methyl derivatives of aromatics (metyl acenaphthylene, methylnaphthalene, toluene and indene)
Class 4	Light poly-aromatic	Indene, naphthalene, methylnaphtalene, biphenyl, acenaphthylene, acenaphthene, fluorene, phenanthrene, anthracene	Condensed tertiary products	Polycyclic aromatic hydrocarbons (PAH) without substituents (benzene, naphthalene, acenaphthylene, anthracene/ phenanthrene and pyrene)
Class 5	Heavy poly-aromatic	Fluoranthene, pyrene, benz(a)anthracene, chrysene, benzo(b)fluoranthene, benzo(k)fluoranthene, benzo(a)phyrene, indeno(1,2,3-cd)pyrene, benzo(g,h,i)perylene, dibenzo(a,b)anthracene.		

2.8.5. Tar removal

To meet the requirement of tar concentration in order for the producer gas to be used in IC engine, tar removal becomes necessary. There are two available methods to control the tar

concentration in the producer gas which include primary (in-situ) method and secondary (post-gasification) method (Kiel et al. 2004). Primary method is a process of tar removal taking place inside the gasifier and it is performed in several ways such as by optimising gasification operation conditions, adding a bed additives or catalysts in the fluidized bed gasifier and using well designed gasifier. In secondary method, tar is separated from the producer gas following the gasifier. In this treatment, both dry and wet gas cleaning methods have been reported. The secondary methods have been extensively studied by many researchers. However, as these are out of the scope of this study, it is advised for curious readers to look into sophisticated reports by (Devi et al. 2003) as well as an excellent literature by (Milne and Evans 1998).

As far as the operation conditions are concerned, the increase of gasification temperature and pressure in the gasifier normally decreases the tar concentrations in the producer gas. Therefore, high-temperature and high-pressure operations are desirable (Devi et al. 2003). In addition, gasification temperature is also found to have the positive effect on producer gas yield (Basu 2010). In a downdraft gasifier, the operation temperature of above 850^{o}C favoured the producer gas composition increasing the contents of CO, CH_4, and H_2 with the expense of CO_2 (Moghadam et al. 2014).

The S/B ratio in steam gasification is other influential parameter on the biomass gasification, and thus it is important to find the optimum value of the S/B ratio in the gasification process. The tar yield in a system depends on the amount of gasification agent per unit mass of biomass gasified (Atnaw et al. 2013). Too much gasification agent applied to a gasifier may not be favourable for the producer gas production and is not cost effective as it will lower the gas quality (Basu 2010).

The use of catalyst, furthermore, is also an important parameter in the gasification process as it can elevate the producer gas yield by cracking the tar and reforming the molecules of hydrocarbon (Knoef 2005). It is reported that the injection of steam to the catalytic bed

significantly reduced the tar concentration and increased the efficiency of the hydrocarbon reforming reaction during biomass gasification. In practice, catalyst can be used for tar reduction either in the primary reactor (gasifier) or in the downstream tar removal as a secondary method (Moghadam et al. 2014). The former may involve impregnating the catalyst in the biomass preceding the gasification process. It can be added directly to the reactor, as in a fluidized bed. In this case, dolomite, olivine, alkali, nickel, and char have been found to have positive effect on tar reduction. Of these bed materials, olivine and dolomite are most effective in gasification of biomass.

Olivine is a magnesium-iron-silicate mineral $(Mg_{1-x}, Fe_x)SiO_2$ that is naturally available and comes in sizes (100-800 μm) and density ranges (2,500-2,900 kg m^{-3}). The concentration of the iron and magnesium often varies depending on where the sand is mined. Olivine has a comparable catalytic activity to calcined dolomite (Bhattacharyya 2014).

In this study, the effect of natural olivine sand as the bed material on the producer gas and tar composition as well as concentration will be investigated which will be discussed in more details in the subsequent chapters.

3. Materials and Equipment

3.1. Research materials

Rice husk pellets (RHP) were purchased from PT. Agro Jaya Dwipa, headquartered in Yogyakarta, Indonesia. Prior to their delivery to New Zealand, the sample were sent to Gadjah Mada University, Indonesia, for proximate analysis and to Sucofindo, Semarang, Indonesia, for ultimate analysis. The results of these analyses are given in in Table 3.1.

Table 3.1. Results from proximate and ultimate analyses of the RHP.

Parameter	**Unit**	**As received (a.r.)**	**Dry basis (d.b.)**
Proximate analysis			
Moisture	[wt.%]	8.85	9.71
Ash content	[wt.%]	18.00	19.75
Volatile matters	[wt.%]	52.60	57.71
Fixed carbon	[wt.%]	20.55	22.55
Ultimate analysis			
Carbon	[wt.%]	42.22	46.32
Hydrogen	[wt.%]	4.04	4.43
Nitrogen	[wt.%]	0.32	0.35
Oxygen	[wt.%]	22.02	24.16
Heating value			
LHV	[MJ kg^{-1}]	13.46	14.77
Physical measurement			
Bulk density	[$kg.m^{-3}$]	650	-
Diameter	[mm]	6	-
Length	[mm]	20-30	-

From Table 3.1, it can be seen that the RHP has a low moisture content in as received basis (8.85% a.r.) and relatively high ash content (18.00% a.r.) in comparison with wood pellets, and the high ash content will influence the characteristics of the fluidisation, gasification and combustion. The low moisture content in the biomass feedstock is expected to positively affect the heating value of the producer gas, the efficiency of the gasification

reactor and tar content. However, the high ash content could possibly trigger a significant cause of concern associated with agglomeration and de-fluidisation of bed material. The high volatile matter (52.60% a.r.) means that the RHP can be combusted easily, but the control of combustion may need care (Armesto et al. 2002). Meanwhile, the fairly low fixed carbon (20.55% a.r.) is also expected to influence the overall producer gas production since there are more fractions of biomass that can volatize to the gaseous product. The RHP could be expressed as the $C_xH_yO_z$ molecule, where the molarities of C, H and O were found to be $CH_{1.15}O_{0.39}$, according to the fuel ultimate analysis (wt.% d.b.). It was found that the values of the proximate and ultimate analysis were closely comparable to those of solid materials used in other studies referenced in Table 2.4.

Physically, the RHP has a diameter of 6 mm with a maximum length of 30 mm and a mass density of 650 kg m^{-3}. Compared to the pellet standard of final draft prEN 14961-2 in all classes mentioned in Section 2.5.3, it seems that the physical dimensions of the RHP were close to the threshold measurement requirements. The high density of the RHP (650 kg m^{-3}) makes it easy for its transportation, storage, processing and firing.

Two types of bed materials were used in the experiments which include silica sand as inert material and olivine sand as catalytic bed material. The silica sand was supplied by Industrial Sand Limited, while the olivine sand was obtained from Metcast Services Limited, both in New Zealand. The chemical and mechanical properties of these two types of sands are presented in Table 3.2. In the experiments, the bed material acted as heat carrier to transfer heat from the combustion column to the gasification column for the endothermic reactions during steam gasification of the biomass.

From Table 3.2, it is seen that as an inert material, silica sand is comprised of more than 96% of silicate in SiO_2 form, resulting in no catalytic effect on the gasification process. On the other hand, olivine sand has 39% silicate, in addition to 43% of magnesium oxide (MgO) as

the major fraction. With the notably high proportion of MgO, olivine sand is expected to be a catalytically active bed material for the enhancement of gaseous product of gasification.

The particle density of the bed material influences the fluidisation characteristics in the experiments. The high mineral hardness measured in Mohs scale confirms their suitability for the fluidized bed application. Finally, Brunauer-Emmet-Teller (BET) number shows values for both sand particles indicating they are suitable as heat transfer agents.

Table 3.2. Chemical and mechanical properties of silica and olivine sand.

Component	Unit	Silica sand in this study[1)]	Silica sand in literature[2)]	Olivine sand in this study[1)]	Olivine sand in literature[2)]
MgO	[wt.%]	-	-	43.0	48.0-50.0
SiO_2	[wt.%]	99.32	96.0-98.0	39	39.0-42.0
Fe_2O_3	[wt.%]	0.07	< 0.25	8	8.0-10.0
$Al_2O_3 + Cr_2O_3 + Mg_3O_4$	[wt.%]	0.16	< 2.0 (Al_2O_3)	1.9 (Al_2O_3)	0.8
CaO	[wt.%]	0.10	-	-	< 0.4
NiO	[wt.%]	-	-	-	< 0.1
Loss on ignition	[wt.%]	0.20	-	2	-
Particle density	$kg.m^{-3}$	2,560	≈ 2,650	3,250	≈ 2,850
Hardness	Mohs scale	-	7	-	6.7
BET surface area	$m^2.g^{-1}$	-	< 0.5	-	< 1.0

[1)] as indicated by suppliers

[2)] Koppatz et al. (2011)

3.2. Experimental setup

All experiments took place at the special-purposes laboratory of Chemical and Process Engineering (CAPE) department, University of Canterbury, from December 2016 to October 2017. The biomass steam gasification experiments were performed in a 100 kW_{th} DFB gasifier, whose schematic design is presented in Figure 3.1. The pilot scale gasifier consists of two main columns including a bubbling fluidized bed (BFB) column as the gasification reactor or a circulating fluidized bed (CFB) column as the combustion reactor.

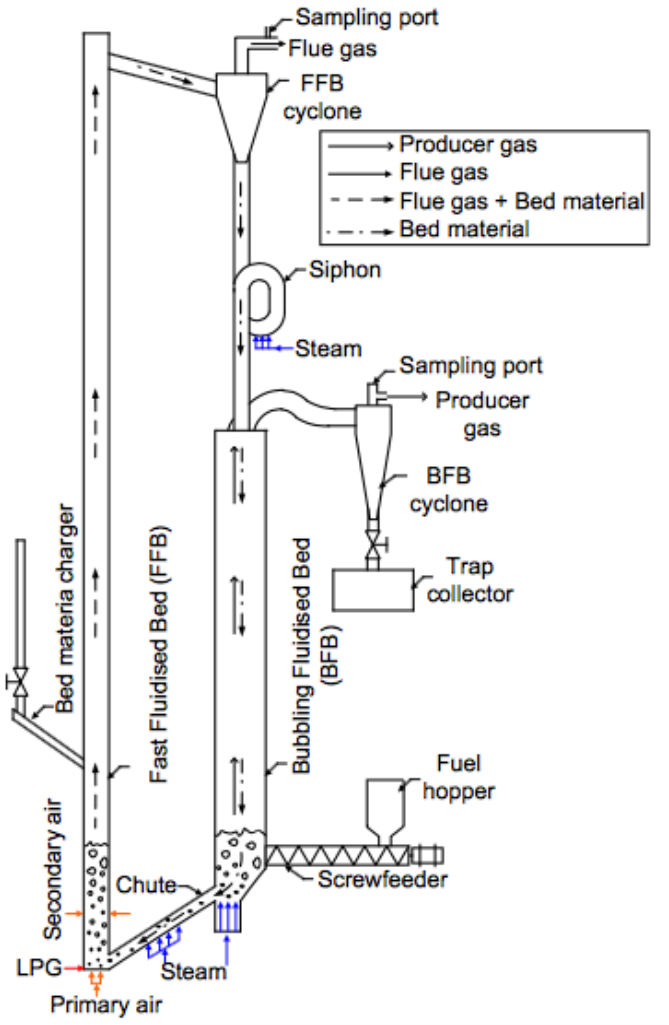

Figure 3.1. Schematic design of DFB gasifier (Saw and Pang 2013).

The CFB combustion reactor has an internal diameter of 0.1 m and a height of 3.7 m. The corresponding dimensions for the BFB gasification reactor are 0.2 m and 2 m, respectively. A cyclone was installed at the top of the CFB column to separate heated bed material and flue gas. A syphon is connected to the bottom of the cyclone for pressure seal but it allows hot bed material to flow through to the BFB gasification reactor. The other cyclone was connected to the top of the BFB column to remove solid particles from producer gas stream. At the base of the gasification column, a chute is connected to the CFB combustor which allows the bed material and char to flow from the gasifier to the CFB combustion reactor in which the char is combusted by the injected air.

To feed the biomass into the gasification reactor, a feeding system comprised of lock hoppers and calibrated screw feeder, termed as auger, was put into operation. The biomass feed rate was adjustable by changing the rotation frequency of the auger. A cylindrical container that is called trap collector and connected below the BFB cyclone was also used for the collection of ash and fine particles exiting the gasification reactor which could be emptied at any time, when required.

A pilot burners were installed at the middle height of the CFB column for ignition of char and addition fuel, LPG, if needed. A sand charger was installed at the lower side of the CFB column to feed the bed material for compensation of lost material. To control the flows of various streams entering and leaving the system such as steam, LPG, air, nitrogen (N_2), helium (He) and low pressurised cooling water, some valves, rotameters and flowmeters were also utilised.

To fluidize bed material in CFB combustion column, air as the fluidizing agent is injected from two different pipes, named primary air pipe and secondary air pipes (orange arrows), both of which are located at the bottom of the column. During the heat up process of the gasifier operation, air is also supplied from the bottom of the BFB gasification column (blue arrows). To avoid any gas leakage between the columns and make sure a high throughput of bed material, both the upper loop seal (syphon) and chute are fluidized with air (blue arrows). When the gasification process is started at targeted operation conditions, the fluidizing agent in the BFB gasification column, syphon and chute are replaced with steam.

4. Experimental procedures and analysis

The operation of the DFB gasifier comprises three essential stages towards the desired operation conditions at which gaseous products are ready to be drawn.

- Stage 1: Cold run experiment to identify the fluidisation characteristics of bed material inside the DFB gasifier.
- Stage 2: The heating up stage which is critical to elevate the gasification reactor temperature. This stage indicates the thermal energy transfer from the CFB column to the BFB column, from which heat is provided for the endothermal reactions of gasification.
- Stage 3: The third stage is the steam gasification of biomass, which is the main part of the experiments in this study, in which samples of tar-containing producer gas are collected.

  During the gas sample collection, the operation parameters were kept steady. Constant flow rates of material entering the gasifier such as biomass and steam into the BFB column as well as air into the CFB column were maintained stable so that the gasifier operation was steady before samples were drawn. However, in order to keep the gasification temperature steady, the flow rate of supplementary fuel (LPG) to the CFB column may be adjusted.

These stages allow a number of necessary parameters to be determined for the successful operation of the gasifier that is explained in the following sections.

4.1. Cold test run

A number of experiments were carried out during the cold runs, in which the gasifier was operated with no addition of heat. Two important objectives at this stage were to calibrate the feed rate of the auger, and to theoretically and experimentally identify the fluidisation characteristics of the bed material in both CFB (combustion) column and in BFB (gasification)

column. The essential information acquired from this part of experiments was then used for basic calculations of operation parameters applied in the hot test runs.

4.1.1. Auger calibration for rice husk pellets

The auger calibration aimed to determine the correlation between the rotation speed of auger (Ω_A, r.p.m.) and the rice husk pellets ($\dot{m}_{f,wet}$, kg_{wet} h^{-1}) fed into the gasification reactor, from which a linear equation has been generated as shown in Figure 4.1. Each data point in the graph represents an average of three repeated measurements.

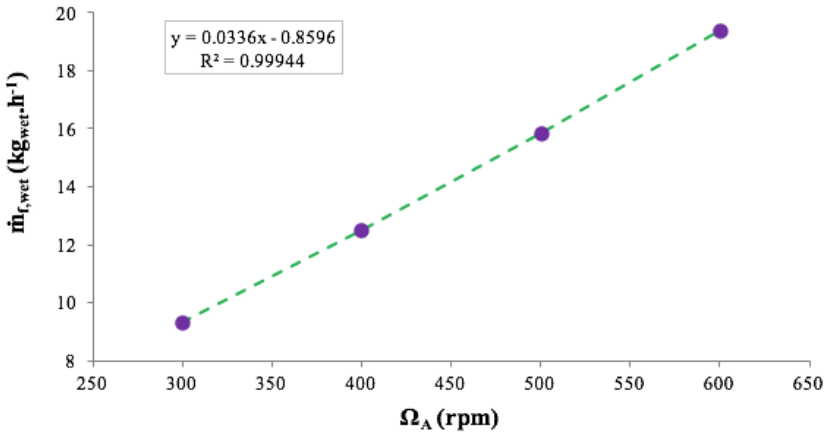

Figure 4.1. Calibration curve for rice husk pellets in the DFB gasification feeding system.

From the graph above, a linear equation has been generated as follows:

$$\dot{m}_{f,wet} = 0.0336\Omega_A - 0.8569 \quad (4.1)$$

The above calibrated curve is applied to the rice husk pellet feedstock ($\dot{m}_{f,wet}$, kg $h^{-1}{}_{wet}$) thus the oven-dry (od) biomass feed rate ($\dot{m}_{f,od}$) can be calculated once the moisture content (MC_{wet}) and the biomass feed rate are known:

$$\dot{m}_{f,od} = \frac{\dot{m}_{f,wet}}{(1 + MC_{od})} \quad (4.2)$$

where MC_{od} represents moisture content in dry basis and can be related to the wet-based moisture content, MC_{wet}, using the following equation:

$$MC_{od} = \frac{MC_{wet}}{(1 - MC_{wet})} \tag{4.3}$$

From the oven-dry biomass feed rate (kg h^{-1}_{dry}), dry-based moisture content (wt.%, d.b.) and the steam feed rate ($\dot{m}_s$, kg h^{-1}), the values of S/B ratio ($Ø_{SB}$) can be determined by the following formula (Göransson et al. (2011) and Saw and Pang (2013)):

$$Ø_{SB} = \frac{\dot{m}_s + MC_{od} \,.\, \dot{m}_{f,od}}{\dot{m}_{f,od}} = \frac{\dot{m}_s + MC_{od} \cdot \frac{\dot{m}_{f,wet}}{(1 + MC_{od})}}{\frac{\dot{m}_{f,wet}}{(1 + MC_{od})}} = \frac{(1 + MC_{od}) \,.\, \dot{m}_s + MC_{od} \,.\, \dot{m}_{f,wet}}{\dot{m}_{f,wet}} \tag{4.4}$$

Alternatively, if the value of $Ø_{SB}$ is known, the biomass feed rate can be determined by:

$$\dot{m}_{f,wet} = \frac{(1 + MC_{od}) \,.\, \dot{m}_s}{Ø_{SB} - MC_{od}} \tag{4.5}$$

In some cases, the wet biomass feed rate and the steam to biomass ratio are known and the steam feed rate is then determined by

$$\dot{m}_s = \frac{(Ø_{SB} - MC_{od}) \,.\, \dot{m}_{f,wet}}{(1 + MC_{od})} \tag{4.6}$$

Based on the equation (4.1) and (4.5), the auger speed is determined through the following equation:

$$\Omega_A = \left[\frac{(1 + MC_{od}) \,.\, \dot{m}_s}{0.0336 \text{ x } (Ø_{SB} - MC_{od})} \right] + 25.50 \tag{4.7}$$

4.1.2. Theoretical analysis of fluidisation characteristics

As far as the fluidisation characteristics are concerned, minimum fluidisation (u_{mf}) and terminal velocity (u_t) are two indicators that can be theoretically calculated according to the following formulae (Kunii and Levenspiel 1969):

- For Reynold number particle (Re_p) < 20 : $u_{mf} = \frac{d_p^2 (\rho_s - \rho_g) g}{1650 \mu}$ (4.8)

- For Re_p > 1,000 : $u_{mf}^2 = \frac{d_p (\rho_s - \rho_g) g}{24.5 \rho_g}$ (4.9)

where:

$$Re_p = \frac{d_p . u_{mf} . \rho_g}{\mu} \quad (4.10)$$

To obtain u_t, the following formulae are introduced.

- For $Re_p < 0.4$: $u_t = \frac{g (\rho_s - \rho_g) d_p^2}{\mu}$ (4.11)

- For $0.4 < Re_p < 500$: $u_t = \sqrt[3]{\frac{4}{225} . \frac{(\rho_s - \rho_g)^2 g^2}{\rho_g . \mu}} . d_p$ (4.12)

- For $500 < Re_p < 200{,}000$: $u_t = \sqrt[2]{\frac{3.1 g (\rho_s - \rho_g) d_p}{\rho_g}}$ (4.13)

where:

$$Re_p = \frac{d_p . u_t . \rho_g}{\mu} \quad (4.14)$$

In the equations above, d_p represents mean particle size (m), ρ_s represents solid (particle) density (kg m^{-3}), ρ_g represents fluid (gas) density (kg m^{-3}), g represents gravity (9.81 m s^{-2}) and μ represents dynamic viscosity of the fluid (kg m^{-1} s^{-1}).

To calculate u_{mf} and u_t, particle size distribution is needed which can be measured. In this study, the dimensions of the silica and olivine sands were measured using sieves and the results are shown in Figure 4.2 on the cumulative mass fractions of different particle sizes. The result shows that the silica was comprised of sand particles with average size ranging from 53 to 362.5 μm, while the olivine sands had a wider range of mean particle sizes, varying between 53 and 925 μm. For silica sand, all particles had sizes less than 360 μm, of which about 90%

was less than 256 µm. On the other hand, the particle sizes of olivine sands spread in a much wider range and over 98% of them fell on the range from 159 to 675 µm.

Table 4.1 presents a summary on calculated values of u_{mf} and u_t for different particles sizes of both silica and olivine sands, assuming that air is used as the fluidizing agent at room temperature (25°C). Detailed calculations of these values are presented in Appendix F. From these results, it is found that u_{mf} and u_t increase linearly with the particle size for both sands.

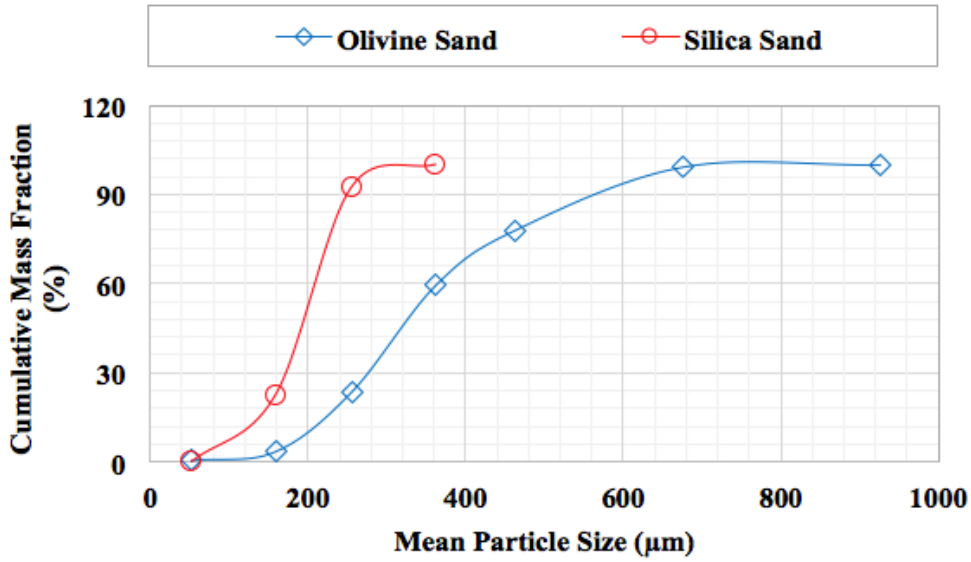

Figure 4.2. Cumulative mass fraction of silica and olivine sands against particles sizes.

The distinctive fluidisation regime requirements of the bed materials both in CFB column and in BFB column need different values for the solid flows. In the CFB column, the gas flow velocity should be above the terminal velocity as particle entrainment is desirable aiming to facilitate heat transfer from the CFB column to the BFB column. Therefore, desirable circulation of bed material is important to allow the heat carrying sand to move at a stable pace.

In contrast, in the BFB column, bubbling flow regime is required and sand particle entrainments should be prevented to minimize bed material loss from the system. Instead, the heat carrying sand in the BFB column (gasification reactor) should be recycled back to the combustion reactor. Consequently, the gas flow velocity in CFB column (combustion reactor)

should be higher than u_t, whereas that in the BFB column (gasification reactor) should be kept between u_{mf} as the lower limit and u_t as the upper limit.

Table 4.1. The values of umf and ut of bed materials at room temperature.

Mean Particle Size, d_p (µm)	**Silica sand**		**Olivine sand**	
	u_{mf} (m s^{-1})	u_t (m s^{-1})	u_{mf} (m s^{-1})	u_t (m s^{-1})
53	0.0014	0.3033	0.0029	0.4971
159	0.0126	0.9100	0.0264	1.4912
256	0.0326	1.4652	0.0685	2.4009
362.5	0.0654	2.0747	0.1373	3.3996
462.5	-	-	0.2235	4.3375
675	-	-	0.4760	6.3304
925	-	-	0.8938	8.6750

To determine the gas superficial velocity, u_{sf}, the following expressions can be used:

$$u_{sf} = \frac{\dot{v}_f}{A} \tag{4.15}$$

$$A = \pi \cdot r^2 \tag{4.16}$$

in which, $\dot{v}_f$ is the volumetric flow rate (m^3 s^{-1}) of fluid, A is the cross-section area of the pipe (m^2) and r is the radius of the pipe (m).

The increase of operation temperature gives an influence to the gas velocity in both CFB and BFB columns, resulting in a higher u_{sf} based on the equation as follow:

$$\frac{u_{sf,1}}{u_{sf,2}} = \frac{T_2}{T_1}$$

Theoretically, when silica is used as bed material at the the operation temperature of 25°C, the air flow rate to CFB should be controlled so that u_{sf} in the CFB column is higher than 2 m s^{-1}, whereas that in the BFB (gasification) column should be much lower than 2 m s^{-1}, but higher than 0.066 m s^{-1} in order for all the range of the particle size can be fluidized. For the olivine

sand, the corresponding values of the gas velocities should be higher than 8.66 m s^{-1} in the CFB column and between 0.476 to 0.497 m s^{-1} in the BFB column respectively, provided that the olivine sand is used without any pre-treatment in terms of particle size selection.

4.1.3. Experimental determination of fluidisation characteristics

Before gasification experiments, observations were performed in the DFB gasifier at cold conditions to visually investigate the extent of bed material fluidisation with varying gas flow rate without any supplementary heat in the both combustion and gasification reactors. This was performed by looking directly at the circulation of the flowing sand particles via a viewport installed at the stand pipe above the syphon. In these tests, the mass of sand particles carried out by gases from the cyclones were collected and measured after having the cold operation for 30 minutes. Rapid circulation of bed material with the minimum bed material loss was an indication of desired fluidisation. However, if at a certain gas velocity in the CFB column the particles were no longer carried out, this gas velocity was the terminal velocity (u_t). If the sands in the bed remain stagnant before the gas flow was increased to certain value, then this velocity was the u_{mf}. The results from the fluidisation observation tests revealed that when 10 kg silica sand was used as the inventory, the values of air u_{sf} in CFB column were found to be 3.43 m s^{-1} (primary air and secondary rotameter readings show "scale 20"). Whereas, the u_{sf} in the BFB column was found to be 0.12 m s^{-1}, in which the gas flow equivalent to a gas velocity of 0.08 m s^{-1} through the column was from BFB base and the remaining gas flow equivalent to a gas velocity of 0.04 m s^{-1} was from chute.

For the olivine sand, the fluidisation test in cold condition required more preparations because of two main reasons. Firstly, the maximum u_{sf} which could be tested in the existing gasifier's CFB column was 4.12 m s^{-1}. Therefore, based on the results given in Table 4.1, the

olivine sand with a mean particle size of more than 462.5 μm was not able to be tested. Secondly, as the mean particle size of the olivine mixture varied from 53 to 925 μm, there was approximately 40% (wt.%) of the bed material with mean particle size above 462.5 μm that needed to be removed.

Surprisingly, at the air of 4.12 m s^{-1}, circulation was insignificant and it appeared that only very fine particles with diameter less than 200 μm were entrained in the gas from the CFB column. To solve this issue, sands only with particle sizes between 200 μm and 300 μm were used which had a mean particle size of 256 μm. As a result, an appreciable circulation of bed material was then obtained using 10 kg of olivine sand, in which the values of u_{sf} in CFB and BFB columns were found to be 3.77 and 0.12 m s^{-1}, respectively. In the CFB column, the gas flow equivalent to velocity of 3.14 m s^{-1} was from the primary air and the remaining gas flow equivalent to gas velocity of 0.63 m s^{-1} was from the secondary air. Whereas, in the BFB column, the gas flow equivalent to velocity of 0.08 m s^{-1} was from the primary air and the remaining gas flow equivalent to gas velocity of 0.04 m s^{-1} was from the secondary air. Therefore, in order to achieve required circulation of the olivine sand as bed material in the future gasification, the olivine sands were sieved to select and use those with particle size between 200 and 300 μm, while no pre-treatment is required for the use of silica sand.

4.1.4. Assessment of fluidisation regime based on given gas velocities

Once the boundaries of gas velocities are known and bed material is selected, the actual gas velocity can be determined from a flow map based on target fluidisation regime. The type of fluidisation both in the CFB combustion reactor and in the BFB gasification reactor were determined using gas-solid fluidisation regime map which was proposed by Bi and Grace (1995) and was modified by Kern et al. (2013) as shown in Figure 4.3. In the figure, U^* and

d_p^* represent dimensionless gas velocity and dimensionless particle diameter, respectively. U^* and d_p^* were calculated from the following equations:

$$dp^* = \sqrt[3]{Ar} \tag{4.17}$$

$$Ar = \frac{\rho_g \cdot u_{mf}^3 \cdot (\rho_s - \rho_g) \cdot g}{\mu^2} \tag{4.18}$$

$$U^* = \frac{Re_p}{\sqrt[3]{Ar}} \tag{4.19}$$

$$Re_p = \frac{u_{se}\, d_{sv}\, \rho_g}{\mu} \tag{4.20}$$

in which Ar is the dimensionless Archimedes number, u_{se} is superficial velocity in which the solids begin to be significantly entrained (m s^{-1}) and d_{sv} is sauter diameter (µm). Other variables of the equations share the same definitions as those aforementioned in Section 4.1.2.

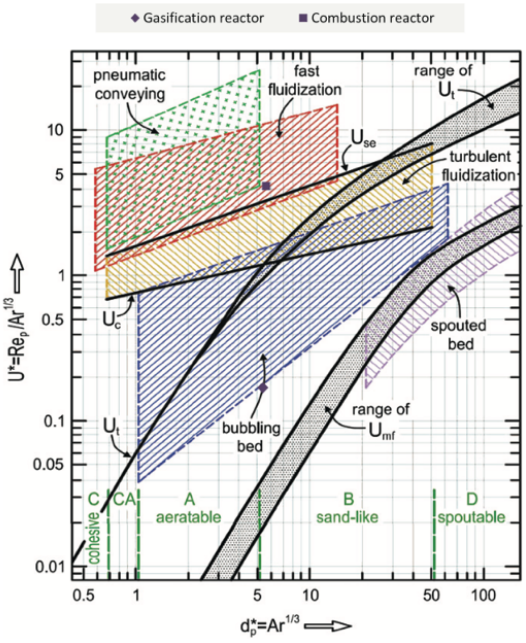

Figure 4.3. Fluidisation map of gas-solid fluidisation proposed by Bi and Grace (1995) and modified by Kern et al. (2013).

Based on the above equations, in the CFB combustion reactor, the U^* value during the cold test runs at 25°C was 5.46 for the silica sand and 5.04 for the selected olivine sand, while

the corresponding values of d_p^* were 10.06 and 12.28, respectively. In the BFB gasification reactor, the values of U^* were 0.17 for the silica sand and 0.16 for the olivine sand. Meanwhile, values of d_p^* in the BFB gasification reactor for silica and olivine sands, respectively, were the same as those in CFB combustion reactor since the Archimedes number of any bed material remains unchanged regardless of their specific location in the gasification system. As required, the fluidisation regime in the CFB combustion reactor should be in the fast fluidisation region as indicated in the map with the chosen operations and known properties of solid and gas. Similarly, in the BFB gasification reactor, the fluidisation regime should be in the region of bubbling bed as illustrated in the map.

4.2. Experiments of Biomass Gasification

The experimental procedures of biomass gasification can be divided to two phases, heating up and gasification. The initial phase of heating up is to heat the system to the desired gasification temperature, before the steam gasification of RHP could start. At the second step, samples of producer gas and tar were collected for chemical analysis and determination of yields.

4.2.1. Heating up phase

The heating up phase was started with supplying air into the gasifier system through all the pipelines mentioned in Section 3.2 adopting the flow velocities determined in the cold tests. Next 10 kg of bed material (silica or olivine) was progressively introduced into the CFB column through the sand charger. Once this was done, LPG burner was switched on with heat input of up to 50 kW. The LPG combustion continued until the target operation temperatures both in the CFB column and the BFB column were reached. At this time, another 20 kg of fresh bed

material was added into the CFB column progressively, each time with 5 kg, thus a total of 30 kg of sand inside the gasification system was used. In the meantime, additional fresh sand was also introduced into the gasifier system to compensate the bed material loss during the heating up process.

The target temperature in the BFB column was about 650-800°C and that in the CFB column needed to be 50-100°C higher than the BFB column temperature depending on the target gasification temperature in the BFB column. To successfully achieve the target operation temperature in BFB column, it is important to regularly monitor the temperature increase and the circulation of bed material at least once in 30 minutes. Failure to do this regular check-up may result in the uncontrolled and rapid temperature change in certain parts of the system as well as huge bed material loss.

It was observed that at the elevated operation temperature above 500^{o}C, the sand particle was likely to be carried out of the combustion reactor. After assessing this, it was thought that the increase of dynamic viscosity and the decrease of fluid density could lead to increased drag force on the particles, making the fluidisation circulating faster. The rapid and vast accumulation of sand particles lifted up out of the CFB cyclone would lessen the cyclone capability to separate the gas-solid phase so that instead of being transferred to the BFB column, the sand particles would be thrown out of the CFB cyclone along with the flue gas stream. To address this, adjustment of air velocity and LPG flow rate in the combustion reactor became the essential procedure to minimize these foreseeable issues during the heat-up phase.

The typical flow rates of LPG and air velocity used in the CFB column during normal operation of the gasifier are provided in Table 4.2 which are applicable to both silica sands and olivine sands. The increase of temperature profile in the BFB column, in which the gasification took place, was used as the main indicator to change the LPG flow rate and the air velocity.

Table 4.2. The typical profile of temperature increase in the gasification heat up stage.

Time (min)	Temperature in BFB column (^{o}C)	Temperature change (^{o}C)	LPG flow rate in CFB column (L min^{-1})	Air velocity in CFB column (m s^{-1})
0-30	70	50	10	3.48-3.77
30-60	150	120	20	3.48-3.77
60-120	300	150	30	2.43-2.71
120-240	500	150	30	2.43-2.71
240-300	650	150	30	1.58-1.82
300-360	800	150	30	1.58-1.82

During the heating-up phase, in the first 30 minutes, the temperature in the BFB column increased by 50^{o}C, from 20 to 70^{o}C, with the LPG flow rate of 10 L min^{-1} and air velocity ranging between 3.48 and 3.77 m s^{-1} in the CFB combustion column. To further heat up the reactor, the LPG flow rate was progressively increased to 20 L min^{-1}, while keeping the air velocity unchanged at the initial value. This change in LPG flow rate brought the temperature of BFB column up to 150^{o}C in 30 minutes. A temperature increase of approximately 150^{o}C h^{-1} was obtained when the LPG flow rate was at 30 L min^{-1}, thus reaching the target temperature of 650^{o}C in 5 hours.

Alternatively, in order to reduce bed material loss, lower air velocity was tried which was between 2.43 and 2.71 m s^{-1} until the reactor temperature reached 500^{o}C. After then the air velocity was further decreased to as low as 1.51 m s^{-1}. Under this operation procedure, the amount of sand particle entrained out of the gasifier varied between 10% and 15% from 10 kg of bed material fed into the system during the heating up process.

Another essential part of heating up phase was the charging of further 20 kg of fresh bed material. The increased quantity of bed material in the system could interrupt the steady state operation of the gasifier, leading to a short fluctuation of temperature in both CFB and BFB columns. To prevent such severe fluctuation of the bed material circulation in the system, the

sand was fed in 4 times (each time 5 kg), and in each time, feeding the sand slowly at a loading rate of about 1 kg min^{-1}. The loading time for 20 kg of fresh bed material plus 1 to 2 kg of the bed material for loss compensation took approximately 22 minutes in total. This ensured that the inventory of bed material was about 30 kg in the gasifier when the target operation temperature was achieved.

4.2.2. Gasification phase

The gasification phase was the most important part of the gasifier operation. Once the target operation temperature in the gasification reactor was stable, the gasification phase started. Firstly superheated steam injection was turned on to replace air, respectively, to the BFB gasification reactor, chute and siphon. Afterwards, the RHP was fed into the bed of sand particles by an auger at the pre-set rotation speed. Once the system had reached a steady state condition at the desired operation parameters and maintained at the steady condition for about 10 minutes, the tracer gas, helium (He) with a flow rate of 5 L min^{-1} was injected into the gasification column. About 1 minute after He being injected, producer gas and tar samples were collected from a sampling port located at the top of BFB cyclone. In the meantime, the producer gas from the biomass gasification was passed into the after-burner for combustion before being released into the environment through a chimney.

The entrained bed material, remaining char and ash exiting the BFB reactor were collected through a collector connected to the BFB cyclone bottom and then removed approximately every 30 minutes during the gasification process. A complete standard operation procedure of the DFB gasifier is provided in Appendix I.

4.2.2.1. Steam injection

At the start of the gasification phase, when steam was injected into the base of the gasification reactor, chute and syphon, the temperature in the BFB column was reduced by 15 - 20^{o}C depending on the total steam injection rate, due to the heat used to heat up the steam from approximately 300°C to the gasification temperature. At standard operation conditions with total steam injection rate of 10.5 kg h^{-1}, it took approximately 10 minutes when the gasification temperature was brought back to target temperature automatically.

It was interesting to note that when the steam was introduced, replacing the equivalent amount of air, the fluidisation behaviour of the bed in the gasification reactor was not apparently interrupted. When lower steam injection rates were used for lower steam to biomass ratios, for example at 1.5 kg h^{-1}, 2 kg h^{-1} and 7 kg h^{-1}, respectively, the BFB bed still remained in the bubbling fluidisation regime. At the steam flow rate of 10.5 kg h^{-1}, the steam velocity in the BFB column was 0.32 m s^{-1} at 650^{o}C and this became 0.37 m s^{-1} at the highest operation temperature of 800^{o}C. The change of fluid density and dynamic viscosity in this temperature range (650-800°C) did not affect the bed fluidisation regime (bubbling) either as the above steam velocities remained between u_{mf} and u_t of both silica and olivine sands. Details on calculation of the superficial velocity for the fluidizing agents (air and steam) can be found in Appendix G.

4.2.2.2. Biomass feeding

Once the steam injection was stabilised, biomass was fed into the BFB bed midlayer by activating the auger. The initial introduction of the biomass also decreased the temperature in the gasification reactor but the temperature was then stable after about 10 minutes. The biomass feed rate was determined by target S/B ratio as the steam injection rate was normally kept

constant. The details of the biomass feed rate and the steam flow rate for each operation parameter are provided in Section 2.5.

4.2.2.3. Producer gas and tar sample collection

The method of gas sampling in this study was adopted from previous study of this research team (Bull 2008), while the tar extraction method was based on that developed by (Brage et al. 1997) and modified by (Saw and Pang 2013). To take the samples of the producer gas and tar from the sampling port on the gasifier system, a special apparatus was used which is depicted in Figure 4.4.

The sampling device consists of a 100-ml glass syringe (A) coupled with a "T" stopcock at its lower end. A 60-ml plastic syringe (B) is attached to one end of the stopcock while a 3-ml Solid Phase Adsorption (SPA) cartridge with Supelclean LC-NH2, commonly known as Solid Phase Extraction (SPE) tube (C), is attached at the other end. A custom-made stainless steel adaptor, called sampling rod (D) with a length and diameter of 20 cm and 3 mm, respectively, is attached to the SPE tube on the side with a wider diameter. The sampling rod enabled the connection to the SPE tube with the producer gas stream exiting through the sampling port.

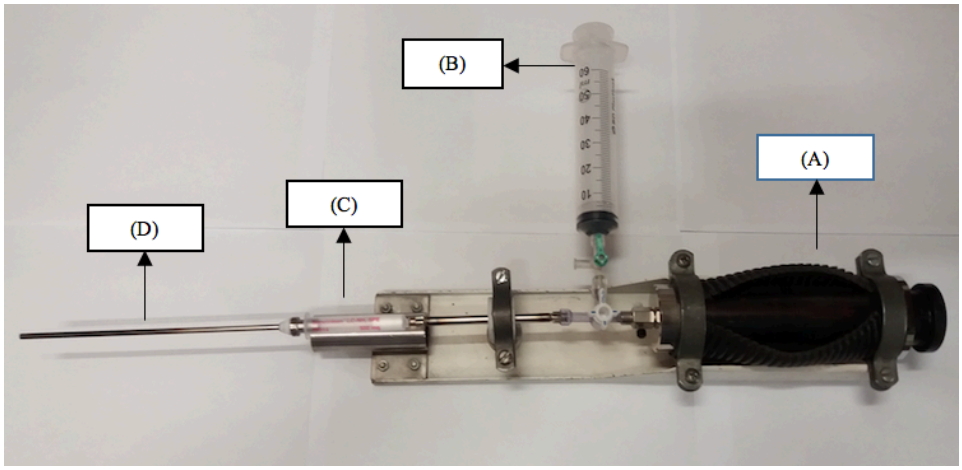

Figure 4.4. Sampling apparatus of producer gas and tar used in this study.

In the gasification experiments, when the gasification process reached steady state at the desired operation conditions, the sample of tar-containing producer gas was drawn through the sampling rod and then the glass syringe attached to the SPE tube, in which the tar compounds were trapped. To get sufficient quantity of tar for the gas chromatography (GC) analysis, 200 ml of tar-containing producer gas was drawn in total. The first 50 ml aliquot was manually drawn from the sampling port using the glass sample collection syringe. The first sample was then transferred into the plastic syringe, after which the gas was flushed out of the plastic container. Afterwards, the second and third 50 ml aliquots were extracted and flushed out in the same way. Then the last 50 ml aliquot was taken and stored in the plastic syringe as gas sample. The gas sample was then sealed, removed from the sampling apparatus and transported to an Agilent 3000 micro-GC for gas composition analysis.

In practice, a potential problem that might occur during the sample collection is the leakage of sampling apparatus. Loose connection between plastic syringe tip and the stopcock was often the main cause of this issue, leading to oxygen contamination in the gas sample. Therefore, care should be taken to ensure that all parts of the sampling instrument have been firmly tightened prior to drawing the gas sample.

After sampling was completed, the tar sample in each SPE column was eluted with 1 ml of dichloromethane (DCM) to crack the fraction of aromatic compounds from the trapped tar mixture into a 2 ml vial. The same SPE column was then eluted again with 1 ml mixture of DCM and isopropanol (IPA) (50:50 %vol.) for the extraction of phenolic fractions remained inside the packed bed of the SPE tube. As an internal standard (IS), *n*-dodecane with a concentration of 40 ppm was used for the analysis of individual tar compounds. The specific procedures for the tar sample extraction and GC analysis are provided in Appendix J.

For a given feedstock (such as RHP), the required supplementary heat from LPG can be estimated according to the gasification temperature and biomass feed rate. For example, steady

state operation at 650^{o}C normally required additional heat of LPG from 4 to 6 L min^{-1} with a dry biomass feed rate of 17.5 kg h^{-1}. An increase of every 50^{o}C in the gasification temperature required the supply of approximately an additional 2 L min^{-1} of LPG. Therefore, to keep the gasification temperature steady at 800^{o}C, 10-12 L min^{-1} of LPG was required.

4.2.2.4. Dust trap collector replacement

Rice husk is well known as a biomass resource containing high ash content. For the rice husk pellets (RHP) tested in this study, it has 18% of ash content, which would result in a considerable quantity of ash formed during the gasification phase. Therefore, it is necessary to empty the cylindrical ash container regularly every 30 minutes during the gasification. Failure to do this part of the gasifier operation may lead to the blockage of a pipe connecting the BFB cyclone and ash container. In the worst case, solid residue may fly into the after burner column along with the stream of producer gas.

If too much ash accumulates surrounding the inner wall of after burner it would cover the sparking wire of the pilot burner, and once this occurred, a barrier was formed blocking the nozzles of air and LPG. This blockage would negatively affect the combustion of producer gas in the after burner that could stop at any time leading to the termination of the gasifier operation.

4.3. Measurement apparatus

A micro-GC equipped with thermal conductivity detector (TCD) and two columns was used to determine the concentration of each gas component of producer gas. The first column with a 10 m x 0.32 mm molecular sieve 5A Plot was operated at 110^{o}C to separate H_2, N_2, CH_4 and CO. The other column with an 8 m x 0.32 mm Plot-Q, was operated at 60^{o}C to detect CO_2, C_2H_4 and C_2H_6.

For the individual tar analysis, a Varian CP-3800 GC with Flame Ionization Detector (FID) was used to separate and measure each of tar fractions in 50% phenyl and 50% dimethylpolysiloxane, fused in silica capillary column of 26 m x 0.25 mm x 0.25 μm with variant of Rxi-17Sil MS. The temperature of the injector and the FID was set at 300^{o}C. Each tar sample of 1 μl was transferred into the injector with an auto-sampler. To provide a good separation for all of the GC-detectable tar compounds, the column temperature was programmed with the column conditions controlled at: (i) 50^{o}C hold for 1 minute, (ii) from 50 to 210^{o}C at a rate of 10^{o}C min^{-1}, (iii) from 210 to 340^{o}C at a rate of 50^{o}C min^{-1} and hold for 11 minutes. The flow rate of the carrier gas, He, was set at 1 ml min^{-1}.

4.4. Method of calculations

This section explains a number of equations used for the calculation of major parameters examined in this study. These include the volumetric flow rate of producer gas, gas heating value, carbon conversion, cold gas efficiency and tar concentration.

4.4.1. The calculation of producer gas volumetric flow rate

The volumetric flow rate of dry producer gas ($\dot{v}_{dry\text{-}pg}$) was determined based on mass balance of tracer gas (He) with a known flow rate injected into the BFB reactor, in which the steam gasification took place. Along with the stream of producer gas, He as the tracer gas flew out of the reactor and passed through the sampling port and collected together with the gaseous product for the quantitative analysis. The volumetric flow rate of producer gas was determined through the following procedures adopted from Bull (2008).

- When the system reached steady state at the targeted operation conditions, He with a flow rate of 5 L min^{-1} was injected into the BFB column. Gas was first sampled 1 minute later

after the injection of He started and three repeated samples were collected within a period of 5 minutes.

- 50 ml of producer gas containing He, tar and unreacted steam was then drawn from a sampling port with the sampling apparatus described in Section 4.2.2.3.
- As the He-containing producer gas was passed through the SPE tube before getting into the plastic syringe container, the tar and steam in the producer gas were trapped in the packed silica gel inside the tube, making the producer gas dry and tar free.
- The dry producer gas was then injected into the micro GC to analyse the concentration of each gas element including He.

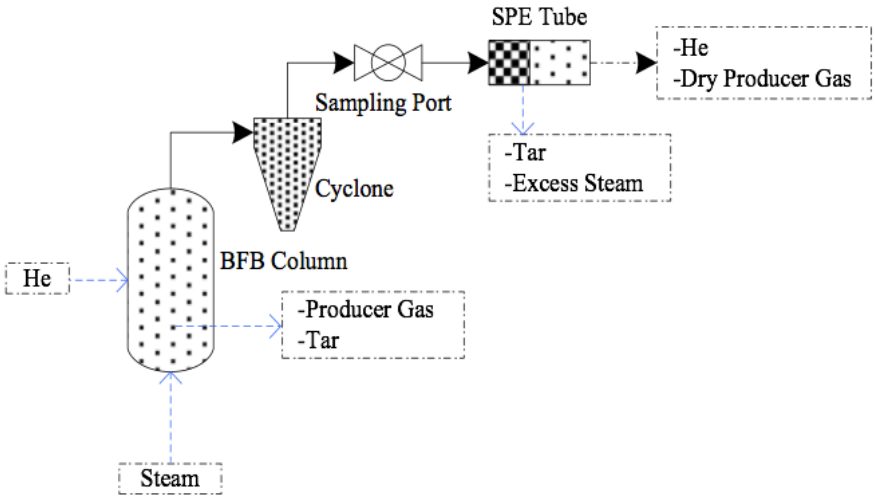

Figure 4.5. Schematic diagram of the helium flow in the system.

Mass balance for the tracer gas, He:

$$\dot{V}_{He,in} = \dot{V}_{He,out} \tag{4.21}$$

$$\dot{V}_{He,\,in} = x_{He,out} \cdot (\dot{V}_{He,out} + \dot{V}_{dry\text{-}pg}) \tag{4.22}$$

$$\dot{V}_{dry\text{-}pg} = \frac{\dot{V}_{He,in}}{x_{He,out}} - \dot{V}_{He,out} \tag{4.23}$$

where $\dot{v}_{He,in}$ is volumetric flux or flow rate of He entering the BFB column (L min^{-1}), $\dot{v}_{He,out}$ is volumetric flux rate of He exiting the BFB column (L min^{-1}), x_{He} is concentration of He flowing out of the BFB column (mol.%) and $\dot{v}_{dry\text{-}pg}$ is volumetric flux rate of dry producer gas (L min^{-1}). Since He enters and exits the BFB gasification column at the same flow rate, the following formula can be derived from equation (4.22) as follows,

$$\dot{v}_{dry\text{-}pg} = \dot{v}_{He} \left(\frac{1}{x_{He}} - 1\right) \quad (4.24)$$

For the above equation, the following assumptions were applied:

- Ideal Gas Law applies, meaning that mol.% = vol.%. It means that at 25^{o}C and 1 atm, 1 mole of ideal gas is equal to 0.02446 m^3 or approximately 24.46 L.
- All samples of producer gas analysed in this experiment are tar and moisture free.
- All of the samples is cooled down to the room temperature (25^{o}C) prior to being injected into the micro GC.
- The ambient temperature in the gasifier room is constant at 25^{o}C.

At 0^{o}C (273.15 K) and 1 atm (101,325 Pa), the unit of producer gas flow rate is changed into $Nm^3\ h^{-1}$, following the calculation procedure provided in Appendix E.1.

4.4.2. The calculation of producer gas lower heating value

The heating value of producer gas was determined based on the dry gas composition. It was referred to LHV which is defined as the heat released from combustion while the product water exists in state of vapour thus its latent heat of water vaporation is not taken into account. The calculation of LHV was based on the following equation (Manatura et al. (2017) and Bull (2008)).

$$LHV_{dry\text{-}pg} = \sum (y_i \,.\, LHV_i) \quad (4.25)$$

In the equation above, *y* represents mole fraction of each combustible gas component (*i*) including H_2, CH_4, CO, C_2H_4 and C_2H_6. The LHV values of these gaseous components are summarized in Table 4.3.

Table 4.3. LHV of each combustible gas component (Bull 2008).

Gas component	LHV (MJ Nm^{-3})
H_2	9.9
CH_4	32.8
CO	11.6
C_2H_4	49.8
C_2H_6	58.4

4.4.3. The calculation of carbon conversion

According to Kern et al. (2013), carbon conversion is the ratio of carbon leaving the gasification reactor in the form of gaseous products in the producer gas to the amount of carbon introduced by the feedstock entering the gasification reactor.

$$x_C\ (\%) = \frac{\dot{m}_{C,pg}}{y_{C,f}\ .\ \dot{m}_{f,od}} \tag{4.26}$$

$$\dot{m}_{C,pg} = \sum (y_{Ci,pg}\ .\ \dot{v}_{dry\text{-}pg}) \tag{4.27}$$

$$\dot{m}_{C,pg} = (y_{C,CH4} + y_{C,CO} + y_{C,CO2} + y_{C,C2H4} + y_{C,C2H6})\ .\ \dot{v}_{dry\text{-}pg} \tag{4.28}$$

$$y_{Ci,pg} = y_{i,pg}\ .\ \frac{A_{r,C}}{M_{r,Ci}} \tag{4.29}$$

where x_C is carbon conversion (%), $\dot{m}_{C,pg}$ the mass flow rate of carbon leaving the reactor (kg h^{-1}), $y_{C,f}$ mole fraction of carbon-containing molecules in oven-dry feedstock (%), $\dot{m}_{f,od}$ is mass feed rate of oven-dry biomass (RHP) (kg_{od} h^{-1}), $y_{Ci,pg}$ is mole fraction of carbon-containing molecules in producer gas mixture (%), $M_{r,Ci}$ is relative molecular mass of carbon-containing molecules including CH_4, CO, CO_2, C_2H_4 and C_2H_6 (dimensionless), $A_{r,C}$ is

atomic weight of carbon (dimensionless, A_r carbon = 12) and $\dot{v}_{dry\text{-}pg}$ is volumetric flux rate of dry producer gas (mol h^{-1} or $Nm^3\ h^{-1}$).

4.4.4. The calculation of cold gas efficiency

The cold efficiency (η_c) is defined as the chemical energy from the combustion of syngas produced divided by the input energy, including biomass feedstock (rice husk pellets), LPG, and power usage for steam generation, which is determined based on the equations adopted from Bull (2008) and Knoef (2005) as follows

$$\eta_c = \frac{q_{dry\text{-}pg}}{q_{LPG} + q_b + q_s} \tag{4.30}$$

$$q_{dry\text{-}pg} = \dot{v}_{dry\text{-}pg} \,.\, LHV_{dry\text{-}pg} \,.\, m_{f,od} \tag{4.31}$$

$$q_{LPG} = \dot{v}_{LPG} \,.\, \Delta H_{LPG} \tag{4.32}$$

$$q_b = LHV_{RHP} \,.\, \dot{m}_{f,od} \tag{4.33}$$

$$q_s = \Delta H_s \,.\, \dot{m}_s \tag{4.34}$$

where $q_{dry\text{-}pg}$ is chemical energy of producer gas combustion (kW), q_{LPG} is chemical energy of supplementary LPG in combustion column (kW), q_b is chemical energy of RHP in BFB gasification column (kW) and q_s is energy consumed for steam generation. $LHV_{dry\text{-}pg}$ represents chemical energy of producer gas combustion. While v_{LPG} refers to volumetric flux rate of LPG injected into the CFB combustion column (L min^{-1}), $\dot{m}_s$ is total mass flux rate of steam in the BFB column, chute and syphon ($kg.h^{-1}$). ΔH_{LPG} and ΔH_s respectively define heating value of LPG (~87.50 $MJ.m^{-3}$) and total heat energy for steam generation (J).

4.4.5. The calculation of tar concentration

In this study, two different methods of tar analysis were applied to determined tar concentration in the producer gas, one termed as Light Tar Method (LTM) and the other Heavy Tar Method (HTM). LTM was the set-up of GC column with split ratio designed to specifically measure concentrations of the light tar compounds with lower molecular weights, whereas the HTM was designed to estimate the amount of tar contents of heavy molecules. These methods had the same column temperature settings, but the split ratios of these methods were different. Details of these two methods are described in Appendix J.

The concentration of each tar component was determined by comparing the signal count ratio from the GC analysis to those from individual tar standard calibration. For the tar calibration, five different concentrations were prepared and analysed, and each concentration was measured three times. The tar classification in the current study was adopted from the study of Kiel et al. (2004). Detailed procedures for tar extraction and the example of quantitative analyses were provided in Appendix J. In determination of tar content by using the method described above, the following assumptions were applied:

- The effect of mass or volume of the tar compounds in the sample solution is negligible due to their small concentration.
- The density of tar sample is then assumed to be the same as those of the solvents used for the tar extraction.
- The small fraction of unreacted steam that may contaminate the tar sample solution is ignored.
- The LTM is used to specifically measure the light tar compounds focusing on benzene, toluene, pyridine, p-xylene + ethylbenzene, m-xylene, o-xylene and styrene.

- The LTM is used to specifically measure the heavy tar compounds focusing on bens(a)anthracene, chrysene, benso(b)fluoranthene, benso(k)fluoranthene, benso(a)pyrene, indeno(1,2,3-cd)pyrene, benso(g,h,i)perylene and dibenso(a,h)anthracene.
- For other tar compounds, the concentration measured is determined from the average value of tar concentration calculated from LTM and HTM.

Therefore, tar concentration from DCM extraction (T_{D0}) and DCM-IPA extraction (T_{D1}), total mass of tar (T_{TM}) and yield (T_{TY}) from the tar sample mixture can be calculated using the following formulae

$$T_{D0} = \frac{\text{Tar concentration in ppm (mg L}^{-1}\text{) x mass of tar sample solution (g)}}{\rho_{DCM}\ (\text{g ml}^{-1})} \text{ x } \frac{1000\ \mu g}{1\ mg} \text{ x } \frac{1\ L}{1000\ ml} = \ldots \mu g \quad (4.35)$$

$$T_{D1} = \frac{\text{Tar concentration in ppm (mg.L}^{-1}\text{) . mass of tar sample solution (g)}}{\rho_{DCM+IPA}\ (\text{g ml}^{-1})} \text{ x } \frac{1000\ \mu g}{1\ mg} \text{ x } \frac{1\ L}{1000\ ml} = \cdots \mu g \quad (4.36)$$

$$T_{TM} = T_{D0} + T_{D1} = \ldots \mu g \quad (4.37)$$

Furthermore, the total tar concentration in the producer gas (T_{TCP}) and total tar yield (T_{TY}) are calculated as follows

$$T_{TCP} = \frac{T_{TM}\ (\mu g)}{V_{dry\text{-}pg}\ (ml)} = \ldots \mu g\ ml^{-1} \quad (4.38)$$

At 1 atm and 0^{o}C,

$$T_{TCP} = \frac{T_{TCP} \text{ x } 273.15}{\dot{v}_{dry\text{-}pg} \text{ x } 303.15} \text{x } \frac{10^{6}\ ml}{m^{3}} \text{ x } \frac{10^{-6}\ g}{\mu g} = \ldots g\ Nm^{-3} \quad (4.39)$$

$$T_{TY} = \dot{v}_{dry\text{-}pg}\ (Nm^{3}\ kg^{-1}{}_{od}) \text{ x } T_{TCP}\ (g\ Nm^{-3}) = \ldots g\ kg^{-1}{}_{od} \quad (4.40)$$

4.5. Operation parameters investigated

4.5.1. Parameter 1: Gasification temperature

Gasification temperature (T_g) was an important operation parameter investigated in this study to determine its impact on the composition and yield of producer gas. In the gasification experiments, four temperatures, ranging from 650 to 800^{o}C with 50°C increments, were used.

In the experiments for investigation of gasification temperature effect, the wet feed rate of the biomass, RHP, was controlled at 19.1 kg h^{-1}, while the total steam injection rate 10.50 kg h^{-1}. The moisture content of the wet RHP was contact at 8.85%, therefore, the oven-dry feed rate of RHP was 17.5 kg h^{-1}. As the fluidized solid particles, 30 kg of fresh silica sand was added into the gasifier. The specific experimental conditions for parameter 1 were summarised in Table 4.4.

Table 4.4. Experimental conditions for investigation of temperature effect.

Parameter	**Unit**	**Condition**			
		Run 1.1	**Run 1.2**	**Run 1.3**	**Run 1.4**
Steam to biomass ratio, $Ø_{SB}$	wt./wt.	0.7	0.7	0.7	0.7
Oven-dry biomass feed rate, $\dot{m}_{f,\,od}$	kg h^{-1}	17.5	17.5	17.5	17.5
Gasification temperature, T_g	^oC	650	700	750	800
Total steam injection rate, $\dot{m}_s$	kg h^{-1}	10.50	10.50	10.50	10.50
Inventory of bed material (Silica sand)	kg	30	30	30	30

4.5.2. Parameter 2: S/B ratio

In steam biomass gasification, steam to biomass ratio is another important operation parameter which also affects the gasification performance. This part of experiments was performed at the optimum temperature from the results in part 1 as described above, in which the producer gas yield was high and had high hydrogen concentration and thus greater calorific value. This part of study aimed to examine how $Ø_{SB}$, varied from 0.7 to 1.3 (wt./wt.), affect the quality of the gasification products (producer gas and tar) and yield. The steam to biomass ratio can be varied either by changing the biomass feed rate while keeping the steam injection rate constant or by changing the steam injection rate while keeping the biomass feed rate constant. Therefore, in one series of runs, the wet biomass feed rate was decreased from 17.5 to

10.7 kg h^{-1} while the steam flow rate was constant at 10.5 kg h^{-1}. The details of this series of runs are given in Table 4.5.

In second series of runs, the dry biomass feed rate was set at a constant value of 14.5 kg_{od} h^{-1}, while the total steam flow rate was increased from 9.2 to 18.4 kg h^{-1}, as is presented in Table 4.6. In both series of runs, the gasification temperature and the bed materials were the same. Fresh silica sand at inventory of 30 kg was used as the bed material in both series of the experimental runs.

Table 4.5. Experimental conditions for investigation of steam to biomass ratio - constant steam feed rate.

Parameter	**Unit**	**Condition**				
		2. 1	**2.2**	**2.3**	**2.4**	**2.5**
$Ø_{SB}$	wt./wt.	0.7	0.8	0.9	1.0	1.1
$\dot{m}_{f,\,od}$	kg h^{-1}	17.5	14.9	13.1	11.6	10.7
T_g	^oC	750	750	750	750	750
$\dot{m}_s$	kg h^{-1}	10.5	10.5	10.5	10.5	10.5
Inventory of bed material (Silica sand)	kg	30	30	30	30	30

Table 4.6. Experimental conditions for investigation of steam to biomass ratio - constant biomass feed rate.

Parameter	**Unit**	**Condition**		
		2.6	**2.7**	**2.8**
$Ø_{SB}$	wt./wt.	0.7	1.0	1.3
$\dot{m}_{f,\,od}$	kg h^{-1}	14.5	14.5	14.5
$\dot{m}_s$	kg h^{-1}	9.2	13.8	18.4

4.5.3. Parameter 3: The variation of bed material

A further study was conducted to analyse the catalytic effect of olivine sand with a particle size of 256 μm for the enhancement of the gasification products. The experiment was performed at optimum conditions based on the experimental results from the above two parts of experimental studies, with 30 kg of olivine sand being used as the bed material.

Table 4.7. Impact of catalytic bed material: experimental conditions.

Parameter	Unit	Condition
$Ø_{SB}$	wt./wt.	0.7
$\dot{m}_{f,dry}$	kg h^{-1}	17.5
T_g	^oC	750
$\dot{m}_s$	kg h^{-1}	10.5

5. Result and Discussion

5.1. Producer gas properties

The measurement results of dry producer gas formation under the investigated parameters discussed in Section 4.5 are presented and discussed in this chapter. In general, the main producer gas compounds (He-free) of H_2, CO, CH_4 and CO_2 accounted for 91-93%, with contents of individual gaseous species being 14-28% for H_2, 31-38% for CO, 11-12% for CH_4 and 19-25% for CO_2. The remaining gas components were comprised of N_2 (2-4%), C_2H_4 (2-4%) and C_2H_6 (0.5-1%), termed as minor gas components. Furthermore, the gas yield and LHV range, respectively, between 0.44 and 0.66 Nm^{-3} kg_{od}, and from 12.12 to 13.08 MJ Nm^{-3}.

5.1.1. Effect of gasification temperature

To examine the effect of gasification temperature on producer gas composition and lower heating (LHV), the gasification temperature was increased from 650 to 800^oC at a constant S/B ratio of 0.7. Producer gas with significant variations in gas composition can be observed from Figure 5.1. It was found that the H_2 concentration increased with gasification temperature at the expense of CO, CO_2 and CH_4, all of which were measured in He-free basis. With the gasification temperature increasing from 650 to 800°C, the H_2 content increased from 14.75 to 28.66%, while those of CO and CO_2 dropped from 38.47% to 32.42% and from 25.87% to 19.60%, respectively. Meanwhile, the concentration of CH_4 was observed with a slight decrease of 0.08%, going down from 12.33% at 650^oC to 12.28% at 800^oC.

Stelt et al. (2011) has reported that higher temperature favours forward direction for the products in endothermic reactions but favours the reverse direction for the reactants in exothermic reactions. The increasing concentration of H_2 resulted from the steam addition with which some reactions are associated, such as steam-char reaction and water-gas shift reaction.

The steam-char generates more CO which further enhances the water-gas shift reaction rate, which leads to the formation of CO_2 and this subsequently promotes Boudouard reaction. As a result more CO is released and is transformed into H_2 through the water-gas shift reaction. These reactions are subsequently enhanced by the increase of gasification temperature which is favourable for the enhancement of H_2 concentration.

The decrease of the CH_4 concentration could be explained by considering both exothermic and endothermic reduction reactions, depending on the temperature level. At low temperature, the exothermic hydro-reaction tends to be more active in respect to the chemical equilibrium (Zhang and Pang 2017), hence, more CH_4 was produced. However, endothermic reactions including steam-methane reforming and dry reforming were more dominant when the gasification temperature was increased up to 800^{o}C, causing more consumption of CH_4 in the thermal reduction.

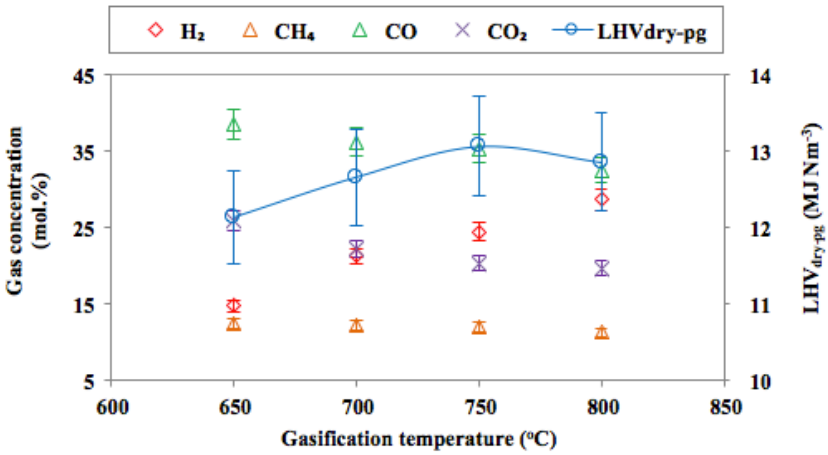

Figure 5.1. The variation of producer gas concentration and LHV with the increase in gasification temperature.

The heating value is an important aspect of producer gas which needs to be considered for its application as a gaseous fuel (Atnaw et al. 2013). Highlighted in Figure 5.1 is the variation of the dry producer gas LHV ($LHV_{dry\text{-}pg}$) as a function of gasification temperature for

the range of 650-800^{o}C. At the lowest temperature, the gas LHV was 12.12 MJ Nm^{-3} and it reached the optimum value of 13.06 MJ Nm^{-3} at 750^{o}C. This may be attributed to the concentration increase of H_2 and C_2H_4 as a minor compound in the gas mixture. However, the gas LHV was found to be 12.85 MJ Nm^{-3} when the gasification temperature was further increased to 800^{o}C. This indicated that to an extent the increase of gasification temperature is not favourable to the producer gas LHV.

The increase of gasification temperature was found to be desirable for the increase of producer gas yield, expressed in the volumetric flux rate of dry producer gas ($\dot{v}_{dry\text{-}pg}$) with a unit of Nm^3 kg$^{-1}_{od}$. The similar increasing trend was also found for the carbon conversion (x_C). As can be seen in Figure 5.2, the gas yield increased considerably from 0.50 to 0.61 Nm^3 kg$_{od}^{-1}$ and this could be attributed to the higher carbon conversion (x_C) achieved with the increasing temperature, at which the carbon conversion increased from 42.45 to 46.15%.

The experimental data presented in Figure 5.1 and Figure 5.2 shows convincing evidence of substantial improvement of both the gas yield and LHV with increase of gasification temperature. Although, the steam gasification process at a higher temperature was likely to increase the gas yield, the thermal conversion above 750^{o}C tended to lower the gas LHV and this is undesirable for the application of producer gas as the gaseous fuel. Therefore, the optimum temperature of gasification was considered to be at 750^{o}C.

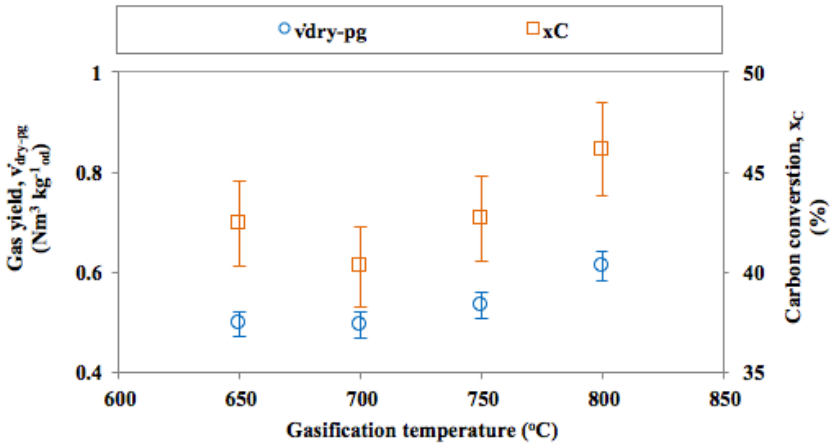

Figure 5.2. The variation of producer gas yield and carbon conversion with the increase in gasification temperature.

5.1.2. Effect of S/B ratio

5.1.2.1. Investigation on a constant steam flux rate

Figure 5.3 plots the producer gas composition and LHV as a function of S/B ratio ($Ø_{SB}$), in which the gasification temperature and steam flow rate were kept constant at 750°C and 10.5 kg h^{-1}, respectively. The $Ø_{SB}$ was increased from 0.7 to 1.1 by decreasing the oven-dry (od) biomass feed rate from 17.42 to 10.72 kg h^{-1}_{od}. Under these operation conditions, slight fluctuation in the gas composition was observed.

The concentration of H_2 experienced a slight rise over the given range of $Ø_{SB}$ (0.7 - 1.1), changing from 24.44 to 26.20%. Meanwhile, the CH_4 and CO concentrations were each reduced as the $Ø_{SB}$ was increased, giving 11.59% of CH_4 and 31.92% of CO in the producer gas mixture at $Ø_{SB}$ 1.1, in comparison with their corresponding values at $Ø_{SB}$ 0.7 (11.92% and 35.34%, respectively). The concentration of CO_2 was 20.27% at the initial $Ø_{SB}$ (0.7) and increased to 21.53% at the higher $Ø_{SB}$ (1.1). In the range of $Ø_{SB}$ 0.7- 1.1, the average individual concentrations of the main gas components were found approximately to be 25.51% for H_2,

11.88% for CH_4, 33.43% for CO and 21.10% for CO_2. The remaining 8.08% of gas was made up of N_2, C_2H_4 and C_2H_6.

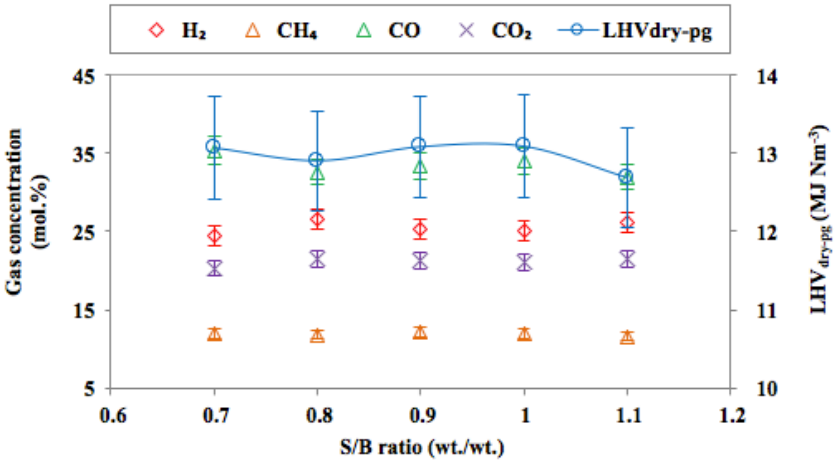

Figure 5.3. The variation of producer gas concentration and LHV with increase in S/B ratio holding steam flux rate constant.

As far as the gas heating value is concerned, no obvious trend was observed in examining the impact of the increased $Ø_{SB}$ on the gas LHV. It was found that the gas LHV was nearly constant at approximately 13 MJ Nm^{-3} over the $Ø_{SB}$ range tested from 0.7 to 1.0, decreasing slightly to 12.68 MJ Nm^{-3} at $Ø_{SB}$ 1.1. The nearly constant gas LHV is likely due to the stable proportion of the major combustible gas components including H_2, CH_4 and CO. At $Ø_{SB}$ 1.1, the concentration of H_2 was increased slightly at the expense of CO and the other minor gas compounds, in which the concentration of C_2H_4 and C_2H_6 dropped from 4.41 to 4.37% and from 0.75 to 0.69%, respectively, which was found to be the main cause of the LHV decrease.

Under the given range of $Ø_{SB}$, a similar trend was found for the gas yield and carbon conversion, in which gas yield fluctuated between 0.52 and 0.57 $Nm^3\ kg^{-1}_{od}$ over the range of $Ø_{SB}$, as can be seen in Figure 5.4. At the lowest $Ø_{SB}$ (1.1), the gas yield was 0.54 $Nm^3\ kg^{-1}_{od}$ and this decreased by 0.1 $Nm^{-3}\ kg^{-1}_{od}$ at $Ø_{SB}$ of 0.8. However, as the biomass feed rate was

further decreased, the gas yield peaked at 0.57 $Nm^3\ kg^{-1}_{od}$ at $Ø_{SB}$ of 1.0, before decreasing back to 0.52 $Nm^3\ kg^{-1}_{od}$ at the highest $Ø_{SB}$ (1.1).

It was expected that the raise of S/B ratio would result in more producer gas yield due to the enhanced carbon conversion through the water-gas shift and steam reforming reactions. However, no obvious trend can be observed from the fluctuated data of the gas yield and carbon conversion. The experimental results in Figure 5.4 show that the increase of $Ø_{SB}$ while maintaining the steam flow rate at 10.5 kg h^{-1} had promoted a slight impact on the gas yield and carbon conversion. The discovery of this evidence has good agreement with a study carried out by Saw and Pang (2012).

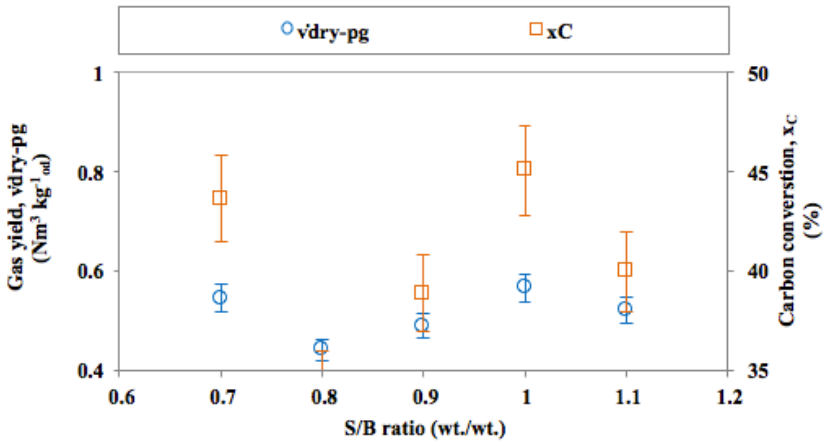

Figure 5.4. The variation of producer gas yield and carbon conversion with increase in S/B ratio holding steam flux rate constant.

However, since $Ø_{SB}$ is relative to both biomass feed rate or steam feed rate involved in the gasification process, two possible ways in determining the value of $Ø_{SB}$ should be compared in order to find a strong correlation between the variation of $Ø_{SB}$ and the measured parameters. Therefore, it was decided to conduct another set of experiment under a constant biomass feed rate as discussed in the succeeding section.

5.1.2.2. Investigation on effect of S/B ratio at a constant biomass feed rate

To further measure the consistency of $Ø_{SB}$ influence, another set of experimental study was performed with a constant biomass (RHP) feed rate of 14.5 $_{od}$ kg h^{-1}. The total amount of steam flux rate injected into the BFB column was increased from 9.2 to 18.4 kg h^{-1}, giving a variation to the $Ø_{SB}$ from 0.7 and 1.3. Under this operation condition, more regular changing trend in the gas composition and yield can be observed as provided in Figure 5.5.

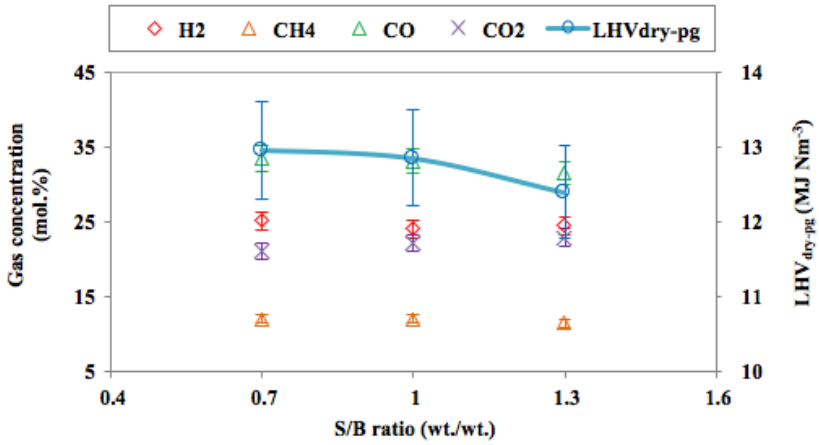

Figure 5.5. The variation of producer gas concentration and LHV with increase in S/B ratio holding biomass feed rate constant.

Amongst the main producer gas compounds, CO_2 was the only gas species gaining a bigger proportion at higher $Ø_{SB}$ with the gas species having a concentration rise from 21.03% at the lowest $Ø_{SB}$ (0.7) to 22.87% at the highest $Ø_{SB}$ (1.3). In the meantime, slight decrease occurred to H_2, CO and CH_4 at the same range of $Ø_{SB}$. H_2 showed 2% drop in concentration (from 33.46 to 31.46%), while the concentration drops occurred, respectively, to CO (from 20.10 to 24.49%) and CH_4 (from 12.01 to 11.45%).

A minor decrease in the gas LHV was observed over the tested range of $Ø_{SB}$, from 12.95 to 12.40 MJ Nm^{-3}. This downward trend could be attributed to the concentration increase of non-combustible gas compound (CO_2) and the concentration decrease of combustible gas

elements (H_2, CO and CH_4) as can be seen in Figure 5.5. Thus, the increase of $Ø_{SB}$ in this study was not favourable for the improvement of the producer gas LHV.

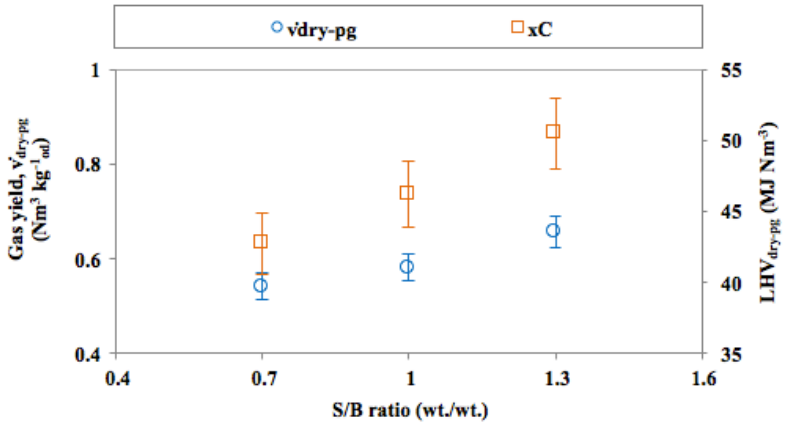

Figure 5.6. The variation of producer gas yield and carbon conversion with increase in S/B ratio holding biomass feed rate constant.

As expected the increase of $Ø_{SB}$, meaning that more steam was fed into the gasification reactor, showed a positive influence on the yield and concentration of the dry gas product at higher $Ø_{SB}$. As provided in Figure 5.6, the gas yield was 0.54 Nm^3 kg^{-1}_{od} at $Ø_{SB}$ of 0.7, and this value increased by 22% to 0.66 Nm^3 kg^{-1}_{od} at $Ø_{SB}$ of 1.3. The upward trend was followed by the carbon conversion, rising from 42.75 to 50.48% in the given range of $Ø_{SB}$. The increase of the producer gas yield could be linked to the increase of the carbon conversion due to the enhanced activity of water-gas reaction at the higher amount of steam fed in the gasification reactor, in which H_2 and CO_2 is formed by the transformation of CO with H_2O.

Based on the experimental results discussed in Section 5.1.2, it can be concluded that the variation of $Ø_{SB}$ by varying either steam or biomass feed rate, while keeping one of these constant resulted in slight variation of producer gas composition, yield and LHV. Although the steam involvement in biomass gasification leads to the enrichment of H_2 composition, the increase of S/B ratio above 0.7 in this study was found disadvantageous to the gas LHV.

The optimum S/B ratio is determined by assessing the cold gas efficiency of BFB gasification column for each of the investigated S/B ratio whose calculation details are provided in Appendix E.4. Although the total energy input from the biomass (RHP) feeding decreased from 17.42 to 10.72 $kg_{od}\ h^{-1}$, leading to a 29% decrease (from 87.57 kW at S/B ratio of 0.7 to 62.52 kW at S/B of 1.1), the energy output reduced more significantly by 43% (from 34.43 to 19.67 kW) over the range of the investigated S/B ratio. This resulted in the highest cold gas efficiency of 39.32% for the S/B ratio of 0.7. Whereas, the lowest efficiency was observed at S/B ratio of 0.8 (30.11%). Therefore, 0.7 was be considered to be the optimum S/B ratio.

5.1.3. Effect of catalytic bed material

An experiment of olivine-fluidized steam gasification has been done at the optimum operation conditions to investigate the effect of catalytic bed material (olivine) on producer gas composition and yield. The gasification temperature was held at 750°C and the $Ø_{SB}$ was operated at 0.7. To measure the catalytic effect of the olivine sand, the experimental results obtained from the gasification with olivine were compared with those generated from the gasification with silica, as can be seen in Figure 5.7.

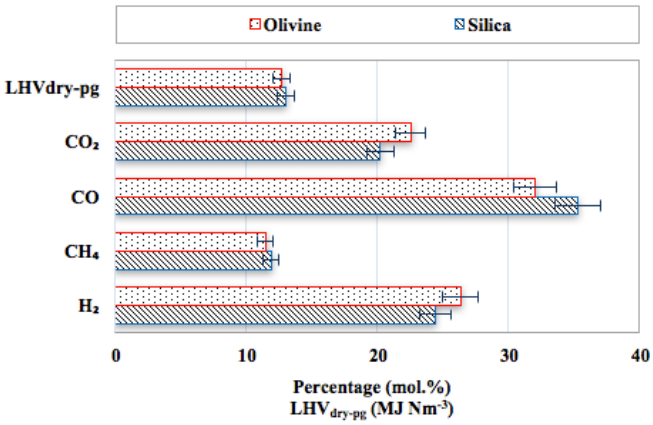

Figure 5.7. The influence of catalytic bed material on the gas concentration.

In general, more H_2 and CO_2 but less CO and CH_4 were produced with the olivine sand than the silica sand. The H_2 content increased from 24.44% (silica) to 26.36% (olivine), whereas the concentration increase for CO_2 was from 20.27% to 22.57%, respectively. Meanwhile, over 3% decrease of concentration was experienced by CO, in which 32.08% of CO was generated with olivine, while the corresponding values for methane, CH_4, was 11.50%, slightly decreasing from 11.92% when the active olivine was used replacing silica.

In this study, the further enhancement of H_2 and CO_2 at the expense of CO and CH_4 indicated a positive response of catalytic bed material through the activity of exothermic water-gas shift reaction. This trend has a strong agreement with a study performed by Li et al. (2010). Due to the concentration change in the major gas compounds (H_2, CO, CO_2 and CH_4), however, the olivine usage resulted in the lower producer gas LHV (12.72 MJ Nm^{-3}), compared to that obtained with the use of silica sand (13.06 MJ Nm^{-3}).

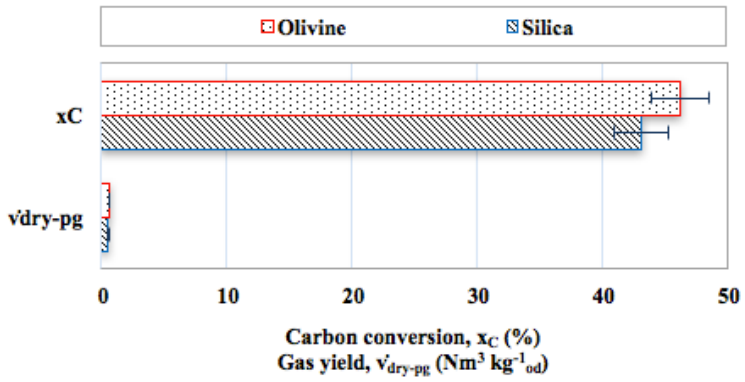

Figure 5.8.The variation of producer gas LHV and carbon conversion with the increase of S/B ratio under the optimum operation conditions.

Figure 5.8 provides a comparison of producer gas yield and carbon conversion obtained from the steam biomass gasification with two different types of bed material at the optimum conditions mentioned in Section 5.1.4. As can be seen in Figure 5.8, it was observed that olivine sand promoted higher gas yield (0.6 Nm^3 kg^{-1}_{od}) than silica sand (0.54 Nm^3 kg^{-1}_{od}). This

indicates that olivine sand is more favourable for the biomass-to-gas conversion, with which 46.20% of carbon conversion was achieved, over 3% higher than that of silica sand.

5.2. Tar formation

It has been identified that the thermal process of biomass gasification not only generates producer gas as the primary product, but also tar as the secondary product although in most cases it is undesirable. Tar is a complex mixture of condensable gas products that are not desirable in gasification since a high concentration of tar in the product can lead to serious issues for use in downstream applications. Belgiorno et al. (2003) defines tar as bituminous oil constituted of a complex mixture of oxygenated hydrocarbons existing in vapour phase in the producer gas at high temperatures, however, the tar contains numerous compounds which are difficult to remove by simple condensation and could cause problems such as filters and valves clogging, as well as metallic corrosion. Therefore, tar removal becomes highly necessary and this can be done through several measures such as dry or wet gas cleaning (mechanical or physical method), catalytic tar decomposition and thermal tar cracking (Anis and Zainal 2011).

In this study, a series of experiments were undertaken to investigate the effect of operation parameters of the gasification process on the GC-detectable tar concentration and yield. This includes gasification temperature and S/B ratio. The evolution of tar yield and concentration were also tested on the effect of using the catalytic bed material olivine sand at the optimum temperature and S/B ratio. It is important to keep in mind that the amount of total tar measured in this research work is only part of those existing in the system as it does not include the unidentified heavy or very light tars since they are undetectable by the method of SPA analysis. The results are presented following tar classification proposed by Kiel et al. (2004) where, for example, benzene is considered as a tar compound and included in the graphs.

5.2.1. Effect of gasification temperature

Figure 5.9 presents the change in the tar yield and concentration with the increase of gasification temperature. While the tar yield had an increasing trend, it was observed that the tar concentration decreased significantly when the gasification temperature was increased from 650 to 800°C. At the initial tested temperature (650°C), the amount of tar was 5.39 g per kg of oven-dry (od) biomass (RHP) and this value decreased to 4.61 g kg^{-1}_{od} as the gasification temperature was increased to 800°C. Meanwhile, the tar concentration in the producer gas decreased considerably from 10.85 to 7.53 g Nm^{-3} over the range of operation temperature. The examined results for the tar yield and concentration are comparable with studies performed by Zhang and Pang (2017). They observed that the tar yield decreased at higher temperature as the result of tar conversion producing more gaseous product. Another study performed by Zanzi et al. (1996) revealed the same result, in which higher gasification temperature has brought about lower tar yield and higher amount of gaseous product.

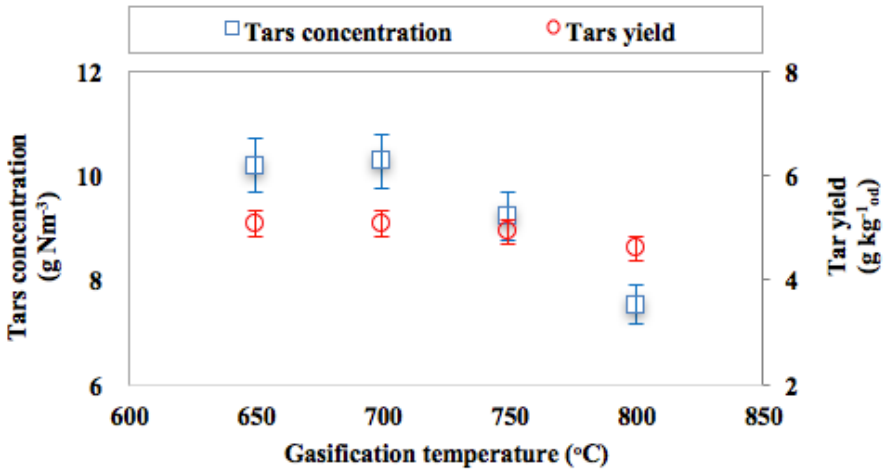

Figure 5.9. Impact of gasification temperature on the tar yield and concentration.

As can be seen in Figure 5.10, the detailed examination on the individual tar classes shows that the change of tar concentration mainly happened to class 2, class 3 and class 4 tars, while that of class 5 tars was unlikely to transform at the given temperature range 650-800°C.

At 650°C the concentration of class 2 tars was 6.63 g Nm^{-3}. However, when the gasification temperature was increased to 800°C, the tar content decreased by 3.60 g Nm^{-3} to reach 3.02 g Nm^{-3}. On the other hand, the corresponding values for the class 3 tars increased from 2.92 to 3.49 g Nm^{-3} with the temperature rise.

The class 2 tars contain heteroatoms, which are highly water soluble compounds (Devi et al. 2005) whose cracking activities are enhanced by the increase of reaction temperature (Morf et al. 2002). Furthermore, the tar decomposition can be associated with the breaking of chemical bonds generating two radicals, which can react with other tar components forming a new tar compound in addition to a radical, or a larger radical (Vreugdenhil and Zwart 2009). Consequently, the heterocyclic tar class is significantly decomposed with increase of gasification temperature. Furthermore, the increase of class 3 tars can be attributed to the cracking activity of class 4 and class 5 tars whose tar contents decreased from 1.07 to 0.85 g Nm^{-3} and from 0.23 to 0.16 g Nm^{-3}, respectively, with the temperature increase.

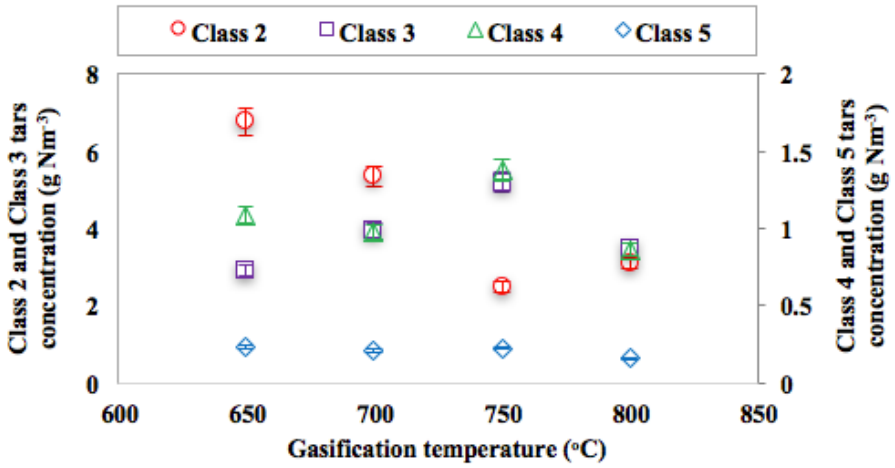

Figure 5.10. Impact of gasification temperature on the concentration of individual tar classification.

To gain a better understanding of the mechanism of tar formation and decomposition, a detailed examination of individual tar compounds is presented in Figure 5.11. At low

temperature (650°C), phenol was the major compound of class 2 tars with a concentration of 4.44 g Nm^{-3}. It began to decompose at higher temperatures becoming 1.92 g Nm^{-3} at 800°C, as can be seen in Figure 5.11 (A). El-Rub et al. (2004) reported that the thermal conversion of phenol takes place between 700 and 900°C. Between 650 and 700°C, the phenol concentration in the present study was stable at around 3.95 - 4.44 g Nm^{-3}, but started to lose its stability at higher temperature. Therefore, the compound of heterocyclic was significantly reduced with the rise of reaction temperature.

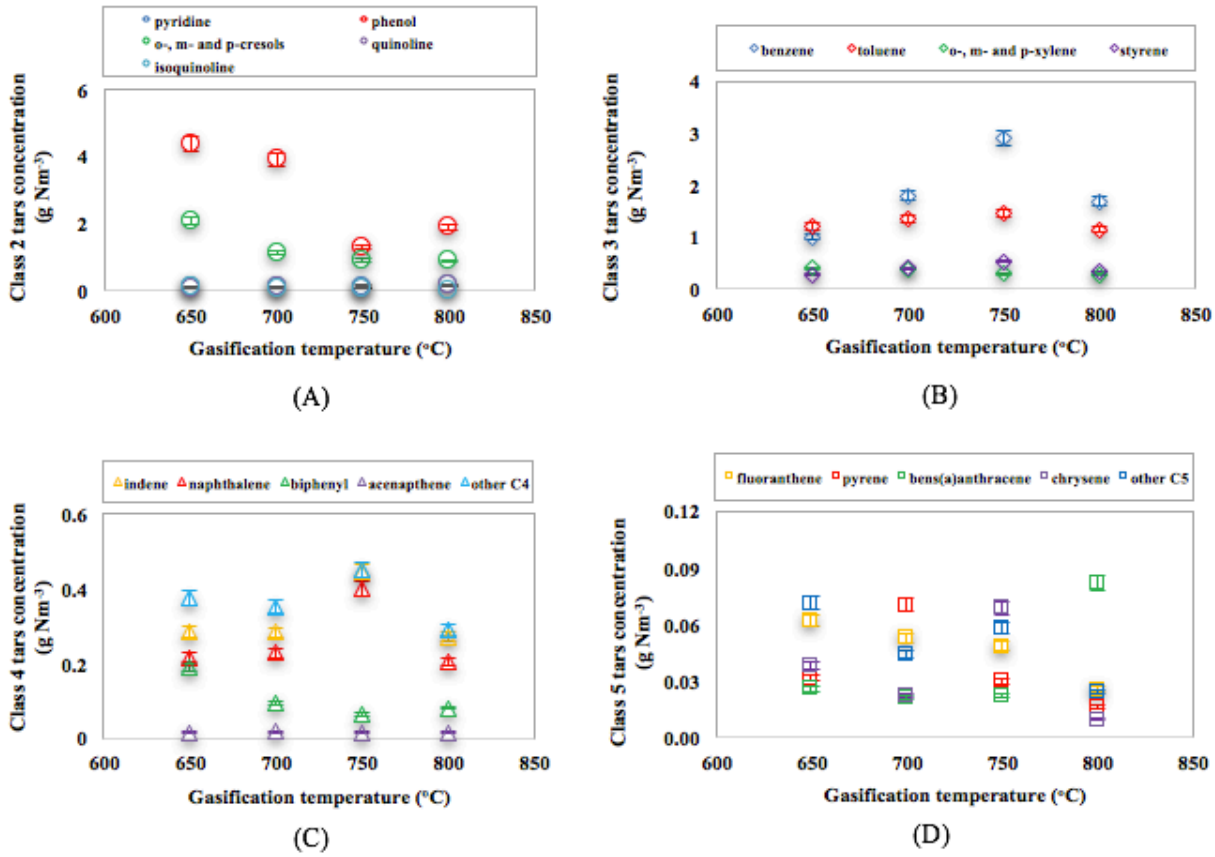

Figure 5.11. Impact of gasification temperature on the concentration of individual tar compounds in class 2 tars (A); class 3 tars (B); class 4 tars (C); and class 5 tars (D).

Meanwhile, the other compounds of class 2 tars were found to be more stable with the temperature change. The cresols group collectively had a concentration decrease from 1.92 to 0.79 g Nm^{-3}, while that of quinoline increased slightly from 0.08 to 0.14 g Nm^{-3}. Isoquinoline

was the other less reactive compound in class 2 tars with the concentration reducing from 0.10 to 0.02 g Nm^{-3}. Similar to quinoline, pyridine was a compound of class 2 tars with content increasing considerably from 0.1 to 0.15 g Nm^{-3}. Based on this strong quantitative evidence, phenol is believed to be the key determining compound in the group of class 2 tars.

For the class 3 tars, higher temperature appeared to be favourable for the formation of benzene with a maximum concentration at 750^{o}C (2.89 g Nm^{-3}) as depicted in Figure 5.11 (B). Toluene and xylenes followed the similar trend. The concentration of these components was found to reduce at higher temperature from 1.22 to 1.16 g Nm^{-3} for the former and from 0.28 to 0.34 g Nm^{-3} for the latter. Anis and Zainal (2011) reported that benzene and toluene are the most difficult tar components to be destroyed. To achieve a complete removal of those components, they investigated that the gasification temperature should be set very high above 1200^{o}C, in which all types gasification medium reveal less impact on the tar cracking reaction. As a result, the tested range of gasification temperature in the current study brought about only very little change in the reduction of class 3 tars. Styrene, a compound of the class 3 tars, was at a low concentration of 0.28 g Nm^{-3} at 650^{o}C, which increased to 0.34 g Nm^{-3} at 800^{o}C. According to the investigated data trend in Figure 5.11 (B), the increase of reaction temperature is believed to have less cracking activity to reduce the amount of styrene.

A decreasing overall concentration was found in both class 4 (Figure 5.11 (C)) and class 5 (Figure 5.11 (D)) tars. The formations of indene and naphthalene were observed to be favoured with the increase in reaction temperature between 650 and 750^{o}C, but their concentration was reduced as the temperature was further increased to 800^{o}C. This trend was followed by other compounds of class 4 tars (C4). Acenapthene was observed to be likely the most stable compound having a steady concentration of 0.02 g Nm^{-3} throughout the temperature test range. Therefore, the overall decrease of concentration in class 4 tars was believed to be due to

biphenyl decomposing activity, resulting in much lower concentration at higher reaction temperature.

Class 5 tars was observed to be thermally stable as the content and yield of this class tar compounds were reduced very slightly with the temperature increase. The detail examination on the individual tar components of class 5 depicted in Figure 5.11 (D) reveals that less tar formation was detected at higher temperature, except that of bens(a)anthracene. The mechanism in this study for the increase in concentration of bens(a)anthracene is thought to be complicated. However, the presence of this higher molecular weight compound could be from the cracking of a heavier tar compound presenting in the non-GC-detectable tars (class 1). It could also be the product of growing reactions of PAH which involve small PAH compounds or unsaturated hydrocarbons (Milne and Evans 1998).

5.2.2. Effect of S/B ratio

The variation of S/B ratio from 0.7 to 1.1 is found to significantly affect the tar yield and concentration, in which less amount of tar was obtained at the higher S/B ratio. As can be seen in Figure 5.12, at the lowest tested S/B ratio (0.7), there was approximately 5.05 g of tar per kg oven-dry (od) biomass (RHP) and the condensable product of gasification decreased to 3.8 g kg^{-1}_{od} at the highest S/B ratio (1.1). Meanwhile, the tar content had a similar declining trend with the concentration going down from 9.28 to 7.29 g Nm^{-3} over the given range of S/B ratio.

As far as the individual tar classes is concerned, the concentration decrease of class 3, class 4 and class 5 tars had lowered the overall tar concentration and this can be identified from Figure 5.13. In contrast, there was a slight increase in the concentration of class 2 tars, but it only made a small difference to the final amount of total GC-detectable tar. With a

concentration of 2.49 g Nm^{-3} at S/B ratio 0.7, the class 2 tars content rose slightly by 0.38 g Nm^{-3} reaching 2.87 g Nm^{-3} at S/B ratio 1.1. On the other hand, class 3 tars decreased significantly by 1.81 g Nm^{-3} (from 5.18 to 3.37 g Nm^{-3}), followed by 0.44 g Nm^{-3} decrease for the class 4 tars (from 1.38 to 0.94 g Nm^{-3}) and 0.12 g Nm^{-3} decrease for the tar components of class 5 (from 0.23 to 0.11 g Nm^{-3}).

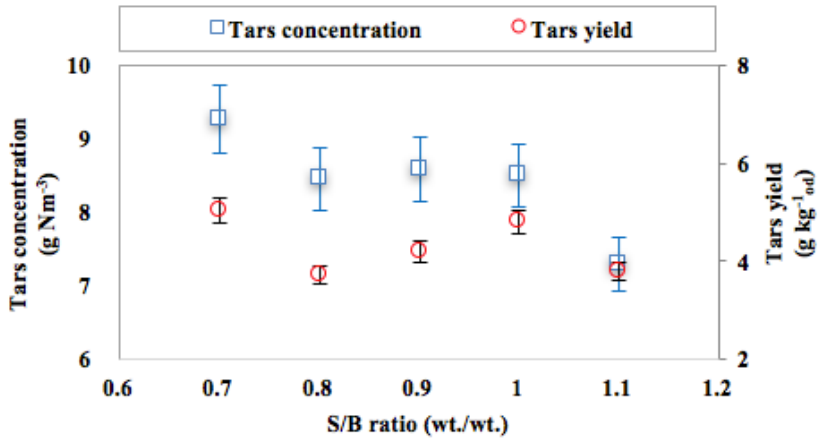

Figure 5.12. Impact of S/B ratio on the tar yield and concentration.

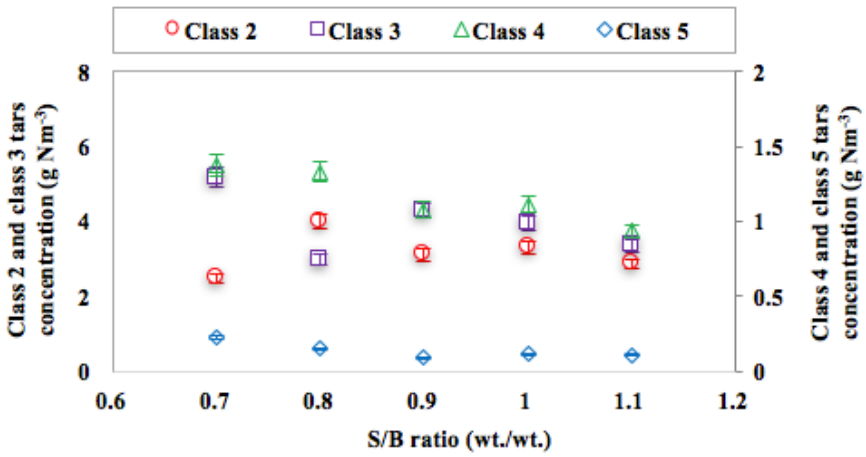

Figure 5.13. Impact of S/B ratio on the concentration of individual tar classification.

Figure 5.14 (A) - (D) plots the individual compounds of each tar classes as a function of S/B ratio. For the class 2 tars, phenol was found to be a major compound, in which its content increased from 1.29 to 2.05 g Nm^{-3} within the tested range of S/B ratio. Meanwhile, other compounds of the class 2 tars remained unchanged and together they accounted for a

concentration of 1.21 at S/B ratio 0.7, decreasing to as low as 0.82 g Nm^{-3} at S/B ratio 1.1. Moreover, benzene had the largest concentration (2.89 g Nm^{-3}) of the tar compounds found in class 3 tars at S/B ratio 0.7, representing 55.8% of total tar in this group. Following this was toluene with a concentration of 1.46 g Nm^{-3} in the class 3 tars at S/B ratio 0.7. Although the concentration of these two compounds respectively decreased to 1.83 and 0.94 g Nm^{-3}, at S/B ratio 1.1, they collectively remained the dominant elements representing 82.19% of the total tar in class 3 tars. Meanwhile, there was no significant change observed for the other class 3 elements including o-, m- and p- xylenes as well as styrene. While the former had a concentration of 0.30 g Nm^{-3} at S/B ratio 0.7, the latter accounted for 0.53 g Nm^{-3} at the same S/B ratio. At S/B ratio 1.1, the corresponding concentrations for these individual tar elements were 0.2 and 0.41g Nm^{-3}, respectively.

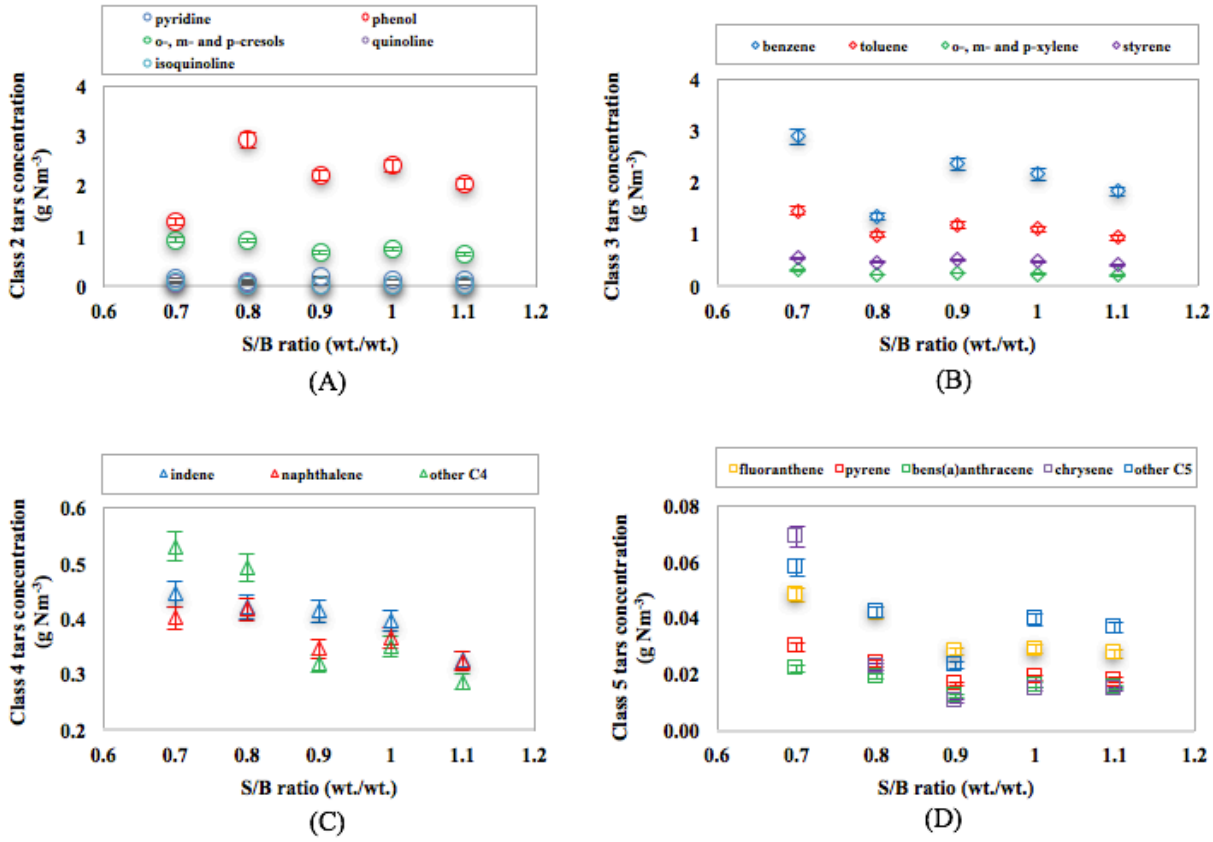

Figure 5.14. Impact of S/B ratio on the concentration of individual tar compounds in class 2 tars (A); class 3 tars (B); class 4 tars (C); and class 5 tars (D).

As the compounds of class 4 tars, indene, naphthalene and other C4 compounds were slightly differed in concentration with a respective concentration of 0.44 and 0.53 g Nm^{-3}. However, the increase of S/B ratio to 1.1 resulted in a concentration decrease for these compounds to approximately 0.3 g Nm^{-3}. A very small amount of class 5 tars was found in the producer gas generated with the varying S/B ratio. With the increase value of the given S/B ratios, the class 5 tars content decreased by over 50% from 0.23 to 0.11 g Nm^{-3}.

It is clear that all of the individual tar compounds had a declining trend of concentration with increasing S/B ratio, except the case of phenol with less tar concentration observed at the lowest tested S/B ratio. This exceptional trend may be linked to the transformation of heavy tars (class 4 and class 5) into lighter components which is enhanced as the S/B ratio increases.

5.2.3. Effect of catalytic bed material

The test of olivine sand as bed material was undertaken for the steam gasification of RHP. The influence of the active sand on the change of tar yield and concentration was examined by comparing the experimental results obtained from the gasification with olivine to those obtained with silica under the same investigated conditions as mentioned in Section 4.5.3. For easy understanding, the tars generated with silica discussed in this section is sometimes termed as “silica-tars”, while that produced using olivine could also be named as “olivine-tars”.

As can be seen in Figure 5.15, it is obvious that the use of olivine sand resulted in a lower tar yield and concentration compared to those of silica sand. At the optimum operation conditions, where the gasification temperature was set at 750^{o}C and the S/B ratio was kept at 0.7, the total amount of tar generated from silica-fluidized gasification was 5.36 g kg^{-1}_{od}. Approximately 31.3% of tar reduction was achieved when olivine sand was put into operation as the fluidized bed material, producing tar for 3.66 g kg^{-1}_{od}. The same trend was also found

for the tar content, in which the concentration decreased from 9.96 (with silica) to 6.15 g Nm^{-3} (with olivine).

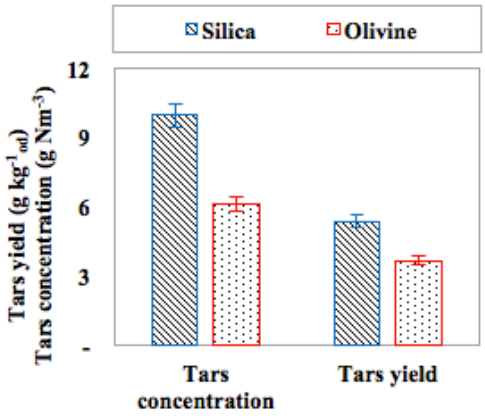

Figure 5.15. Comparison of tar yield and concentration generated from the steam gasification of RHP with silica and olivine sand.

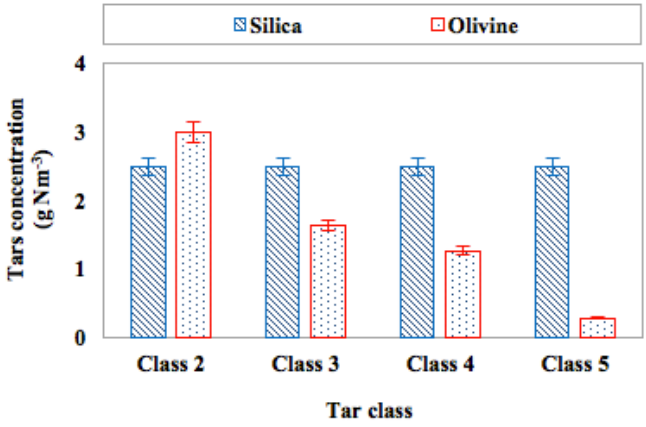

Figure 5.16. Comparison of tar concentration based on two different type of bed material

A detailed examination of the tar classification data in Figure 5.16 indicates that the use of olivine promotes a signification overall reduction of tar. Despite producing more class 2 tars, the use of olivine resulted in lower concentration of the other tar classes. In comparison with the class 2 of silica-tars, approximately 20% increase of class 2 olivine-tars was observed. However, the olivine bed material produced about 52% less class 3 tars than the silica; 1.63 g Nm^{-3} with olivine compared with 2.49 g Nm^{-3} with silica. Significant reduction was

found in class 5 with about 89% better conversion, while the conversion of class 4 tars with olivine was found to be approximately 49%.

Similar to class 2 silica-tars, phenol was the most dominant compound in class 2 olivine-tars, followed by o-, m- and p-cresols, pyridine, isoquinoline and quinoline. The olivine usage favoured the formation of more phenol and pyridine, each of which had a concentration of 1.98 and 0.21 g Nm^{-3}, respectively, in comparison with 1.29 g Nm^{-3} (phenol) and 0.15 g Nm^{-3} (pyridine) obtained with the silica. However, 0.28 g Nm^{-3} lower concentration for the o-, m- and p- cresols was obtained with olivine (0.64 g Nm^{-3}). Surprisingly, the same amount of quinoline (0.06 g Nm^{-3}) was produced with the use of either olivine or silica, indicating that no cracking activity occurring to this compound. Isoquinoline was found to have a good stability with a minor change in concentration.

Moreover, all of the concentration of individual tar compounds in class 3 and class 4 olivine-tars were lower than those of silica-tars, in which benzene and toluene had the most significant reduction. The concentration of benzene decreased from 2.89 to 0.71 g Nm^{-3} when olivine was used to replace silica, while the corresponding concentration decrease for the toluene was from 1.46 to 0.49 g Nm^{-3}. About half concentration reduction occurred for the group of o-, m- and p-xylenes as well as styrene with the former reducing from 0.3 to 0.15 g Nm^{-3} and the latter dropping from 0.53 to 0.29 g Nm^{-3}.

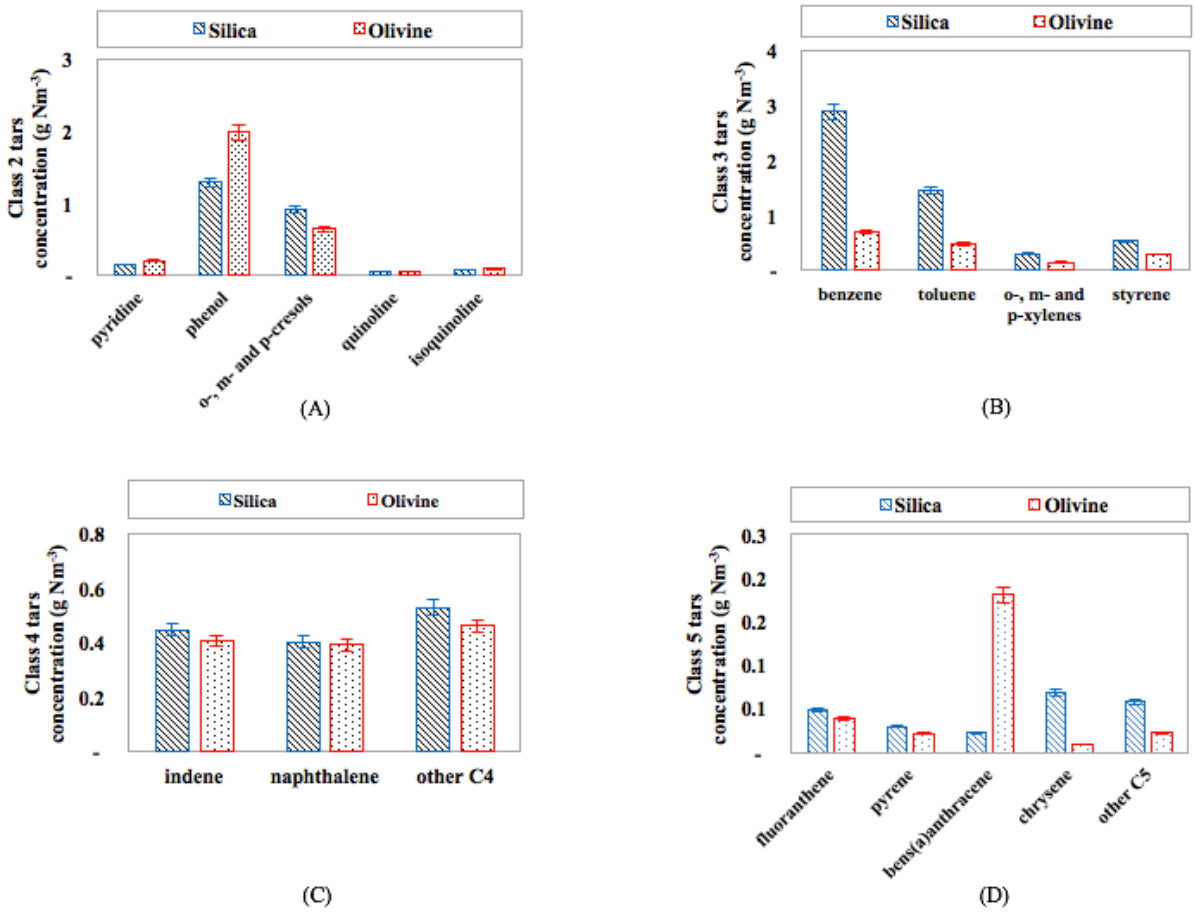

Figure 5.17. Comparison of concentration of individual tar compounds based on two different bed material types.

Meanwhile, less significant change occurred in all concentrations of class 4 tar compounds with the individual tar content ranging from 0.39 to 0.53 g Nm^{-3}, whereas in class 5 olivine-tars, the use of olivine was observed to favour the formation of bens(a)anthracene. According to Devi et al. (2005), tar decomposition in catalytic gasification occurs in a series of complex, multiple and simultaneous reactions involving:

Thermal cracking : $pC_nH_x \rightarrow qC_mH_y + rH_2$

Steam reforming : $C_nH_x + nH_2O \rightarrow (n + \frac{x}{2})H_2 + nCO$

Dry reforming : $C_nH_x + nCO_2 \rightarrow (\frac{x}{2})H_2 + 2nCO$

Carbon formation : $C_nH_x \rightarrow nC + \frac{x}{2}H_2$

where C_nH_x represents tar and it can be a mixture of several individual tar compounds. They also found that different tars can react with each other to form a new tar product so that understanding the behaviour of tar cracking activity becomes very complicated. Therefore, comparing the tar content generated from non-catalytic and active bed material is an easy way to measure the effect of the active catalyst of the bed material, as discussed previously.

6. Conclusion

This study has successfully examined the impact of important research parameters used generally in steam gasification of biomass, in which different gasification temperature and S/B ratio have been investigated to determine the optimum gasifier operation condition for the steam gasification of rice husk pellets (RHP). The biomass feedstock, which is abundantly available in Indonesia, is considered as a potential renewable energy resource since it can be transformed into hydrogen-rich producer gas, which can be further applied as a gaseous fuel for an internal combustion (IC) engine to produce electricity.

The experimental results discussed in this study demonstrate that the optimum operation condition of the gasifier was found to be at 750^{o}C with a S/B ratio of 0.7, at which the highest gas LHV reached 13.06 MJ Nm^{-3}. The presence of tar reaching a concentration of 9.23 g Nm^{-3} needs a further gas treatment in order to achieve the minimum tar level suitable for the application of the IC engine (50 mg Nm^{-3}). However, this finding provides a fundamental information which is expected to be useful for developing the application of RHP producer gas as a fuel for internal combustion engine.

Olivine sand was found to have a catalytic effect on the reduction of the overall tar formation in the producer gas, showing a better tar conversion when compared with silica sand. Apart from the group of class 2 tars, cracking activity driven by the olivine is detected in other tar classes. In order to investigate the most effective method of tar cracking with the active bed material, secondary tar treatment may be considered as part of great importance for the future study.

A number of general recommendations are proposed for the future research of RHP steam gasification in terms of gasifier operation and producer gas cleaning. Firstly, to improve the operation of the gasifier when a high ash content biomass such as RHP is the solid feedstock

fed into the gasifier, the separation of gas-solid phase between producer gas and ash particle in the cyclone installed at the top of BFB column needs to be improved to prevent excessive ash deposition blocking the combustion room of the after burner. This may be done by either scaling up the cyclone capacity or installing another typical cyclone, so they can work in parallel. Secondly, to fluidize a wider size range of bed material, increasing the air blower capacity would be necessary so it could raise the air u_{sf} in the CFB column. Thirdly, in order to better understand the total tar formation and decomposition from steam gasification of RHP, the measurement of tar yield with total gravimetric tar method would be essential. Finally, mechanical tar cracking such as wet or dry scrubbing could be considered as future area of research to further reduce the tar concentration so it could meet the required standard limit of producer application as a fuel of internal combustion engine.

7. Reference

Administration, U. S. E. I. (2016). "International Energy Outlook 2016." U.S. Energy Information Administration, Washington, 163.

Affendi, M., Sugiyatno, Djunaedi, I., and Wahyu, H. (2010). "Uji variasi beban listrik dan rasio gas hasil gasifikasi sekam padi pada mesin diesel dual fuel." *Seminar Nasional Rekayasa Kimia dan Proses*, Universitas Diponegoro, Semarang, 1-6.

Agency, I. E. (2016). "Key world energy trend, excerpt from: World energy balances ", 4-5.

Agency, I. R. E. (2012). "Renewable energy technologies: Cost analysis series."

Akgün, O., and Luukkanen, J. (2012). "Extension of rice husk gasification technology for electricity generation in Cambodia." *Energy Procedia*, 14, 1244-1249.

Al-Amin, A. Q., Rasiah, R., and Chenayah, S. (2015). "Prioritizing climate change mitigation:

An assessment using Malaysia to reduce carbon emissions in future." *environmental science & policy*, 50, 24-33.

Alamsyah, R., Loebisa, E. H., Susantoa, E., Junaidia, L., and Siregar, N. C. (2015). "An Experimental Study on Synthetic Gas (Syngas) Production Through Gasification of Indonesian Biomass Pellet." *Energy Procedia*, 65, 292–299.

Alsaleh, M., Rahim, A. S. A., and Mohd-Shahwahid, H. O. (2017). "Determinants of technical efficiency in the bioenergy industry in the EU28 region." *Renewable and Sustainable Energy Reviews*, 78, 1331–1349.

Amri, F. (2017). "The relationship amongst energy consumption (renewable and non-renewable), and GDP in Algeria." *Renewable and Sustainable Energy Reviews* 76(qwe), 62-71.

Anis, S., and Zainal, Z. A. (2011). "Tar reduction in biomass producer gas via mechanical, catalytic and thermal methods: A review." *Renewable and Sustainable Energy Reviews*, 15, 2355–2377.

Armesto, L., Bahillo, A., Veijonen, K., Cabanillas, A., and Otero, J. (2002). "Combustion behaviour of rice husk in a bubbling fluidised bed." *Biomass and Bioenergy*, 23, 171–179.

Atnaw, S. M., Sulaiman, S. A., and Yusup, S. (2013). "Syngas production from downdraft gasification of oil palm fronds." *Energy*, 61, 491-501.

Baratieri, M., Baggio, P., Bosio, B., Grigiante, M., and Longo, G. A. (2009). "The use of biomass syngas in IC engines and CCGT plants: A comparative analysis." *Applied Thermal Engineering*, 29, 3309–3318.

Basu, P. (2010). *Biomass gasification and pyrolysis: Practical design and theory*, Academic Press, Burlington, MA.

Bauen, A., Berndes, G. r., Junginger, M., Londo, M., and Vuille, F. o. (2009). "Bioenergy – a Sustainable and Reliable Energy Source." 2.

Belgiorno, V., Feo, G. D., Rocca, C. D., and Napoli, R. M. (2003). "Energy from gasification of solid wastes." *Waste Manage*, 23, 1-15.

Bhattacharyya, S. C. (2014). "Viability of off-grid electricity supply using rice husk: A case study from South Asia." *Biomass and Bioenergy*, 68, 44-54.

Bi, H. T., and Grace, J. R. (1995). "Flow regime diagrams for gas-solid fluidization and upward transport." *Int. J. Multiphase Flow*, 21, 1229-1236.

BP (2016). "BP Statistical Review of World Energy 2016." BP p.l.c., London, 42.

Brage, C., Yu, Q., Chen, G., and Sjöström, K. (1997). "Use of amino phase absorbent for biomass tar sampling and separation." *Fuel*, 76, 137-142.

Bridgwater, A. V. (1995). "The technical and economic feasibility of biomass gasification for power generation." *Fuel*, 74(5), 631-653.

Bull, D. (2008). "Performance Improvement to a Fast Internally Circulating Fluidized Bed (FICFB) Biomass Gasifier for Combined Heat and Power Plants." Master of Engineering, University of Canterbury, Christchurch.

Caneghem, J. V., Brems, A., Lievens, P., Block, C., Billen, P., Vermeulen, I., Dewil, R., Baeyens, J., and Vandecasteele, C. (2012). "Fluidized bed waste incinerators: Design, operational and environmental issues." *Progress in Energy and Combustion Science*, 38, 551-582.

Century, R. E. P. N. f. t. s. (2016). "Renewables 2016: Global status report." *we*, Adam, ed., er, Paris, 56.

Chiari, L., and Zecca, A. (2011). "Constraints of fossil fuels depletion on global warming projections." *Energy Policy*, 39, 5026–5034.

Demirbas, A. (2001). "Biomass resource facilities and biomass conversion processing for fuels and chemicals." *Energy Conversion and Management*, 42, 1357-1378.

Demirbas, A. (2004). "Combustion characteristics of different biomass fuels." *Progress in Energy and Combustion Science*, 30, 219-230.

Devi, L., Ptasinski, K. J., and Janssen, F. J. J. G. (2003). "A review of the primary measures for tar elimination in biomass gasication processes." *Biomass and Bioenergy*, 24, 125-140.

Devi, L., Ptasinski, K. J., Janssen, F. J. J. G., Paasen, S. V. B. v., Bergman, P. C. A., and Kiel, J. H. A. (2005). "Catalytic decomposition of biomass tars: use of dolomite and untreated olivine." *Renewable Energy*, 30, 565-587.

Ding, L., Zou, B., Shen, L., Zhao, C., Wang, Z., Guo, Y., Wang, X., and Liu, Y. (2014). "A simple route for consecutive production of activated carbon and liquid compound

fertilizer from rice husk." *Colloids and Surfaces A: Physicochem. Eng. Aspects*, 446, 90–96.

Drift, A. v. d., Boerrigter, H., Coda, B., Cieplik, M. K., and Hemmes, K. (2004). "Entrained flow gasification of biomass: Ash behaviour, feeding issues and system analysis." Energy Research Centre of the Netherlands, 1-58.

El-Rub, Z. A., Bramer, E. A., and Brem, G. (2004). "Review of catalysts for tar elimination in biomass gasification processes." *Ind. Eng. Chem. Res.*, 43, 6911-6919.

Göransson, K., Söderlind, U., and Zhang, W. (2011). "Experimental test on a novel dual fluidised bed biomass gasifier for synthetic fuel production." *Fuel* 90 1340–1349.

Hasler, P., and Nussbaumer, T. (1999). "Gas cleaning for IC engine applications from fixed bed biomass gasifcation." *Biomass and Bioenergy*, 16, 385-395.

Hernández, J. J., Aranda-Almansa, G., and Bula, A. (2010). "Gasification of biomass wastes in an entrained flow gasifier: Effect of the particle size and the residence time." *Fuel Processing Technology*, 91, 681-692.

Hsieh, Y. Y., Tsai, Y. C., He, J. R., Yang, P. F., Lin, H. P., Hsu, C. H., and Loganathan, A. (2017). "Rice husk agricultural waste-derived low ionic content carbon–silica nanocomposite for green reinforced epoxy resin electronic packaging material." *Journal of the Taiwan Institute of Chemical Engineers*, 78, 493–499.

Indonesia, D. E. N. R. (2014). "Outlook energy Indonesia 2014."Jakarta, 7-81.

Indonesia, S. (2017). "Production of paddy by province (ton), 1993-2015." Statistics Indonesia, Jakarta.

Kern, S., Pfeifer, C., and Hofbauer, H. (2013). "Gasification of wood in a dual fluidized bed gasifier: Influence of fuel feeding on process performance." *Chemical Engineering Science*, 90, 284–298.

Ketenagalistrikan, D. J. (2016). "Statistik Ketenagalistrikan 2015." K. E. d. S. D. Mineral, ed.Jakarta, 1-33.

Kiel, J. H. A., Paasen, S. V. B. v., Neeft, J. P. A., Devi, L., Ptasinski, K. J., Janssen, F. J. J. G., Meijer, R., Berends, R. H., Temmink, H. M. G., Brem, G., Padban, N., and Bramer, E. A. (2004). "Primary measure to reduce tar formation in fluidised-bed biomass gasifiers." Energy Research Centre of the Netherlands, 1-108.

Knoef, H. A. M. (2005). "Practical aspects of biomass gasification." *Handbook Biomass Gasification*, H. Knoef, ed., BTG biomass technology group, The Netherlands, 13-37.

Kook, J. W., Choi, H. M., Kim, B. H., Ra, H. W., Yoon, S. J., Mun, T. Y., Kim, J. H., Kim, Y. K., Lee, J. G., and Seo, M. W. (2016). "Gasification and tar removal characteristics of rice husk in a bubbling fluidized bed reactor." *Fuel*, 181, 942-950.

Koppatz, S., Pfeifer, C., and Hofbauer, H. (2011). "Comparison of the performance behaviour of silica sand and olivine in a dual fluidised bed reactor system for steam gasification of biomass at pilot plant scale." *Chemical Engineering Journal*, 175, 468-483.

Kunii, D., and Levenspiel, O. (1969). *Fluidization Engineering*, John Wiley & Sons, Inc, United States of America.

Kwofie, E. M., Ngadi, M., and Sotocinal, S. (2017). "Thermodynamic evaluation of a rice husk fired integrated steam and hot air generation unit for rice parboiling." *Energy*, 128, 39-49.

Laboratory, N. E. T. (2017). "High Temperature Wrinkler Gasifier ", U.S. Department of Energy.

Li, C., and Suzuki, K. (2009). "Tar property, analysis, reforming mechanism and model for biomass gasification—An overview." *Renewable and Sustainable Energy Reviews*, 13, 594-604.

Li, J., Liu, J., Liao, S., and Yan, R. (2010). "Hydrogen-rich gas production by airesteam gasification of rice husk using supported nano-NiO/g-Al2O3 catalyst." *international journal of hydrogen energy*, 35, 7399-7404.

Lim, J. S., Manan, Z. A., Alwi, S. R. W., and Hashim, H. (2012). "A review on utilisation of biomass from rice industry as a source of renewable energy." *Renewable and Sustainable Energy Reviews*, 16, 3084–3094.

Manatura, K., Lu, J. H., Wu, K. T., and Hsu, H. T. (2017). "Exergy analysis on torrefied rice husk pellet in fluidized bed gasification." *Applied Thermal Engineering*, 111, 1016–1024.

Milne, T. A., and Evans, R. J. (1998). "Biomass gasifier "tars": Their nature, formation and conversion ", National Renewable Energy Laboratory, Colorado, 1-68.

Moghadam, R. A., Yusup, S., Azlina, W., Nehzati, S., and Tavasoli, A. (2014). "Investigation on syngas production via biomass conversion through the integration of pyrolysis and air–steam gasification processes." *Energy Conversion and Management*, 87, 670–675.

Mohamed, R. M., Mkhalid, I. A., and Barakat, M. A. (2015). "Rice husk ash as a renewable source for the production of zeolite NaY and its characterization." *Arabian Journal of Chemistry*, 8, 48-53.

Morf, P., Hasler, P., and Nussbaumer, T. (2002). "Mechanisms and kinetics of homogeneous secondary reactions of tar from continuous pyrolysis of wood chips." *Fuel*, 81, 843-853.

Neeft, J. P. A., Knoef, H. A. M., and Onaji, P. (1999). "Behaviour of tar in biomass gasification systems. Tar related problems and their solutions.", Energy from Waste and Biomass (EWAB), The Netherlands.

Obernberger, I., and Thek, G. (2010). "The pellet handbook." *The production and utilisation of biomass pellets*, Taylor & Francis, New York, 501.

Organization, F. a. A. (2017). "Rice market monitor." United Nations, 1-32.

Paine, L. K., Peterson, T. L., Undersander, D. J., Rineer, K. C., Bartelt, G. A., Temple, S., Sample, D. W., and Klemme, R. M. (1995). "Some ecological and socio-economic considerations for biomass energy

crop production." *Biomass and Bioenergy*, 10, 231-242.

Pang, S. (2016). "Fuel flexible gas production: Biomass, coal and bio-solid wastes " *Fuel Flexible Energy Generation*, J. Oakey, ed., Elsevier, 241-269.

Patel, H. K., Paswan, M., Kadir, A., and Parha, O. P. (2015). "Rice husk, its application, power generation & environmental impact – An overview." *Journal for Studies in Management and Planning*, 1(4), 438-445.

Phillips, J. (2017). "Different types of gasifier and their integration with gas turbine." Electric Power Research Institute, 67-76.

Pode, R. (2016). "Potential applications of rice husk ash waste from rice husk biomass power plant." *Renewable and Sustainable Energy Reviews*, 53, 1468-1485.

Rapagnà, S., Jand, N., Kiennemann, A., and Foscolo, P. U. (2000). "Steam-gasi cation of biomass in a uidised-bed of olivine particles." *Biomass and Bioenergy*, 19, 187-197.

Roy, P., and Dias, G. (2017). "Prospects for pyrolysis technologies in the bioenergy sector: A review." *Renewable and Sustainable Energy Reviews*, 77, 59-69.

Ruiz, J. A., Juárez, M. C., Morales, M. P., Muñoz, P., and Mendívil, M. A. (2013). "Biomass gasification for electricity generation: Review of current technology barriers." *Renewable and Sustainable Energy Reviews*, 18.

Saw, W., McKinnon, H., Gilmour, I., and Pang, S. (2012). "Production of hydrogen-rich syngas from steam gasification of blend of biosolids and wood using a dual fluidised bed gasifier." *Fuel*, 93, 473-478.

Saw, W. L., and Pang, S. (2012). "The influence of calcite loading on producer gas composition and tar concentration of radiata pine pellets in a dual fluidised bed steam gasifier." *Fuel*, 102, 445-452.

Saw, W. L., and Pang, S. (2013). "Co-gasification of blended lignite and wood pellets in a 100 kW dual fluidised bed steam gasifier: The influence of lignite ratio on producer gas composition and tar content." *Fuel*, 112, 117-124.

Sembiring, S., Simanjuntak, W., Situmeang, R., Riyanto, A., and Sebayang, K. (2016). "Preparation of refractory cordierite using amorphous rice husk silica for thermal insulation purposes." *Ceramics International*, 42, 8431–8437.

Shafie, S. M., Mahlia, T. M. I., Masjuki, H. H., and Rismanchi, B. (2012). "Life cycle assessment (LCA) of electricity generation from rice husk in Malaysia." *Energy Procedia*, 14, 499 – 504.

Shu, K., Schneider, U. A., and Scheffran, J. r. (2017). "Optimizing the bioenergy industry infrastructure: Transportation networks and bioenergy plant locations." *Applied Energy*, 192, 247-261.

Simone, M., Barontini, F., Nicolella, C., and Tognotti, L. (2012). "Gasification of pelletized biomass in a pilot scale downdraft gasifier." *Bioresource Technology*, 116, 403–412.

Sobrosa, F. Z., Stochero, N. P., Marangon, E., and Tier, M. D. (2017). "Development of refractory ceramics from residual silica derived from rice husk ash." *Ceramics International*, 43, 7142–7146.

Srinath, S., and Reddy, G. V. (2011). "Combustion and emission characteristics of rice husk in a rectangular fluidized bed combustor." *2nd International Conference on Environmental Science and Technology*, IACSIT Press, Singapore, 343-346.

Stelt, M. J. C. v. d., Gerhauser, H., Kiel, J. H. A., and Ptasinski, K. J. (2011). "Biomass upgrading by torrefaction for the production of biofuels: A review." *Biomass and Bioenergy*, 35, 3748-3762.

Susastriawana, A. A. P., Saptoadib, H., and Purnomo (2017). "Small-scale downdraft gasifiers for biomass gasification: A review." *Renewable and Sustainable Energy Reviews*, 76, 989–1003.

Thakkara, M., Makwanab, J. P., Mohantyb, P., Shaha, M., and Singh, V. (2016). "In bed catalytic tar reduction in the autothermal fluidized bed gasification of rice husk: Extraction of silica, energy and cost analysis." *Industrial Crops and Products*, 87, 324–332.

Toolbox, T. E. (2018). "The definition of STP - Standard Temperature and Pressure and NTP - Normal Temperature and Pressure." <https://www.engineeringtoolbox.com/stp-standard-ntp-normal-air-d_772.html>. (15 February, 2018).

Uslu, A., Faaij, A. P. C., and Bergman, P. C. A. (2008). "Pre-treatment technologies, and their effect on international bioenergy supply chain logistics. Techno-economic evaluation of torrefaction, fast pyrolysis and pelletisation." *Energy*, 33, 1206-1223.

Venvika, H. J., and Yang, J. (2017). "Catalysis in microstructured reactors: Short review on small-scale syngas production and further conversion into methanol, DME and Fischer-Tropsch products." *Catalysis Today*, 285, 135-146.

Vreugdenhil, B. J., and Zwart, R. W. R. (2009). "Tar formation in pyrolysis and gasification." Energy research Centre of the Netherlands, 1-37.

Wicaksono (2017). "Target pemakaian energi baru terbarukan meningkat." <http://bisnis.liputan6.com/read/3069123/nasib-energi-terbarukan-tumpuan-ri-di-masa-depan>. (21 September, 2017).

Wielgosinski, G., Łechtanska, P., and Namiecinska, O. (2017). "Emission of some pollutants from biomass combustion in comparison to hard coal combustion." *Journal of the Energy Institute*, 90, 787-796.

Yadav, J. P., and Singh, B. R. (2011). "Study on comparison of boiler efficiency using husk and coal as fuel in rice mill " *Samriddhi*, 2(2), 1-15.

Yank, A., Ngadi, M., and Kok, R. (2016). "Physical properties of rice husk and bran briquettes under low pressure densification for rural applications." *Biomass and Bioenergy*, 84, 22-30.

Yoon, S. J., Son, Y. I., Kim, Y. K., and Lee, J. G. (2012). "Gasification and power generation characteristics of rice husk and rice husk pellet using a downdraft fixed-bed gasifier." *Renewable Energy*, 42, 163-167.

Zainal, Z. A., Rifau, A., Quadir, G. A., and Seetharamu, K. N. (2002). "Experimental investigation of a downdraft biomass gasi er." *Biomass and Bioenergy*, 23, 283-289.

Zanzi, R., Sjöström, K., and Björbom, E. (1996). "Rapid high-temperature pyrolysis of biomass in a free-fall reactor." *Fuel*, 75(5), 545-550.

Zecca, A., and Chiari, L. (2010). "Fossil-fuel constraints on global warming." *Energy Policy*, 38, 1-3.

Zhai, M., Zhang, Y., Dong, P., and Liu, P. (2015). "Characteristics of rice husk char gasification with steam." *Fuel*, 158, 42-49.

Zhang, Z., and Pang, S. (2017). "Experimental investigation of biomass devolatilization in steam gasification in a dual fluidised bed gasifier." *Fuel*, 188, 628-635.

8. Appendices

Appendix A. Report of elemental analysis of the tested fuel: Rice husk pellets

A.1. Proximate analysis

UNIVERSITAS GADJAH MADA
PUSAT STUDI PANGAN DAN GIZI

LAPORAN HASIL UJI
(Analysys Certificate)
No.PS/389/XII/2016

Nomor Pengujian : PS/485/XI/2016
(Analysis Report Number)
Nama Pelanggan : **CV Agro Jawa Dwipa**
(Name of client)
Alamat Pelanggan :
(Addres of client)
No. Telepon Pelanggan :
(Phone No. of client)
Contoh Uji : **Padatan**
(type og sample)
Tanggal Penerimaan Contoh Uji : 24 November 2016
Tanggal Pengujian : 25 November 2016
Metode Uji :
(Analysis Method)
Hasil Uji :
(Analysis Result)

No.	Kode sampel	Hasil Analisa				
		Abu %	Air %	Volatil matter %	Fix Carbon %	Kalori kalori/g
1.	Pellet Sekam	18,060	9,222	52,792	19,926	3237,686
	Padi	17,947	8,478	52,408	21,167	3196,268

Yogyakarta, 6 Desember 2016
Wakil Kepala Bidang Program PSPG – UGM

Dr. Ir. Nurliyani, MS
NIP. 196008171986032003

Gedung PAU Universitas Gadjah Mada
Jl. Teknika Utara, Barek, Yogyakarta 55281
Telp. (0274) 6492282, 589242 Fax. (0274) 589242
E-mail: cfns@ugm.ac.id; Website: www.cfns.ugm.ac.id

A.2. Ultimate analysis

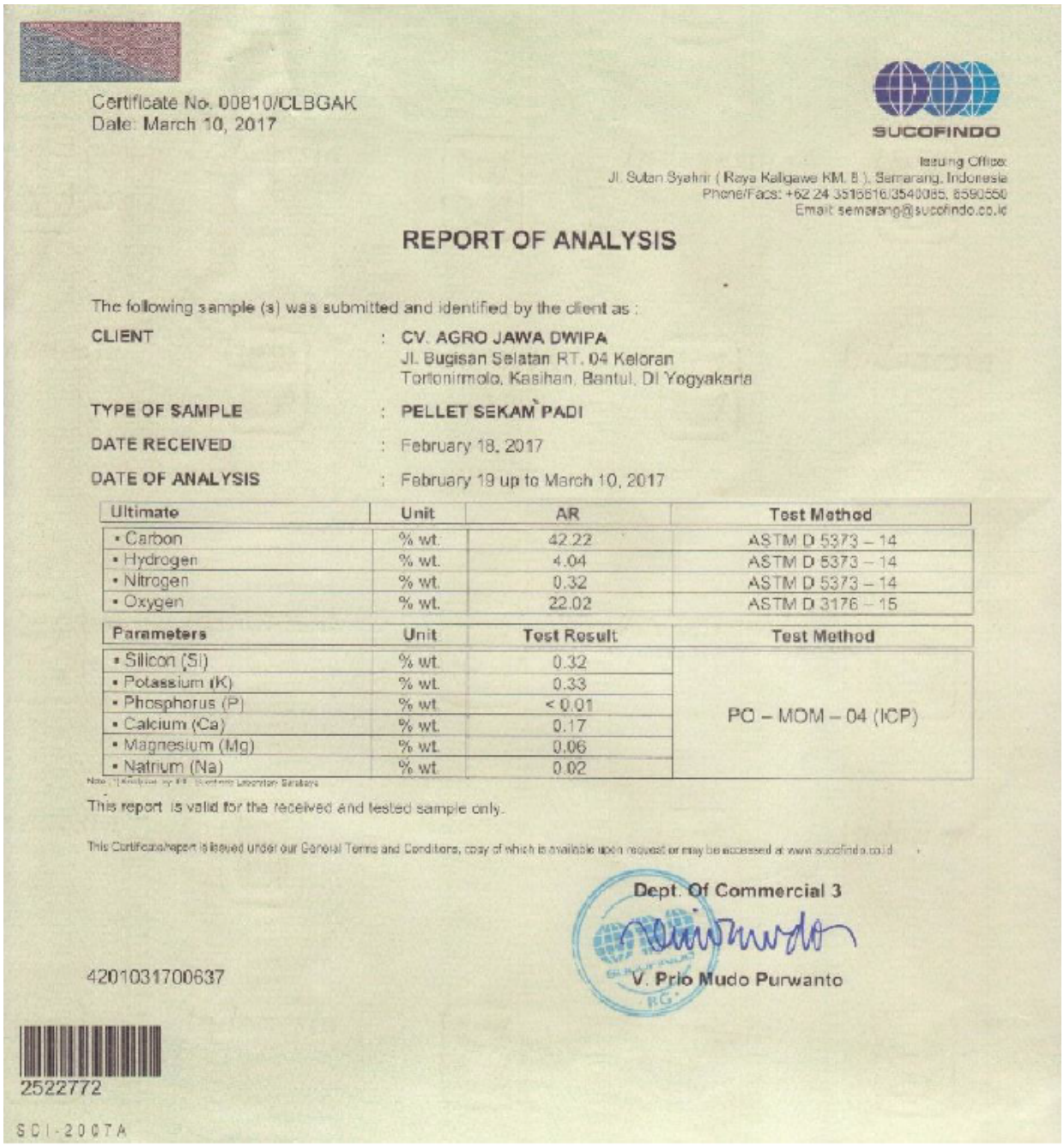

Certificate No. 00810/CLBGAK
Date: March 10, 2017

SUCOFINDO

Issuing Office:
Jl. Sultan Syahrir (Raya Kaligawe KM. 8), Semarang, Indonesia
Phone/Facs: +62 24 3516816/3540065, 6590550
Email: semarang@sucofindo.co.id

REPORT OF ANALYSIS

The following sample (s) was submitted and identified by the client as :

CLIENT	:	**CV. AGRO JAWA DWIPA** Jl. Bugisan Selatan RT. 04 Keloran Tortonirmolo, Kasihan, Bantul, DI Yogyakarta
TYPE OF SAMPLE	:	**PELLET SEKAM PADI**
DATE RECEIVED	:	February 18, 2017
DATE OF ANALYSIS	:	February 19 up to March 10, 2017

Ultimate	Unit	AR	Test Method
• Carbon	% wt.	42.22	ASTM D 5373 – 14
• Hydrogen	% wt.	4.04	ASTM D 5373 – 14
• Nitrogen	% wt.	0.32	ASTM D 5373 – 14
• Oxygen	% wt.	22.02	ASTM D 3176 – 15

Parameters	Unit	Test Result	Test Method
• Silicon (Si)	% wt.	0.32	PC – MOM – 04 (ICP)
• Potassium (K)	% wt.	0.33	
• Phosphorus (P)	% wt.	< 0.01	
• Calcium (Ca)	% wt.	0.17	
• Magnesium (Mg)	% wt.	0.06	
• Natrium (Na)	% wt.	0.02	

This report is valid for the received and tested sample only.

This Certificate/Report is issued under our General Terms and Conditions, copy of which is available upon request or may be accessed at www.sucofindo.co.id

Dept. Of Commercial 3

V. Prio Mudo Purwanto

4201031700637

2522772

SCI-2007A

Appendix B. Chemical properties of the olivine sand

Cast Metal Services

Certificate of Analysis

01 Aug 2016

Customer:

Attention:

Customer Order No.:

Delivery Date:

Product Description: **OLIVINE SAND**

Product Batch No: **NZA07813**

Product Code: **KS1190**

Lot No:

Chemistry & Physical Data:

Magnesium Oxide (MgO)	%	43
Silicon Dioxide (SiO_2)	%	39
Iron Oxide (Fe_2O_3)	%	8
Alumina (Al_2O_3)	%	1.9
Loss On Ignition (LOI)	%	2

Certificate Prepared By: Holla Niranjan **Date: 01/08/2016**

Certificate Authorized By: Holla Niranjan **Date: 01/08/2016**

Appendix C. The calculation of biomass feed rate

C.1. Auger calibration

Table C.1. The correlation between auger rotation speed and biomass feed rate

Auger speed (rpm)	Speed range (rpm)	Duration (minute)	Mass of biomass fed into reactor (g)	Feed rate (kg_{wet} h^{-1})
300	296-306	5	964	9.35
300		5	955	9.24
300		5	962	9.32
400	396-406	5	1233	12.58
400		5	1219	12.41
400		5	1226	12.49
500	497-507	5	1487	15.62
500		5	1505	15.84
500		5	1523	16.06
600	596-608	5	1820	19.62
600		5	1786	19.21
600		5	1795	19.32

C.2. Determination of auger rotation speed and biomass feed rate

- For investigated parameter 1 and parameter 3

In parameter 1 and parameter 3, the following operation conditions were applied:

$\dot{m}_s = 10.5$ kg h^{-1}; $Ø_{SB} = 0.7$; $MC_{od} = 9.71\%$

The value of Ω_A was calculated based on equation 4.7

$$\Omega_A = \left[\frac{(1 + MC_{od}) \,.\, \dot{m}_s}{0.0336 \text{ x } (Ø_{SB} - MC_{od})} \right] + 25.50$$

$$\Omega_A = \left[\frac{(1 + 0.0971) \text{ x } 10.5}{0.0336 \text{ x } (0.7 - 0.0971)} \right] + 25.50$$

$\Omega_A = 594.16 \cong 594$

From equation 4.2 and 4.5, $\dot{m}_{f,od}$ is then calculated as follows:

$$\dot{m}_{f,od} = \frac{\dot{m}_{f,wet}}{(1 + MC_{od})}$$

since : $$\dot{m}_{f,wet} = \frac{(1 + MC_{od}) \cdot \dot{m}_s}{Ø_{SB} - MC_{od}}$$

then : $$\dot{m}_{f,od} = \frac{(1 + MC_{od}) \cdot \dot{m}_s}{(1 + MC_{od})\,(Ø_{SB} - MC_{od})}$$

$$\dot{m}_{f,od} = \frac{(1 + 0.0971) \text{ x } 10.5}{(1 + 0.0971)\,(0.7 - 0.0971)}$$

$$\dot{m}_{f,od} = 17.45 \cong 17.5 \text{ kg}_{od}\text{ h}^{-1}$$

- For investigated parameter 2

For a constant steam feed rate, the following operation conditions were applied:

$\dot{m}_s$ = 10.5 kg h^{-1}; $Ø_{SB}$ = 0.7, 0.8, 0.9, 1.0 and 1.1; MC_{od} = 9.71%

For a constant biomass (RHP) feed rate, the operation conditions were applied as follows:

$\dot{m}_{f,od}$ = 10.5 kg h^{-1}; $Ø_{SB}$ = 0.7, 1.0 and 1.3 ; MC_{od} = 9.71%

with the same procedure of calculation as those adopted for parameter 1, the auger rotation speed and oven-dry biomass feed rate for the investigated parameter 2 were summarised in Table C2.

Table C.2. Auger rotation speed and dry biomass feed rate of the investigated parameter 2.

Constant steam				**Constant feeding rate**			
$Ø_{SB}$	**$\dot{m}_s$ (kg h^{-1})**	**$Ω_A$ (r.p.m.)**	**$\dot{m}_{f,od}$ (kg h^{-1})**	**$Ø_{SB}$**	**$\dot{m}_s$ (kg h^{-1})**	**$Ω_A$ (r.p.m.)**	**$\dot{m}_{f,od}$ (kg h^{-1})**
0.7	10.5	594	17.4	0.7	9.2	500	14.5
0.8	10.5	513	14.9	1.0	13.8	500	14.5
0.9	10.5	453	13.1	1.3	18.4	500	14.5
1.0	10.5	405	11.6	-	-	-	-
1.1	10.5	375	10.7	-	-	-	-

Appendix D. Producer gas composition generated from hot test runs

- **Parameter 1 (Experiment performed on 13th April 2017)**

Table D1. Gas composition from a gasification experiment between 650 and 800°C.

No	Producer gas	(T_g = 650 °C)						(T_g = 700 °C)					
		y_i				y_i (He-free)		y_i				y_i (He-free)	
		R1	R2	R3	Avg	mol.%	g kg_{od}^{-1}	R1	R2	R3	Avg	mol.%	g kg_{od}^{-1}
1	He	3.05	2.98	3.20	3.08	-	-	2.34	3.01	3.93	3.09	-	-
2	H_2	14.31	13.84	14.78	14.31	14.75	6.54	19.27	21.83	20.66	20.59	21.23	9.36
3	N_2	4.89	4.40	3.29	4.19	4.32	26.83	2.25	4.39	3.43	3.35	3.46	21.36
4	CH_4	12.22	12.07	11.59	11.96	12.33	43.73	12.04	11.75	11.82	11.87	12.24	43.19
5	CO	37.14	36.61	38.21	37.32	38.47	238.83	38.50	32.53	34.23	35.09	36.17	223.39
6	CO_2	24.40	26.11	24.79	25.10	25.87	252.42	20.88	22.30	21.52	21.57	22.24	215.81
7	C_2H_4	2.74	2.68	2.93	2.78	2.87	17.80	3.72	3.24	3.49	3.48	3.59	22.18
8	C_2H_6	1.19	1.25	1.21	1.21	1.25	8.33	0.99	0.87	0.91	0.93	0.95	6.32

No	Producer gas	(T_g = 750 °C)						(T_g = 800 °C)					
		y_i				y_i (He-free)		y_i				y_i (He-free)	
		R1	R2	R3	Avg	mol.%	g kg_{od}^{-1}	R1	R2	R3	Avg	mol.%	g kg_{od}^{-1}
1	He	2.95	2.72	2.95	2.88	-	-	2.46	2.44	2.64	2.51	-	-
2	H_2	24.11	24.08	23.09	23.76	24.44	11.63	27.93	27.70	28.23	27.95	28.66	15.65
3	N_2	3.11	2.41	2.61	2.71	2.79	18.58	2.71	2.93	2.97	2.87	2.94	22.50
4	CH_4	11.52	11.63	11.59	11.58	11.92	45.34	11.17	11.06	10.78	11.00	11.28	49.30
5	CO	33.95	34.34	34.77	34.35	35.34	235.35	31.53	32.04	31.32	31.63	32.42	247.96
6	CO_2	19.57	19.75	19.80	19.70	20.27	212.13	19.27	18.84	19.24	19.12	19.60	235.50
7	C_2H_4	4.07	4.33	4.46	4.29	4.41	29.38	4.40	4.47	4.33	4.40	4.51	34.50
8	C_2H_6	0.72	0.74	0.74	0.73	0.75	5.37	0.54	0.51	0.49	0.51	0.53	4.32

- **Parameter 2**

Constant steam feed rate (Experiment performed on 4th May 2017)

Table D2 (A). Gas composition from a gasification experiment at 750°C with the variation of $Ø_{SB}$ between 0.7 and 1.1.

No	Producer gas	($Ø_{SB}$ = 0.7)						($Ø_{SB}$ = 0.8)					
		y_i				y_i (He-free)		y_i				y_i (He-free)	
		R1	R2	R3	Avg	mol.%	g kg_{od}^{-1}	R1	R2	R3	Avg	mol.%	g kg_{od}^{-1}
1	He	2.95	2.72	2.77	2.82			3.16	4.55	4.31	4.01		
2	H_2	24.11	24.08	23.13	23.77	24.44	11.88	23.98	25.81	26.96	25.59	26.61	10.46
3	N_2	3.11	2.41	2.61	2.71	2.79	18.98	1.86	2.5	2.23	2.2	2.29	12.58
4	CH_4	11.52	11.63	11.62	11.59	11.92	46.34	11.63	11.43	11.02	11.36	11.82	37.17
5	CO	33.95	34.34	34.83	34.37	35.34	240.54	34.23	29.85	29.88	31.32	32.57	179.3
6	CO_2	19.57	19.75	19.83	19.72	20.27	216.81	19.66	21.17	21	20.61	21.43	185.4
7	C_2H_4	4.07	4.33	4.47	4.29	4.41	30.03	4.73	4.03	3.97	4.25	4.42	24.3
8	C_2H_6	0.72	0.74	0.74	0.73	0.75	5.49	0.75	0.65	0.63	0.68	0.7	4.15

No	Producer gas	($Ø_{SB}$ = 0.9)						($Ø_{SB}$ = 1.0)					
		y_i				y_i (He-free)		y_i				y_i (He-free)	
		R1	R2	R3	Avg	mol.%	g kg_{od}^{-1}	R1	R2	R3	Avg	mol.%	g kg_{od}^{-1}
1	He	4.49	4.31	3.56	4.12			3.91	4.36	3.77	4.01		
2	H_2	25.76	23.64	23.23	24.21	25.21	11	23.28	25.05	24.08	24.14	25.1	12.67
3	N_2	2.86	2.62	1.84	2.44	2.54	15.51	2.29	2.34	2.4	2.34	2.43	17.2
4	CH_4	11.19	11.74	12.01	11.65	12.13	42.31	11.79	11.18	11.48	11.48	11.94	48.24
5	CO	29.75	32.31	34.24	32.1	33.42	204.08	33.77	30.77	33.2	32.58	33.89	239.46
6	CO_2	21.09	20.28	19.65	20.34	21.18	203.2	19.63	21.44	19.71	20.26	21.07	234.01
7	C_2H_4	4.18	4.39	4.72	4.43	4.62	28.18	4.6	4.21	4.67	4.49	4.67	33.03
8	C_2H_6	0.67	0.71	0.74	0.71	0.74	4.83	0.73	0.66	0.7	0.7	0.72	5.49

No	Producer gas	($Ø_{SB}$ = 1.1)					
		y_i				y_i (He-free)	
		R1	R2	R3	Avg	mol.%	g kg_{od}^{-1}
1	He	4.79	4.68	4.6	4.69		
2	H_2	25.69	25.52	24.27	25.16	26.2	12.18
3	N_2	3.56	2.57	2.35	2.83	2.94	19.16
4	CH_4	10.82	11.32	11.24	11.13	11.59	43.11
5	CO	29.27	31.06	31.62	30.65	31.92	207.8
6	CO_2	21.17	19.92	20.93	20.68	21.53	220.25
7	C_2H_4	4.05	4.24	4.3	4.2	4.37	28.46
8	C_2H_6	0.65	0.68	0.68	0.67	0.69	4.85

Constant biomass feed rate (Experiment performed on 3rd October 2017)

Table D2 (B). Gas composition from a gasification experiment at 750°C with the variation of $Ø_{SB}$ between 0.7 and 1.3.

No	Producer gas	0.7						1.0					
		y_i				y_i (He-free)		y_i				y_i (He-free)	
		R1	R2	R3	Avg	mol.%	g kg_{od}^{-1}	R1	R2	R3	Avg	mol.%	g kg_{od}^{-1}
1	He	3.48	3.14	3.5	3.37			3.36	3.21	2.89	3.15		
2	H_2	24.58	23.24	25.01	24.28	25.1	12.13	23.16	23.24	23.4	23.27	24	12.45
3	N_2	3.58	2.97	2.46	3	3.1	21.01	3.65	3.44	2.64	3.24	3.35	24.31
4	CH_4	11.24	11.66	11.96	11.62	12.01	46.46	11.8	11.54	11.61	11.65	12.02	49.87
5	CO	30.7	33.88	32.53	32.37	33.46	226.5	33.16	31.27	31.76	32.06	33.07	240.2
6	CO_2	21.68	19.86	19.49	20.34	21.03	223.6	19.74	22.3	22.5	21.51	22.19	253.2
7	C_2H_4	4.02	4.46	4.32	4.27	4.41	29.85	4.38	4.26	4.42	4.35	4.49	32.6
8	C_2H_6	0.72	0.79	0.74	0.75	0.77	5.61	0.76	0.75	0.77	0.76	0.78	6.09

No	Producer gas	1.3					
		y_i				y_i (He-free)	
		R1	R2	R3	Avg	mol.%	g kg_{od}^{-1}
1	He	2.34	3.39	2.66	2.8		
2	H_2	24.19	24.01	23.26	23.82	24.49	14.36
3	N_2	4.54	4.7	4.23	4.49	4.62	37.91
4	CH_4	10.96	11.14	11.33	11.14	11.45	53.75
5	CO	30.25	29.8	31.77	30.61	31.46	258.4
6	CO_2	22.84	22.27	21.64	22.25	22.87	295.2
7	C_2H_4	4.18	4.02	4.4	4.2	4.32	35.45
8	C_2H_6	0.7	0.67	0.72	0.7	0.72	6.29

- **Parameter 3 (Experiment performed on 27th September 2017)**

Table D3. Gas composition from a gasification experiment at 750°C and S/B ratio of 0.7.

No	Producer gas	Olivine						Silica					
		y_i				x_{pg} (He-free)		y_i				x_{pg} (He-free)	
		R1	R2	R3	Avg	mol.%	g kg_{od}^{-1}	R1	R2	R3	Avg	mol.%	g kg_{od}^{-1}
1	He	2.54	3.79	2.63	2.99			2.95	2.72	2.95	2.88	0.00	0.00
2	H_2	26.32	28.21	26.37	26.97	27.77	12.70	24.11	24.08	23.09	23.76	24.44	11.63
3	N_2	1.77	2.14	1.55	1.82	1.87	11.98	3.11	2.41	2.61	2.71	2.79	18.58
4	CH_4	11.31	11.32	11.19	11.27	11.61	42.46	11.52	11.63	11.59	11.58	11.92	45.34
5	CO	30.32	27.00	30.52	29.28	30.15	192.98	33.95	34.34	34.77	34.35	35.34	235.35
6	CO_2	22.98	23.38	22.85	23.07	23.76	238.95	19.57	19.75	19.80	19.70	20.27	212.13
7	C_2H_4	4.02	3.49	4.17	3.89	4.01	25.64	4.07	4.33	4.46	4.29	4.41	29.38
8	C_2H_6	0.74	0.68	0.72	0.71	0.73	5.04	0.72	0.74	0.74	0.73	0.75	5.37

Appendix E. Determination producer gas yield (volumetric flux rate), lower heating value and carbon conversion.

This section is aimed to explain how the numerical data from the gasification experiments mentioned in Appendix D were processed to calculate producer gas yields, lower heating value and carbon conversion. The data presented in the following calculations were generated from the experiment performed on 13th April 2017 (parameter 1), in accordance with the investigated operation parameters as mentioned in Section 4.5.1.

$\dot{m}_{f,od}$ = 17.5 $kg_{od}\,h^{-1}$; MC_{od} = 9.71%; $Ø_{SB}$ = 0.7;

T_g = 650 °C; $\dot{v}_{He}$ = 5 L min^{-1}; $\dot{v}_{LPG}$ = 6 L min^{-1};

ΔH_{LPG} = 87 MJ m^{-3}; LHV_{RHP} = 13 MJ kg^{-1}; $y_{C,f}$ = 46.32% (d.b.)

The fractions of He-free producer gas compounds ($y_{i,He\text{-}free}$ mol.%) along with their individual heating values (LHV_i, MJ Nm^{-3}) as well as relative molecular weight are summarised in Table E.1.

Table E.1. Composition, lower heating value and molecular weight of He-free producer gas.

No	Gas compounds	Producer gas composition (y_i, mol.% ≈ vol.%)					LHV	M_R
		R1	R2	R3	Average	He-free	(MJ Nm^{-3})	(g mol^{-1})
1	He	3.05	2.98	3.20	3.08	0.00	-	4
2	H_2	14.31	13.84	14.78	14.31	14.75	9.9	2
3	N_2	4.89	4.40	3.29	4.19	4.32	0	28
4	CH_4	12.22	12.07	11.59	11.96	12.33	32.8	16
5	CO	37.14	36.61	38.21	37.32	38.47	11.6	28
6	CO_2	24.40	26.11	24.79	25.10	25.87	0	44
7	C_2H_4	2.74	2.68	2.93	2.78	2.87	49.8	28
8	C_2H_6	1.19	1.25	1.21	1.21	1.25	58.4	30

E.1. Determination of producer gas volumetric flow rate

The following calculation of producer gas volumetric flow rate is based on equation 4.23 and the experimental data provided in Table D1, in which the known y_{He} is 4.08% at 650°C, and thus:

$$\dot{v}_{dry\text{-}pg} = \dot{v}_{He} \left(\frac{1}{x_{He}} - 1\right)$$

$$\dot{v}_{dry\text{-}pg} = 5 \text{ L min}^{-1} \left(\frac{1}{0.0308} - 1\right)$$

$$\dot{v}_{dry\text{-}pg} = 157.45 \text{ L min}^{-1}$$

Based on the ideal gas law, at 25°C and 1 atm, 1 mol of ideal gas is equal to 0.024465 m^3 (≈24.465 L)

$$\dot{v}_{dry\text{-}pg} = \frac{157.45 \text{ L min}^{-1} . 1 \text{ mol}}{24.465 \text{ L}}$$

$$\dot{v}_{dry\text{-}pg} = 6.4357 \text{ mol min}^{-1}$$

$$\dot{v}_{dry\text{-}pg} = 386.14 \text{ mol h}^{-1}$$

$$P.\dot{v}_{dry\text{-}pg} = n.R.T$$

$$\dot{v}_{dry\text{-}pg} = \frac{n.R.T}{P}$$

At 0°C (273.15 K) and 1 atm (101,325 Pa), the producer gas flow rate:

$$\dot{v}_{dry\text{-}pg} = \frac{386.14 \text{ mol h}^{-1} \text{ x } 8.314 \text{ Pa m}^3 \text{ mol}^{-1} \text{ K}^{-1} \text{ x } 273.15 \text{ K}}{101{,}325 \text{ Pa}}$$

$$\dot{v}_{dry\text{-}pg} = 8.65 \text{ Nm}^3 \text{ h}^{-1}$$

$$\dot{v}_{dry\text{-}pg} = \frac{8.65 \text{ Nm}^3 \text{ h}^{-1}}{17.25 \text{ kg}_{od} \text{ h}^{-1}} = 0.50 \text{ Nm}^3 \text{ kg}^{-1}_{od}$$

Note:

The term Nm^3 is considered to be at Standard Temperature and Pressure of to 0 °C and 1 atm respectively (Toolbox 2018).

The same calculation procedures are applied for the determination of producer gas volumetric flow rate from the other operation conditions.

E.2. Determination of producer gas LHV

From equation 4.25 and data provided in Table 4.3, the LHV of producer gas whose composition is provided in Table E1, were calculated as follows:

$$LCV_{dry\text{-}pg} = \sum (y_i \,.\, LHV_i)$$

$$LCV_{dry\text{-}pg} = (y_{H2} \,.\, LHV_{H2}) + (y_{CH4} \,.\, LHV_{CH4}) + (y_{CO} \,.\, LHV_{CO}) + (y_{C2H4} \,.\, LHV_{C2H4}) + (y_{C2H6} \,.\, LHV_{C2H6})$$

$$LCV_{dry\text{-}pg} = [(14.75\% \times 9.9) + (12.33\% \times 32.8) + (37.32\% \times 11.6) + (2.87\% \times 49.8) + (1.25\% \times 58.4)]\ MJ$$

$$LCV_{dry\text{-}pg} = 12.12\ MJ\ Nm^{-3}$$

The same calculation procedures were applied for the determination of producer gas LHV for the other operation conditions.

E.3. Determination of carbon conversion

The carbon conversion was calculated based on equation 4.26 - 4.29, in which y_i was obtained from Table D1 ($T_g = 650^oC$)

$$x_C\ (\%) = \frac{\dot{m}_{C,pg}}{y_{C,f} \,.\, \dot{m}_{f,od}}$$

$$\dot{m}_{C,pg} = \sum (y_{Ci,pg} \cdot \dot{v}_{dry\text{-}pg})$$

$$\dot{m}_{C,pg} = (y_{CH4} \cdot \frac{A_{r,C}}{M_{r,CH4}} + y_{CO} \cdot \frac{A_{r,C}}{M_{r,CO}} + y_{CO2} \cdot \frac{A_{r,C}}{M_{r,CO2}} + y_{CH4} \cdot \frac{A_{r,C}}{M_{r,C2H4}} + y_{CH4} \cdot \frac{A_{r,C}}{M_{r,C2H6}}) \cdot \dot{v}_{dry\text{-}pg}$$

$$x_C\,(\%) = \frac{(y_{CH4} \cdot \frac{A_{r,C}}{M_{r,CH4}} + y_{CO} \cdot \frac{A_{r,C}}{M_{r,CO}} + y_{CO2} \cdot \frac{A_{r,C}}{M_{r,CO2}} + y_{CH4} \cdot \frac{A_{r,C}}{M_{r,C2H4}} + y_{CH4} \cdot \frac{A_{r,C}}{M_{r,C2H6}}) \cdot \dot{v}_{dry\text{-}pg}}{y_{C,f} \cdot \dot{m}_{f,od}}$$

$$y_{Ci,pg} = y_{Ci} \cdot \frac{A_{r,C}}{M_{r,Ci}}$$

$$y_{C,CH4} = 12.33\% \text{ x } \frac{12}{16} = 0.0924$$

$$y_{C,CO} = 38.47\% \text{ x } \frac{12}{28} = 0.1648$$

$$y_{C,CO2} = 25.87\% \text{ x } \frac{12}{44} = 0.0705$$

$$y_{C,C2H4} = 2.87\% \text{ x } \frac{24}{28} = 0.0246$$

$$y_{C,C2H6} = 1.25\% \text{ x } \frac{24}{30} = 0.01$$

$\dot{v}_{dry\text{-}pg} = 157.45 \text{ L m}^{-1}$

as the density of producer gas is assumed to be 1 kg m^{-3},

$$\dot{v}_{dry\text{-}pg} = \frac{157.45 \text{ L min}^{-1} \text{ x } 1 \text{ kg m}^{-3} \text{ x } 60 \text{ min h}^{-1}}{1000 \text{ L m}^{-3}} = 9.45 \text{ kg h}^{-1}$$

$\dot{m}_{C,pg} = (0.0924 + 0.1648 + 0.0705 + 0.0246 + 0.01) \text{ x } 9.45 \text{ kg h}^{-1}$

$\dot{m}_{C,pg} = 3.42 \text{ kg h}^{-1}$

$$x_C = \frac{3.42 \text{ kg h}^{-1}}{46.32\% \text{ x } 17.5 \text{ kg}_{od} \text{ h}^{-1}} \text{ x } 100\%$$

$x_C = 42.45\%$

The same calculation procedures were applied for the determination of carbon conversion for the other operation conditions.

Table E.2. Producer gas yield, LHV and carbon conversion: Summary from investigated parameter 1 (gasification temperature).

Parameter	Gasification Temperature (°C)			
	650	700	750	800
$LHV_{dry\text{-}pg}$ (MJ Nm^{-3})	12.12	12.66	13.06	12.85
$\dot{v}_{dry\text{-}pg}$ ($Nm^3\ kg^{-1}_{od}$)	0.50	0.49	0.53	0.61
x_C (%)	42.45	40.29	42.70	46.15

Table E.3. Producer gas yield, LHV and carbon conversion: Summary from investigated parameter 2 (S/B ratio-keeping the steam feeding constant).

Parameter	S/B ratio				
	0.7	0.8	0.9	1.0	1.1
$LHV_{dry\text{-}pg}$ (MJ Nm^{-3})	13.06	12.90	13.08	13.08	12.68
$\dot{v}_{dry\text{-}pg}$ ($Nm^3\ kg^{-1}_{od}$)	0.54	0.44	0.49	0.57	0.52
x_C (%)	43.65	34.28	38.86	45.08	39.97

Table E.4. Producer gas yield, LHV and carbon conversion: Summary from investigated parameter 2 (S/B ratio-keeping the biomass feeding constant).

Parameter	S/B ratio		
	0.7	1.0	1.3
$LHV_{dry\text{-}pg}$ (MJ Nm^{-3})	12.95	12.85	12.40
$\dot{v}_{dry\text{-}pg}$ ($Nm^3\ kg^{-1}_{od}$)	0.54	0.58	0.66
x_C (%)	42.75	46.18	50.48

Table E.5. Producer gas yield, LHV and carbon conversion: Summary from investigated parameter 3 (catalytic bed material).

Parameter	Bed material	
	Silica	Olivine
$LHV_{dry\text{-}pg}$ (MJ Nm^{-3})	13.06	12.72
$\dot{v}_{dry\text{-}pg}$ (Nm^3 kg^{-1}_{od})	0.54	0.60
x_C (%)	43.11	46.20

E.4. Determination of the cold gas efficiency

The optimum S/B ratio was determined by examining cold gas efficiency of the BFB gasification column. The energy input was considered to be made up of energy consumption for the production of steam used for gasification (q_s), chemical energy of RHP fed into the BFB column (q_b) and chemical energy of supplementary LPG in combustion column (q_{LPG}). The energy output, on the other hand, is referred to the chemical energy from the producer gas combustion.

- Determination of cold gas efficiency

Based on the information summarised in Table E.3, it is known that for S/B ratio of 0.7 and gasification temperature of 750°C, the results are as follow:

$\dot{v}_{dry\text{-}pg}$ = 0.54 Nm^3 kg^{-1}_{od}; $LHV_{dry\text{-}pg}$ = 13.06 MJ Nm^{-3}

to maintain the temperature of gasification at 750°C, the flow rate of the supplementary LPG ($\dot{v}_{LPG}$) and the feed rate of oven-dry RHP ($m_{f,od}$) were kept constant at 10 L min^{-1} and 17.42 kg_{od} h^{-1}. Meanwhile, the amount of steam required was 10.5 kg h^{-1}.

$$\eta_c = \frac{q_{dry\text{-}pg}}{q_{LPG} + q_b + q_s}$$

$$q_{dry\text{-}pg} = \dot{v}_{dry\text{-}pg} \,.\, LHV_{dry\text{-}pg} \,.\, m_{f,od}$$

$q_{dry\text{-}pg} = 0.54\ Nm^3\ kg^{-1}_{od} \times 13.06\ MJ\ Nm^{-3} \times 17.42\ kg_{od}\ h^{-1}$

$q_{dry\text{-}pg} = 123.96\ MJ\ h^{-1}$

$$q_{dry\text{-}pg} = 123.96\ MJ\ h^{-1} \times \frac{1\ h}{3{,}600\ s} \times \frac{1{,}000\ kJ}{1\ MJ}$$

$$q_{dry\text{-}pg} = 123.96\ MJ\ h^{-1} \times \frac{1\ h}{3{,}600\ s} \times \frac{1{,}000\ kJ}{1\ MJ}$$

$\underline{q_{dry\text{-}pg} = 34.43\ kJ\ s^{-1} = 34.43\ kW}$

$q_{LPG} = \dot{v}_{LPG} \,.\, \Delta H_{LPG}$

as the ΔH_{LPG} is assumed to be 87 MJ m^{-3}, then

$$q_{LPG} = 10\ L\ min^{-1} \times 87\ MJ\ m^{-3} \times \frac{1\ min}{60\ s} \times \frac{1m^3}{1{,}000\ L} \times \frac{1{,}000\ kJ}{1\ MJ}$$

$\underline{q_{LPG} = 14.58\ kJ\ s^{-1} = 14.58\ kW}$

$q_b = LHV_{RHP} \,.\, \dot{m}_{f,od}$

Since the LHV_{RHP} is known to be 13 MJ kg^{-1} from the proximate analysis, then

$$q_b = 13.5\ MJ\ kg^{-1} \times 17.42\ kg_{od}\ h^{-1} \times \frac{1\ h}{3{,}600\ s} \times \frac{1{,}000\ kJ}{1\ MJ}$$

$\underline{q_b = 65.11\ kJ\ s^{-1} = 65.11\ kW}$

$q_s = \Delta H_s \,.\, \dot{m}_s$

Basis of calculation: 1 g of 25^oC water

Step 1: Heat required to raise the temperature of 25°C water to 100°C water

$\Delta H_1 = m_w \cdot c_w \cdot \Delta T$

$\Delta H_1 = 1\ g \times 4.18\ J\ g^{-1}\ {}^oC^{-1} \times (100 - 25)\ {}^oC$

$\Delta H_1 = 313.5\ J$

Step 2: Heat required to convert 100°C water to 100°C steam

$\Delta H_2 = m_s \cdot \Delta H_v$

$\Delta H_2 = 1\ g \times 2{,}257\ J\ g^{-1}$

$\Delta H_2 = 2{,}257\ J$

Step 3: Heat required to turn 100°C steam into 170°C steam

$\Delta H_3 = m_s \cdot c_s \cdot \Delta T$

$\Delta H_3 = 1\ g \times 2.09\ J\ g^{-1}\ {}^oC^{-1} \times 70\ {}^oC$

$\Delta H_3 = 146.3\ J$

$\Delta H_s = \Delta H_1 + \Delta H_2 + \Delta H_3$

$\Delta H_s = (313.15 + 2{,}257 + 146.3)\ J$

$\Delta H_s = 2{,}716.8\ J$

To vaporize 1 kg h^{-1} of 25°C water producing 1 kg h^{-1} of 170°C steam,

$\Delta H_s = 2{,}716.8\ kJ\ h^{-1} = 2{,}72\ MJ\ h^{-1}$

$$\Delta H_s = 2{,}72 \text{ MJ h}^{-1} \text{ x } \frac{1 \text{ h}}{3600 \text{ s}}$$

$$\Delta H_s = 0.755 \text{ kJ s}^{-1} = 0.75 \text{ kW}$$

To produce a total of 10.5 kg h^{-1} of 170^{o}C steam, the total energy requirement becomes

$$q_s = \frac{0.75 \text{ kW}}{1 \text{ kg h}^{-1}} \text{ x } 10.5 \text{ kg h}^{-1}$$

$$q_s = 7.88 \text{ kW}$$

Therefore,

$$\eta_c = \frac{34.43 \text{ kW}}{(14.58 + 65.11 + 7.88) \text{ kW}} \text{ x } 100\%$$

$\eta_c = 39.32\ \%$

With the same procedure of calculation, the cold gas efficiency of BFB gasifier for other S/B ratios are summarised in the following table.

Table E.6. Cold gas efficiency for determination of the optimum S/B ratio.

S/B ratio	***0.7***	***0.8***	***0.9***	***1.0***	***1.1***
$LHV_{dry\text{-}pg}$ (MJ Nm^{-3})	13.06	12.90	13.08	13.08	12.68
Yield of producer gas, $\dot{v}_{dry\text{-}pg}$ (Nm^3 kg^{-1}_{od})	0.54	0.44	0.49	0.57	0.52
Fuel feeding rate, $\dot{m}_{f,od}$ (kg_{od} h^{-1})	17.42	14.94	13.08	11.63	10.72
Mass flow rate of steam, $\dot{m}_s$ (kg_{od} h^{-1})	10.5	10.5	10.5	10.5	10.5
Flow rate of LPG, $\dot{v}_{LPG}$ (L min^{-1})	10	10	10	10	10
Heating value of LPG, ΔH_{LPG} (MJ m^{-3})	87.5	87.5	87.5	87.5	87.5
Lower heating value of RHP, LHV_{RHP} (MJ kg^{-1})	13.5	13.5	13.5	13.5	13.5
Energy output from producer gas combustion (MJ h^{-1})	123.96	84.90	83.60	86.07	70.81
Energy output from producer gas combustion (kW)	34.43	23.58	23.22	23.91	19.67
Energy input from the LPG combustion, q_{LPG} (kW)	14.58	14.58	14.58	14.58	14.58
Energy input from the biomass combustion, q_b (kW)	65.11	55.85	48.89	43.48	40.06
Energy input for steam generation (kW)	7.88	7.88	7.88	7.88	7.88
Total energy input (kW)	87.57	78.31	71.35	65.94	62.52
Total energy output (kW)	34.43	23.58	23.22	23.91	19.67
Cold gas efficiency, ηc (%)	***39.32***	***30.11***	***32.55***	***36.26***	***31.46***

Appendix F. Calculation of u_{mf} and u_t

Based on particle separation with the sieving method, the physical measurement of the silica and olivine sands are presented in Table F.1.

Table F.1. Cumulative mass fraction of silica and olivine sands.

Diameter Range (μm)	d_p (μm)	Mass Fraction (%)		Cumulative Mass Fraction (%)	
		Olivine Sand	Silica Sand	Olivine Sand	Silica Sand
0-106	53	0.72	0.38	0.72	0.38
106-212	159	2.91	22.15	3.63	22.53
212-300	256	20.12	69.87	23.74	92.39
300-425	362.5	35.85	7.61	59.59	100
425-500	462.5	18.39	-	77.98	-
500-850	675	21.28	-	99.26	-
850-100	925	0.74	-	100	-

For the cold experiment, the operation temperature was assumed to be at 25^{o}C, while during the hot test experiment, the gasification temperature ranged between 650 and 800^{o}C. The information of dynamic viscosity (μ) and fluid density (ρ_g) of fluidizing agents (air and steam) for each operation temperature are presented in Table F.2.

Table F.2. dynamic viscosity and fluid density of fluidizing agents.

Air at CFB and BFB column	T_g (^{o}C)			Steam at BFB column	T_g (^{o}C)		
	25	650	800		170	650	800
μ (kg m^{-1} s^{-1})	0.00002	0.00004	0.00004	μ (kg m^{-1} s^{-1})	0.00002	0.00003	0.00004
ρ_g (kg m^{-3})	1.18400	0.38340	0.34580	ρ_g (kg m^{-3})	0.4969	0.2506	0.2171

The following calculations were to explain how u_{mf} and u_t were determined. For example, only particles with d_p of 256 μm were mentioned in this section. Those with the other measured particle size were determined with the same procedure.

- Fluidisation properties of olivine sand with **air** as the fluidizing medium in both CFB and BFB columns (ρ_s = 3,250 kg m^{-3})
    - *Determination of minimum fluidisation velocity (u_{mf})*

At 25 ^oC

Assuming that $Re_p < 20$, then:

$$u_{mf} = \frac{d_p^2 (\rho_s - \rho_g) g}{1650 \mu}$$

$$u_{mf} = \frac{(256\ \mu m \times 10^{-6}\ m\ \mu m^{-1})^2 \times (3{,}250 - 1.18400)\ kg\ m^{-3} \times 9.81\ m\ s^{-2}}{1650 \times 0.00002\ kg\ m^{-1}\ s^{-1}}$$

$u_{mf} = 0.068\ m\ s^{-1}$

$$Re_p = \frac{d_p\, u_{mf}\, \rho_g}{\mu}$$

$$Re_p = \frac{(256\ \mu m \times 10^{-6}\ m\ \mu m^{-1}) \times 0.068\ m\ s^{-1} \times 1.18400\ kg\ m^{-3}}{0.00002\ kg\ m^{-1}\ s^{-1}}$$

$Re_p = 1.1223$; $Re_p < 20$

Now that $Re_p < 20$, the calculation of u_{mf} is valid.

At 650 ^oC

$$u_{mf} = \frac{(256\ \mu m \times 10^{-6}\ m\ \mu m^{-1})^2 \times (3{,}250 - 0.38340)\ kg\ m^{-3} \times 9.81\ m\ s^{-2}}{1650 \times 0.00004\ kg\ m^{-1}\ s^{-1}}$$

$u_{mf} = 0.032\ m\ s^{-1}$

$$Re_p = \frac{(256\ \mu m \times 10^{-6}\ m\ \mu m^{-1}) \times 0.032\ m\ s^{-1} \times 0.38340\ kg\ m^{-3}}{0.00004\ kg\ m^{-1}\ s^{-1}}$$

$Re_p = 0.0785$; $Re_p < 20$

Now that $Re_p < 20$, the calculation of u_{mf} is valid.

At 800^{o}C

$$u_{mf} = \frac{(256\ \mu m \times 10^{-6}\ m\ \mu m^{-1})^2 \times (3{,}250 - 0.32890)\ kg\ m^{-3} \times 9.81\ m\ s^{-2}}{1650 \times 0.00004\ kg\ m^{-1}\ s^{-1}}$$

$u_{mf} = 0.029\ m\ s^{-1}$

$$Re_p = \frac{(256\ \mu m \times 10^{-6}\ m\ \mu m^{-1}) \times 0.029\ m\ s^{-1} \times 0.322890\ kg\ m^{-3}}{0.00004\ kg\ m^{-1}\ s^{-1}}$$

$Re_p = 0.0560$, $Re_p < 20$

Now that $Re_p < 20$, the calculation of u_{mf} is valid.

- *Determination of terminal velocity (u_t)*

To calculate u_t, the following formulae are introduced.

Assuming that $0.4 < Re_p < 500$, then:

At 25^{o}C

$$u_t = \sqrt[3]{\frac{4}{225}\frac{(\rho_s-\rho_g)^2 g^2}{\rho_g \mu}}\ .\ d_p$$

$$u_t = \sqrt[3]{\frac{4}{225} \times \frac{\left((3{,}250 - 0.32890)\ kg.m^{-3}\right)^2 \times (9.81\ m\ s^{-2})^2}{1.18400\ kg\ m^{-3} \times 0.00002\ kg\ m^{-1}\ s^{-1}}} \times (256\ \mu m \times 10^{-6}\ m\ \mu m^{-1})$$

$u_t = 2.401\ m\ s^{-1}$

$$Re_p = \frac{d_p\, u_t\, \rho_g}{\mu}$$

$$Re_p = \frac{(256\ \mu m \times 10^{-6}\ m\ \mu m^{-1}) \times 2.401\ m\ s^{-1} \times 1.18400\ kg\ m^{-3}}{0.00002\ kg\ m^{-1}\ s^{-1}}$$

$Re_p = 39.36$

Now that $0.4 < Re_p < 500$, the calculation of u_t is valid.

At 650^{o}C

$$u_t = \sqrt[3]{\frac{4}{225} x \frac{\left((3{,}250 - 0.32890)\ kg.m^{-3}\right)^2 x (9.81\ m\ s^{-2})^2}{0.38340\ kg\ m^{-3} x\ 0.00004\ kg\ m^{-1}\ s^{-1}}} x\ (256\ \mu m\ x\ 10^{-6}\ m\ \mu m^{-1})$$

$u_t = 2.709\ m\ s^{-1}$

$$Re_p = \frac{(256\ \mu m\ x\ 10^{-6}\ m\ \mu m^{-1}) x\ 2.709\ m\ s^{-1} x\ 0.38340\ kg\ m^{-3}}{0.00004\ kg\ m^{-1}\ s^{-1}}$$

$Re_p = 6.68$

Now that $0.4 < Re_p < 500$, the calculation of u_t is valid.

At 800^{o}C

$$u_t = \sqrt[3]{\frac{4}{225} x \frac{\left((3{,}250 - 0.32890)\ kg\ m^{-3}\right)^2 x (9.81\ m\ s^{-2})^2}{0.32890\ kg\ m^{-3} x\ 0.00004\ kg\ m^{-1}\ s^{-1}}} x\ (256\ \mu m\ x\ 10^{-6}\ m\ \mu m^{-1})$$

$u_t = 2.765\ m\ s^{-1}$

$$Re_p = \frac{(256\ \mu m\ x\ 10^{-6}\ m\ \mu m^{-1}) x\ 2.765\ m\ s^{-1} x\ 0.32890\ kg\ m^{-3}}{0.00004\ kg\ m^{-1}\ s^{-1}}$$

$Re_p = 5.34$

Now that $0.4 < Re_p < 500$, the calculation of u_t is valid.

- Fluidisation properties of olivine sand with **steam** as the fluidizing medium in BFB column ($\rho_s = 3{,}250\ kg\ m^{-3}$)

At 650^{o}C

Assuming that $Re_p < 20$, then:

$$u_{mf} = \frac{d_p^2 (\rho_s - \rho_g) g}{1650 \mu}$$

$$u_{mf} = \frac{(256\ \mu m \times 10^{-6}\ m\ \mu m^{-1})^2 \times (3{,}250 - 0.2506)\ kg\ m^{-3} \times 9.81\ m\ s^{-2}}{1650 \times 0.00003\ kg\ m^{-1}\ s^{-1}}$$

$$u_{mf} = 0.037\ m\ s^{-1}$$

$$Re_p = \frac{d_p\, u_{mf}\, \rho_g}{\mu}$$

$$Re_p = \frac{(256\ \mu m \times 10^{-6}\ m\ \mu m^{-1}) \times 0.037\ m\ s^{-1} \times 0.2506\ kg\ m^{-3}}{0.00003\ kg\ m^{-1}\ s^{-1}}$$

$Re_p = 0.0694$, $Re_p < 20$

Now that $Re_p < 20$, the calculation of u_{mf} is valid.

<u>At 800^{o}C</u>

$$u_{mf} = \frac{(256\ \mu m \times 10^{-6}\ m\ \mu m^{-1})^2 \times (3{,}250 - 0.2171)\ kg\ m^{-3} \times 9.81\ m\ s^{-2}}{1650 \times 0.00004\ kg\ m^{-1}\ s^{-1}}$$

$$u_{mf} = 0.032\ m\ s^{-1}$$

$$Re_p = \frac{(256\ \mu m \times 10^{-6}\ m\ \mu m^{-1}) \times 0.032\ m\ s^{-1} \times 0.2171\ kg\ m^{-3}}{0.00004\ kg\ m^{-1}\ s^{-1}}$$

$Re_p = 0.0441$, $Re_p < 20$

Now that $Re_p < 20$, the calculation of u_{mf} is valid.

To calculate u_t, the following formulae are introduced.

Assuming that $0.4 < Re_p < 500$, then:

<u>At 650^{o}C</u>

$$u_t = \sqrt[3]{\frac{4}{225}\frac{(\rho_s - \rho_g)^2 g^2}{\rho_g \mu}}\ .\ d_p$$

$$u_t = \sqrt[3]{\frac{4}{225} x \frac{\left((3{,}250 - 0.2506)\ kg\ m^{-3}\right)^2 x (9.81\ m\ s^{-2})^2}{0.2506\ kg\ m^{-3} x\ 0.00003\ kg\ m^{-1}\ s^{-1}}} x\ (256\ \mu m\ x\ 10^{-6}\ m\ \mu m^{-1})$$

$u_t = 3.282\ m\ s^{-1}$

$$Re_p = \frac{d_p\ u_t\ \rho_g}{\mu}$$

$$Re_p = \frac{(256\ \mu m\ x\ 10^{-6}\ m\ \mu m^{-1}) x\ 3.282\ m\ s^{-1} x\ 0.2506\ kg\ m^{-3}}{0.00003\ kg\ m^{-1}\ s^{-1}}$$

$Re_p = 6.16$

Now that $0.4 < Re_p < 500$, the calculation of u_t is valid.

<u>At 800°C</u>

$$u_t = \sqrt[3]{\frac{4}{225} x \frac{\left((3{,}250 - 0.2506)\ kg\ m^{-3}\right)^2 x (9.81\ m\ s^{-2})^2}{0.2171\ kg\ m^{-3} x\ 0.00004\ kg\ m^{-1}\ s^{-1}}} x\ (256\ \mu m\ x\ 10^{-6}\ m\ \mu m^{-1})$$

$u_t = 3.270\ m\ s^{-1}$

$$Re_p = \frac{(256\ \mu m\ x\ 10^{-6}\ m\ \mu m^{-1}) x\ 3.270\ m\ s^{-1} x\ 0.2171\ kg\ m^{-3}}{0.00004\ kg\ m^{-1}\ s^{-1}}$$

$Re_p = 4.55$

Now that $0.4 < Re_p < 500$, the calculation of u_t is valid.

The overall values of u_{mf} and u_t for each d_p of bed material with different fluidizing mediums and operation temperatures are summarised in Table F.3 and F.4.

Table F.3. u_{mf} and u_t of silica sand at different fluidizing mediums and operation temperatures.

Silica Sand	Location: CFB and BFB columns				Location: BFB column	
	Fluid: Air				Fluid: Steam	
Mean Particle Size (μm)	25		800		800	
	u_{mf} (m s^{-1})	u_t (m s^{-1})	u_{mf} (m s^{-1})	u_t (m s^{-1})	u_{mf} (m s^{-1})	u_t (m s^{-1})
53	0.0023	0.4239	0.0010	0.4882	0.0011	0.4783
159	0.0208	1.2717	0.0088	1.4645	0.0096	1.4349
256	0.0539	2.0476	0.0229	2.3579	0.0250	2.3102
362.5	0.1081	2.8994	0.0458	3.3388	0.0501	3.2713

Table F.4. u_{mf} and u_t of olivine sand at different fluidizing mediums and operation temperatures.

Olivine Sand	Location: CFB and BFB columns				Location: BFB column	
	Fluid: Air				Fluid: Steam	
Mean Particle Size (μm)	25		800		800	
	u_{mf} (m s^{-1})	u_t (m s^{-1})	u_{mf} (m s^{-1})	u_t (m s^{-1})	u_{mf} (m s^{-1})	u_t (m s^{-1})
53	0.0029	0.4971	0.0012	0.5723	0.0014	0.6769
159	0.0264	1.4912	0.0112	1.7170	0.0122	2.0307
256	0.0685	2.4009	0.0290	2.7645	0.0317	3.2696
362.5	0.1373	3.3996	0.0582	3.9146	0.0636	4.6297
462.5	0.2235	4.3375	0.0947	4.9945	0.1035	5.9069
675	0.4760	6.3304	*0.2018*	7.2893	0.2204	8.6209
925	0.8938	8.6750	0.3790	9.9890	0.4138	11.8138

Appendix G. The determination of superficial velocity of the fluid

The following assumptions were applied for the calculations of superficial velocity (u_{sf}) in both CFB combustion column and BFB gasification column.

- All the steam from chute entered and flowed upwards in the BFB column.
- The total steam flowing through the base of BFB column was the summation of those from the BFB base and chute, while the total air entering the CFB column was the summation of air stream from primary and secondary pipelines.
- The flow effect as a result of the oxidised LPG in the CFB column was negligible.

- The air temperature just before entering the system was assumed to be constant at ambient temperature (25^{o}C).

$$u_{sf} = \frac{\dot{v}_f}{A}$$

$$A = \pi \cdot \left(\frac{d}{2}\right)^2$$

$$u_{sf} = \frac{4 \cdot \dot{v}_f}{\pi \cdot d^2}$$

The value of each fluid density in specific operation temperature was referred to Table F.2. Shown in Table G.1 is the summary of air flux in the CFB column corresponding to the rotameter reading, whereas those for BFB column are provided in Table G.2. Since the flow rate units of the rotameter were not explicitly mentioned on its glass cylinder, the determination of the volume flow rate was based on the user manual providing a linear equation as specified in those Tables. The *y-axis* represented the value of volume flow rate (L min^{-1}), while the *x-axis* showed the level of rotameter reading.

Table G.1. Correlation of rotameter reading with the air flow rate in CFB column at 25^{o}C.

Primary air			**Secondary Air**		
y = 63.689x + 74.951	Flow rate at 25^{o}C		y = 12.92x + 12.448	Flow rate at 25^{o}C	
Reading scale (x)	L min^{-1}	m^3 s^{-1}	Reading scale (x)	L min^{-1}	m^3 s^{-1}
8.00	599.74	0.0100	8.00	119.40	0.0020
10.00	715.39	0.0119	10.00	142.54	0.0024
12.00	834.62	0.0139	12.00	166.46	0.0028
14.00	957.31	0.0160	14.00	191.15	0.0032
16.00	1083.32	0.0181	16.00	216.62	0.0036
18.00	1212.53	0.0202	18.00	242.85	0.0040
20.00	1344.81	0.0224	20.00	269.84	0.0045
22.00	1480.02	0.0247	22.00	297.60	0.0050
24.00	1618.04	0.0270	24.00	326.11	0.0054

Table G.2. Correlation of rotameter reading with the air flow rate in BFB column at 25°C.

BFB Fluidisation			**Chute air**		
y = 7.4971x + 4.6189	Flow rate at 25°C		y = 3.1095x + 4.8135	Flow rate at 25°C	
Reading scale (x)	L min^{-1}	m^3 s^{-1}	Reading scale (x)	L min^{-1}	m^3 s^{-1}
8.00	67.00	0.0011	8.00	30.39	0.0005
10.00	80.22	0.0013	10.00	36.10	0.0006
12.00	93.92	0.0016	12.00	41.95	0.0007
14.00	108.12	0.0018	14.00	47.92	0.0008
16.00	122.83	0.0020	16.00	54.05	0.0009
18.00	138.06	0.0023	18.00	60.33	0.0010
20.00	153.82	0.0026	20.00	66.77	0.0011
22.00	170.15	0.0028	22.00	73.39	0.0012
24.00	187.03	0.0031	24.00	80.19	0.0013

- u_{sf} in CFB column

<u>At 25°C</u>

At level 8 of rotameter readings for both primary and secondary pipes, the u_{sf} was calculated as follows:

$$u_{sf,CFB} = u_{sf,primary} + u_{sf,secondary}$$

$$u_{sf} = \frac{4 \,.\, \dot{v}_f}{\pi \,.\, d^2}$$

$$u_{sf,primary} = \frac{4 \text{ x } 599.74 \text{ L min}^{-1}}{\pi \text{ x } (0.1 \text{ m})^2} \text{ x } \frac{1 \text{ m}^3}{1000 \text{ L}} \text{ x } \frac{1 \text{ min}}{60 \text{ s}}$$

$$u_{sf,primary} = 1.2726 \text{ m s}^{-1}$$

$$u_{sf,secondary} = \frac{4 \text{ x } 119.4 \text{ L min}^{-1}}{\pi \text{ x } (0.1 \text{ m})^2} \text{ x } \frac{1 \text{ m}^3}{1000 \text{ L}} \text{ x } \frac{1 \text{ min}}{60 \text{ s}}$$

$$u_{sf,secondary} = 0.2534 \text{ m s}^{-1}$$

$$u_{sf,CFB} = (1.2726 + 0.2534) \text{ m s}^{-1}$$

$u_{sf,CFB,25} = 1.53 \text{ m s}^{-1}$

At 650^{o}C

The u_{sf} in CFB column increased with the operation temperature as a result of fluid density difference. A generalization was made as follows:

$$\frac{\rho_{g,650C}}{\rho_{g,25C}} = \frac{u_{sf,25C}}{u_{sf,650C}}$$

$$u_{sf,650C} = \frac{\rho_{g,25C}}{\rho_{g,650C}} \text{ x } u_{sf,25C}$$

At the same level of rotameter reading,

$$u_{sf,CFB,650C} = \frac{1.1840 \text{ kg m}^{-3}}{0.3834 \text{ kg m}^{-3}} \text{ x } 1.526 \text{ m s}^{-1}$$

$u_{sf,CFB,650C} = 4.71 \text{ m s}^{-1}$

The same calculation procedures were also applied for the other rotameter readings, fluidising medium and operation temperature whose results are summarised in Table G3 and Table G4.

Table G.3. u_{sf} of air (m s^{-1}) in CFB and BFB columns at different rotameter readings and operation temperatures (^{o}C).

Rotameter reading	CFB Column						BFB Column			
	Primary			Secondary			BFB Base		Chute	
	25	650	800	25	650	800	25	650	25	650
8	1.27	3.93	4.58	0.25	0.78	0.91	0.04	0.11	0.02	0.05
10	1.52	4.69	5.46	0.30	0.93	1.09	0.04	0.13	0.02	0.06
12	1.77	5.47	6.38	0.35	1.09	1.27	0.05	0.15	0.02	0.07
14	2.03	6.27	7.31	0.41	1.25	1.46	0.06	0.18	0.03	0.08
16	2.30	7.10	8.28	0.46	1.42	1.65	0.07	0.20	0.03	0.09
18	2.57	7.95	9.26	0.52	1.59	1.86	0.07	0.23	0.03	0.10
20	2.85	8.81	10.27	0.57	1.77	2.06	0.08	0.25	0.04	0.11
22	3.14	9.70	11.31	0.63	1.95	2.27	0.09	0.28	0.04	0.12
24	3.43	10.60	12.36	0.69	2.14	2.49	0.10	0.31	0.04	0.13

Table G.4. u_{sf} of steam (m s^{-1}) in the BFB column at different rotameter readings and operation temperatures.

Rotameter reading (kg h^{-1})	BFB Base		Chute	
	650	800	650	800
1	0.04	0.04	0.04	0.04
2	0.07	0.08	0.07	0.08
3	0.11	0.12	0.11	0.12
4	0.14	0.16	0.14	0.16
5	0.18	0.20	0.18	0.20
6	0.21	0.24		
7	0.25	0.29		
8	0.28	0.33		
9	0.32	0.37		
10	0.35	0.41		
11	0.39	0.45		
13	0.46	0.53		
15	0.53	0.61		
16	0.56	0.65		
17	0.60	0.69		

Appendix H. The determination of fluidisation regime

The determination of fluidisation regimes for the silica and olivine sands in both the CFB combustion column and the BFB gasification column were based on equation 4.17 - 4.20. The values of U^* and d_p^* are graphed in Figure 4.3 and show the type of fluidisation regime of bed material in each column based on the operation parameters applied on the gasifier operation. The following calculation example explains how to determine fluidisation behaviour of silica sand in both CFB combustion column and BFB gasification column at the operation temperature of 25^{o}C during the heat up phase.

$$U^* = \frac{Re_p}{Ar^{1/3}}$$

$$Re_p = \frac{u_{se}\, d_{sv}\, \rho_g}{\mu}$$

$$d_p^* = Ar^{1/3}$$

$$Ar = \frac{\rho_g (\rho_s - \rho_g)\, g\, d_p^3}{\mu^2}$$

- From the sand particle information provided in Table F.1, the sauter diameter (d_{sv}, μm) of silica sand can be determined by:

$$d_{sv} = \frac{1}{\Sigma \left(\frac{x}{d_p}\right)_i}$$

in which *x* is the mass fraction of bed material (silica or olivine sand) for a specific range of aperture as mentioned in Table F.1, while d_p is mean diameter that represents the whole range of particle size *i*.

$$\sum \left(\frac{x}{d_p}\right)_i = 0.00007 + 0.00139 + 0.00273 + 0.00021$$

$$\sum \left(\frac{x}{d_p}\right)_i = 0.0044$$

$$d_{sv} = \frac{1}{0.0044}$$

$$d_{sv} = 227\ \mu m$$

- ***<u>At 25 ^oC</u>***

$\rho_g = 1.18\ kg\ m^{-3}$; $\rho_s = 2{,}560\ kg\ m^{-3}$; $\mu = 0.00002\ kg\ m^{-1}\ s^{-1}$; $u_{se} = 3.77\ m\ s^{-1}$

$$Re_p = \frac{3.77\ m\ s^{-1} \times 227 \times 10^{-6}\ m \times 1.18\ kg\ m^{-3}}{0.00002\ kg\ m^{-1}\ s^{-1}}$$

$$Re_p = 54.88$$

$$Ar = \frac{1.18\ kg\ m^{-3} \times (2{,}560 - 1.18)\ kg\ m^{-3} \times 9.81\ m\ s^{-2} \times (227 \times 10^{-6}\ m)^3}{(0.00002\ kg\ m^{-1}\ s^{-1})^2}$$

$$Ar = 1017.75$$

$$U^* = \frac{54.88}{(1{,}017.75)^{1/3}}$$

$$U^* = 5.46$$

$$d_p^* = (1{,}017.75)^{1/3}$$

$$d_p^* = 10.06$$

With the values of U^* (5.46) and d_p^* (10.06), the fluidisation regime in the CFB column during the heat up phase was identified as fast fluidisation.

The determination of fluidisation regime for the silica sand in BFB gasification column, in which the u_{se} was 0.12 m s^{-1}, followed the same procedures as above. This resulted in 0.17 for U^* and 20.06 for d_p^*, leading to a bubbling bed regime in the BFB gasification column. With the same calculation method, the behaviour of bed material fluidisation during the heat up and gasification phases for other operation conditions in each column were determined and the results are summarised in Table H.1 and Table H.2.

Table H.1. Fluidisation regime in CFB and BFB columns during the heat up phase.

Parameters	Unit	Silica				Olivine			
		25°C		650°C		25°C		650°C	
		CFB	BFB	CFB	BFB	CFB	BFB	CFB	BFB
g	$m\ s^{-2}$	9.81	9.81	9.81	9.81	9.81	9.81	9.81	9.81
ρ_s	$kg\ m^{-3}$	2,560	2,560	2,560	2,560	3,250	3,250	3,250	3,250
d_{sv}	µm	227	227	227	227	256	256	256	256
u_{se}	$m\ s^{-1}$	3.77	0.12	5.62	0.36	3.77	0.12	5.62	0.36
ρ_g	$kg\ m^{-3}$	1.1840	1.1840	0.3834	0.3834	1.1840	1.1840	0.3834	0.3834
µ	$kg\ m^{-1}\ s^{-1}$	0.00002	0.00002	0.00004	0.00004	0.00002	0.00002	0.00004	0.00004
Re_p	dimensionless	54.876	1.702	12.304	0.791	61.87	1.92	13.87	0.89
Ar	dimensionless	1017.75	1017.75	71.22	71.22	1851.79	1851.79	129.58	129.58
d_p^*	dimensionless	10.06	10.06	4.15	4.15	12.28	12.28	5.06	5.06
U^*	dimensionless	5.46	0.17	2.97	0.19	5.04	0.16	2.74	0.18
Regime	NA	FF	BB	FF	BB	FF	BB	FF	BB

Table H.2. Fluidisation regime in CFB and BFB columns during the gasification phase.

Parameters	Unit	Silica				Olivine			
		650°C		800°C		650°C		800°C	
		CFB	BFB	CFB	BFB	CFB	BFB	CFB	BFB
g	$m\ s^{-2}$	9.81	9.81	9.81	9.81	9.81	9.81	9.81	9.81
ρ_s	$kg\ m^{-3}$	2560.00	2560.00	2560.00	2560.00	3250.00	3250.00	3250.00	3250.00
d_{sv}	μm	227.07	227.07	227.07	227.07	256.00	256.00	256.00	256.00
u_{se}	$m\ s^{-1}$	5.62	0.32	5.49	0.37	5.62	0.32	5.49	0.37
ρ_g	$kg\ m^{-3}$	0.38	0.25	0.33	0.22	0.38	0.25	0.33	0.22
μ	$kg\ m^{-1}\ s^{-1}$	0.00	0.00	0.00	0.00	0.00	0.00	0.00	0.00
Re_p	dimensionless	14.31	0.53	10.27	0.45	16.13	0.60	11.58	0.51
Ar	dimensionless	96.30	62.95	60.58	39.99	175.21	114.53	110.22	72.76
d_p^*	dimensionless	4.58	3.98	3.93	3.42	5.60	4.86	4.79	4.17
U^*	dimensionless	3.12	0.13	2.61	0.13	2.88	0.12	2.41	0.12
Regime	NA	FF	BB	FF	BB	FF	BB	FF	BB

*) FF = fast fluidized; BB = bubbling bed

Appendix I. Standard operation procedures of the DFB gasifier

This SOP is aimed to provide guidance for operators to appropriately and safely operate with the DFB gasifier. This includes general and detailed explanations before, during and after running the pilot scale rig.

I.1. Pre-experiment

Three days before planned experiment			
1	Let fire engineering know we need the lab facilities		
2	Email we want to run a test to:		
	Prof. Shusheng Pang	shusheng.pang@canterbury.ac.nz	CAPE
	Leigh Richardson	leigh.richardson@canterbury.ac.nz	CAPE
	Tim Moore	tim.moore@canterbury.ac.nz	CAPE
	Stephen Beuzenberg	stephen.beuzenberg@canterbury.ac.nz	CAPE
	Alfred Herritsch	alfred.herritsch@canterbury.ac.nz	CAPE
	Grant Dunlop	grant.dunlop@canterbury.ac.nz	Engineering & Science Annex Rm 200D
3	Check blower availability		
4	Check both Liquefied Petroleum Gas (LPG) cylinders have enough fuel to run		

5	Book use of boiler in workshop logbook
6	Schedule clear, clashes sorted
7	Ensure enough SPE columns are available

I.2 During experiment

Pre-run Checks	
1	Fill 10 kg bed material (Silica sand or Olivine sand) through sand charger into CFB column.
2	Display sign on combustion lab door.
3	Open roller door to particle lab.
4	Screw feeder connected, valve closed (V13).
5	Open black pneumatic valve for photocell and control valve air.
6	Extractor duct open for gasifier lab extraction system.
7	Extractor fan "E1 & E2" on.
8	"Fire Hood Fan" on (should read 65% or higher).
9	Safety glasses and labs jacket are always on.

Air Start-up	
1	Start computer for temperature and pressure readings.
2	Vent valve in particle lab D175 1/3 open and hole covered.
3	Main red handled blower line valve in lab fully open.
4	Check rotameter valves are closed so floats do not hit stoppers.
5	Turn main power switches on to control cabinet.
6	Wait 10-30 seconds for pneumatic valves to open.
7	Turn blower on.
8	Set initial speed of the blower at 5 Hz then increase to 18-20 Hz.
9	Check the blower temperature ensure below 70^{o}C.
10	When control valves open, set rotameter flows as shown in Table I.1.
11	Compressed air (red valve) is open.
12	Controller in normal mode and faults cleared.

LPG Start-up	
1	Ensure switches (S2 & S4) are all OFF.
2	LPG on in control room to combustion lab *(switch on with the key)*.
3	Main LPG supply valve and yellow LPG valve to A/B solenoid are open.

4	Check LPG supply gauge reads 7-15 psig.
5	A/B switch at the control panel (S4) on.
6	A/B controller set to 1, push blue button.
7	Check A/B viewport for flame.
8	Open cold water valve to prevent the pyrolysis in feeding system.
9	CFB switch at the control panel (**S2)** on.
10	Open valve, turn cabinet switch to 1, push blue button.
11	Check CFB Flame visually and temperature.
12	Open air valve to CFB viewport.
13	Turn CBF controller to 2.
14	Open yellow CFB valve and needle valves (slowly).
15	Set the CFB LPG flow to 12 $L.min^{-1}$ for the first 1 hour, then increase to 26~30 $L.min^{-1}$.

General Heat up	
1	All reading monitored constantly and recorded every 30 minutes.
2	Visual inspection for flame and fluidisation every 30 minutes through viewports.
3	Check for leaks.
4	If temperatures plateau on computer, increase air & LPG for heat up.
5	Turn N_2 on low for heat up (5 $L.min^{-1}$) once temperature at #BFB1 is $\geq 500^{o}C$.
6	Check biomass pellets level in main hopper.

Charging Bed Material	
1	When the temperature at CFB1 and BFB1 reach 600 ^{o}C, feed another 20 kg of bed material through the sand charger.
2	Do the sand charging slowly with a feed rate of approximately 0.5-0.75 $kg.min^{-1}$.
3	Make sure to close the sand charger valve back prior to opening its lid.

Boiler Start-up	
1	Check particle lab steam valve is open in room D113.
2	Get boiler room key from mechanical workshop & return afterwards.
3	Check water level in sight tube.
4	Turn boiler “burner” switch on in boiler room.
5	Fill in boiler use book in boiler room (run times, project and initial).

Swapping Air with Steam	
1	Swap the air supply with steam when the temperature at BFB1 is at least 50 ^{o}C higher than the target temperature of gasification (~700^{o}C)
2	Turn trace heating (TH) switch at the control panel on.
3	Turn TH1 and TH2 switches on.
4	Open the main steam valve gradually, while keeping all the other valves over the steam pipe closed.
5	Draw condensed steam through disposing valve for 10-15 seconds.
6	Swap the air supply progressively with the steam at the BFB distribution, syphon, and chute.
7	Check the circulation of bed material to see if the fluidisation is still acceptable.

Wood Feeder Start-up	
1	After swapping the air supply with steam, start feeding the biomass when the temperature at BFB1 is 50 ^{o}C higher than the target temperature of gasification.
2	Operator only in the lab.
3	Turn switch (S1) on (interlock will prevent auger operation).
4	Ensure circulation is adequate and no signs of blockages.
5	Turn cooling fan on for auger motor.
6	Ensure knife gate valve is shut.
7	Open main auger circular valve at the top of main screw feeder.
8	Check auger switches in forward mode (Auger will not run, unless S1 on).
9	Start feeding wood on a low setting and then increase gradually to intended feed rate.
10	Check feed port is not causing pellets to bridge.

Run hot test experiment	
1	Adjust LPG rotameter according to the BFB temperature.
2	When steady state conditions have been reached, record all plant data in a spreadsheet.
3	Supply helium (He) with a flow rate of 5 L min^{-1} before taking the gas and tar samples.
4	Take gas and tar samples, then label both samples with sample code and date.
5	Close the He valve whenever samples have been drawn.
6	Check pellets level in the main hopper regularly.
7	Add some more pellets, if required.

Shutting down the system	
1	Switch the main and in-bed augers off.
2	Swap the steam supply progressively with the air at the BFB distribution, syphon, and chute.
3	Turn off the TH1 and TH2 including that in the main control panel (S7).

4	Switch the LPG burner at the CFB column off.
5	Terminate all the air supplies, except that to syphon, sand charger and LPG burner.
6	After stopping the rotameters supplying air to the A/B, quickly shut the blower too.
7	Wait for the residual producer gas to be completely burnt for 4-5 minutes, then switch the A/B off.
8	Set the rotameter reading for the N_2 supply to level 1.
9	Leave the cooling water flow to induce the temperature decrease along the in-bed auger.
10	Shut down the boiler. To do so, follow the instruction in the boiler room.
11	Turn the main control panel, LPG Key and fan hood off.
12	Turn off the lights both in the gasifier and control rooms.
13	Do general check to make sure the laboratory is safe to be left.

Table I.1. Air flow rate in various condition.

No	Location	Heat up	When BFB1 Temperature ≥ 500°C	When the Steam is Supplied
1	Rotameter A/B Dilution	12	12	12
2	Rotameter A/B Main	6	6	6
3	Rotameter A/B Pilot	4	4	4
4	Rotameter Chute	20	20	-
5	Rotameter BFB fluidisation	20	20	-
6	Rotameter Primary air	16-17	9-10	9-10
7	Rotameter Syphon	20	20	20
8	Rotameter Secondary air	15-16	15-16	15-16

I.3. Post-experiment

Gasifier Cleaning Procedure	
1	Make sure to screw all the nuts and bolts using finger-tighten first, before fasten them using the spanners.
2	Make sure all the valves on the whole system are fully closed before starting cleaning up the system.
	Cleaning up the CFB and BFB Columns
3	Place a hand pallet with a big plastic bag on it or tarpaulin underneath the pallet at the bottom of BFB column base to collect the bed material coming from this cylinder.
4	Open the two nuts connecting BFB column to LPG line and BFB distribution air using two adjustable spanners.
5	Disengage gently the bottom cap of the BFB column by unscrewing bolts surrounding its cylindrical area using spanner no. 18 or 19.
6	Let the bed material flowing down onto the plastic bag and wait for approximately 3 minutes to get all of the sand out of the column.

7	Pour the bed material into a known mass bucket carefully and then measure their weight
8	Put the detached bottom part of the BFB cylinder in a more spacious area for further cleaning process
9	Clean every nozzle and hole using the compressed air, undo the big nut at the end of the BFB column, clean it, and then put it back on.
10	Repeat step 3 to 9 to clean bed material from the CFB column.
	Clean up the CFB Burner
11	Open the pin and remove the cable on the top of the burner from which it is connected to the LPG switch controller.
12	Detach the yellow and blue hose supplying air, respectively, from the LPG burner.
13	Undo the two bolts or nuts using two spanners no. 15 over their two sides.
14	Remove the LPG burner from the CFB column by pulling it up gently.
15	Check the burner column over the CFB cylinder for any agglomeration formed during the hot test run.
16	Clean the whole parts of the burner with compressed air.
17	Use sand paper to remove ash covering the ignitor.
	Clean up the A/B Ignitor
18	Take the pipe supplying air to the pilot burner off by unscrewing its nut using a screw driver.
19	Detach the yellow pipe supplying LPG using two adjustable spanners.
20	Remove two small black hoses from their ports.
21	Remove the flame censor by unscrewing it using fingers.
22	Detach the base of the A/B by unscrewing all 8 nuts with spanner.
23	Clean all parts of the A/B base with compressed air.
24	Use sand paper to remove ash covering the ignitor.
25	Put the base back on along with attaching all of its components.
	Clean up the Censor Ports
26	The next step is cleaning the bed material residues that are trapped in the line of pressure sensors surrounding the BFB and CFB columns.
27	Place two buckets underneath the CFB and BFB cylinders to accommodate the residue flowing out of the bottom part of those two columns.
28	Disconnect the small yellow hose by pushing down the rubber seal while pulling up the hose gently and pushing down its ring.
29	Supply the compressed air through the small hole of the pipe for at least 3 to 5 seconds.
30	Put the yellow hose back on to its hole, and then do the same for the rest of the yellow hoses.
	Clean up the Ash Container
31	Place the hand pallet underneath the container.
32	Unscrew all the nuts at the top of its surrounding cylindrical area with fingers.
33	Take all the carbon-containing ash out of the container and place them into a disposable plastic bag.
34	Put the cleaned container back on to the ash collector end.
35	Tighten the nuts and bolts gently using fingers.
	Install the CFB Burner Back
36	Put the yellow and blue hoses back on to the burner.

37	Install the CFB burner cable back and activate its pin.

Appendix J. The procedures of tar standard calibration, tar extraction and tar compounds analysis

J.1. Solution preparation for tar standard calibration.

J.1.1. General instruction

1) Prepare stock internal standard (IS) solution of approximately 400 ppm. Separate the solution in as many as 20 ml vials as required.

2) Use GC to check consistency of the IS peaks. Discard deviated standards if required.

3) Dilute Light Tar (LT) and Heavy Tar (HT) Standards (2000 ppm) into concentrations of 1000 ppm. Similarly, separate the solution in several 2 ml vials. The detailed procedures for this are given in Section J.1.3.1 and J.1.3.2.

4) Prepare the pre-determined tar standard concentrations by mixing required volume of 1000 ppm LT and HT solutions into 2 ml vials. The detailed procedures for this are given in Section J.1.3.3.

   NOTE: Add the IS solution to the mixture of the tar standards ONLY when they are ready to be used. Make sure to use the same IS solution for tar calibration and tar sample analysis.

J.1.2. Preparation steps for internal standard solution

1) Pipette 0.1 ml of dodecane into a 25 ml volumetric flask using 20-200 µl pipette.

2) Fill DCM into the volumetric flask until the marked line. This should make a 25 ml of 4000 ppm dodecane solution.

3) Transfer 10 ml of 4000 ppm dodecane into a 10 ml volumetric flask until marked line.

4) Then, transfer the 10 ml solution into a 100 ml volumetric flask. Fill DCM into the volumetric flask until marked line to produce 100 ml of 400 ppm IS solution.

5) Transfer the prepared IS solution into several 20 ml vials. Then close their lids.

6) Label the prepared IS in the vials and store them in a fridge for being used during tar standard calibration and tar sample analysis.

J.1.3. Preparation steps for tar standard solutions

Two types of tar standards are used in this experiment, Heavy Tar and Light Tar, coming in a 1 ml and 2 ml containers, respectively.

J.1.3.1. Dilution of LT standard mix

1) Break LT standard mix ampule containing 2 ml of 2000 ppm light tar components.

2) Using disposable pipette, quickly transfer ampule content into a 3 ml centrifuge tube and replace its cap. Label and store the centrifuge tube in fridge if required.

3) When ready, use a 1000 µl pipette to transfer 900 µl of LT standard into a 2 ml vial. Then replace its lid. Repeat this to a second 2 ml vial to use 1800 µl of the LT standard. NOTE: The remaining 200 µl of the standard may not be utilized as it is impossible to extract the ampule completely.

4) Pipette 900 µl of DCM into each vial to dilute the tar standard mix to 1000 µl.

5) Label and store the prepared standard in a fridge.

J.1.3.2. Dilution of HT standard mix

1) Break HT standard mix ampule containing 1ml of 2000 ppm heavy tar components.

2) Using the 1000 µl pipette, transfer 400 µl of HT standard into a 2 ml vial. Then replace its lid. Repeat this to another vial to use 800 µl of the HT standard. NOTE: The remaining 200 µl of the standard may not be utilized as it is impossible to extract the ampule completely.

3) Pipette 400 µl of DCM into each vial to dilute the tar standard mix to 1000 ppm.

4) Label and store the prepared standard in a fridge.

J.1.3.3. Preparation steps for pre-determined concentration of tar standard

1) 0.1 ml of 1000 ppm LT standard + 0.1 ml 1000 ppm HT standard + 0.8 ml DCM = 1 ml of 100 ppm LT-HT solution

2) 0.05 ml of 100 ppm LT-HT + 0.1 ml IS + 0.85 ml DCM = 1 ml of 5 ppm LT-HT-IS solution

3) 0.1 ml of 100 ppm LT-HT + 0.1 ml IS + 0.8 ml DCM = 1 ml of 10 ppm LT-HT-IS solution

4) 0.2 ml of 100 ppm LT-HT + 0.1 ml IS + 0.7 ml DCM = 1 ml of 20 ppm LT-HT-IS solution

5) 0.4 ml of 100 ppm LT-HT + 0.1 ml IS + 0.5 ml DCM = 1 ml of 40 ppm LT-HT-IS solution

6) 0.6 ml of 100 ppm LT-HT + 0.1 ml IS + 0.3 ml DCM = 1 ml of 60 ppm LT-HT-IS solution

7) 0.8 ml of 100 ppm LT-HT + 0.1 ml IS + 0.1 ml DCM = 1 ml of 100 ppm LT-HT-IS solution

8) 0.2 ml of 1000 ppm LT standard + 0.2 ml 1000 ppm HT standard + 0.6 ml DCM = 1 ml of 200 ppm LT-HT solution

9) 0.6 ml of 200 ppm LT-HT + 0.1 ml IS + 0.3 ml DCM = 1 ml of 120 ppm LT-HT-IS solution

J.2. Tar calibration

Tar calibration is carried out to generate essential information related to individual species of tar in the tar standard. This is performed by analysing a set of known concentrations of the tar standard in the GC to determine the retention times of each tar compounds and their signal counts corresponding to the various known concentrations.

To compensate errors from the sample introduction into the GC such as injection, rapid evaporation and transfer to the column, an internal standard is used. In this experiment, dodecane is used as the internal standard with a fixed concentration of 40 ppm, which is added to the prepared solution of both tar standard and tar sample. A standard curve is then established by plotting the values of the signal counts ratios between each tar component and the internal standard with their retention times. Example of information gathered from tar calibration and the resulted standard curves used in this work are presented in Table J.1 and J.2 as well as Figure J.1 and Figure J.2.

Table J.1. Retention times and signal count ratios of each tar component generated from LTM calibration.

No	Compounds	Retention Time	ECN Class	Tar Group	Signal Count					Signal Count Ratio					Correlation from Linear Equatio	
					Species Concentration (μg ml^{-1})					Species Concentration (μg ml^{-1})					Species concentration (*y-axis*)	Signal Count I (*x-axis*)
				Light (L) :	10	20	40	80	120	10	20	40	80	120		
				Heavy (H) :	5	10	20	40	60	5	10	20	40	60		
1	Benzene	2.317	2	L	6182	13325	27029	65662	83896	0.41	0.79	1.62	3.17	4.41	y =	0.0379 x
2	Toluene	3.108	3	L	9497	16278	29731	71942	87667	0.63	0.97	1.79	3.47	4.61	y =	0.0405 x
3	Pyridine	3.402	2	L	2939	7919	17785	48786	61560	0.19	0.47	1.07	2.35	3.24	y =	0.0276 x
4	p-xylene + Ethylbenzene	4.198	3	L	6317	13674	27534	70418	87491	0.42	0.81	1.65	3.40	4.60	y =	0.0398 x
5	m-xylene	4.269	3	L	12831	27905	56492	144745	179630	0.84	1.66	3.39	6.99	9.45	y =	0.0817 x
6	o-xylene	4.715	3	L	6348	13839	28222	72282	89699	0.42	0.82	1.70	3.49	4.72	y =	0.0408 x
7	Styrene	4.917	3	L	6468	13995	28241	72871	90872	0.43	0.83	1.70	3.52	4.78	y =	0.0412 x
8	Phenol	6.637	2	L	3136	8045	17808	50227	63851	0.21	0.48	1.07	2.42	3.36	y =	0.0284 x
9	Indene	7.653	4	L	5714	12699	26202	69210	84961	0.38	0.76	1.57	3.34	4.47	y =	0.0387 x
10	o-cresol (2-methylphenol)	7.800	2	L	3567	8982	19555	54613	67859	0.23	0.53	1.17	2.64	3.57	y =	0.0305 x
11	m+p-cresol (3+4-methylphenol)	8.136	2	L	5616	15383	35382	103012	128134	0.37	0.92	2.13	4.97	6.74	y =	0.0574 x
12	Naphthalene	10.172	4	H	3595	8264	16679	45676	56653	0.24	0.49	1.00	2.20	2.98	y =	0.0512 x
13	Quinoline	11.480	2	L	3375	9204	20737	58327	75682	0.22	0.55	1.25	2.82	3.98	y =	0.0334 x
14	2-Methylnaphthalene	11.648	4	H	4483	9139	18300	47801	62325	0.30	0.54	1.10	2.31	3.28	y =	0.0555 x
15	Isoquinoline	11.825	2	L	2375	7993	19385	55274	70140	0.16	0.48	1.16	2.67	3.69	y =	0.0312 x
16	1-Methylnaphthalene	12.010	4	H	4953	9392	18153	45746	58977	0.33	0.56	1.09	2.21	3.10	y =	0.0530 x
17	Biphenyl	12.935	4	L	5745	13115	27819	75157	96288	0.38	0.78	1.67	3.63	5.06	y =	0.0430 x
18	Acenaphthylene	14.297	4	H	3628	8644	17541	46075	57999	0.24	0.51	1.05	2.22	3.05	y =	0.0523 x
19	Acenapthene	14.615	4	H	3797	8869	17914	47092	58351	0.25	0.53	1.08	2.27	3.07	y =	0.0529 x
20	Fluorene	15.861	4	H	3331	8211	17802	45902	57980	0.22	0.49	1.07	2.22	3.05	y =	0.0522 x
21	Phenanthrene	18.019	4	H	3178	7755	16560	43696	56783	0.21	0.46	0.99	2.11	2.99	y =	0.0505 x
22	Anthracene	18.067	4	H	1680	9049	26201	62820	73124	0.11	0.54	1.57	3.03	3.85	y =	0.0680 x
23	Fluoranthene	19.272	5	H	7071	13147	21327	55077	62668	0.47	0.78	1.28	2.66	3.30	y =	0.0594 x
24	Pyrene	19.507	5	H	12799	15510	22770	111157	108150	0.84	0.92	1.37	5.36	5.69	y =	0.1042 x
25	Bens(a)anthracene	-	5	H	-	-	-	-	-	-	-	-	-	-	-	-
26	Chrysene	-	5	H	-	-	-	-	-	-	-	-	-	-	-	-
27	Benso(b)fluoranthene	-	5	H	-	-	-	-	-	-	-	-	-	-	-	-
28	Benso(k)fluoranthene	-	5	H	-	-	-	-	-	-	-	-	-	-	-	-
29	Benso(a)Pyrene	-	5	H	-	-	-	-	-	-	-	-	-	-	-	-
30	Indeno(1,2,3-cd)pyrene	-	5	H	-	-	-	-	-	-	-	-	-	-	-	-
31	Benso(g,h,i)perylene	-	5	H	-	-	-	-	-	-	-	-	-	-	-	-
32	Dibenso(a,h)anthracene	-	5	H	-	-	-	-	-	-	-	-	-	-	-	-
	Dodecane (internal standard)	7.330			15186	16810	16650	20720	19011							

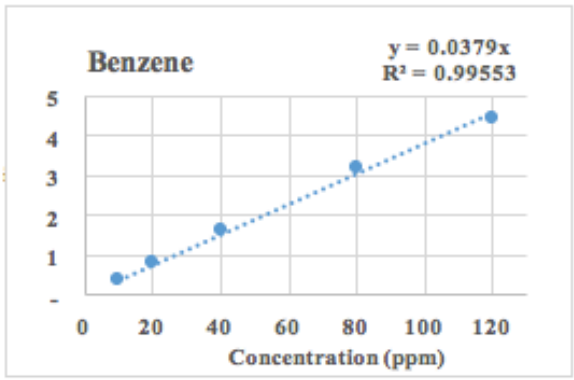

(A)

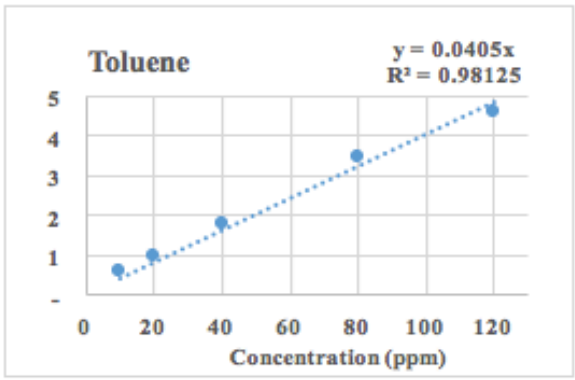

(B)

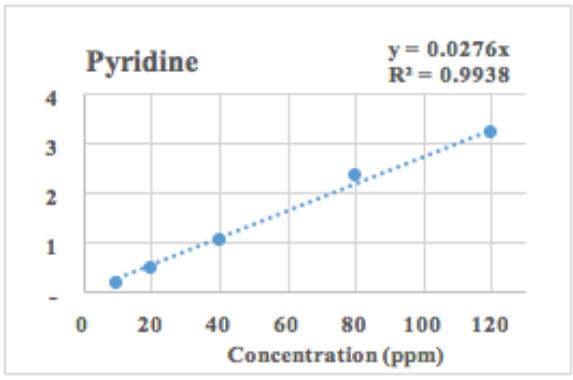

(C)

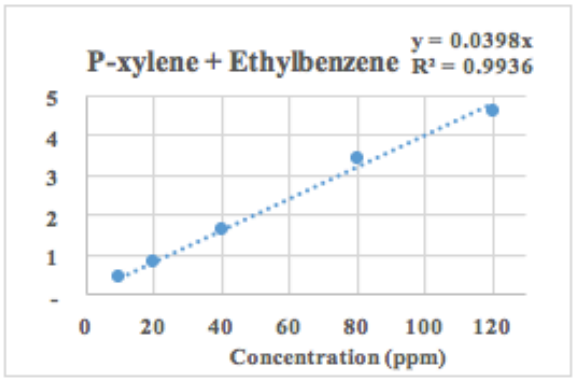

(D)

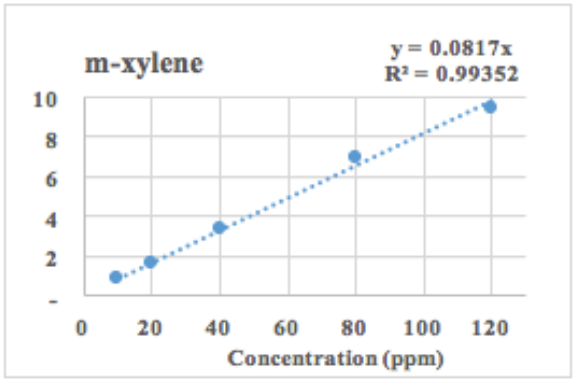

(E)

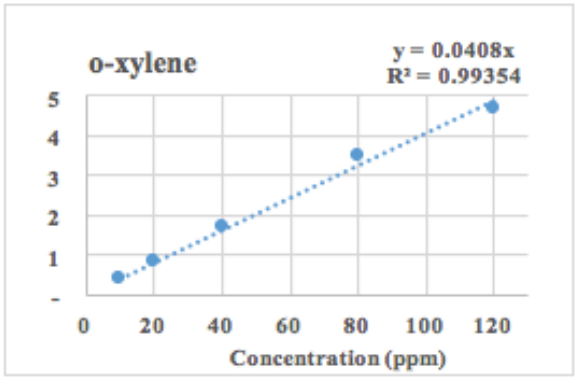

(F)

Figure J.1. Standard curves of each tar compound: (A) benzene; (B) toluene; (C) pyridine; (D) p-xylene + ethylbenzene; (E) m-xylene; (F) 0-xylene.

Table J.2. Retention times and signal count ratios of each tar component generated from HTM calibration.

No	Compounds	Retention Time	ECN Class	Tar Group	Signal Count					Signal Count Ratio					Correlation from Linear Equation	
					Species Concentration (µg ml^{-1})					Species Concentration (µg ml^{-1})					Species concentration (*y-axis*)	Signal Count Ratio (*x-axis*)
				Light (L) :	10	20	40	80	120	10	20	40	80	120		
				Heavy (H) :	5	10	20	40	60	5	10	20	40	60		
1	Benzene	-	2	L	-	-	-	-	-	-	-	-	-	-	-	-
2	Toluene	-	3	L	-	-	-	-	-	-	-	-	-	-	-	-
3	Pyridine	-	2	L	-	-	-	-	-	-	-	-	-	-	-	-
4	p-xylene + Ethylbenzene	-	3	L	-	-	-	-	-	-	-	-	-	-	-	-
5	m-xylene	-	3	L	-	-	-	-	-	-	-	-	-	-	-	-
6	o-xylene	-	3	L	-	-	-	-	-	-	-	-	-	-	-	-
7	Styrene	-	3	L	-	-	-	-	-	-	-	-	-	-	-	-
8	Phenol	6.664	2	L	38884	80973	168793	419898	558855	0.18	0.39	0.88	2.01	2.85	y =	0.0239 x
9	Indene	7.678	4	L	54339	118410	237569	578419	750270	0.26	0.57	1.24	2.76	3.82	y =	0.0325 x
10	o-cresol (2-methylphenol)	7.818	2	L	41631	96765	204533	510557	672526	0.20	0.46	1.07	2.44	3.43	y =	0.0288 x
11	m+p-cresol (3+4-methylphenol)	8.162	2	L	65298	153540	337820	861188	1150009	0.31	0.74	1.77	4.11	5.86	y =	0.0489 x
12	Naphthalene	10.178	4	H	42299	89703	176570	419086	540901	0.20	0.43	0.92	2.00	2.75	y =	0.0470 x
13	Quinoline	11.484	2	L	44987	97383	206306	512447	674204	0.21	0.47	1.08	2.45	3.43	y =	0.0289 x
14	2-Methylnaphthalene	11.652	4	H	46330	89803	179106	426468	551831	0.22	0.43	0.94	2.04	2.81	y =	0.0479 x
15	Isoquinoline	11.811	2	L	33834	81219	179989	465218	619577	0.16	0.39	0.94	2.22	3.16	y =	0.0264 x
16	1-Methylnaphthalene	12.015	4	H	41675	88933	175309	408398	523247	0.20	0.43	0.92	1.95	2.66	y =	0.0457 x
17	Biphenyl	12.938	4	L	66764	142055	284557	680240	883711	0.31	0.68	1.49	3.25	4.50	y =	0.0383 x
18	Acenaphthylene	14.298	4	H	41512	87472	176984	414939	535399	0.19	0.42	0.93	1.98	2.73	y =	0.0466 x
19	Acenapthene	14.615	4	H	38474	83200	171201	409607	533394	0.18	0.40	0.90	1.96	2.72	y =	0.0461 x
20	Fluorene	15.848	4	H	32288	69170	147739	365160	483236	0.15	0.33	0.77	1.74	2.46	y =	0.0414 x
21	Phenanthrene	18.012	4	H	30435	64138	138469	344260	453078	0.14	0.31	0.72	1.64	2.31	y =	0.0389 x
22	Anthracene	18.058	4	H	29253	84664	140243	340428	442498	0.14	0.41	0.73	1.63	2.25	y =	0.0384 x
23	Fluoranthene	19.269	5	H	31782	73336	135911	332491	435558	0.15	0.35	0.71	1.59	2.22	y =	0.0376 x
24	Pyrene	19.505	5	H	32605	129306	157155	365987	475017	0.15	0.62	0.82	1.75	2.42	y =	0.0417 x
25	Bens(a)anthracene	20.435	5	H	26682	53824	110124	272175	351652	0.13	0.26	0.58	1.30	1.79	y =	0.0304 x
26	Chrysene	20.512	5	H	22911	137605	151288	346324	429336	0.11	0.66	0.79	1.65	2.19	y =	0.0385 x
27	Benso(b)fluoranthene	21.582	5	H	24256	53930	106763	271832	362985	0.11	0.26	0.56	1.30	1.85	y =	0.0310 x
28	Benso(k)fluoranthene	21.611	5	H	29346	93263	121732	298031	368767	0.14	0.45	0.64	1.42	1.88	y =	0.0328 x
29	Benso(a)Pyrene	22.168	5	H	25603	86004	123683	380694	456710	0.12	0.41	0.65	1.82	2.33	y =	0.0402 x
30	Indeno(1,2,3-cd)pyrene	24.044	5	H	8497	26021	61155	211712	294058	0.04	0.12	0.32	1.01	1.50	y =	0.0241 x
31	Benso(g,h,i)perylene	24.118	5	H	26386	45618	83165	269816	339589	0.12	0.22	0.44	1.29	1.73	y =	0.0291 x
32	Dibenso(a,h)anthracene	24.945	5	H	25848	48959	87165	394175	467557	0.12	0.23	0.46	1.88	2.38	y =	0.0402 x
	Dodecane (Internal Standard)	7.363	-	-	213000	208847	191065	209292	196346							

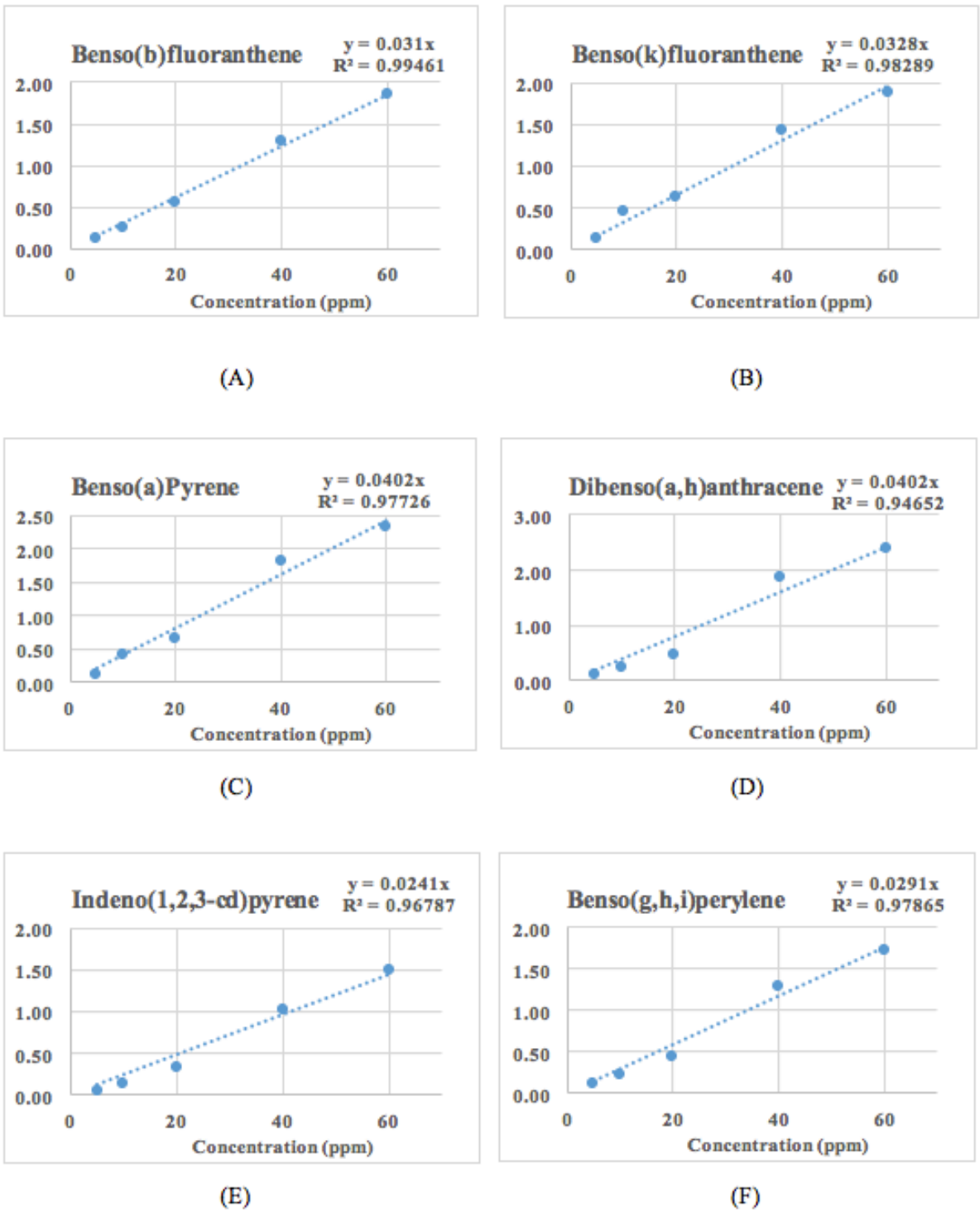

Figure J.2. Standard curves of each tar compound; (a) benso(b)fluoranthene; (b) benso(k)fluoranthene; (c) benso(as)pyrene; (d) dibenso(a,h)antrachene; (e) indeno(1,2,3-cd)pyrene; (f) benso(g,h,i)perylene.

J.3. Tar extraction

J.3.1. Solvent preparation steps for tar extraction

The procedures of preparing the mixture of DCM and IPA are as follows:

1) Fill DCM into a 100 ml volumetric flask until marked line, and then transfer this solvent into a 200 ml volumetric flask.
2) Fill IPA into the 200 ml volumetric flask containing 100 ml DCM until marked line. This should give 200 ml DCM-IPA (50:50 vol. %)
3) Transfer the solvent mixture into 250 ml glass container and replace its lid.
4) Label and store the solvent mixture into a fire safety container. It is ready to be used for tar sample extraction.

J.3.2. Procedures to extract the tar from the SPE tube

1) Weight the mass of two empty 2 ml vials with their lids. Record the values.
2) Clamp the SPE column on a retort stand.
3) Clamp the sampling rod used in sampling on a second retort stand. Place the rod vertically and should be positioned above the SPE column.
4) Place the first 2 ml vial under the SPE column, ready for sample extraction.
5) Then, draw 1 ml of the prepared DCM using 1000 µl pipette and inject into the sampling rode hole. The solvent will flush the rod while flowing downward into the SPE tube.
6) Connect a syringe to the SPE tube using a connector and force the solution in the SPE tube through the packed bed into the 2 ml vial. NOTE: Do this ONCE only to minimise the possible error due to the solvent evaporation.
7) Close the vial using its lid.

8) Repeat steps 4-7 using 1 ml DMC-IPA (50:50 vol. %) for the same SPE tube into the second 2 ml vial.

9) Shake the two vials rigorously to get a perfect mixture of the tar sample solution.

10) Weight the mass of both vials containing tar sample solutions. Record their final masses.

11) Mass of tar sample solution (including the solvent) inside the 2 ml vial is the mass difference of the vial before and after tar extraction.

J.3.3. Preparation steps for tar sample analysis in GC

1) Draw 0.45 ml of tar sample solution from the first 2 ml, then inject into an empty 2 ml vial.

2) Add 0.05 ml of 400 ppm IS solution into the vial, making its concentration to become 40 ppm.

3) Then, shake the vial rigorously to mix the tar sample and IS solution.

4) Repeat steps 1-3 for the other sample in another empty vial

5) Place the vials in GC sample holder. Turn the GC and follow the instruction for its operation.

6) Analyse the samples with GC using the method explained in Section J.4.

J.4. GC-column settings

J.4.1. Column conditioning

At this stage, any residues and contaminants from the previous experiments are removed by gradually heating up the column until the temperature reaches 340^{o}C in three different

conditions. Normally, it takes up to 80 minutes to complete this process as described in the following table.

Table J.3. The condition of column oven for the conditioning.

Condition	Temperature (^{o}C)	Rate (^{o}C min^{-1})	Hold (min)	Total (min)
1	50	-	1	1
2	210	10	0	17
3	340	50	60	79.60

The procedures for column conditioning are as follows:

1) Fill one 2 ml vial with pure DCM and close the lid.
2) Place the vial in GC sample holder.
3) In the GC software, activate the method using 'column conditioning'.
4) Complete required information and click start sample.

J.4.2. Light Tar Method

Light tar method (LTM) is the set-up of GC column and split ratio specifically designed to focus on the light tar compounds in the producer gas. In this method, the tar samples are heated up inside the GC column at several temperature conditions with split ratio as presented in Table J.4 and Table J.5. Generally, it takes up to 30 minutes to complete this process.

Table J.4. The condition of column oven for the LTM and HTM.

Condition	Temperature (^{o}C)	Rate (^{o}C min^{-1})	Hold (min)	Total (min)
1	50	-	1.00	1.00
2	210	10.0	0.00	17.00
3	340	50.0	11.00	30.60

Table J.5. Split ratio for LTM.

Condition	Time	Split State	Split Ratio
1	Initial		20
2	-	-	-

J.4.3. Heavy Tar Method

Heavy tar method (HTM) is the set-up of GC column and split ratio specifically designed to focus on the heavy tar compounds in the producer gas. While the column conditions in HTM is the same as those in LTM, their split ratio is different from each other. Table J.6 presents the split ratio conditions in HTM. Generally, it takes up to 30 minutes to complete this process.

Table J.6. Split ratio for LTM

Condition	Time	Split State	Split Ratio
1	Initial	On	20
2	0.00	Off	Off
3	2.00	On	50
4	5.00	On	20
5	-	-	-

J.5. Determination of individual tar concentration mass (g) and volume (ml)

The following calculation aims to explain how tar concentration and yield are determined.

Assumptions:

1) The effect of mass or volume of the tar compounds in the sample solution is negligible due to their small concentration.
2) The density of the tar sample is assumed to be the same as that of the solvent used the tar extraction.

3) The LTM is used to specifically measure the light tar compounds focusing on benzene, toluene, pyridine, p-xylene + ethylbenzene, m-xylene, o-xylene and styrene.

4) The LTM is used to specifically measure the heavy tar compounds focusing on bens(a)anthracene, chrysene, benso(b)fluoranthene, benso(k)fluoranthene, benso(a)pyrene, indeno(1,2,3-cd)pyrene, benso(g,h,i)perylene and dibenso(a,h)anthracene.

5) For other tar compounds, the concentration measured is determined from the average value of tar concentration calculated from LTM and HTM.

Benzene, phenol and chrysene are taken for the example of the quantitative calculation.

1 ppm = 1 µl L^{-1} = 1 mg L^{-1} = 1 ml m^{-3} = 1 mg kg^{-1}

ρ_{DCM} = 1.32 g ml^{-1}

ρ_{IPA} = 0.78 g ml^{-1}

$$\rho_{DCM\text{-}IPA}\ (50{:}50\ \text{vol.}\%) = \frac{\text{mass of 1 ml DCM (g)} + \text{mass of 1 ml IPA (g)}}{2\ \text{ml}}$$

$$\rho_{DCM\text{-}IPA}\ (50{:}50\ \text{vol.}\%) = \frac{1.32\ \text{g} + 0.78\ \text{g}}{2\ \text{ml}}$$

$\rho_{DCM\text{-}IPA}$ (50:50 vol.%) = 1.05 g ml^{-1}

- **Benzene**

Step 1: Signal count ratio determination.

In Table J.7, from the LTM analysis, for example, it is known that in sample 1 (or repeat 1) the signal count ratios (y) of benzene extracted with DCM and DCM-IPA are 13.40 and 0.63, respectively.

Step 2: Tar concentration determination decided from the correlation between signal count ratio and tar concentration found in the curve of tar standard calibration.

As summarised in Table J1, the LTM calibration curve for benzene gives a linear equation:

$$y = 0.0379x$$

in which y is signal count ratio, whereas x represents the tar concentration in ppm, therefore:

$$x = \frac{y}{0.0379}$$

Step 3: Calculating the mass of tar extracted with DCM and DCM-IPA.

- Tar mass from DCM extraction (T_{D0})

$$x = \frac{13.40}{0.0379}$$

$x = 353.44$ ppm $= 353.44$ mg L^{-1}

As the weighted mass of tars sample solution is 0.8023 g,

$$T_{D0}\ (\mu g) = \frac{\text{Tar concentration in ppm (mg } L^{-1}\text{) x mass of tar sample solution (g)}}{\rho_{DCM}\ (\text{g ml}^{-1})} \times \frac{1000\ \mu g}{1\ mg} \times \frac{1\ L}{1000\ ml}$$

$$T_{D0} = \frac{353.44\ \text{mg } L^{-1} \times 0.8023\ g}{1.32\ \text{g ml}^{-1}} \times \frac{1000\ \mu g}{1\ mg} \times \frac{1\ L}{1000\ ml}$$

$T_{D0} = 214.82\ \mu g$

With the same calculation procedures, the tar mass for sample in repeat 2 and repeat 3 are found to be 211.53 µg and 198.73 µg, respectively. Therefore, the average tar mass can be calculated as follows

$$T_{D0} = \frac{(214.8 + 211.53 + 198.73)\ \mu g}{3}$$

$T_{D0} = 208.36\ \mu g$

- Tar mass from DCM-IPA extraction (T_{D1})

$$x = \frac{0.63}{0.0379}$$

$x = 16.58$ ppm

As the weighted mass of tars sample solution is 1.0546 g,

$$T_{D1} = \frac{16.58\ mg\ L^{-1} \times 1.0546\ g}{1.05\ g\ ml^{-1}} \times \frac{1000\ \mu g}{1\ mg} \times \frac{1\ L}{1000\ ml}$$

$T_{D1} = 16.65\ \mu g$

With the same calculation procedures, the tar mass for sample in repeat 2 and repeat 3 are found to be 16.48 µg and 17.53 µg, respectively. Therefore, the average tar mass can be calculated as follows

$$T_{D1} = \frac{(16.65 + 16.48 + 17.53)\ \mu g}{3}$$

$T_{D1} = 16.89\ \mu g$

Step 4: Calculating the total mass of tar (T_{TM}) defining as the summation of tar mass extracted with DCM and DCM-IPA.

$T_{TM} = T_{D0} + T_{D1}$

$T_{TM} = (208.36 + 16.89)\ \mu g$

$T_{TM} = 225.25\ \mu g$

Step 5: Calculating the total tar concentration (T_{TCP}) in the sample of producer gas.

Now that the total volume of drawn tar-containing producer gas sample is 200 ml, the total tar concentration in producer can be calculated by:

$$T_{TCP} = \frac{T_{TM}}{V_{dry\text{-}pg}}$$

$$T_{TCP} = \frac{225.25\ \mu g}{200\ ml} = 1.13\ \mu g\ ml^{-1}$$

At 1 atm and $0^{o}C$,

$$T_{TCP} = \frac{1.13\ \mu g\ ml^{-1}\ x\ 273.15\ K}{303.15\ K} x\ \frac{10^{6}\ ml}{m^{3}}\ x\ \frac{10^{-6}\ g}{\mu g}$$

$$T_{TCP} = 1.01\ g\ Nm^{-3}$$

From the calculation above, it is found that the concentration of benzene is 1.01 g Nm^{-3}.

- **Phenol**

Another calculation sample is given for the tar element analysed with a combination of LTM and HTM.

- **Calculation for the LTM analysis**

Step 1: Signal count ratio determination.

In this case, phenol is taken for an example with signal count ratios of 0.07 and 29.58 obtained from respectively DCM and DCM-IPA extractions (see Table J7, Repeat 1).

Step 2: Tar concentration determination decided from the correlation between signal count ratio and tar concentration found in the curve of tar standard calibration.

The light tar calibration curve mentioned in Table J.1 gives a linear equation as follow:

$y = 0.0284x$

in which y is signal count ratio, whereas x represents the tar concentration in ppm, therefore:

$$x = \frac{y}{0.0284}$$

Step 3: Calculating the mass of tar extracted with DCM and DCM-IPA.

- Tar mass from DCM extraction (T_{D0})

$$x = \frac{0.07}{0.0379}$$

$x = 2.36$ ppm $= 2.36$ mg L^{-1}

As the weighted mass of tars sample solution is 0.8023 g,

$$T_{D0} = \frac{2.36 \text{ mg } L^{-1} \text{ x } 0.8023 \text{ g}}{1.32 \text{ g ml}^{-1}} \text{ x } \frac{1000 \text{ µg}}{1 \text{ mg}} \text{ x } \frac{1 \text{ L}}{1000 \text{ ml}}$$

$T_{D0} = 1.44$ µg

With the same calculation procedures, the tar mass for sample in repeat 2 and repeat 3 are found to be 1.41 µg and 0.70 µg, respectively. Therefore, the average tar mass can be calculated as follows

$$T_{D0} = \frac{(1.44 + 1.41 + 0.70) \text{ µg}}{3}$$

$T_{D0} = 1.18$ µg

- Tar mass from DCM-IPA extraction (T_{D1})

$$x = \frac{29.58}{0.0379}$$

$x = 1{,}041.49$ ppm

As the weighted mass of tars sample solution is 1.0546 g,

$$T_{D1} = \frac{1{,}041.49 \text{ mg L}^{-1} \text{ x } 1.0546 \text{ g}}{1.05 \text{ g ml}^{-1}} \text{ x } \frac{1000 \text{ µg}}{1 \text{ mg}} \text{ x } \frac{1 \text{ L}}{1000 \text{ ml}}$$

$T_{D1} = 1046.65$ µg

With the same calculation procedures, the tar mass for sample 2 and 3 are found to be 1,317.75 µg and 993.91 µg, respectively. Therefore, the average tar mass can be calculated as follows

$$T_{D1} = \frac{(1{,}046.65 + 1{,}317.75 + 993.91) \text{ µg}}{3}$$

$T_{D1} = 1{,}119.24$ µg

Step 4: Calculating the total mass of tar (T_{TM}) defining as the summation of tar mass extracted with DCM and DCM-IPA.

$T_{TM} = T_{D0} + T_{D1}$

$T_{TM} = (1.18 + 1{,}119.24)$ µg

$T_{TM} = 1{,}120.42$ µg

Step 5: Calculating the total tar concentration (T_{TCP}) in the sample of producer gas.

Now that the total volume of drawn tar-containing producer gas sample is 200 ml, the tar concentration in producer can be calculated by:

$$T_{TCP} = \frac{1{,}120.42\ \mu g}{200\ ml} = 5.60\ \mu g\ ml^{-1}$$

At 1 atm and $0^{o}C$,

$$T_{TCP} = \frac{5.60\ \mu g\ ml^{-1}\ x\ 273.15\ K}{303.15\ K} x\ \frac{10^{6}\ ml}{m^{3}}\ x\ \frac{10^{-6}\ g}{\mu g}$$

$$T_{TCP} = 5.04\ g\ Nm^{-3}$$

From the calculation above, it is found that the concentration of phenol (LTM) is 5.04 g Nm^{-3}.

- **Calculation for the HTM analysis**

Step 1: Signal count ratio determination.

From Table J.8 (Repeat 1), it is known that the signal count ratio of phenol in DCM is 0.18, while that with DCM-IPA is 20.54.

Step 2: Tar concentration determination decided from the correlation between signal count ratio and tar concentration found in the curve of tar standard calibration.

The light tar calibration curve mentioned in Table J.1 gives an equation as follow:

$y = 0.0239x$

in which y is signal count ratio, whereas x represents the tar concentration in ppm, therefore:

$$x = \frac{y}{0.0239}$$

Step 3: Calculating the mass of tar extracted with DCM and DCM-IPA.

- Tar mass from DCM extraction (T_{D0})

$$x = \frac{0.18}{0.0239}$$

$x = 7.55$ ppm $= 7.55$ mg L^{-1}

As the weighted mass of tars sample solution is 0.8023 g,

$$T_{D0} = \frac{7.55 \text{ mg } L^{-1} \text{ x } 0.8023 \text{ g}}{1.32 \text{ g ml}^{-1}} \text{ x } \frac{1000 \text{ µg}}{1 \text{ mg}} \text{ x } \frac{1 \text{ L}}{1000 \text{ ml}}$$

$T_{D0} = 4.59$ µg

With the same calculation procedures, the tar mass for sample in repeat 2 and repeat 3 are found to be 5.89 µg and 2.01 µg, respectively. Therefore, the average tar mass can be calculated as follows

$$T_{D0} = \frac{(4.59 + 5.89 + 2.01) \text{ µg}}{3}$$

$T_{D0} = 3.42$ µg

- Tar mass from DCM-IPA extraction (T_{D1})

$$x = \frac{20.54}{0.0239}$$

$x = 859.57$ ppm $= 859.57$ mg L^{-1}

As the weighted mass of tars sample solution is 1.0546 g,

$$T_{D1} = \frac{859.57 \text{ mg L}^{-1} \text{ x } 1.0546 \text{ g}}{1.05 \text{ g ml}^{-1}} \text{ x } \frac{1000 \text{ µg}}{1 \text{ mg}} \text{ x } \frac{1 \text{ L}}{1000 \text{ ml}}$$

$T_{D1} = 863.34$ µg

With the same calculation procedures, the tar mass for sample in repeat 2 and repeat 3 are found to be 842.74 µg and 829.44 µg, respectively. Therefore, the average tar mass can be calculated as follows

$$T_{D1} = \frac{(863.34 + 842.74 + 829.44) \text{ µg}}{3}$$

$T_{D1} = 845.17$ µg

Step 4: Calculating the total mass of tar (T_{TM}) defining as the summation of tar mass extracted with DCM and DCM-IPA.

$T_{TM} = T_{D0} + T_{D1}$

$T_{TM} = (3.42 + 845.17)$ µg

$T_{TM} = 848.59$ µg

Step 5: Calculating the total tar concentration (T_{TCP}) in the sample of producer gas.

Now that the total volume of drawn tar-containing producer gas sample is 200 ml, the tar concentration in producer can be calculated by:

$$T_{TCP} = \frac{848.59 \text{ µg}}{200 \text{ ml}} = 4.24 \text{ µg ml}^{-1}$$

At 1 atm and $0^{o}C$,

$$T_{TCP} = \frac{4.24\ \mu g\ ml^{-1}\ x\ 273.15\ K}{303.15\ K} x\ \frac{10^{6}\ ml}{m^{3}}\ x\ \frac{10^{-6}\ g}{\mu g}$$

$T_{TCP} = 3.82\ g\ Nm^{-3}$

From the calculation above, it is found that the concentration of phenol (HTM) is 3.82 g Nm^{-3}.

The final concentration of phenol is considered as the average concentration from LTM and HTM calculations, thus:

$$T_{TCP} = \frac{(5.60 + 4.24)\ g\ Nm^{-3}}{2}\ \mu g\ ml^{-1}$$

$T_{TCP} = 4.92\ \mu g\ ml^{-1} = 4.43\ g\ Nm^{-3}$

The concentration of phenol in the producer gas is found to be 4.43 g Nm^{-3}.

- **Chrysene**

Step 1: Signal count ratio determination.

From Table J.8 (Repeat 1), it is known that the signal count ratio of chrysene in DCM is 0.27, while that with DCM-IPA is 0.25.

Step 2: Tar concentration determination decided from the correlation between signal count ratio and tar concentration found in the curve of tar standard calibration.

The light tar calibration curve mentioned in J.1 gives an equation as follow:

$y = 0.0385x$

in which y is signal count ratio, whereas x represents the tar concentration in ppm, therefore:

$$x = \frac{y}{0.0385}$$

Step 3: Calculating the mass of tar extracted with DCM and DCM-IPA.

- Tar mass from DCM extraction (T_{D0})

$$x = \frac{0.27}{0.0385}$$

$x = 6.98$ ppm $= 6.98$ mg L^{-1}

As the weighted mass of tars sample solution is 0.8023 g,

$$T_{D0} = \frac{6.98 \text{ mg } L^{-1} \text{ x } 0.8023 \text{ g}}{1.32 \text{ g ml}^{-1}} \text{ x } \frac{1000 \text{ µg}}{1 \text{ mg}} \text{ x } \frac{1 \text{ L}}{1000 \text{ ml}}$$

$T_{D0} = 4.24$ µg

With the same calculation procedures, the tar mass for sample in repeat 2 and repeat 3 are found to be 2.84 µg and 2.02 µg, respectively. Therefore, the average tar mass can be calculated as follows

$$T_{D0} = \frac{(4.24 + 2.84 + 2.02) \text{ µg}}{3}$$

$T_{D0} = 3.04$ µg

- Tar mass from DCM-IPA extraction (T_{D1})

$$x = \frac{0.25}{0.0385}$$

$x = 6.40$ ppm $= 6.40$ mg L^{-1}

As the weighted mass of tars sample solution is 1.0546 g,

$$T_{D1} = \frac{6.40 \text{ mg L}^{-1} \text{ x } 1.0546 \text{ g}}{1.05 \text{ g ml}^{-1}} \text{ x } \frac{1000 \text{ µg}}{1 \text{ mg}} \text{ x } \frac{1 \text{ L}}{1000 \text{ ml}}$$

$T_{D1} = 6.43$ µg

With the same calculation procedures, the tar mass for sample in repeat 2 and repeat 3 are found to be 6.36 µg and 4.00 µg, respectively. Therefore, the average tar mass can be calculated as follows

$$T_{D1} = \frac{(6.43 + 6.36 + 4.00) \text{ µg}}{3}$$

$T_{D1} = 5.59$ µg

Step 4: Calculating the total mass of tar (T_{TM}) defining as the summation of tar mass extracted with DCM and DCM-IPA.

$T_{TM} = T_{D0} + T_{D1}$

$T_{TM} = (3.04 + 5.59)$ µg

$T_{TM} = 8.63$ µg

Step 5: Calculating the total tar concentration (T_{TCP}) in the sample of producer gas.

Now that the total volume of drawn tar-containing producer gas sample is 200 ml, the tar concentration in producer can be calculated by:

$$T_{TCP} = \frac{8.63 \text{ µg}}{200 \text{ ml}} = 0.04 \text{ µg ml}^{-1}$$

At 1 atm and 0^{o}C,

$$T_{TCP} = \frac{0.04\ \mu g\ ml^{-1}\ x\ 273.15\ K}{303.15\ K} x\ \frac{10^6\ ml}{m^3}\ x\ \frac{10^{-6}\ g}{\mu g}$$

$T_{TCP} = 0.04\ g\ Nm^{-3}$

From the calculation above, it is found that the concentration of phenol (HTM) is 0.04 g Nm^{-3}.

By following the aforementioned step 1-5 for the determination of concentration of benzene, toluene and chrysene, the concentration of other tar compounds can be determined. The whole calculated data are presented in Table J.7 and J.8, while the concentration and yield of each tar compounds are summarised in Table J.19 and J.20.

- Total tar yield (T_{TY})

From Table J.19, the tar concentration at 650^oC is 12.04 µg ml^{-1} or equal to 10.85 g Nm^{-3}. Since the producer gas volumetric flux rate (gas yield) at 650^oC is 0.50 $Nm^3\ kg^{-1}_{od}$ as presented in Table E.2, thus:

$T_{TY} = \dot{v}_{dry\text{-}pg}\ x\ T_{TCP}$

$T_{TY} = 0.05\ Nm^3\ kg^{-1}_{od}\ x\ 10.85\ g\ Nm^{-3}$

$T_{TY} = 5.39\ g\ kg^{-1}_{od}$ (at 650^oC)

Tar yields for other gasification temperature are summarised in Table J.20.

For investigated parameter 2 and 3, the summaries of tar yield and concentration are given in Table J.37 and J.45, respectively.

J.6. Tar composition data generated from hot test runs

The following tables summarise the concentration for each tar compounds detected in the extracting solvents (DCM and DCM-IPA), corresponding to the signal count ratio obtained from GC analysis.

J.6.1. Tar composition measured from the investigated parameter 1 (Experiment performed on 13th April 2017)

Table J.7. Signal count ratio and concentration of each tar compound at 650°C analysed with LTM.

No	Method	LTM																			
	Solvent	DCM				ρ_{DCM} = 1.32 g ml^{-1}				DCM-IPA						$\rho_{DCM-IPA}$ = 1.05 g ml^{-1}		Average tar mass		Tar amount	
	Category	Signal Count Ratio			Concentration					Signal Count Ratio			Concentration					DCM (G): (A+B+C) / 3	DCM-IPA (H): (D+E+F) / 3	in sample solution (I): (G+H)	in PG (I / 200)
	Repeat	1	2	3	1		2		3	1	2	3	1		2		3				
	Mass of Tar Sample Solution (g)	NA	NA	NA	0.8023		0.8212		0.8081	NA	NA	NA	1.0546		1.1132		1.0536				
	Measurement unit	NA	NA	NA	ppm	µg (A)	ppm	µg (B)	ppm	µg (C)	NA	NA	NA	ppm	µg (D)	ppm	µg (E)	ppm	µg (F)	µg	µg	µg	µg ml^{-1}
1	Benzene	13.40	12.89	12.30	353.44	214.82	340.02	211.53	324.62	198.73	0.63	0.59	0.66	16.58	16.65	15.54	16.48	17.47	17.53	208.36	16.89	225.25	1.13
2	Toluene	15.81	16.64	15.31	390.31	237.23	410.87	255.61	377.92	231.36	1.17	1.09	1.30	28.90	29.02	26.97	28.59	31.98	32.09	241.40	29.90	271.30	1.36
3	Pyridine	0.98	1.02	0.89	35.38	21.51	36.97	23.00	32.23	19.73	0.01	0.01	0.01	0.42	0.42	0.42	0.44	0.47	0.48	21.41	0.45	21.86	0.11
4	p-xylene + Ethylbenzene	1.85	2.02	1.86	46.46	28.24	50.80	31.60	46.67	28.57	0.10	0.13	0.15	2.52	2.53	3.21	3.40	3.70	3.71	29.47	3.22	32.69	0.16
5	m-xylene	3.24	3.59	3.20	39.71	24.14	43.99	27.37	39.11	23.94	0.21	0.31	0.40	2.61	2.62	3.83	4.06	4.85	4.87	25.15	3.85	29.00	0.15
6	o-xylene	1.57	1.75	1.57	38.55	23.43	42.96	26.73	38.50	23.57	0.14	0.14	0.14	3.44	3.45	3.39	3.60	3.43	3.44	24.58	3.50	28.07	0.14
7	Styrene	3.60	3.56	3.42	87.38	53.11	86.32	53.70	83.09	50.87	0.32	0.40	0.36	7.71	7.75	9.74	10.33	8.86	8.89	52.56	8.99	61.55	0.31
8	Phenol	0.07	0.06	0.03	2.36	1.44	2.27	1.41	1.14	0.70	29.58	35.30	28.13	1041.49	1046.05	1242.94	1317.75	990.52	993.91	1.18	1119.24	1120.42	5.60
9	Indene	2.27	2.30	2.25	58.61	35.62	59.31	36.90	58.15	35.60	0.24	0.22	0.23	6.29	6.32	5.65	6.00	5.87	5.89	36.04	6.07	42.11	0.21
10	o-cresol (2-methylphenol)	1.24	1.01	0.40	40.77	24.78	32.99	20.52	13.11	8.03	5.15	6.66	5.33	168.98	169.72	218.25	231.38	174.86	175.46	17.78	192.19	209.96	1.05
11	m+p-cresol (3+4-methylphenol)	0.56	0.41	0.23	9.70	5.90	7.19	4.47	3.92	2.40	15.37	18.80	14.35	267.85	269.02	327.51	347.22	250.04	250.90	4.26	289.05	293.30	1.47
12	Naphthalene	2.12	2.08	2.02	41.43	25.18	40.55	25.23	39.45	24.15	0.56	0.46	0.47	10.97	11.02	8.89	9.43	9.17	9.20	24.85	9.88	34.74	0.17
13	Quinoline	0.21	0.24	0.16	6.22	3.78	7.04	4.38	4.84	2.96	0.63	0.65	0.82	19.00	19.09	19.34	20.51	24.54	24.62	3.71	21.41	25.11	0.13
14	2-Methylnaphthalene	0.90	0.83	0.70	16.30	9.91	14.90	9.27	12.59	7.71	0.51	0.64	0.42	9.13	9.17	11.54	12.23	7.49	7.51	8.96	9.64	18.60	0.09
15	Isoquinoline	0.13	0.14	0.04	4.25	2.59	4.46	2.77	1.25	0.76	0.31	0.42	0.29	10.03	10.08	13.56	14.37	9.42	9.45	2.04	11.30	13.34	0.07
16	1-Methylnaphthalene	0.65	0.67	0.55	12.24	7.44	12.67	7.88	10.33	6.32	0.68	0.92	0.72	12.77	12.83	17.45	18.50	13.63	13.67	7.22	15.00	22.22	0.11
17	Biphenyl	0.23	0.24	0.19	5.23	3.18	5.52	3.44	4.43	2.71	1.84	2.49	2.10	42.89	43.08	57.81	61.29	48.91	49.08	3.11	51.15	54.26	0.27
18	Acenaphthylene	0.24	0.24	0.25	4.68	2.84	4.59	2.85	4.78	2.93	0.23	0.23	0.21	4.49	4.51	4.49	4.76	4.09	4.11	2.87	4.46	7.33	0.04
19	Acenapthene	0.11	0.12	0.09	2.10	1.28	2.32	1.44	1.64	1.01	0.10	0.12	0.10	1.92	1.93	2.23	2.36	1.86	1.86	1.24	2.05	3.29	0.02
20	Fluorene	0.46	0.38	0.29	8.89	5.40	7.31	4.55	5.53	3.38	0.30	0.25	0.23	5.80	5.82	4.81	5.10	4.48	4.49	4.44	5.14	9.58	0.05
21	Phenanthrene	0.35	0.32	0.28	6.96	4.23	6.36	3.96	5.57	3.41	0.36	0.25	0.31	7.05	7.08	4.86	5.15	6.16	6.18	3.87	6.14	10.00	0.05
22	Anthracene	0.16	0.22	0.13	2.38	1.45	3.17	1.97	1.90	1.16	0.11	0.10	0.10	1.58	1.59	1.54	1.63	1.40	1.40	1.53	1.54	3.07	0.02
23	Fluoranthene	0.48	0.49	0.39	8.11	4.93	8.30	5.17	6.56	4.01	0.63	0.63	0.61	10.66	10.71	10.66	11.30	10.24	10.27	4.70	10.76	15.46	0.08
24	Pyrene	0.32	0.33	0.44	3.08	1.87	3.20	1.99	4.19	2.57	0.46	0.24	0.47	4.41	4.43	2.26	2.40	4.52	4.54	2.14	3.79	5.93	0.03
25	Bens(a)anthracene																						
26	Chrysene																						
27	Benso(b)fluoranthene																						
28	Benso(k)fluoranthene																						
29	Benso(a)Pyrene																						
30	Indeno(1,2,3-cd)pyrene																						
31	Benso(g,h,i)perylene																						
32	Dibenso(a,h)anthracene																						

Table J.8. Signal count ratio and concentration of each tar compound at 650°C analysed with HTM.

No	Method	HTM																			
	Solvent	DCM				$\dot{\rho}_{DCM}$ = 1.32 g ml^{-1}				DCM-IPA						$\dot{\rho}_{DCM-IPA}$ = 1.05 g ml^{-1}				Average tar mass		Tar amount	
	Category	Signal Count Ratio			Concentration					Signal Count Ratio			Concentration							DCM (G): (A+B+C) / 3	DCM-IPA (H): (D+E+F) / 3	in sample solution (I): (G+H)	in PG (I / 200)
	Repeat	1	2	3	1		2		3				1		2		3						
	Mass of Tar Sample Solution (g)	NA	NA	NA	0.8023		0.8212		0.8081	NA	NA	NA	1.0546		1.1132		1.0536						
	Concentration unit	NA	NA	NA	ppm	µg (A)	ppm	µg (B)	ppm	µg (C)	NA	NA	NA	ppm	µg (D)	ppm	µg (E)	ppm	µg (F)	µg	µg	µg	µg ml^{-1}
1	Benzene																						
2	Toluene																						
3	Pyridine																						
4	p-xylene + Ethylbenzene																						
5	m-xylene																						
6	o-xylene																						
7	Styrene																						
8	Phenol	0.18	0.14	0.08	7.55	4.59	5.89	3.66	3.28	2.01	20.54	19.00	19.76	859.57	863.34	794.90	842.74	826.60	829.44	3.42	845.17	848.59	4.24
9	Indene	3.86	4.11	4.12	118.77	72.19	126.34	78.60	126.77	77.61	0.22	0.26	0.23	6.70	6.73	8.00	8.48	7.02	7.05	76.13	7.42	83.55	0.42
10	o-cresol (2-methylphenol)	0.20	0.29	0.16	6.93	4.21	10.03	6.24	5.73	3.51	3.93	3.66	3.84	136.29	136.89	126.98	134.63	133.19	133.65	4.65	135.05	139.71	0.70
11	m+p-cresol (3+4-methylphenol)	0.47	0.51	0.47	9.60	5.83	10.53	6.55	9.64	5.90	9.99	9.10	9.82	204.37	205.26	186.13	197.33	200.73	201.42	6.10	201.34	207.43	1.04
12	Naphthalene	3.48	3.33	3.64	73.99	44.97	70.81	44.05	77.50	47.45	0.55	0.82	0.77	11.64	11.70	17.52	18.57	16.33	16.39	45.49	15.55	61.04	0.31
13	Quinoline	0.18	0.14	0.06	6.10	3.71	4.76	2.96	2.13	1.30	0.21	0.27	0.21	7.42	7.45	9.33	9.90	7.21	7.23	2.66	8.19	10.85	0.05
14	2-Methylnaphthalene	0.71	0.76	0.73	14.74	8.96	15.85	9.86	15.19	9.30	0.35	0.45	0.44	7.28	7.31	9.40	9.97	9.29	9.32	9.37	8.87	18.24	0.09
15	Isoquinoline	1.05	0.97	1.04	39.69	24.13	36.86	22.93	39.50	24.18	0.15	0.14	0.16	5.62	5.64	5.22	5.53	6.03	6.05	23.75	5.74	29.49	0.15
16	1-Methylnaphthalene	0.87	0.76	0.84	19.04	11.57	16.64	10.35	18.35	11.23	0.47	0.48	0.50	10.36	10.41	10.53	11.16	10.96	11.00	11.05	10.86	21.91	0.11
17	Biphenyl	0.28	0.26	0.27	7.27	4.42	6.90	4.29	7.02	4.30	1.08	0.83	0.90	28.20	28.33	21.78	23.09	23.60	23.68	4.34	25.03	29.37	0.15
18	Acenaphthylene	0.59	0.56	0.68	12.67	7.70	12.03	7.48	14.53	8.89	0.31	0.36	0.39	6.75	6.78	7.82	8.29	8.27	8.30	8.02	7.79	15.82	0.08
19	Acenapthene	0.15	0.13	0.13	3.32	2.02	2.92	1.81	2.82	1.73	0.08	0.09	0.10	1.65	1.66	1.90	2.01	2.06	2.07	1.85	1.91	3.77	0.02
20	Fluorene	0.61	0.58	0.56	14.76	8.97	14.13	8.79	13.64	8.35	0.25	0.30	0.31	5.96	5.99	7.27	7.71	7.56	7.59	8.70	7.09	15.80	0.08
21	Phenanthrene	0.50	0.45	0.41	12.85	7.81	11.51	7.16	10.47	6.41	0.25	0.28	0.28	6.43	6.45	7.13	7.56	7.19	7.22	7.13	7.08	14.20	0.07
22	Anthracene	0.30	0.25	0.23	7.74	4.70	6.48	4.03	5.91	3.62	0.09	0.11	0.09	2.40	2.41	2.78	2.95	2.45	2.46	4.12	2.61	6.72	0.03
23	Fluoranthene	0.41	0.34	0.28	10.84	6.59	9.08	5.65	7.38	4.52	0.25	0.24	0.24	6.52	6.55	6.45	6.84	6.28	6.30	5.59	6.57	12.15	0.06
24	Pyrene	0.26	0.22	0.19	6.34	3.86	5.35	3.33	4.47	2.73	0.25	0.23	0.22	5.97	6.00	5.62	5.96	5.36	5.37	3.31	5.78	9.08	0.05
25	Bens(a)anthracene	0.16	0.13	0.10	5.11	3.10	4.29	2.67	3.23	1.98	0.10	0.09	0.09	3.20	3.21	3.01	3.19	2.88	2.89	2.58	3.10	5.68	0.03
26	Chrysene	0.27	0.18	0.13	6.98	4.24	4.56	2.84	3.30	2.02	0.25	0.23	0.15	6.40	6.43	6.00	6.36	3.98	4.00	3.04	5.59	8.63	0.04
27	Benso(b)fluoranthene	0.10	0.08	0.07	3.15	1.91	2.65	1.65	2.29	1.40	0.11	0.12	0.11	3.45	3.46	3.88	4.11	3.48	3.49	1.65	3.69	5.34	0.03
28	Benso(k)fluoranthene	0.06	0.06	0.05	1.97	1.20	1.83	1.14	1.38	0.84	0.08	0.08	0.08	2.45	2.46	2.47	2.62	2.34	2.35	1.06	2.48	3.54	0.02
29	Benso(a)Pyrene	0.05	0.05	0.04	1.27	0.77	1.30	0.81	0.95	0.58	0.08	0.09	0.09	2.06	2.06	2.23	2.37	2.29	2.30	0.72	2.24	2.96	0.01
30	Indeno(1,2,3-cd)pyrene	0.00	0.01	0.00	0.05	0.03	0.54	0.33	0.16	0.10	0.04	0.01	0.05	1.52	1.52	0.54	0.57	1.92	1.92	0.15	1.34	1.49	0.01
31	Benso(g,h,i)perylene	0.01	0.03	0.01	0.28	0.17	1.01	0.63	0.36	0.22	0.03	0.03	0.04	1.06	1.07	1.10	1.16	1.33	1.33	0.34	1.19	1.53	0.01
32	Dibenso(a,h)anthracene	0.01	0.03	0.01	0.24	0.15	0.74	0.46	0.24	0.15	0.03	0.06	0.07	0.73	0.73	1.40	1.49	1.66	1.67	0.25	1.30	1.55	0.01

Table J.9. Total tar concentration for each tar compounds at 650^{o}C.

No	Tar component	Tar concentration (µg ml^{-1})		Average (µg ml^{-1})	Total tar (µg ml^{-1})
		LTM	HTM		
1	Benzene	1.13			1.13
2	Toluene	1.36			1.36
3	Pyridine	0.11			0.11
4	p-xylene + Ethylbenzene	0.16			0.16
5	m-xylene	0.15			0.15
6	o-xylene	0.14			0.14
7	Styrene	0.31			0.31
8	Phenol	5.60	4.24	4.92	4.92
9	Indene	0.21	0.42	0.31	0.31
10	o-cresol (2-methylphenol)	1.05	0.70	0.87	0.87
11	m+p-cresol (3+4-methylphenol)	1.47	1.04	1.25	1.25
12	Naphthalene	0.17	0.31	0.24	0.24
13	Quinoline	0.13	0.05	0.09	0.09
14	2-Methylnaphthalene	0.09	0.09	0.09	0.09
15	Isoquinoline	0.07	0.15	0.11	0.11
16	1-Methylnaphthalene	0.11	0.11	0.11	0.11
17	Biphenyl	0.27	0.15	0.21	0.21
18	Acenaphthylene	0.04	0.08	0.06	0.06
19	Acenapthene	0.02	0.02	0.02	0.02
20	Fluorene	0.05	0.08	0.06	0.06
21	Phenanthrene	0.05	0.07	0.06	0.06
22	Anthracene	0.02	0.03	0.02	0.02
23	Fluoranthene	0.08	0.06	0.07	0.07
24	Pyrene	0.03	0.05	0.04	0.04
25	Bens(a)anthracene		0.03		0.03
26	Chrysene		0.04		0.04
27	Benso(b)fluoranthene		0.03		0.03
28	Benso(k)fluoranthene		0.02		0.02
29	Benso(a)Pyrene		0.01		0.01
30	Indeno(1,2,3-cd)pyrene		0.01		0.01
31	Benso(g,h,i)perylene		0.01		0.01
32	Dibenso(a,h)anthracene		0.01		0.01

Table J.10. Signal count ratio and concentration of each tar compound at 700°C analysed with LTM.

No	Method	LTM																				
	Solvent	DCM					ρ_{DCM} = 1.32 g ml^{-1}				DCM-IPA					$\rho_{DCM-IPA}$ = 1.05 g ml^{-1}				Average tar mass		Tar amount	
	Category	Signal Count Ratio			Concentration						Signal Count Ratio			Concentration						DCM (G): (A+B+C) / 3	DCM-IPA (H): (D+E+F) / 3	in sample solution (I): (G+H)	in PG (I / 200)
	Repeat	1	2	3	1		2		3		1	2	3	1		2		3					
	Mass of Tar Sample Solution (g)	NA	NA	NA	0.8321		0.7671		0.7722		NA	NA	NA	1.0787		0.9757		1.0552					
	Concentration unit	NA	NA	NA	ppm	µg (A)	ppm	µg (B)	ppm	µg (C)	NA	NA	NA	ppm	µg (D)	ppm	µg (E)	ppm	µg (F)	µg	µg	µg	µg ml^{-1}
1	Benzene	23.11	25.66	25.58	609.89	384.46	676.93	393.39	674.84	394.78	0.62	0.47	0.48	16.33	16.78	12.47	11.59	12.74	12.80	390.88	13.72	404.60	2.02
2	Toluene	18.78	19.51	19.43	463.63	292.26	481.80	279.99	479.65	280.60	0.93	0.21	0.73	22.96	23.59	5.24	4.87	18.08	18.17	284.28	15.54	299.82	1.50
3	Pyridine	0.70	0.43	0.29	25.27	15.93	15.45	8.98	10.41	6.09	0.24	0.36	0.49	8.71	8.95	13.16	12.23	17.84	17.92	10.33	13.03	23.37	0.12
4	p-xylene + Ethylbenzene	1.96	1.96	1.96	49.29	31.07	49.24	28.62	49.21	28.79	0.09	0.05	0.04	2.18	2.24	1.23	1.15	1.08	1.08	29.49	1.49	30.98	0.15
5	m-xylene	3.20	3.28	3.28	39.22	24.72	40.17	23.34	40.16	23.50	0.51	0.56	0.52	6.29	6.46	6.82	6.34	6.37	6.40	23.85	6.40	30.26	0.15
6	o-xylene	1.50	1.51	1.50	36.81	23.20	37.03	21.52	36.86	21.56	0.06	0.22	0.19	1.46	1.50	5.29	4.92	4.57	4.59	22.10	3.67	25.76	0.13
7	Styrene	5.61	5.85	5.78	136.26	85.90	141.91	82.47	140.39	82.13	0.24	0.20	0.19	5.93	6.09	4.80	4.46	4.62	4.64	83.50	5.06	88.56	0.44
8	Phenol	0.18	0.16	0.16	6.43	4.05	5.62	3.27	5.79	3.39	24.67	21.38	21.74	868.78	892.52	752.84	699.56	765.66	769.45	3.57	787.18	790.75	3.95
9	Indene	3.54	3.69	3.76	91.59	57.74	95.25	55.35	97.05	56.77	0.24	0.30	0.27	6.26	6.43	7.74	7.19	6.90	6.94	56.62	6.85	63.47	0.32
10	o-cresol (2-methylphenol)	0.15	0.10	0.08	4.99	3.14	3.38	1.96	2.76	1.62	4.64	4.05	4.18	152.28	156.44	132.71	123.32	137.12	137.80	2.24	139.19	141.43	0.71
11	m+p-cresol (3+4-methylphenol)	0.53	0.54	0.51	9.17	5.78	9.37	5.45	8.87	5.19	12.14	10.31	10.85	211.51	217.30	179.59	166.88	188.96	189.90	5.47	191.36	196.83	0.98
12	Naphthalene	3.43	3.25	3.55	66.93	42.19	63.45	36.87	69.35	40.57	0.66	0.92	0.85	12.84	13.19	17.99	16.71	16.67	16.76	39.88	15.55	55.43	0.28
13	Quinoline	0.82	0.76	0.81	24.70	15.57	22.65	13.16	24.33	14.23	0.84	0.76	0.19	25.26	25.95	22.90	21.28	5.77	5.80	14.32	17.68	32.00	0.16
14	2-Methylnaphthalene	1.14	0.99	1.09	20.48	12.91	17.82	10.35	19.60	11.47	0.43	0.52	0.50	7.70	7.91	9.34	8.68	8.94	8.98	11.58	8.53	20.10	0.10
15	Isoquinoline	0.04	0.05	0.05	1.34	0.85	1.47	0.86	1.50	0.88	0.20	0.16	0.18	6.35	6.52	5.04	4.68	5.78	5.80	0.86	5.67	6.53	0.03
16	1-Methylnaphthalene	0.84	0.73	0.84	15.92	10.04	13.72	7.97	15.90	9.30	0.50	0.56	0.57	9.41	9.67	10.51	9.76	10.71	10.76	9.10	10.06	19.17	0.10
17	Biphenyl	0.30	0.25	0.29	7.03	4.43	5.91	3.44	6.78	3.97	1.64	1.10	1.15	38.12	39.17	25.63	23.81	26.70	26.83	3.94	29.94	33.88	0.17
18	Acenaphthylene	0.62	0.55	0.65	11.93	7.52	10.55	6.13	12.41	7.26	0.43	0.45	0.45	8.17	8.39	8.52	7.91	8.67	8.71	6.97	8.34	15.31	0.08
19	Acenapthene	0.15	0.13	0.15	2.89	1.82	2.40	1.40	2.76	1.62	0.09	0.09	0.10	1.65	1.70	1.79	1.66	1.90	1.90	1.61	1.75	3.37	0.02
20	Fluorene	0.67	0.59	0.44	12.93	8.15	11.22	6.52	8.42	4.93	0.31	0.24	0.35	5.92	6.08	4.64	4.31	6.70	6.73	6.53	5.71	12.24	0.06
21	Phenanthrene	0.60	0.49	0.53	11.96	7.54	9.63	5.60	10.56	6.18	0.34	0.35	0.35	6.70	6.88	6.95	6.46	6.84	6.87	6.44	6.74	13.18	0.07
22	Anthracene	0.28	0.21	0.22	4.05	2.55	3.11	1.81	3.22	1.88	0.10	0.11	0.10	1.52	1.56	1.67	1.55	1.54	1.55	2.08	1.55	3.63	0.02
23	Fluoranthene	0.57	0.48	0.38	9.66	6.09	8.02	4.66	6.47	3.79	0.58	0.54	0.54	9.72	9.98	9.14	8.50	9.02	9.07	4.85	9.18	14.03	0.07
24	Pyrene	0.41	0.35	0.35	3.95	2.49	3.38	1.96	3.34	1.95	0.48	0.45	0.41	4.57	4.69	4.35	4.04	3.98	4.00	2.13	4.24	6.38	0.03
25	Bens(a)anthracene																						
26	Chrysene																						
27	Benso(b)fluoranthene																						
28	Benso(k)fluoranthene																						
29	Benso(a)Pyrene																						
30	Indeno(1,2,3-cd)pyrene																						
31	Benso(g,h,i)perylene																						
32	Dibenso(a,h)anthracene																						

Table J.11. Signal count ratio and concentration of each tar compound at 700°C analysed with HTM.

No	Method	HTM																				
	Solvent	DCM					ρ_{DCM} = 1.32 g ml^{-1}				DCM-IPA						$\rho_{DCM-IPA}$ = 1.05 g ml^{-1}				Average tar mass		Tar amount	
	Category	Signal Count Ratio			Concentration						Signal Count Ratio			Concentration							DCM (G): (A+B+	DCM-IPA (H): (D+E+F) /	in sample solution (I): (G+H)	in PG (I / 200)
	Repeat	1	2	3	1		2		3		1	2	3	1		2		3					
	Mass of Tar Sample Solution (g)	NA	NA	NA	0.8321		0.7671		0.7722		NA	NA	NA	1.0787		0.9757		1.0552					
	Concentration unit	NA	NA	NA	ppm	µg (A)	ppm	µg (B)	ppm	µg (C)	NA	NA	NA	ppm	µg (D)	ppm	µg (E)	ppm	µg (F)		µg	µg	µg	µg ml^{-1}
1	Benzene																							
2	Toluene																							
3	Pyridine																							
4	p-xylene + Ethylbenzene																							
5	m-xylene																							
6	o-xylene																							
7	Styrene																							
8	Phenol	0.03	0.01	0.03	1.36	0.86	0.30	0.17	1.25	0.73	23.36	25.99	20.66	977.21	1003.92	1087.57	1010.61	864.33	868.61		0.59	961.05	961.63	4.81
9	Indene	2.24	2.11	2.04	68.82	43.38	65.05	37.80	62.71	36.68	0.23	0.17	0.24	7.21	7.41	5.33	4.96	7.33	7.36		39.29	6.57	45.86	0.23
10	o-cresol (2-methylphenol)	1.06	1.04	0.47	36.85	23.23	36.18	21.03	16.18	9.47	0.15	0.26	0.15	5.31	5.45	9.06	8.42	5.10	5.12		17.91	6.33	24.24	0.12
11	m+p-cresol (3+4-methylphenol)	0.49	0.38	0.18	9.93	6.26	7.85	4.56	3.74	2.19	3.91	4.59	3.78	80.02	82.20	93.89	87.25	77.35	77.74		4.34	82.40	86.74	0.43
12	Naphthalene	2.00	2.22	1.90	42.65	26.89	47.23	27.45	40.39	23.63	0.51	0.32	0.39	10.86	11.15	6.75	6.27	8.32	8.36		25.99	8.60	34.58	0.17
13	Quinoline	0.18	0.14	0.14	6.08	3.83	4.97	2.89	4.96	2.90	0.32	0.81	0.28	11.03	11.33	28.11	26.12	9.56	9.60		3.21	15.68	18.89	0.09
14	2-Methylnaphthalene	0.60	0.49	0.28	12.56	7.92	10.28	5.97	5.87	3.43	0.83	0.25	0.63	17.39	17.87	5.22	4.85	13.10	13.17		5.78	11.96	17.74	0.09
15	Isoquinoline	0.84	0.86	0.64	31.84	20.07	32.72	19.01	24.42	14.29	0.18	0.15	0.17	7.01	7.20	5.79	5.38	6.50	6.54		17.79	6.37	24.16	0.12
16	1-Methylnaphthalene	0.63	0.67	0.52	13.78	8.69	14.61	8.49	11.29	6.61	0.16	0.13	0.13	3.40	3.49	2.74	2.55	2.74	2.76		7.93	2.93	10.86	0.05
17	Biphenyl	0.21	0.39	0.18	5.56	3.50	10.14	5.89	4.70	2.75	0.11	0.05	0.10	2.99	3.07	1.35	1.26	2.50	2.51		4.05	2.28	6.33	0.03
18	Acenaphthylene	0.32	0.37	0.21	6.78	4.28	7.97	4.63	4.51	2.64	0.05	0.12	0.03	1.15	1.18	2.48	2.30	0.67	0.67		3.85	1.39	5.24	0.03
19	Acenapthene	0.10	0.08	0.07	2.25	1.42	1.69	0.98	1.59	0.93	0.10	0.14	0.10	2.19	2.25	3.10	2.88	2.25	2.26		1.11	2.46	3.57	0.02
20	Fluorene	0.05	0.04	0.04	1.24	0.78	0.96	0.56	0.91	0.54	0.31	0.26	0.20	7.37	7.57	6.21	5.77	4.74	4.77		0.62	6.04	6.66	0.03
21	Phenanthrene	0.27	0.86	0.19	6.88	4.34	21.98	12.77	5.01	2.93	0.24	0.22	0.20	6.29	6.46	5.58	5.18	5.08	5.10		6.68	5.58	12.26	0.06
22	Anthracene	0.13	0.07	0.13	3.51	2.21	1.86	1.08	3.26	1.91	0.10	0.09	0.08	2.53	2.60	2.26	2.10	1.99	2.00		1.73	2.24	3.97	0.02
23	Fluoranthene	0.17	0.54	0.12	4.52	2.85	14.34	8.33	3.28	1.92	0.11	0.12	0.10	2.93	3.01	3.12	2.90	2.62	2.64		4.37	2.85	7.22	0.04
24	Pyrene	0.16	2.19	0.12	3.87	2.44	52.60	30.57	2.99	1.75	0.26	0.35	0.31	6.32	6.49	8.41	7.81	7.55	7.59		11.59	7.30	18.88	0.09
25	Bens(a)anthracene	0.08	0.03	0.11	2.72	1.72	0.83	0.48	3.60	2.11	0.04	0.10	0.12	1.34	1.38	3.20	2.97	3.94	3.96		1.44	2.77	4.20	0.02
26	Chrysene	0.10	0.03	0.09	2.58	1.63	0.77	0.45	2.22	1.30	0.14	0.14	0.13	3.67	3.77	3.58	3.32	3.28	3.30		1.12	3.46	4.59	0.02
27	Benso(b)fluoranthene	0.05	0.02	0.04	1.60	1.01	0.48	0.28	1.32	0.77	0.07	0.09	0.09	2.30	2.36	3.05	2.83	2.78	2.80		0.69	2.66	3.35	0.02
28	Benso(k)fluoranthene	0.03	0.01	0.03	0.96	0.61	0.31	0.18	0.89	0.52	0.07	0.09	0.08	2.01	2.07	2.65	2.47	2.33	2.34		0.43	2.29	2.73	0.01
29	Benso(a)Pyrene	0.03	0.02	0.03	0.82	0.51	0.49	0.29	0.85	0.50	0.05	0.06	0.06	1.17	1.20	1.48	1.38	1.50	1.51		0.43	1.36	1.80	0.01
30	Indeno(1,2,3-cd)pyrene	0.00	0.00	0.00	0.10	0.06	0.03	0.02	0.12	0.07	0.01	0.01	0.01	0.40	0.41	0.22	0.21	0.59	0.59		0.05	0.40	0.45	0.00
31	Benso(g,h,i)perylene	0.01	0.01	0.01	0.29	0.18	0.28	0.16	0.46	0.27	0.01	0.02	0.03	0.42	0.43	0.76	0.71	0.87	0.88		0.21	0.67	0.88	0.00
32	Dibenso(a,h)anthracene	0.00	0.00	0.00	0.02	0.02	0.02	0.01	0.07	0.04	0.01	0.01	0.01	0.13	0.13	0.23	0.21	0.19	0.19		0.02	0.18	0.20	0.00

Table J.12. Total tar concentration for each tar compounds at 700°C.

No	Tar component	Tar concentration (µg ml^{-1})		Average (µg ml^{-1})	Total tar (µg ml^{-1})
		LTM	HTM		
1	Benzene	2.02			2.02
2	Toluene	1.50			1.50
3	Pyridine	0.12			0.12
4	p-xylene + Ethylbenzene	0.15			0.15
5	m-xylene	0.15			0.15
6	o-xylene	0.13			0.13
7	Styrene	0.44			0.44
8	Phenol	3.95	4.81	4.38	4.38
9	Indene	0.32	0.23	0.27	0.27
10	o-cresol (2-methylphenol)	0.71	0.12	0.41	0.41
11	m+p-cresol (3+4-methylphenol)	0.98	0.43	0.71	0.71
12	Naphthalene	0.28	0.17	0.23	0.23
13	Quinoline	0.16	0.09	0.13	0.13
14	2-Methylnaphthalene	0.10	0.09	0.09	0.09
15	Isoquinoline	0.03	0.12	0.08	0.08
16	1-Methylnaphthalene	0.10	0.05	0.08	0.08
17	Biphenyl	0.17	0.03	0.10	0.10
18	Acenaphthylene	0.08	0.03	0.05	0.05
19	Acenapthene	0.02	0.02	0.02	0.02
20	Fluorene	0.06	0.03	0.05	0.05
21	Phenanthrene	0.07	0.06	0.06	0.06
22	Anthracene	0.02	0.02	0.02	0.02
23	Fluoranthene	0.07	0.04	0.05	0.05
24	Pyrene	0.03	0.09	0.06	0.06
25	Bens(a)anthracene		0.02		0.02
26	Chrysene		0.02		0.02
27	Benso(b)fluoranthene		0.02		0.02
28	Benso(k)fluoranthene		0.01		0.01
29	Benso(a)Pyrene		0.01		0.01
30	Indeno(1,2,3-cd)pyrene		0.00		0.00
31	Benso(g,h,i)perylene		0.00		0.00
32	Dibenso(a,h)anthracene		0.00		0.00

Table J.13. Signal count ratio and concentration of each tar compound at 750°C analysed with LTM.

No	Method	LTM																					
	Solvent	DCM						ρ_{DCM} =	1.32 g ml^{-1}		DCM-IPA							$\rho_{DCM-IPA}$ =	1.05 g ml^{-1}		Average tar mass		Tar amount	
	Category	Signal Count Ratio			Concentration						Signal Count Ratio			Concentration							DCM (G): (A+B+C) / 3	DCM-IPA (H): (D+E+F) / 3	in sample solution (I): (G+H)	in PG (I / 200)
	Repeat	1	2	3	1		2		3		1	2	3	1		2		3					
	Mass of Tar Sample Solution (g)	NA	NA	NA	0.8320		0.8019		0.7916		NA	NA	NA	1.0194		1.0068		1.0357					
	Concentration unit	NA	NA	NA	ppm	µg (A)	ppm	µg (B)	ppm	µg (C)	NA	NA	NA	ppm	µg (D)	ppm	µg (E)	ppm	µg (F)		µg	µg	µg ml^{-1}
1	Benzene	37.74	37.73	41.84	995.73	627.61	995.53	604.78	1103.88	661.99	0.66	0.59	0.81	17.40	16.90	15.68	15.04	21.27	20.98	631.46	17.64	649.10	3.25
2	Toluene	20.10	19.66	21.34	496.28	312.81	485.35	294.85	526.94	316.01	0.81	0.64	0.78	20.12	19.53	15.69	15.04	19.24	18.98	307.89	17.85	325.74	1.63
3	Pyridine	0.15	0.20	0.22	5.27	3.32	7.18	4.36	8.05	4.82	1.01	0.73	0.74	36.60	35.54	26.40	25.32	26.73	26.37	4.17	29.07	33.24	0.17
4	p-xylene + Ethylbenzene	1.37	1.17	1.30	34.36	21.66	29.45	17.89	32.55	19.52	0.22	0.19	0.10	5.57	5.41	4.75	4.56	2.56	2.52	19.69	4.16	23.85	0.12
5	m-xylene	2.71	2.61	2.83	33.19	20.92	31.93	19.40	34.62	20.76	0.34	0.26	0.61	4.15	4.03	3.17	3.04	7.50	7.40	20.36	4.82	25.18	0.13
6	o-xylene	1.15	1.09	1.19	28.28	17.82	26.81	16.29	29.23	17.53	0.02	0.02	0.03	0.59	0.57	0.55	0.52	0.70	0.69	17.21	0.60	17.81	0.09
7	Styrene	7.54	7.40	8.23	182.91	115.29	179.50	109.05	199.77	119.80	0.18	0.15	0.20	4.27	4.15	3.76	3.61	4.86	4.80	114.71	4.18	118.90	0.59
8	Phenol	0.01	0.00	0.01	0.23	0.15	0.16	0.10	0.18	0.11	16.52	16.48	17.59	581.55	564.60	580.30	556.43	619.45	611.01	0.12	577.35	577.46	2.89
9	Indene	4.90	5.03	5.60	126.54	79.76	129.98	78.96	144.73	86.79	0.38	0.32	0.45	9.72	9.43	8.28	7.94	11.56	11.41	81.84	9.59	91.43	0.46
10	o-cresol (2-methylphenol)	0.10	0.07	0.10	3.32	2.09	2.28	1.38	3.15	1.89	2.41	2.20	2.47	78.97	76.66	71.97	69.01	80.87	79.76	1.79	75.15	76.93	0.38
11	m+p-cresol (3+4-methylphenol)	0.22	0.12	0.17	3.87	2.44	2.00	1.22	2.94	1.76	6.12	6.17	6.86	106.53	103.43	107.47	103.05	119.59	117.96	1.81	108.15	109.95	0.55
12	Naphthalene	4.71	4.98	5.60	92.00	57.99	97.22	59.06	109.39	65.60	1.43	1.30	1.68	27.84	27.02	25.38	24.34	32.83	32.38	60.88	27.91	88.80	0.44
13	Quinoline	0.10	0.09	0.10	2.89	1.82	2.84	1.72	3.12	1.87	0.19	0.17	0.20	5.84	5.67	5.12	4.90	5.88	5.80	1.80	5.46	7.26	0.04
14	2-Methylnaphthalene	1.04	0.96	1.13	18.68	11.77	17.29	10.50	20.39	12.23	0.57	0.51	0.63	10.20	9.91	9.26	8.88	11.32	11.16	11.50	9.98	21.48	0.11
15	Isoquinoline	0.01	0.01	0.01	0.38	0.24	0.40	0.24	0.48	0.29	0.13	0.13	0.14	4.09	3.97	4.07	3.91	4.55	4.48	0.26	4.12	4.38	0.02
16	1-Methylnaphthalene	0.73	0.66	0.79	13.76	8.67	12.40	7.53	14.85	8.90	0.59	0.52	0.67	11.09	10.76	9.86	9.45	12.56	12.39	8.37	10.87	19.24	0.10
17	Biphenyl	0.30	0.28	0.33	6.90	4.35	6.59	4.00	7.71	4.62	0.71	0.41	0.69	16.43	15.95	9.64	9.25	15.97	15.75	4.32	13.65	17.97	0.09
18	Acenaphthylene	0.81	0.77	0.91	15.52	9.78	14.78	8.98	17.40	10.44	0.72	0.68	0.82	13.76	13.36	13.01	12.48	15.68	15.46	9.73	13.77	23.50	0.12
19	Acenapthene	0.12	0.11	0.17	2.36	1.49	2.02	1.23	3.15	1.89	0.10	0.12	0.12	1.91	1.85	2.22	2.12	2.20	2.17	1.53	2.05	3.58	0.02
20	Fluorene	0.60	0.50	0.64	11.52	7.26	9.67	5.88	12.19	7.31	0.43	0.39	0.47	8.21	7.97	7.53	7.22	9.05	8.93	6.81	8.04	14.85	0.07
21	Phenanthrene	0.59	0.50	0.67	11.68	7.36	9.93	6.03	13.35	8.01	0.43	0.42	0.53	8.54	8.29	8.37	8.02	10.50	10.35	7.13	8.89	16.02	0.08
22	Anthracene	0.22	0.19	0.29	3.21	2.02	2.82	1.71	4.31	2.58	0.14	0.14	0.18	2.13	2.07	2.11	2.02	2.59	2.55	2.11	2.21	4.32	0.02
23	Fluoranthene	0.44	0.38	0.51	7.46	4.70	6.45	3.92	8.55	5.13	0.45	0.48	0.55	7.52	7.30	8.03	7.70	9.20	9.07	4.58	8.02	12.61	0.06
24	Pyrene	0.43	0.51	0.54	4.12	2.60	4.92	2.99	5.21	3.13	0.39	0.37	0.59	3.74	3.63	3.56	3.42	5.62	5.55	2.90	4.20	7.10	0.04
25	Bens(a)anthracene																						
26	Chrysene																						
27	Benso(b)fluoranthene																						
28	Benso(k)fluoranthene																						
29	Benso(a)Pyrene																						
30	Indeno(1,2,3-cd)pyrene																						
31	Benso(g,h,i)perylene																						
32	Dibenso(a,h)anthracene																						

Table J.14. Signal count ratio and concentration of each tar compound at 750°C analysed with HTM.

No	Method	HTM																				
	Solvent	DCM						ρ_{DCM} = 1.32 g ml^{-1}		DCM-IPA						$\rho_{DCM-IPA}$ = 1.05 g ml^{-1}				Average tar mass		Tar amount	
	Category	Signal Count Ratio			Concentration					Signal Count Ratio			Concentration							DCM (G): (A+B+C) / 3	DCM-IPA (H): (D+E+F) / 3	in sample solution (I): (G+H)	in PG (I / 200)
	Repeat	1	2	3	1		2		3	1	2	3	1		2		3						
	Mass of Tar Sample Solution (g)	NA	NA	NA	0.8320		0.8019		0.7916	NA	NA	NA	1.0194		1.0068		1.0357						
	Concentration unit	NA	NA	NA	ppm	µg (A)	ppm	µg (B)	ppm	µg (C)	NA	NA	NA	ppm	µg (D)	ppm	µg (E)	ppm	µg (F)	µg	µg	µg	µg ml^{-1}
1	Benzene																						
2	Toluene																						
3	Pyridine																						
4	p-xylene + Ethylbenzene																						
5	m-xylene																						
6	o-xylene																						
7	Styrene																						
8	Phenol	0.02	0.05	0.02	0.96	0.60	2.09	1.27	1.02	0.61	0.05	0.05	0.06	2.26	2.20	2.25	2.16	2.33	2.30	0.83	2.22	3.05	0.02
9	Indene	4.89	4.85	5.53	150.34	94.76	149.25	90.67	170.07	101.99	0.33	0.27	0.38	10.13	9.83	8.40	8.06	11.64	11.48	95.81	9.79	105.60	0.53
10	o-cresol (2-methylphenol)	0.04	0.12	0.05	1.40	0.88	4.02	2.44	1.64	0.98	2.16	1.91	2.14	75.02	72.83	66.15	63.42	74.27	73.26	1.44	69.84	71.28	0.36
11	m+p-cresol (3+4-methylphenol)	0.19	0.09	0.12	3.79	2.39	1.92	1.17	2.55	1.53	5.42	5.02	5.49	110.75	107.52	102.68	98.45	112.18	110.65	1.70	105.54	107.24	0.54
12	Naphthalene	4.53	4.78	5.38	96.42	60.77	101.68	61.77	114.40	68.60	1.20	1.09	1.41	25.54	24.79	23.27	22.32	30.10	29.69	63.71	25.60	89.31	0.45
13	Quinoline	0.10	0.10	0.13	3.39	2.13	3.49	2.12	4.47	2.68	0.45	0.29	0.40	15.48	15.03	10.00	9.59	13.90	13.71	2.31	12.78	15.09	0.08
14	2-Methylnaphthalene	0.48	0.24	0.42	10.10	6.37	4.93	3.00	8.73	5.24	0.48	0.44	0.53	10.01	9.71	9.10	8.73	11.08	10.93	4.87	9.79	14.66	0.07
15	Isoquinoline	1.01	0.92	1.10	38.07	24.00	34.99	21.25	41.56	24.92	0.10	0.09	0.10	3.67	3.57	3.45	3.31	3.95	3.89	23.39	3.59	26.98	0.13
16	1-Methylnaphthalene	0.76	0.66	0.82	16.65	10.50	14.50	8.81	18.04	10.82	0.40	0.37	0.45	8.73	8.48	8.17	7.83	9.82	9.69	10.04	8.67	18.71	0.09
17	Biphenyl	0.40	0.29	0.33	10.50	6.62	7.49	4.55	8.68	5.21	0.16	0.17	0.20	4.10	3.98	4.44	4.26	5.13	5.06	5.46	4.43	9.89	0.05
18	Acenaphthylene	0.87	0.73	0.94	18.66	11.76	15.64	9.50	20.14	12.08	0.51	0.51	0.60	11.03	10.71	11.00	10.55	12.97	12.79	11.11	11.35	22.47	0.11
19	Acenapthene	0.13	0.10	0.13	2.84	1.79	2.24	1.36	2.80	1.68	0.09	0.08	0.10	1.87	1.81	1.73	1.66	2.08	2.06	1.61	1.84	3.45	0.02
20	Fluorene	0.59	0.47	0.62	14.22	8.96	11.46	6.96	14.87	8.92	0.34	0.31	0.39	8.27	8.03	7.60	7.29	9.32	9.20	8.28	8.17	16.45	0.08
21	Phenanthrene	0.50	0.46	0.59	12.93	8.15	11.72	7.12	15.25	9.14	0.31	0.32	0.38	7.92	7.69	8.14	7.81	9.66	9.53	8.14	8.34	16.48	0.08
22	Anthracene	0.38	0.18	0.26	9.86	6.22	4.80	2.92	6.68	4.01	0.10	0.11	0.13	2.71	2.63	2.80	2.69	3.37	3.32	4.38	2.88	7.26	0.04
23	Fluoranthene	0.33	0.22	0.29	8.65	5.45	5.75	3.50	7.67	4.60	0.17	0.16	0.19	4.54	4.41	4.36	4.18	5.04	4.97	4.52	4.52	9.04	0.05
24	Pyrene	0.36	0.17	0.22	8.66	5.46	4.05	2.46	5.39	3.24	0.19	0.13	0.15	4.56	4.43	3.12	2.99	3.62	3.57	3.72	3.66	7.38	0.04
25	Bens(a)anthracene	0.14	0.12	0.15	4.56	2.87	3.91	2.37	4.80	2.88	0.07	0.06	0.07	2.20	2.13	2.06	1.97	2.43	2.39	2.71	2.17	4.88	0.02
26	Chrysene	2.04	0.13	0.18	52.90	33.34	3.45	2.10	4.72	2.83	0.10	0.10	0.12	2.59	2.51	2.65	2.54	3.00	2.95	12.76	2.67	15.43	0.08
27	Benso(b)fluoranthene	0.04	0.09	0.10	1.13	0.71	2.83	1.72	3.34	2.00	0.08	0.08	0.08	2.49	2.41	2.52	2.42	2.69	2.65	1.48	2.49	3.97	0.02
28	Benso(k)fluoranthene	0.02	0.06	0.06	0.60	0.38	1.75	1.06	1.85	1.11	0.05	0.06	0.06	1.63	1.58	1.72	1.65	1.84	1.82	0.85	1.69	2.53	0.01
29	Benso(a)Pyrene	0.03	0.07	0.08	0.80	0.50	1.84	1.12	1.96	1.17	0.06	0.07	0.06	1.48	1.44	1.67	1.60	1.60	1.58	0.93	1.54	2.47	0.01
30	Indeno(1,2,3-cd)pyrene	0.00	0.02	0.02	0.20	0.13	0.87	0.53	0.77	0.46	0.02	0.02	0.01	0.99	0.96	0.65	0.63	0.58	0.57	0.37	0.72	1.09	0.01
31	Benso(g,h,i)perylene	0.01	0.04	0.04	0.38	0.24	1.51	0.92	1.28	0.77	0.03	0.04	0.03	1.07	1.04	1.32	1.26	1.15	1.13	0.64	1.14	1.79	0.01
32	Dibenso(a,h)anthracene	0.01	0.05	0.05	0.36	0.23	1.20	0.73	1.13	0.68	0.05	0.03	0.04	1.20	1.16	0.83	0.79	1.02	1.01	0.54	0.99	1.53	0.01

Table J.15. Total tar concentration for each tar compounds at 750^{o}C.

No	Tar component	Tar concentration (µg ml^{-1})		Average (µg ml^{-1})	Total tar (µg ml^{-1})
		LTM	HTM		
1	Benzene	3.25			3.25
2	Toluene	1.63			1.63
3	Pyridine	0.17			0.17
4	p-xylene + Ethylbenzene	0.12			0.12
5	m-xylene	0.13			0.13
6	o-xylene	0.09			0.09
7	Styrene	0.59			0.59
8	Phenol	2.89	0.02	1.45	1.45
9	Indene	0.46	0.53	0.49	0.49
10	o-cresol (2-methylphenol)	0.38	0.36	0.37	0.37
11	m+p-cresol (3+4-methylphenol)	0.55	0.54	0.54	0.54
12	Naphthalene	0.44	0.45	0.45	0.45
13	Quinoline	0.04	0.08	0.06	0.06
14	2-Methylnaphthalene	0.11	0.07	0.09	0.09
15	Isoquinoline	0.02	0.13	0.08	0.08
16	1-Methylnaphthalene	0.10	0.09	0.09	0.09
17	Biphenyl	0.09	0.05	0.07	0.07
18	Acenaphthylene	0.12	0.11	0.11	0.11
19	Acenapthene	0.02	0.02	0.02	0.02
20	Fluorene	0.07	0.08	0.08	0.08
21	Phenanthrene	0.08	0.08	0.08	0.08
22	Anthracene	0.02	0.04	0.03	0.03
23	Fluoranthene	0.06	0.05	0.05	0.05
24	Pyrene	0.04	0.04	0.04	0.04
25	Bens(a)anthracene		0.02		0.02
26	Chrysene		0.08		0.08
27	Benso(b)fluoranthene		0.02		0.02
28	Benso(k)fluoranthene		0.01		0.01
29	Benso(a)Pyrene		0.01		0.01
30	Indeno(1,2,3-cd)pyrene		0.01		0.01
31	Benso(g,h,i)perylene		0.01		0.01
32	Dibenso(a,h)anthracene		0.01		0.01

Table J.16. Signal count ratio and concentration of each tar compound at 800°C analysed with LTM.

No	Method	LTM																				
	Solvent	DCM						ρ_{DCM} = 1.32 g ml^{-1}			DCM-IPA						$\rho_{DCM-IPA}$ = 1.05 g ml^{-1}				Average tar mass		Tar amount	
	Category	Signal Count Ratio			Concentration						Signal Count Ratio			Concentration									
	Repeat	1	2	3	1		2		3		1	2	3	1		2		3		DCM (G): (A+B+C) / 3	DCM-IPA (H): (D+E+F) / 3	in sample solution (I): (G+H)	in PG (I / 200)
	Mass of Tar Sample Solution (g)	NA	NA	NA	0.8363		0.7938		0.6807		NA	NA	NA	1.0709		1.0472		0.9934					
	Concentration unit	NA	NA	NA	ppm	µg (A)	ppm	µg (B)	ppm	µg (C)	NA	NA	NA	ppm	µg (D)	ppm	µg (E)	ppm	µg (F)	µg	µg	µg	µg ml^{-1}
1	Benzene	21.01	24.36	28.86	554.33	351.20	642.86	386.59	761.56	392.72	0.13	0.10	0.17	3.36	3.42	2.71	2.70	4.39	4.15	376.84	3.43	380.27	1.90
2	Toluene	16.36	16.54	20.34	404.01	255.96	408.34	245.56	502.32	259.04	0.14	0.12	0.16	3.53	3.60	2.95	2.94	3.90	3.69	253.52	3.41	256.93	1.28
3	Pyridine	1.36	1.23	1.57	49.30	31.23	44.67	26.87	57.06	29.43	0.14	0.13	0.14	4.98	5.08	4.61	4.60	5.12	4.85	29.17	4.84	34.02	0.17
4	p-xylene + Ethylbenzene	1.70	1.57	1.97	42.62	27.00	39.35	23.67	49.43	25.49	0.08	0.07	0.10	2.05	2.09	1.72	1.71	2.44	2.31	25.39	2.04	27.42	0.14
5	m-xylene	2.75	2.66	3.33	33.62	21.30	32.54	19.57	40.76	21.02	0.06	0.05	0.08	0.73	0.75	0.60	0.60	0.99	0.94	20.63	0.76	21.39	0.11
6	o-xylene	0.07	1.20	1.51	1.81	1.15	29.49	17.73	37.07	19.12	0.02	0.01	0.02	0.42	0.43	0.34	0.34	0.45	0.43	12.67	0.40	13.07	0.07
7	Styrene	4.70	4.98	6.00	114.17	72.34	120.97	72.75	145.55	75.06	0.12	0.10	0.12	2.94	3.00	2.41	2.40	2.98	2.82	73.38	2.74	76.12	0.38
8	Phenol	1.46	1.46	1.81	51.38	32.55	51.33	30.87	63.60	32.80	11.22	11.07	13.86	395.11	402.98	389.78	388.74	488.17	461.86	32.08	417.86	449.93	2.25
9	Indene	2.99	3.08	3.80	77.35	49.01	79.56	47.84	98.25	50.66	0.21	0.17	0.22	5.34	5.44	4.30	4.29	5.58	5.28	49.17	5.00	54.17	0.27
10	o-cresol (2-methylphenol)	0.11	0.15	0.12	3.51	2.23	4.86	2.92	3.87	2.00	2.30	2.01	2.78	75.56	77.06	65.92	65.74	91.05	86.14	2.38	76.31	78.70	0.39
11	m+p-cresol (3+4-methylphenol)	0.95	0.53	0.90	16.61	10.52	9.23	5.55	15.66	8.07	5.95	5.33	6.99	103.63	105.69	92.94	92.70	121.86	115.29	8.05	104.56	112.61	0.56
12	Naphthalene	2.79	3.02	3.49	54.44	34.49	59.03	35.50	68.24	35.19	0.48	0.50	0.66	9.39	9.58	9.84	9.81	12.83	12.13	35.06	10.51	45.57	0.23
13	Quinoline	1.05	0.61	1.02	31.41	19.90	18.30	11.00	30.41	15.68	0.57	0.43	0.70	17.12	17.46	12.93	12.90	21.08	19.94	15.53	16.77	32.29	0.16
14	2-Methylnaphthalene	1.01	0.96	1.09	18.20	11.53	17.22	10.35	19.59	10.10	0.30	0.28	0.36	5.43	5.54	5.12	5.11	6.53	6.17	10.66	5.61	16.27	0.08
15	Isoquinoline	0.05	0.05	0.05	1.71	1.08	1.48	0.89	1.63	0.84	0.10	0.08	0.12	3.34	3.40	2.68	2.68	3.87	3.66	0.94	3.25	4.19	0.02
16	1-Methylnaphthalene	0.75	0.69	0.79	14.18	8.98	13.06	7.86	14.92	7.70	0.37	0.28	0.42	6.97	7.11	5.26	5.25	7.91	7.49	8.18	6.62	14.79	0.07
17	Biphenyl	0.27	0.26	0.28	6.21	3.93	6.09	3.66	6.59	3.40	0.98	0.06	1.04	22.86	23.31	1.36	1.36	24.24	22.93	3.66	15.87	19.53	0.10
18	Acenaphthylene	0.66	0.57	0.66	12.65	8.02	10.98	6.60	12.64	6.52	0.41	0.34	0.46	7.90	8.06	6.44	6.43	8.84	8.36	7.05	7.62	14.66	0.07
19	Acenapthene	0.16	0.18	0.16	3.11	1.97	3.33	2.00	3.09	1.59	0.11	0.08	0.13	2.10	2.14	1.54	1.54	2.55	2.41	1.85	2.03	3.88	0.02
20	Fluorene	0.33	0.21	0.27	6.36	4.03	3.99	2.40	5.20	2.68	0.09	0.07	0.15	1.73	1.77	1.42	1.41	2.78	2.63	3.04	1.94	4.97	0.02
21	Phenanthrene	0.50	0.35	0.40	9.88	6.26	6.87	4.13	7.86	4.06	0.17	0.17	0.25	3.32	3.39	3.34	3.33	4.90	4.63	4.82	3.78	8.60	0.04
22	Anthracene	0.25	0.18	0.21	3.67	2.32	2.66	1.60	3.11	1.60	0.09	0.09	0.13	1.33	1.36	1.37	1.36	1.93	1.83	1.84	1.52	3.36	0.02
23	Fluoranthene	0.27	0.26	0.26	4.50	2.85	4.36	2.62	4.39	2.26	0.25	0.24	0.32	4.22	4.30	4.04	4.03	5.35	5.06	2.58	4.47	7.04	0.04
24	Pyrene	0.43	0.28	0.26	4.15	2.63	2.67	1.60	2.48	1.28	0.23	0.22	0.43	2.18	2.23	2.08	2.08	4.16	3.94	1.84	2.75	4.58	0.02
25	Bens(a)anthracene																						
26	Chrysene																						
27	Benso(b)fluoranthene																						
28	Benso(k)fluoranthene																						
29	Benso(a)Pyrene																						
30	Indeno(1,2,3-cd)pyrene																						
31	Benso(g,h,i)perylene																						
32	Dibenso(a,h)anthracene																						

Table J.17. Signal count ratio and concentration of each tar compound at 800°C analysed with LTM.

No	Method	LTM																				
	Solvent	DCM					ρ_{DCM} = 1.32 g ml^{-1}				DCM-IPA						$\rho_{DCM-IPA}$ = 1.05 g ml^{-1}				Average tar mass		Tar amount	
	Category	Signal Count Ratio			Concentration						Signal Count Ratio			Concentration							DCM (G): (A+B+C) / 3	DCM-IPA (H): (D+E+F) / 3	in sample solution (I): (G+H)	in PG (I / 200
	Repeat	1	2	3	1		2		3		1	2	3	1		2		3					
	Mass of Tar Sample Solution (g)	NA	NA	NA	0.8363		0.7938		0.6807		NA	NA	NA	1.0709		1.0472		0.9934					
	Concentration unit	NA	NA	NA	ppm	µg (A)	ppm	µg (B)	ppm	µg (C)	NA	NA	NA	ppm	µg (D)	ppm	µg (E)	ppm	µg (F)		µg	µg	µg	µg ml
1	Benzene	21.01	24.36	28.86	554.33	351.20	642.86	386.59	761.56	392.72	0.13	0.10	0.17	3.36	3.42	2.71	2.70	4.39	4.15	376.84	3.43	380.27	1.90
2	Toluene	16.36	16.54	20.34	404.01	255.96	408.34	245.56	502.32	259.04	0.14	0.12	0.16	3.53	3.60	2.95	2.94	3.90	3.69	253.52	3.41	256.93	1.28
3	Pyridine	1.36	1.23	1.57	49.30	31.23	44.67	26.87	57.06	29.43	0.14	0.13	0.14	4.98	5.08	4.61	4.60	5.12	4.85	29.17	4.84	34.02	0.17
4	p-xylene + Ethylbenzene	1.70	1.57	1.97	42.62	27.00	39.35	23.67	49.43	25.49	0.08	0.07	0.10	2.05	2.09	1.72	1.71	2.44	2.31	25.39	2.04	27.42	0.14
5	m-xylene	2.75	2.66	3.33	33.62	21.30	32.54	19.57	40.76	21.02	0.06	0.05	0.08	0.73	0.75	0.60	0.60	0.99	0.94	20.63	0.76	21.39	0.11
6	o-xylene	0.07	1.20	1.51	1.81	1.15	29.49	17.73	37.07	19.12	0.02	0.01	0.02	0.42	0.43	0.34	0.34	0.45	0.43	12.67	0.40	13.07	0.07
7	Styrene	4.70	4.98	6.00	114.17	72.34	120.97	72.75	145.55	75.06	0.12	0.10	0.12	2.94	3.00	2.41	2.40	2.98	2.82	73.38	2.74	76.12	0.38
8	Phenol	1.46	1.46	1.81	51.38	32.55	51.33	30.87	63.60	32.80	11.22	11.07	13.86	395.11	402.98	389.78	388.74	488.17	461.86	32.08	417.86	449.93	2.25
9	Indene	2.99	3.08	3.80	77.35	49.01	79.56	47.84	98.25	50.66	0.21	0.17	0.22	5.34	5.44	4.30	4.29	5.58	5.28	49.17	5.00	54.17	0.27
10	o-cresol (2-methylphenol)	0.11	0.15	0.12	3.51	2.23	4.86	2.92	3.87	2.00	2.30	2.01	2.78	75.56	77.06	65.92	65.74	91.05	86.14	2.38	76.31	78.70	0.39
11	m+p-cresol (3+4-methylphenol)	0.95	0.53	0.90	16.61	10.52	9.23	5.55	15.66	8.07	5.95	5.33	6.99	103.63	105.69	92.94	92.70	121.86	115.29	8.05	104.56	112.61	0.56
12	Naphthalene	2.79	3.02	3.49	54.44	34.49	59.03	35.50	68.24	35.19	0.48	0.50	0.66	9.39	9.58	9.84	9.81	12.83	12.13	35.06	10.51	45.57	0.23
13	Quinoline	1.05	0.61	1.02	31.41	19.90	18.30	11.00	30.41	15.68	0.57	0.43	0.70	17.12	17.46	12.93	12.90	21.08	19.94	15.53	16.77	32.29	0.16
14	2-Methylnaphthalene	1.01	0.96	1.09	18.20	11.53	17.22	10.35	19.59	10.10	0.30	0.28	0.36	5.43	5.54	5.12	5.11	6.53	6.17	10.66	5.61	16.27	0.08
15	Isoquinoline	0.05	0.05	0.05	1.71	1.08	1.48	0.89	1.63	0.84	0.10	0.08	0.12	3.34	3.40	2.68	2.68	3.87	3.66	0.94	3.25	4.19	0.02
16	1-Methylnaphthalene	0.75	0.69	0.79	14.18	8.98	13.06	7.86	14.92	7.70	0.37	0.28	0.42	6.97	7.11	5.26	5.25	7.91	7.49	8.18	6.62	14.79	0.07
17	Biphenyl	0.27	0.26	0.28	6.21	3.93	6.09	3.66	6.59	3.40	0.98	0.06	1.04	22.86	23.31	1.36	1.36	24.24	22.93	3.66	15.87	19.53	0.10
18	Acenaphthylene	0.66	0.57	0.66	12.65	8.02	10.98	6.60	12.64	6.52	0.41	0.34	0.46	7.90	8.06	6.44	6.43	8.84	8.36	7.05	7.62	14.66	0.07
19	Acenapthene	0.16	0.18	0.16	3.11	1.97	3.33	2.00	3.09	1.59	0.11	0.08	0.13	2.10	2.14	1.54	1.54	2.55	2.41	1.85	2.03	3.88	0.02
20	Fluorene	0.33	0.21	0.27	6.36	4.03	3.99	2.40	5.20	2.68	0.09	0.07	0.15	1.73	1.77	1.42	1.41	2.78	2.63	3.04	1.94	4.97	0.02
21	Phenanthrene	0.50	0.35	0.40	9.88	6.26	6.87	4.13	7.86	4.06	0.17	0.17	0.25	3.32	3.39	3.34	3.33	4.90	4.63	4.82	3.78	8.60	0.04
22	Anthracene	0.25	0.18	0.21	3.67	2.32	2.66	1.60	3.11	1.60	0.09	0.09	0.13	1.33	1.36	1.37	1.36	1.93	1.83	1.84	1.52	3.36	0.02
23	Fluoranthene	0.27	0.26	0.26	4.50	2.85	4.36	2.62	4.39	2.26	0.25	0.24	0.32	4.22	4.30	4.04	4.03	5.35	5.06	2.58	4.47	7.04	0.04
24	Pyrene	0.43	0.28	0.26	4.15	2.63	2.67	1.60	2.48	1.28	0.23	0.22	0.43	2.18	2.23	2.08	2.08	4.16	3.94	1.84	2.75	4.58	0.02
25	Bens(a)anthracene																						
26	Chrysene																						
27	Benso(b)fluoranthene																						
28	Benso(k)fluoranthene																						
29	Benso(a)Pyrene																						
30	Indeno(1,2,3-cd)pyrene																						
31	Benso(g,h,i)perylene																						
32	Dibenso(a,h)anthracene																						

Table J.18. Total tar concentration for each tar compounds at 800°C.

No	Tar component	Tar concentration (µg ml^{-1})		Average (µg ml^{-1})	Total tar (µg ml^{-1})
		LTM	HTM		
1	Benzene	1.90			1.90
2	Toluene	1.28			1.28
3	Pyridine	0.17			0.17
4	p-xylene + Ethylbenzene	0.14			0.14
5	m-xylene	0.11			0.11
6	o-xylene	0.07			0.07
7	Styrene	0.38			0.38
8	Phenol	2.25	2.02	2.13	2.13
9	Indene	0.27	0.33	0.30	0.30
10	o-cresol (2-methylphenol)	0.39	0.32	0.35	0.35
11	m+p-cresol (3+4-methylphenol)	0.56	0.48	0.52	0.52
12	Naphthalene	0.23	0.22	0.23	0.23
13	Quinoline	0.16	0.15	0.16	0.16
14	2-Methylnaphthalene	0.08	0.08	0.08	0.08
15	Isoquinoline	0.02	0.01	0.02	0.02
16	1-Methylnaphthalene	0.07	0.07	0.07	0.07
17	Biphenyl	0.10	0.08	0.09	0.09
18	Acenaphthylene	0.07	0.06	0.07	0.07
19	Acenapthene	0.02	0.02	0.02	0.02
20	Fluorene	0.02	0.05	0.04	0.04
21	Phenanthrene	0.04	0.04	0.04	0.04
22	Anthracene	0.02	0.02	0.02	0.02
23	Fluoranthene	0.04	0.02	0.03	0.03
24	Pyrene	0.02	0.02	0.02	0.02
25	Bens(a)anthracene		0.09		0.09
26	Chrysene		0.01		0.01
27	Benso(b)fluoranthene		0.00		0.00
28	Benso(k)fluoranthene		0.01		0.01
29	Benso(a)Pyrene		0.01		0.01
30	Indeno(1,2,3-cd)pyrene		0.00		0.00
31	Benso(g,h,i)perylene		0.00		0.00
32	Dibenso(a,h)anthracene		0.00		0.00

Table J.19. Concentration of each tar compound from the investigated parameter 1: summary

Tar class	Compounds	650 °C		700 °C		750 °C		800 °C	
		µg ml^{-1}	g Nm^{-3}	µg ml^{-1}	g Nm^{-3}	µg ml^{-1}	g Nm^{-3}	µg ml^{-1}	g Nm^{-3}
2	Pyridine	0.11	0.10	0.12	0.11	0.17	0.15	0.17	0.15
	Phenol	4.92	4.44	4.38	3.95	1.45	1.31	2.13	1.92
	o-cresol (2-methylphenol)	0.87	0.79	0.41	0.37	0.37	0.33	0.35	0.32
	m+p-cresol (3+4-methylphenol)	1.25	1.13	0.71	0.64	0.54	0.49	0.52	0.47
	Quinoline	0.09	0.08	0.13	0.11	0.06	0.05	0.16	0.14
	Isoquinoline	0.107	0.10	0.08	0.07	0.08	0.07	0.017	0.02
	Subtotal class 2 tars concentration	***7.35***	***6.63***	***5.82***	***5.25***	***2.67***	***2.40***	***3.36***	***3.02***
3	Benzene	1.13	1.01	2.02	1.82	3.25	2.92	1.90	1.71
	Toluene	1.36	1.22	1.50	1.35	1.63	1.47	1.28	1.16
	p-xylene + Ethylbenzene	0.16	0.15	0.15	0.14	0.12	0.11	0.14	0.12
	m-xylene	0.15	0.13	0.15	0.14	0.13	0.11	0.11	0.10
	o-xylene	0.14	0.13	0.13	0.12	0.09	0.08	0.07	0.06
	Styrene	0.31	0.28	0.44	0.40	0.59	0.54	0.38	0.34
	Subtotal class 3 tars concentration	***3.24***	***2.92***	***4.40***	***3.96***	***5.80***	***5.23***	***3.88***	***3.49***
4	Indene	0.31	0.28	0.27	0.25	0.49	0.44	0.30	0.27
	Naphthalene	0.24	0.22	0.23	0.20	0.45	0.40	0.23	0.20
	2-Methylnaphthalene	0.09	0.08	0.09	0.09	0.09	0.08	0.08	0.07
	1-Methylnaphthalene	0.11	0.10	0.08	0.07	0.09	0.09	0.07	0.07
	Biphenyl	0.21	0.19	0.10	0.09	0.07	0.06	0.09	0.08
	Acenaphthylene	0.06	0.05	0.05	0.05	0.11	0.10	0.07	0.06
	Acenapthene	0.02	0.02	0.02	0.02	0.02	0.02	0.02	0.02
	Fluorene	0.06	0.06	0.05	0.04	0.08	0.07	0.04	0.03
	Phenanthrene	0.06	0.05	0.06	0.06	0.08	0.07	0.04	0.04
	Anthracene	0.02	0.02	0.02	0.02	0.03	0.03	0.02	0.01
	Subtotal class 4 tars concentration	***1.19***	***1.07***	***0.97***	***0.87***	***1.51***	***1.36***	***0.95***	***0.85***
5	Fluoranthene	0.07	0.06	0.05	0.05	0.05	0.05	0.03	0.03
	Pyrene	0.04	0.03	0.06	0.06	0.04	0.03	0.02	0.02
	Bens(a)anthracene	0.03	0.03	0.02	0.02	0.02	0.02	0.09	0.08
	Chrysene	0.04	0.04	0.02	0.02	0.08	0.07	0.01	0.01
	Benso(b)fluoranthene	0.03	0.02	0.02	0.02	0.02	0.02	0.00	0.00
	Benso(k)fluoranthene	0.02	0.02	0.01	0.01	0.01	0.01	0.01	0.01
	Benso(a)Pyrene	0.01	0.01	0.01	0.01	0.01	0.01	0.01	0.01
	Indeno(1,2,3-cd)pyrene	0.01	0.01	0.00	0.00	0.01	0.00	0.00	0.00
	Benso(g,h,i)perylene	0.01	0.01	0.00	0.00	0.01	0.01	0.00	0.00
	Dibenso(a,h)anthracene	0.01	0.01	0.00	0.00	0.01	0.01	0.00	0.00
	Subtotal class 5 tars concentration	***0.26***	***0.23***	***0.21***	***0.19***	***0.26***	***0.23***	***0.18***	***0.16***
Total tars concentration		**12.04**	**10.85**	**11.40**	**10.27**	**10.24**	**9.23**	**8.36**	**7.53**

Table J.20. Total concentration and yield of tars at each measured gasification temperature

Tar Class	Gasification temperature (°C)				Unit
	650	700	750	800	
Class 2	6.63	5.25	2.40	3.02	g Nm^{-3}
Class 3	2.92	3.96	5.23	3.49	
Class 4	1.07	0.87	1.36	0.85	
Class 5	0.23	0.19	0.23	0.16	
Tars concentration	*10.85*	*10.27*	*9.23*	*7.53*	
Gas yield	*0.50*	*0.49*	*0.53*	*0.61*	Nm^3 kg$^{-1}_{od}$
Tars yield	*5.39*	*5.08*	*4.92*	*4.61*	g kg$^{-1}_{od}$

J.6.2. Investigated parameter 2 (Experiment performed on 4th May 2017)

Table J.21. Signal count ratio and concentration of each tar compound at S/B ratio of 0.7 analysed with LTM.

No	Method	LTM																					
	Solvent	DCM			ρ_{DCM} = 1.32 g ml^{-1}						DCM-IPA			$\rho_{DCM-IPA}$ = 1.05 g ml^{-1}						Average tar mass		Tar amount	
	Category	Signal Count Ratio			Concentration						Signal Count Ratio			Concentration						DCM (G): (A+B+C) / 3	DCM-IPA (H): (D+E+F) / 3	in sample solution (I): (G+H)	in PG (I / 200)
	Repeat	1	2	3	1		2		3		1	2	3	1		2		3					
	Mass of Tar Sample Solution (g)	NA	NA	NA	0.8320		0.8019		0.7916		NA	NA	NA	1.0194		1.0068		1.0357					
	Concentration unit	NA	NA	NA	ppm	µg (A)	ppm	µg (B)	ppm	µg (C)	NA	NA	NA	ppm	µg (D)	ppm	µg (E)	ppm	µg (F)	µg	µg	µg	µg ml^{-1}
1	Benzene	37.74	37.73	41.84	995.73	627.61	995.53	604.78	1103.88	661.99	0.66	0.59	0.81	17.40	16.90	15.68	15.04	21.27	20.98	631.46	17.64	649.10	3.25
2	Toluene	20.10	19.66	21.34	496.28	312.81	485.35	294.85	526.94	316.01	0.81	0.64	0.78	20.12	19.53	15.69	15.04	19.24	18.98	307.89	17.85	325.74	1.63
3	Pyridine	0.15	0.20	0.22	5.27	3.32	7.18	4.36	8.05	4.82	1.01	0.73	0.74	36.60	35.54	26.40	25.32	26.73	26.37	4.17	29.07	33.24	0.17
4	p-xylene + Ethylbenzene	1.37	1.17	1.30	34.36	21.66	29.45	17.89	32.55	19.52	0.22	0.19	0.10	5.57	5.41	4.75	4.56	2.56	2.52	19.69	4.16	23.85	0.12
5	m-xylene	2.71	2.61	2.83	33.19	20.92	31.93	19.40	34.62	20.76	0.34	0.26	0.61	4.15	4.03	3.17	3.04	7.50	7.40	20.36	4.82	25.18	0.13
6	o-xylene	1.15	1.09	1.19	28.28	17.82	26.81	16.29	29.23	17.53	0.02	0.02	0.03	0.59	0.57	0.55	0.52	0.70	0.69	17.21	0.60	17.81	0.09
7	Styrene	7.54	7.40	8.23	182.91	115.29	179.50	109.05	199.77	119.80	0.18	0.15	0.20	4.27	4.15	3.76	3.61	4.86	4.80	114.71	4.18	118.90	0.59
8	Phenol	0.01	0.00	0.01	0.23	0.15	0.16	0.10	0.18	0.11	16.52	16.48	17.59	581.55	564.60	580.30	556.43	619.45	611.01	0.12	577.35	577.46	2.89
9	Indene	4.90	5.03	5.60	126.54	79.76	129.98	78.96	144.73	86.79	0.38	0.32	0.45	9.72	9.43	8.28	7.94	11.56	11.41	81.84	9.59	91.43	0.46
10	o-cresol (2-methylphenol)	0.10	0.07	0.10	3.32	2.09	2.28	1.38	3.15	1.89	2.41	2.20	2.47	78.97	76.66	71.97	69.01	80.87	79.76	1.79	75.15	76.93	0.38
11	m+p-cresol (3+4-methylphenol)	0.22	0.12	0.17	3.87	2.44	2.00	1.22	2.94	1.76	6.12	6.17	6.86	106.53	103.43	107.47	103.05	119.59	117.96	1.81	108.15	109.95	0.55
12	Naphthalene	4.71	4.98	5.60	92.00	57.99	97.22	59.06	109.39	65.60	1.43	1.30	1.68	27.84	27.02	25.38	24.34	32.83	32.38	60.88	27.91	88.80	0.44
13	Quinoline	0.10	0.09	0.10	2.89	1.82	2.84	1.72	3.12	1.87	0.19	0.17	0.20	5.84	5.67	5.12	4.90	5.88	5.80	1.80	5.46	7.26	0.04
14	2-Methylnaphthalene	1.04	0.96	1.13	18.68	11.77	17.29	10.50	20.39	12.23	0.57	0.51	0.63	10.20	9.91	9.26	8.88	11.32	11.16	11.50	9.98	21.48	0.11
15	Isoquinoline	0.01	0.01	0.01	0.38	0.24	0.40	0.24	0.48	0.29	0.13	0.13	0.14	4.09	3.97	4.07	3.91	4.55	4.48	0.26	4.12	4.38	0.02
16	1-Methylnaphthalene	0.73	0.66	0.79	13.76	8.67	12.40	7.53	14.85	8.90	0.59	0.52	0.67	11.09	10.76	9.86	9.45	12.56	12.39	8.37	10.87	19.24	0.10
17	Biphenyl	0.30	0.28	0.33	6.90	4.35	6.59	4.00	7.71	4.62	0.71	0.41	0.69	16.43	15.95	9.64	9.25	15.97	15.75	4.32	13.65	17.97	0.09
18	Acenaphthylene	0.81	0.77	0.91	15.52	9.78	14.78	8.98	17.40	10.44	0.72	0.68	0.82	13.76	13.36	13.01	12.48	15.68	15.46	9.73	13.77	23.50	0.12
19	Acenapthene	0.12	0.11	0.17	2.36	1.49	2.02	1.23	3.15	1.89	0.10	0.12	0.12	1.91	1.85	2.22	2.12	2.20	2.17	1.53	2.05	3.58	0.02
20	Fluorene	0.60	0.50	0.64	11.52	7.26	9.67	5.88	12.19	7.31	0.43	0.39	0.47	8.21	7.97	7.53	7.22	9.05	8.93	6.81	8.04	14.85	0.07
21	Phenanthrene	0.59	0.50	0.67	11.68	7.36	9.93	6.03	13.35	8.01	0.43	0.42	0.53	8.54	8.29	8.37	8.02	10.50	10.35	7.13	8.89	16.02	0.08
22	Anthracene	0.22	0.19	0.29	3.21	2.02	2.82	1.71	4.31	2.58	0.14	0.14	0.18	2.13	2.07	2.11	2.02	2.59	2.55	2.11	2.21	4.32	0.02
23	Fluoranthene	0.44	0.38	0.51	7.46	4.70	6.45	3.92	8.55	5.13	0.45	0.48	0.55	7.52	7.30	8.03	7.70	9.20	9.07	4.58	8.02	12.61	0.06
24	Pyrene	0.43	0.51	0.54	4.12	2.60	4.92	2.99	5.21	3.13	0.39	0.37	0.59	3.74	3.63	3.56	3.42	5.62	5.55	2.90	4.20	7.10	0.04
25	Bens(a)anthracene																						
26	Chrysene																						
27	Benso(b)fluoranthene																						
28	Benso(k)fluoranthene																						
29	Benso(a)Pyrene																						
30	Indeno(1,2,3-cd)pyrene																						
31	Benso(g,h,i)perylene																						
32	Dibenso(a,h)anthracene																						

Table J.22. Signal count ratio and concentration of each tar compound at S/B ratio of 0.7 analysed with HTM.

No	Method	HTM																					
	Solvent	DCM						ρ_{DCM} = 1.32 g ml^{-1}			DCM-IPA						$\rho_{DCM-IPA}$ = 1.05 g ml^{-1}				Average tar mass		Tar amount	
	Category	Signal Count Ratio			Concentration						Signal Count Ratio			Concentration									
	Repeat	1	2	3	1		2		3		1	2	3	1		2		3		DCM (G): (A+B+C) / 3	DCM-IPA (H): (D+E+F) / 3	in sample solution (I): (G+H)	in PG (I / 200)
	Mass of Tar Sample Solution (g)	NA	NA	NA	0.8320		0.8019		0.7916		NA	NA	NA	1.0194		1.0068		1.0357					
	Concentration unit	NA	NA	NA	ppm	µg (A)	ppm	µg (B)	ppm	µg (C)	NA	NA	NA	ppm	µg (D)	ppm	µg (E)	ppm	µg (F)	µg	µg	µg	µg ml^{-1}
1	Benzene																						
2	Toluene																						
3	Pyridine																						
4	p-xylene + Ethylbenzene																						
5	m-xylene																						
6	o-xylene																						
7	Styrene																						
8	Phenol	0.02	0.05	0.02	0.96	0.60	2.09	1.27	1.02	0.61	0.05	0.05	0.06	2.26	2.20	2.25	2.16	2.33	2.30	0.83	2.22	3.05	0.02
9	Indene	4.89	4.85	5.53	150.34	94.76	149.25	90.67	170.07	101.99	0.33	0.27	0.38	10.13	9.83	8.40	8.06	11.64	11.48	95.81	9.79	105.60	0.53
10	o-cresol (2-methylphenol)	0.04	0.12	0.05	1.40	0.88	4.02	2.44	1.64	0.98	2.16	1.91	2.14	75.02	72.83	66.15	63.42	74.27	73.26	1.44	69.84	71.28	0.36
11	m+p-cresol (3+4-methylphenol)	0.19	0.09	0.12	3.79	2.39	1.92	1.17	2.55	1.53	5.42	5.02	5.49	110.75	107.52	102.68	98.45	112.18	110.65	1.70	105.54	107.24	0.54
12	Naphthalene	4.53	4.78	5.38	96.42	60.77	101.68	61.77	114.40	68.60	1.20	1.09	1.41	25.54	24.79	23.27	22.32	30.10	29.69	63.71	25.60	89.31	0.45
13	Quinoline	0.10	0.10	0.13	3.39	2.13	3.49	2.12	4.47	2.68	0.45	0.29	0.40	15.48	15.03	10.00	9.59	13.90	13.71	2.31	12.78	15.09	0.08
14	2-Methylnaphthalene	0.48	0.24	0.42	10.10	6.37	4.93	3.00	8.73	5.24	0.48	0.44	0.53	10.01	9.71	9.10	8.73	11.08	10.93	4.87	9.79	14.66	0.07
15	Isoquinoline	1.01	0.92	1.10	38.07	24.00	34.99	21.25	41.56	24.92	0.10	0.09	0.10	3.67	3.57	3.45	3.31	3.95	3.89	23.39	3.59	26.98	0.13
16	1-Methylnaphthalene	0.76	0.66	0.82	16.65	10.50	14.50	8.81	18.04	10.82	0.40	0.37	0.45	8.73	8.48	8.17	7.83	9.82	9.69	10.04	8.67	18.71	0.09
17	Biphenyl	0.40	0.29	0.33	10.50	6.62	7.49	4.55	8.68	5.21	0.16	0.17	0.20	4.10	3.98	4.44	4.26	5.13	5.06	5.46	4.43	9.89	0.05
18	Acenaphthylene	0.87	0.73	0.94	18.66	11.76	15.64	9.50	20.14	12.08	0.51	0.51	0.60	11.03	10.71	11.00	10.55	12.97	12.79	11.11	11.35	22.47	0.11
19	Acenapthene	0.13	0.10	0.13	2.84	1.79	2.24	1.36	2.80	1.68	0.09	0.08	0.10	1.87	1.81	1.73	1.66	2.08	2.06	1.61	1.84	3.45	0.02
20	Fluorene	0.59	0.47	0.62	14.22	8.96	11.46	6.96	14.87	8.92	0.34	0.31	0.39	8.27	8.03	7.60	7.29	9.32	9.20	8.28	8.17	16.45	0.08
21	Phenanthrene	0.50	0.46	0.59	12.93	8.15	11.72	7.12	15.25	9.14	0.31	0.32	0.38	7.92	7.69	8.14	7.81	9.66	9.53	8.14	8.34	16.48	0.08
22	Anthracene	0.38	0.18	0.26	9.86	6.22	4.80	2.92	6.68	4.01	0.10	0.11	0.13	2.71	2.63	2.80	2.69	3.37	3.32	4.38	2.88	7.26	0.04
23	Fluoranthene	0.33	0.22	0.29	8.65	5.45	5.75	3.50	7.67	4.60	0.17	0.16	0.19	4.54	4.41	4.36	4.18	5.04	4.97	4.52	4.52	9.04	0.05
24	Pyrene	0.36	0.17	0.22	8.66	5.46	4.05	2.46	5.39	3.24	0.19	0.13	0.15	4.56	4.43	3.12	2.99	3.62	3.57	3.72	3.66	7.38	0.04
25	Bens(a)anthracene	0.14	0.12	0.15	4.56	2.87	3.91	2.37	4.80	2.88	0.07	0.06	0.07	2.20	2.13	2.06	1.97	2.43	2.39	2.71	2.17	4.88	0.02
26	Chrysene	2.04	0.13	0.18	52.90	33.34	3.45	2.10	4.72	2.83	0.10	0.10	0.12	2.59	2.51	2.65	2.54	3.00	2.95	12.76	2.67	15.43	0.08
27	Benso(b)fluoranthene	0.04	0.09	0.10	1.13	0.71	2.83	1.72	3.34	2.00	0.08	0.08	0.08	2.49	2.41	2.52	2.42	2.69	2.65	1.48	2.49	3.97	0.02
28	Benso(k)fluoranthene	0.02	0.06	0.06	0.60	0.38	1.75	1.06	1.85	1.11	0.05	0.06	0.06	1.63	1.58	1.72	1.65	1.84	1.82	0.85	1.69	2.53	0.01
29	Benso(a)Pyrene	0.03	0.07	0.08	0.80	0.50	1.84	1.12	1.96	1.17	0.06	0.07	0.06	1.48	1.44	1.67	1.60	1.60	1.58	0.93	1.54	2.47	0.01
30	Indeno(1,2,3-cd)pyrene	0.00	0.02	0.02	0.20	0.13	0.87	0.53	0.77	0.46	0.02	0.02	0.01	0.99	0.96	0.65	0.63	0.58	0.57	0.37	0.72	1.09	0.01
31	Benso(g,h,i)perylene	0.01	0.04	0.04	0.38	0.24	1.51	0.92	1.28	0.77	0.03	0.04	0.03	1.07	1.04	1.32	1.26	1.15	1.13	0.64	1.14	1.79	0.01
32	Dibenso(a,h)anthracene	0.01	0.05	0.05	0.36	0.23	1.20	0.73	1.13	0.68	0.05	0.03	0.04	1.20	1.16	0.83	0.79	1.02	1.01	0.54	0.99	1.53	0.01

Table J.23. Total tar concentration for each tar compounds at S/B ratio of 0.7.

No	Tar component	Tar concentration (µg ml^{-1})		Average (µg ml^{-1})	Total tar (µg ml^{-1})
		LTM	HTM		
1	Benzene	3.25			3.25
2	Toluene	1.63			1.63
3	Pyridine	0.17			0.17
4	p-xylene + Ethylbenzene	0.12			0.12
5	m-xylene	0.13			0.13
6	o-xylene	0.09			0.09
7	Styrene	0.59			0.59
8	Phenol	2.89	0.02	1.45	1.45
9	Indene	0.46	0.53	0.49	0.49
10	o-cresol (2-methylphenol)	0.38	0.36	0.37	0.37
11	m+p-cresol (3+4-methylphenol)	0.55	0.54	0.54	0.54
12	Naphthalene	0.44	0.45	0.45	0.45
13	Quinoline	0.04	0.08	0.06	0.06
14	2-Methylnaphthalene	0.11	0.07	0.09	0.09
15	Isoquinoline	0.02	0.13	0.08	0.08
16	1-Methylnaphthalene	0.10	0.09	0.09	0.09
17	Biphenyl	0.09	0.05	0.07	0.07
18	Acenaphthylene	0.12	0.11	0.11	0.11
19	Acenapthene	0.02	0.02	0.02	0.02
20	Fluorene	0.07	0.08	0.08	0.08
21	Phenanthrene	0.08	0.08	0.08	0.08
22	Anthracene	0.02	0.04	0.03	0.03
23	Fluoranthene	0.06	0.05	0.05	0.05
24	Pyrene	0.04	0.04	0.04	0.04
25	Bens(a)anthracene		0.02		0.02
26	Chrysene		0.08		0.08
27	Benso(b)fluoranthene		0.02		0.02
28	Benso(k)fluoranthene		0.01		0.01
29	Benso(a)Pyrene		0.01		0.01
30	Indeno(1,2,3-cd)pyrene		0.01		0.01
31	Benso(g,h,i)perylene		0.01		0.01
32	Dibenso(a,h)anthracene		0.01		0.01

Table J.24. Signal count ratio and concentration of each tar compound at S/B ratio of 0.8 analysed with LTM.

No	Method	LTM																				
	Solvent	DCM					$\dot{\rho}_{DCM}$ = 1.32 g ml^{-1}				DCM-IPA						$\dot{\rho}_{DCM-IPA}$ = 1.05 g ml^{-1}				Average tar mass		Tar amount	
	Category	Signal Count Ratio			Concentration						Signal Count Ratio			Concentration							DCM (G): (A+B+C) / 3	DCM-IPA (H): (D+E+F) / 3	in sample solution (I): (G+H)	in PG (I / 200)
	Repeat	1	2	3	1		2		3		1	2	3	1		2		3					
	Mass of Tar Sample Solution (g)	NA	NA	NA	0.7471		0.7552		0.7429		NA	NA	NA	1.031		1.0058		0.9581					
	Concentration unit	NA	NA	NA	ppm	µg (A)	ppm	µg (B)	ppm	µg (C)	NA	NA	NA	ppm	µg (D)	ppm	µg (E)	ppm	µg (F)		µg	µg	µg	µg ml^{-1}
1	Benzene	13.35	20.08	20.05	352.25	199.37	529.90	303.17	528.95	297.69	1.24	1.39	1.30	32.60	32.01	36.66	35.12	34.25	31.26		266.74	32.80	299.54	1.50
2	Toluene	12.07	14.17	14.00	298.05	168.69	349.95	200.21	345.71	194.57	1.58	1.27	1.25	38.96	38.26	31.37	30.05	30.80	28.11		187.82	32.14	219.96	1.10
3	Pyridine	1.04	0.86	0.95	37.64	21.30	31.17	17.84	34.34	19.33	0.04	0.16	0.13	1.38	1.36	5.63	5.39	4.77	4.35		19.49	3.70	23.19	0.12
4	p-xylene + Ethylbenzene	0.77	0.85	0.89	19.40	10.98	21.42	12.25	22.39	12.60	0.12	0.10	0.11	2.97	2.91	2.58	2.47	2.83	2.58		11.95	2.65	14.60	0.07
5	m-xylene	1.92	2.17	2.16	23.50	13.30	26.55	15.19	26.42	14.87	0.39	0.29	0.33	4.79	4.70	3.54	3.39	4.00	3.65		14.45	3.91	18.37	0.09
6	o-xylene	0.81	0.90	0.92	19.84	11.23	22.10	12.65	22.48	12.65	0.13	0.09	0.10	3.29	3.23	2.29	2.19	2.34	2.14		12.17	2.52	14.70	0.07
7	Styrene	5.86	6.38	6.53	142.23	80.50	154.97	88.66	158.47	89.19	0.82	0.57	0.56	19.86	19.50	13.88	13.30	13.59	12.40		86.12	15.07	101.18	0.51
8	Phenol	0.19	0.03	0.05	6.59	3.73	1.01	0.58	1.91	1.08	18.58	17.86	19.95	654.10	642.26	628.92	602.44	702.54	641.05		1.80	628.58	630.38	3.15
9	Indene	4.54	5.09	5.14	117.21	66.34	131.40	75.18	132.94	74.82	0.90	0.57	0.60	23.14	22.72	14.75	14.13	15.60	14.23		72.11	17.03	89.14	0.45
10	o-cresol (2-methylphenol)	0.43	0.20	0.23	14.18	8.03	6.40	3.66	7.50	4.22	1.95	2.18	2.37	64.02	62.86	71.50	68.49	77.73	70.93		5.30	67.42	72.73	0.36
11	m+p-cresol (3+4-methylphenol)	0.06	0.02	0.02	1.00	0.56	0.42	0.24	0.41	0.23	6.26	6.07	6.78	109.06	107.08	105.80	101.34	118.19	107.85		0.35	105.43	105.77	0.53
12	Naphthalene	6.03	6.16	6.18	117.81	66.68	120.39	68.88	120.70	67.93	1.49	1.08	1.18	29.01	28.49	21.18	20.29	23.03	21.02		67.83	23.27	91.10	0.46
13	Quinoline	0.19	0.15	0.19	5.65	3.20	4.58	2.62	5.58	3.14	0.15	0.17	0.19	4.49	4.41	5.23	5.01	5.70	5.20		2.99	4.87	7.86	0.04
14	2-Methylnaphthalene	1.20	1.14	1.20	21.59	12.22	20.54	11.75	21.68	12.20	0.56	0.53	0.52	10.03	9.85	9.50	9.10	9.37	8.55		12.06	9.17	21.22	0.11
15	Isoquinoline	0.04	0.03	0.04	1.39	0.79	1.02	0.58	1.34	0.75	0.04	0.10	0.09	1.29	1.27	3.35	3.21	2.80	2.56		0.71	2.34	3.05	0.02
16	1-Methylnaphthalene	0.83	0.80	0.86	15.60	8.83	15.03	8.60	16.16	9.09	0.36	0.42	0.33	6.86	6.74	7.84	7.51	6.29	5.74		8.84	6.66	15.50	0.08
17	Biphenyl	0.32	0.30	0.35	7.45	4.22	7.06	4.04	8.08	4.55	0.17	0.19	0.19	4.05	3.98	4.48	4.29	4.34	3.96		4.27	4.08	8.34	0.04
18	Acenaphthylene	0.82	0.85	0.98	15.66	8.86	16.21	9.27	18.75	10.55	0.69	0.71	0.73	13.23	12.99	13.52	12.95	13.88	12.67		9.56	12.87	22.43	0.11
19	Acenapthene	0.11	0.12	0.14	2.01	1.14	2.20	1.26	2.57	1.45	0.10	0.11	0.11	1.81	1.78	2.10	2.01	2.16	1.97		1.28	1.92	3.20	0.02
20	Fluorene	0.37	0.49	0.56	7.06	4.00	9.41	5.38	10.69	6.02	0.36	0.43	0.39	6.91	6.78	8.25	7.91	7.44	6.79		5.13	7.16	12.29	0.06
21	Phenanthrene	0.50	0.55	0.65	9.81	5.55	10.82	6.19	12.91	7.27	0.54	0.53	0.59	10.61	10.42	10.57	10.12	11.69	10.67		6.34	10.40	16.74	0.08
22	Anthracene	0.23	0.25	0.29	3.33	1.88	3.64	2.08	4.22	2.38	0.26	0.25	0.27	3.82	3.75	3.64	3.49	3.96	3.61		2.11	3.62	5.73	0.03
23	Fluoranthene	0.41	0.44	0.48	6.95	3.93	7.41	4.24	8.06	4.53	0.27	0.63	0.42	4.60	4.52	10.68	10.23	7.09	6.47		4.24	7.07	11.31	0.06
24	Pyrene	0.31	0.32	0.35	2.94	1.67	3.09	1.77	3.37	1.90	0.33	0.38	0.38	3.15	3.09	3.67	3.51	3.60	3.29		1.78	3.30	5.08	0.03
25	Bens(a)anthracene																							
26	Chrysene																							
27	Benso(b)fluoranthene																							
28	Benso(k)fluoranthene																							
29	Benso(a)Pyrene																							
30	Indeno(1,2,3-cd)pyrene																							
31	Benso(g,h,i)perylene																							
32	Dibenso(a,h)anthracene																							

Table J.25. Signal count ratio and concentration of each tar compound at S/B ratio of 0.8 analysed with HTM.

No	Method	HTM																			
	Solvent	DCM					ρ_{DCM} = 1.32 g ml^{-1}			DCM-IPA						$\rho_{DCM-IPA}$ = 1.05 g ml^{-1}		Average tar mass		Tar amount	
	Category	Signal Count Ratio			Concentration					Signal Count Ratio			Concentration								
	Repeat	1	2	3	1		2		3	1	2	3	1		2		3		DCM (G): (A+B+	DCM-IPA (H): (D+E+F) /	in sample solution (I): (G+H)	in PG (I / 200)
	Mass of Tar Sample Solution (g)	NA	NA	NA	0.7471		0.7552		0.7429	NA	NA	NA	1.031		1.0058		0.9581					
	Concentration unit	NA	NA	NA	ppm	µg (A)	ppm	µg (B)	ppm	µg (C)	NA	NA	NA	ppm	µg (D)	ppm	µg (E)	ppm	µg (F)	µg	µg	µg	µg ml^{-1}
1	Benzene																					
2	Toluene																					
3	Pyridine																					
4	p-xylene + Ethylbenzene																					
5	m-xylene																					
6	o-xylene																					
7	Styrene																					
8	Phenol	1.45	1.58	1.54	60.51	34.25	66.04	37.79	64.51	36.31	16.14	15.46	17.38	675.34	663.12	646.78	619.55	727.34	663.68	36.11	648.79	684.90	3.42
9	Indene	4.23	4.76	4.79	130.28	73.74	146.46	83.79	147.35	82.93	0.79	0.49	0.52	24.18	23.74	15.02	14.39	16.15	14.74	80.15	17.62	97.78	0.49
10	o-cresol (2-methylphenol)	0.56	0.29	0.37	19.60	11.10	10.01	5.73	12.75	7.18	1.78	2.02	2.19	61.96	60.84	70.25	67.29	76.18	69.51	8.00	65.88	73.88	0.37
11	m+p-cresol (3+4-methylphenol)	0.04	0.02	0.02	0.84	0.47	0.33	0.19	0.32	0.18	5.37	5.30	5.91	109.86	107.87	108.29	103.73	120.76	110.19	0.28	107.27	107.55	0.54
12	Naphthalene	5.87	5.92	5.93	124.85	70.67	125.94	72.05	126.10	70.97	1.31	0.95	1.04	27.84	27.34	20.14	19.29	22.04	20.11	71.23	22.25	93.48	0.47
13	Quinoline	0.19	0.08	0.18	6.44	3.65	2.65	1.52	6.30	3.54	0.17	0.20	0.21	5.75	5.65	6.75	6.46	7.25	6.62	2.90	6.24	9.15	0.05
14	2-Methylnaphthalene	1.17	1.08	1.16	24.40	13.81	22.64	12.95	24.21	13.62	0.39	0.38	0.39	8.19	8.04	7.92	7.59	8.14	7.43	13.46	7.69	21.15	0.11
15	Isoquinoline	0.03	0.01	0.04	1.22	0.69	0.46	0.26	1.60	0.90	0.06	0.07	0.08	2.31	2.27	2.78	2.67	3.11	2.84	0.62	2.59	3.21	0.02
16	1-Methylnaphthalene	0.84	0.80	0.86	18.39	10.41	17.48	10.00	18.74	10.55	0.33	0.36	0.34	7.30	7.17	7.78	7.45	7.43	6.78	10.32	7.13	17.45	0.09
17	Biphenyl	0.32	0.30	0.34	8.25	4.67	7.79	4.46	8.91	5.02	0.16	0.16	0.16	4.11	4.03	4.21	4.03	4.19	3.82	4.71	3.96	8.68	0.04
18	Acenaphthylene	0.75	0.77	0.89	16.14	9.13	16.54	9.46	19.19	10.80	0.56	0.64	0.59	11.97	11.75	13.72	13.14	12.75	11.63	9.80	12.17	21.97	0.11
19	Acenapthene	0.10	0.10	0.12	2.17	1.23	2.07	1.18	2.51	1.41	0.09	0.08	0.10	2.01	1.98	1.83	1.75	2.24	2.04	1.28	1.92	3.20	0.02
20	Fluorene	0.32	0.43	0.49	7.82	4.43	10.33	5.91	11.79	6.64	0.30	0.36	0.37	7.30	7.17	8.80	8.43	8.91	8.13	5.66	7.91	13.57	0.07
21	Phenanthrene	0.39	0.41	0.51	9.90	5.60	10.45	5.98	13.14	7.40	0.39	0.38	0.43	10.08	9.89	9.74	9.33	10.97	10.01	6.33	9.74	16.07	0.08
22	Anthracene	0.16	0.15	0.21	4.16	2.36	3.98	2.28	5.46	3.07	0.14	0.13	0.15	3.63	3.57	3.44	3.30	3.89	3.55	2.57	3.47	6.04	0.03
23	Fluoranthene	0.18	0.14	0.24	4.75	2.69	3.81	2.18	6.38	3.59	0.19	0.14	0.22	5.02	4.92	3.62	3.47	5.89	5.37	2.82	4.59	7.41	0.04
24	Pyrene	0.15	0.17	0.20	3.69	2.09	4.08	2.34	4.73	2.66	0.19	0.14	0.22	4.46	4.38	3.47	3.32	5.20	4.75	2.36	4.15	6.51	0.03
25	Bens(a)anthracene	0.09	0.07	0.12	2.97	1.68	2.21	1.27	3.96	2.23	0.10	0.02	0.12	3.28	3.22	0.78	0.75	3.92	3.57	1.72	2.51	4.24	0.02
26	Chrysene	0.11	0.11	0.15	2.87	1.62	2.77	1.59	3.81	2.14	0.16	0.06	0.18	4.08	4.01	1.64	1.57	4.68	4.27	1.78	3.28	5.07	0.03
27	Benso(b)fluoranthene	0.05	0.03	0.07	1.77	1.00	1.09	0.63	2.25	1.27	0.09	0.02	0.11	2.94	2.89	0.55	0.52	3.43	3.13	0.96	2.18	3.14	0.02
28	Benso(k)fluoranthene	0.03	0.01	0.04	0.85	0.48	0.43	0.24	1.13	0.63	0.04	0.01	0.05	1.27	1.25	0.26	0.25	1.41	1.28	0.45	0.93	1.38	0.01
29	Benso(a)Pyrene	0.04	0.04	0.05	1.05	0.59	1.09	0.62	1.33	0.75	0.06	0.02	0.07	1.53	1.50	0.49	0.47	1.81	1.65	0.65	1.21	1.86	0.01
30	Indeno(1,2,3-cd)pyrene	0.01	0.01	0.01	0.50	0.29	0.24	0.14	0.58	0.33	0.03	0.01	0.04	1.09	1.07	0.21	0.20	1.76	1.60	0.25	0.96	1.21	0.01
31	Benso(g,h,i)perylene	0.02	0.02	0.03	0.78	0.44	0.77	0.44	0.90	0.50	0.04	0.00	0.02	1.36	1.33	0.07	0.07	0.83	0.75	0.46	0.72	1.18	0.01
32	Dibenso(a,h)anthracene	0.02	0.02	0.03	0.54	0.30	0.50	0.28	0.78	0.44	0.03	0.00	0.04	0.79	0.78	0.12	0.12	1.08	0.99	0.34	0.63	0.97	0.00

Table J.26. Total tar concentration for each tar compounds at S/B ratio of 0.8.

No	Tar component	Tar concentration (µg ml^{-1})		Average (µg ml^{-1})	Total tar (µg ml^{-1})
		LTM	HTM		
1	Benzene	1.50			1.50
2	Toluene	1.10			1.10
3	Pyridine	0.12			0.12
4	p-xylene + Ethylbenzene	0.07			0.07
5	m-xylene	0.09			0.09
6	o-xylene	0.07			0.07
7	Styrene	0.51			0.51
8	Phenol	3.15	3.42	3.29	3.29
9	Indene	0.45	0.49	0.47	0.47
10	o-cresol (2-methylphenol)	0.36	0.37	0.37	0.37
11	m+p-cresol (3+4-methylphenol)	0.53	0.54	0.53	0.53
12	Naphthalene	0.46	0.47	0.46	0.46
13	Quinoline	0.04	0.05	0.04	0.04
14	2-Methylnaphthalene	0.11	0.11	0.11	0.11
15	Isoquinoline	0.02	0.02	0.02	0.02
16	1-Methylnaphthalene	0.08	0.09	0.08	0.08
17	Biphenyl	0.04	0.04	0.04	0.04
18	Acenaphthylene	0.11	0.11	0.11	0.11
19	Acenapthene	0.02	0.02	0.02	0.02
20	Fluorene	0.06	0.07	0.06	0.06
21	Phenanthrene	0.08	0.08	0.08	0.08
22	Anthracene	0.03	0.03	0.03	0.03
23	Fluoranthene	0.06	0.04	0.05	0.05
24	Pyrene	0.03	0.03	0.03	0.03
25	Bens(a)anthracene		0.02		0.02
26	Chrysene		0.03		0.03
27	Benso(b)fluoranthene		0.02		0.02
28	Benso(k)fluoranthene		0.01		0.01
29	Benso(a)Pyrene		0.01		0.01
30	Indeno(1,2,3-cd)pyrene		0.01		0.01
31	Benso(g,h,i)perylene		0.01		0.01
32	Dibenso(a,h)anthracene		0.00		0.00

Table J.27. Signal count ratio and concentration of each tar compound at S/B ratio of 0.9 analysed with LTM.

No	Method	LTM																			
	Solvent	DCM					ρ_{DCM} = 1.32 g ml^{-1}				DCM-IPA						$\rho_{DCM-IPA}$ = 1.05 g ml^{-1}		Average tar mass		Tar amount	
	Category	Signal Count Ratio			Concentration						Signal Count Ratio			Concentration							DCM (G): (A+B+C) / 3	DCM-IPA (H): (D+E+F) / 3	in sample solution (I): (G+H)	in PG (I / 200)
	Repeat	1	2	3	1		2		3		1	2	3	1		2		3					
	Mass of Tar Sample Solution (g)	NA	NA	NA	0.7871		0.6159		0.7837		NA	NA	NA	0.9767		1.0136		1.0528					
	Concentration unit	NA	NA	NA	ppm	µg (A)	ppm	µg (B)	ppm	µg (C)	NA	NA	NA	ppm	µg (D)	ppm	µg (E)	ppm	µg (F)		µg	µg	µg	µg ml^{-1}
1	Benzene	30.43	9.16	32.51	802.82	478.71	241.77	112.81	857.70	509.23	1.65	1.31	1.26	43.49	44.60	34.69	33.49	33.17	33.25		366.92	37.11	404.03	2.02
2	Toluene	16.25	10.65	16.92	401.16	239.21	262.99	122.71	417.76	248.03	1.07	0.87	0.79	26.52	27.20	21.52	20.77	19.58	19.64		203.32	22.54	225.85	1.13
3	Pyridine	1.41	0.87	1.43	51.23	30.55	31.55	14.72	51.94	30.84	0.23	0.36	0.28	8.28	8.49	12.93	12.48	10.24	10.27		25.37	10.41	35.78	0.18
4	p-xylene + Ethylbenzene	1.03	0.70	1.01	25.79	15.38	17.68	8.25	25.37	15.06	0.19	0.23	0.18	4.88	5.01	5.73	5.54	4.46	4.48		12.90	5.01	17.90	0.09
5	m-xylene	2.28	1.80	2.34	27.86	16.61	22.08	10.30	28.66	17.02	0.23	0.22	0.18	2.85	2.92	2.65	2.56	2.16	2.16		14.64	2.55	17.19	0.09
6	o-xylene	0.97	0.75	0.99	23.80	14.19	18.39	8.58	24.21	14.37	0.08	0.08	0.06	1.94	1.99	1.86	1.79	1.42	1.42		12.38	1.74	14.12	0.07
7	Styrene	7.01	5.46	7.17	170.04	101.39	132.43	61.79	174.12	103.38	0.49	0.42	0.35	11.93	12.23	10.22	9.86	8.44	8.46		88.85	10.19	99.04	0.50
8	Phenol	1.90	1.61	1.95	67.02	39.96	56.79	26.50	68.83	40.87	16.32	17.43	11.77	574.76	589.44	613.78	592.50	414.56	415.67		35.78	532.54	568.31	2.84
9	Indene	4.90	4.19	5.08	126.54	75.46	108.23	50.50	131.20	77.89	0.44	0.43	0.36	11.45	11.74	11.14	10.76	9.38	9.40		67.95	10.63	78.58	0.39
10	o-cresol (2-methylphenol)	0.08	0.43	0.10	2.55	1.52	14.05	6.55	3.30	1.96	2.31	2.42	1.63	75.72	77.65	79.21	76.47	53.42	53.56		3.34	69.23	72.57	0.36
11	m+p-cresol (3+4-methylphenol)	0.02	0.06	0.01	0.28	0.17	1.10	0.51	0.24	0.14	5.62	5.87	4.29	97.96	100.47	102.23	98.69	74.82	75.02		0.27	91.39	91.67	0.46
12	Naphthalene	5.20	5.57	5.39	101.63	60.60	108.81	50.77	105.18	62.45	0.94	0.83	0.73	18.44	18.91	16.12	15.56	14.18	14.21		57.94	16.23	74.17	0.37
13	Quinoline	0.13	0.18	0.13	3.77	2.25	5.33	2.49	3.85	2.28	0.12	0.13	0.08	3.47	3.56	3.93	3.79	2.34	2.35		2.34	3.23	5.57	0.03
14	2-Methylnaphthalene	0.87	0.08	0.91	15.64	9.33	1.50	0.70	16.41	9.74	0.40	0.34	0.29	7.15	7.34	6.05	5.84	5.24	5.26		6.59	6.15	12.74	0.06
15	Isoquinoline	0.03	1.06	0.03	0.86	0.52	34.12	15.92	0.88	0.52	0.08	0.09	0.06	2.49	2.55	2.74	2.64	1.91	1.91		5.65	2.37	8.02	0.04
16	1-Methylnaphthalene	0.58	0.73	0.60	10.91	6.51	13.78	6.43	11.31	6.71	0.43	0.40	0.32	8.03	8.23	7.56	7.30	5.99	6.00		6.55	7.18	13.73	0.07
17	Biphenyl	0.20	0.29	0.21	4.70	2.80	6.76	3.15	4.78	2.84	0.15	0.11	0.11	3.49	3.58	2.60	2.51	2.47	2.48		2.93	2.85	5.78	0.03
18	Acenaphthylene	0.48	0.76	0.49	9.18	5.47	14.47	6.75	9.39	5.57	0.59	0.53	0.43	11.25	11.54	10.21	9.85	8.24	8.26		5.93	9.88	15.82	0.08
19	Acenapthene	0.06	0.10	0.07	1.16	0.69	1.83	0.86	1.35	0.80	0.10	0.08	0.09	1.85	1.89	1.59	1.53	1.66	1.66		0.78	1.70	2.48	0.01
20	Fluorene	0.26	0.40	0.25	5.03	3.00	7.67	3.58	4.74	2.82	0.33	0.30	0.24	6.32	6.48	5.81	5.61	4.54	4.55		3.13	5.54	8.68	0.04
21	Phenanthrene	0.30	0.51	0.30	6.02	3.59	10.04	4.68	5.90	3.51	0.40	0.35	0.30	7.87	8.07	7.00	6.76	5.87	5.89		3.93	6.91	10.83	0.05
22	Anthracene	0.15	0.22	0.15	2.27	1.35	3.24	1.51	2.22	1.32	0.16	0.13	0.11	2.31	2.37	1.92	1.85	1.63	1.63		1.39	1.95	3.35	0.02
23	Fluoranthene	0.27	0.33	0.26	4.49	2.68	5.48	2.56	4.36	2.59	0.37	0.39	0.28	6.26	6.42	6.53	6.31	4.68	4.69		2.61	5.81	8.41	0.04
24	Pyrene	0.28	0.31	0.30	2.70	1.61	2.99	1.39	2.87	1.71	0.41	0.35	0.32	3.96	4.07	3.33	3.22	3.11	3.12		1.57	3.47	5.04	0.03
25	Bens(a)anthracene																							
26	Chrysene																							
27	Benso(b)fluoranthene																							
28	Benso(k)fluoranthene																							
29	Benso(a)Pyrene																							
30	Indeno(1,2,3-cd)pyrene																							
31	Benso(g,h,i)perylene																							
32	Dibenso(a,h)anthracene																							

Table J.28. Signal count ratio and concentration of each tar compound at S/B ratio of 0.9 analysed with HTM.

No	Method	HTM																				
	Solvent	DCM					ρ_{DCM} = 1.32 g ml^{-1}				DCM-IPA						$\rho_{DCM-IPA}$ = 1.05 g ml^{-1}				Average tar mass		Tar amount	
	Category	Signal Count Ratio			Concentration						Signal Count Ratio			Concentration										
	Repeat	1	2	3	1		2		3		1	2	3	1		2		3		DCM (G): (A+B+C) / 3	DCM-IPA (H): (D+E+F) / 3	in sample solution (I): (G+H)	in PG (I / 200)
	Mass of Tar Sample Solution (g)	NA	NA	NA	0.7871		0.6159		0.7837		NA	NA	NA	0.9767		1.0136		1.0528					
	Concentration unit	NA	NA	NA	ppm	µg (A)	ppm	µg (B)	ppm	µg (C)	NA	NA	NA	ppm	µg (D)	ppm	µg (E)	ppm	µg (F)	µg	µg	µg	µg ml^{-1}
1	Benzene																						
2	Toluene																						
3	Pyridine																						
4	p-xylene + Ethylbenzene																						
5	m-xylene																						
6	o-xylene																						
7	Styrene																						
8	Phenol	1.61	1.37	1.66	67.46	40.22	57.42	26.79	69.35	41.18	14.38	14.85	11.52	601.63	559.63	621.34	599.80	482.02	483.30	36.07	547.58	583.64	2.92
9	Indene	4.76	3.91	4.91	146.48	87.34	120.37	56.16	151.17	89.75	0.39	0.38	0.31	12.13	11.28	11.70	11.29	9.42	9.44	77.75	10.67	88.42	0.44
10	o-cresol (2-methylphenol)	0.12	0.06	0.12	4.13	2.46	1.93	0.90	4.05	2.41	2.14	2.19	1.66	74.45	69.25	76.19	73.55	57.55	57.71	1.92	66.84	68.76	0.34
11	m+p-cresol (3+4-methylphenol)	0.07	0.04	0.06	1.39	0.83	0.83	0.39	1.32	0.78	4.98	5.16	3.99	101.76	94.65	105.54	101.89	81.59	81.81	0.67	92.78	93.45	0.47
12	Naphthalene	5.06	5.43	5.22	107.64	64.19	115.56	53.92	111.01	65.91	0.85	0.73	0.71	18.17	16.90	15.55	15.01	15.16	15.20	61.34	15.71	77.04	0.39
13	Quinoline	0.14	0.17	0.14	4.78	2.85	6.02	2.81	4.91	2.92	0.16	0.17	0.11	5.38	5.00	5.89	5.69	3.69	3.70	2.86	4.80	7.66	0.04
14	2-Methylnaphthalene	0.84	0.08	0.88	17.51	10.44	1.59	0.74	18.31	10.87	0.36	0.30	0.28	7.51	6.98	6.23	6.02	5.92	5.93	7.35	6.31	13.66	0.07
15	Isoquinoline	0.03	1.03	0.02	1.18	0.71	38.94	18.17	0.81	0.48	0.06	0.07	0.06	2.37	2.21	2.59	2.50	2.19	2.20	6.45	2.30	8.75	0.04
16	1-Methylnaphthalene	0.60	0.73	0.63	13.09	7.81	16.05	7.49	13.69	8.13	0.32	0.30	0.30	6.97	6.48	6.46	6.23	6.49	6.51	7.81	6.41	14.22	0.07
17	Biphenyl	0.21	0.29	0.22	5.48	3.27	7.45	3.47	5.73	3.40	0.14	0.11	0.11	3.55	3.30	2.75	2.66	2.87	2.87	3.38	2.94	6.33	0.03
18	Acenaphthylene	0.45	0.68	0.47	9.70	5.79	14.52	6.78	9.98	5.93	0.48	0.41	0.44	10.19	9.48	8.81	8.51	9.51	9.54	6.16	9.18	15.34	0.08
19	Acenapthene	0.06	0.08	0.06	1.30	0.78	1.76	0.82	1.25	0.74	0.08	0.06	0.10	1.63	1.52	1.39	1.35	2.15	2.15	0.78	1.67	2.45	0.01
20	Fluorene	0.24	0.34	0.23	5.88	3.50	8.24	3.85	5.59	3.32	0.28	0.19	0.23	6.84	6.36	4.65	4.49	5.51	5.52	3.56	5.46	9.01	0.05
21	Phenanthrene	0.25	0.38	0.24	6.35	3.79	9.83	4.59	6.14	3.65	0.27	0.23	0.23	7.00	6.51	5.94	5.74	5.79	5.80	4.01	6.02	10.02	0.05
22	Anthracene	0.12	0.16	0.11	3.16	1.88	4.07	1.90	2.81	1.67	0.11	0.09	0.09	2.77	2.58	2.36	2.28	2.27	2.28	1.82	2.38	4.20	0.02
23	Fluoranthene	0.15	0.19	0.12	3.86	2.30	5.08	2.37	3.30	1.96	0.14	0.11	0.11	3.71	3.45	2.99	2.88	2.91	2.92	2.21	3.08	5.29	0.03
24	Pyrene	0.11	0.16	0.10	2.69	1.60	3.89	1.82	2.41	1.43	0.12	0.09	0.09	2.97	2.76	2.19	2.11	2.06	2.07	1.62	2.31	3.93	0.02
25	Bens(a)anthracene	0.10	0.18	0.08	3.24	1.93	5.77	2.69	2.78	1.65	0.06	0.03	0.07	1.93	1.79	1.01	0.98	2.14	2.15	2.09	1.64	3.73	0.02
26	Chrysene	0.09	0.10	0.08	2.37	1.42	2.59	1.21	2.12	1.26	0.09	0.03	0.07	2.24	2.08	0.78	0.75	1.69	1.70	1.29	1.51	2.80	0.01
27	Benso(b)fluoranthene	0.05	0.07	0.05	1.59	0.95	2.17	1.01	1.70	1.01	0.06	0.02	0.05	1.99	1.85	0.49	0.48	1.71	1.71	0.99	1.35	2.33	0.01
28	Benso(k)fluoranthene	0.03	0.03	0.03	0.89	0.53	0.99	0.46	0.97	0.57	0.05	0.01	0.04	1.37	1.28	0.31	0.30	1.22	1.22	0.52	0.93	1.46	0.01
29	Benso(a)Pyrene	0.04	0.05	0.04	0.90	0.54	1.18	0.55	1.03	0.61	0.05	0.02	0.07	1.14	1.06	0.39	0.37	1.64	1.64	0.57	1.03	1.60	0.01
30	Indeno(1,2,3-cd)pyrene	0.02	0.03	0.02	0.67	0.40	1.32	0.62	0.89	0.53	0.01	0.00	0.01	0.36	0.33	0.19	0.18	0.34	0.34	0.52	0.28	0.80	0.00
31	Benso(g,h,i)perylene	0.01	0.01	0.01	0.38	0.23	0.49	0.23	0.32	0.19	0.01	0.00	0.02	0.39	0.36	0.02	0.02	0.60	0.60	0.21	0.33	0.54	0.00
32	Dibenso(a,h)anthracene	0.02	0.03	0.04	0.43	0.26	0.75	0.35	0.88	0.52	0.01	0.00	0.02	0.17	0.16	0.03	0.02	0.40	0.40	0.38	0.19	0.57	0.00

Table J.29. Total tar concentration for each tar compounds at S/B ratio of 0.9.

No	Tar component	Tar concentration (µg ml^{-1})		Average (µg ml^{-1})	Total tar (µg ml^{-1})
		LTM	HTM		
1	Benzene	2.02			2.02
2	Toluene	1.13			1.13
3	Pyridine	0.18			0.18
4	p-xylene + Ethylbenzene	0.09			0.09
5	m-xylene	0.09			0.09
6	o-xylene	0.07			0.07
7	Styrene	0.50			0.50
8	Phenol	2.84	2.92	2.88	2.88
9	Indene	0.39	0.44	0.42	0.42
10	o-cresol (2-methylphenol)	0.36	0.34	0.35	0.35
11	m+p-cresol (3+4-methylphenol)	0.46	0.47	0.46	0.46
12	Naphthalene	0.37	0.39	0.38	0.38
13	Quinoline	0.03	0.04	0.03	0.03
14	2-Methylnaphthalene	0.06	0.07	0.07	0.07
15	Isoquinoline	0.04	0.04	0.04	0.04
16	1-Methylnaphthalene	0.07	0.07	0.07	0.07
17	Biphenyl	0.03	0.03	0.03	0.03
18	Acenaphthylene	0.08	0.08	0.08	0.08
19	Acenapthene	0.01	0.01	0.01	0.01
20	Fluorene	0.04	0.05	0.04	0.04
21	Phenanthrene	0.05	0.05	0.05	0.05
22	Anthracene	0.02	0.02	0.02	0.02
23	Fluoranthene	0.04	0.03	0.03	0.03
24	Pyrene	0.03	0.02	0.02	0.02
25	Bens(a)anthracene		0.02		0.02
26	Chrysene		0.01		0.01
27	Benso(b)fluoranthene		0.01		0.01
28	Benso(k)fluoranthene		0.01		0.01
29	Benso(a)Pyrene		0.01		0.01
30	Indeno(1,2,3-cd)pyrene		0.00		0.00
31	Benso(g,h,i)perylene		0.00		0.00
32	Dibenso(a,h)anthracene		0.00		0.00

Table J.30. Signal count ratio and concentration of each tar compound at S/B ratio of 1.0 analysed with LTM.

No	Method	LTM																			
	Solvent	DCM					ρ_{DCM} = 1.32 g ml^{-1}			DCM-IPA					$\rho_{DCM-IPA}$ = 1.05 g ml^{-1}				Average tar mass		Tar amount	
	Category	Signal Count Ratio			Concentration					Signal Count Ratio			Concentration						DCM (G): (A+B+C) / 3	DCM-IPA (H): (D+E+F) / 3	in sample solution (I): (G+H)	in PG (I / 200)
	Repeat	1	2	3	1		2		3	1	2	3	1		2		3					
	Mass of Tar Sample Solution (g)	NA	NA	NA	0.8650		0.8152		0.8427	NA	NA	NA	1.0104		0.9936		0.9862					
	Concentration unit	NA	NA	NA	ppm	µg (A)	ppm	µg (B)	ppm	µg (C)	NA	NA	NA	ppm	µg (D)	ppm	µg (E)	ppm	µg (F)	µg	µg	µg	µg ml^{-1}
1	Benzene	25.48	24.34	30.38	672.24	440.52	642.18	396.60	801.53	511.71	1.71	1.92	0.72	45.09	43.39	50.68	47.96	18.88	17.74	449.61	36.36	485.97	2.43
2	Toluene	13.77	14.09	15.05	340.00	222.80	348.00	214.92	371.61	237.24	1.10	1.30	0.41	27.11	26.09	32.16	30.43	10.15	9.54	224.99	22.02	247.01	1.24
3	Pyridine	0.90	0.97	0.70	32.62	21.37	35.02	21.63	25.43	16.24	0.05	0.04	0.36	1.95	1.88	1.53	1.44	13.19	12.39	19.75	5.24	24.98	0.12
4	p-xylene + Ethylbenzene	0.86	0.87	0.83	21.65	14.19	21.84	13.49	20.85	13.31	0.13	0.08	0.17	3.27	3.14	2.04	1.93	4.34	4.07	13.66	3.05	16.71	0.08
5	m-xylene	1.94	2.01	2.05	23.69	15.52	24.57	15.17	25.09	16.02	0.24	0.32	0.10	2.93	2.82	3.94	3.73	1.17	1.10	15.57	2.55	18.12	0.09
6	o-xylene	0.81	0.84	0.85	19.88	13.03	20.63	12.74	20.95	13.38	0.09	0.11	0.03	2.12	2.04	2.62	2.48	0.80	0.75	13.05	1.76	14.80	0.07
7	Styrene	5.81	6.17	6.34	140.93	92.35	149.75	92.48	153.82	98.20	0.52	0.62	0.17	12.51	12.03	15.07	14.26	4.10	3.85	94.35	10.05	104.39	0.52
8	Phenol	1.63	1.72	1.79	57.36	37.59	60.42	37.31	62.92	40.17	15.02	15.95	13.29	528.95	509.00	561.74	531.57	467.97	439.54	38.36	493.37	531.72	2.66
9	Indene	4.03	4.32	4.77	104.14	68.25	111.72	69.00	123.32	78.73	0.49	0.61	0.18	12.67	12.19	15.75	14.90	4.64	4.36	71.99	10.48	82.47	0.41
10	o-cresol (2-methylphenol)	0.07	0.00	0.00	2.20	1.44	0.00	0.00	0.00	0.00	2.05	2.14	1.72	67.31	64.77	70.26	66.48	56.48	53.05	0.48	61.43	61.91	0.31
11	m+p-cresol (3+4-methylphenol)	0.01	0.01	0.02	0.25	0.16	0.21	0.13	0.27	0.17	5.13	5.69	4.35	89.40	86.03	99.07	93.75	75.73	71.13	0.15	83.64	83.79	0.42
12	Naphthalene	4.49	5.31	5.27	87.60	57.40	103.71	64.05	102.99	65.75	0.96	1.14	0.70	18.67	17.97	22.32	21.12	13.73	12.90	62.40	17.33	79.73	0.40
13	Quinoline	0.12	0.15	0.10	3.61	2.36	4.52	2.79	3.11	1.99	0.11	0.09	0.11	3.20	3.08	2.83	2.68	3.38	3.17	2.38	2.98	5.36	0.03
14	2-Methylnaphthalene	0.78	0.95	0.86	14.10	9.24	17.17	10.60	15.46	9.87	0.34	0.41	0.32	6.19	5.96	7.42	7.02	5.81	5.46	9.90	6.15	16.05	0.08
15	Isoquinoline	0.03	0.04	0.01	0.97	0.64	1.18	0.73	0.44	0.28	0.06	0.07	0.06	1.81	1.74	2.31	2.19	1.80	1.69	0.55	1.87	2.42	0.01
16	1-Methylnaphthalene	0.51	0.64	0.56	9.70	6.36	12.02	7.42	10.49	6.70	0.33	0.46	0.30	6.24	6.01	8.63	8.17	5.59	5.25	6.83	6.48	13.30	0.07
17	Biphenyl	0.18	0.23	0.19	4.21	2.76	5.35	3.30	4.42	2.82	0.11	0.15	0.12	2.63	2.53	3.42	3.23	2.71	2.55	2.96	2.77	5.73	0.03
18	Acenaphthylene	0.43	0.55	0.46	8.14	5.34	10.45	6.45	8.74	5.58	0.52	0.58	0.48	9.94	9.57	11.18	10.58	9.22	8.66	5.79	9.60	15.39	0.08
19	Acenapthene	0.05	0.07	0.06	0.99	0.65	1.26	0.78	1.19	0.76	0.07	0.09	0.08	1.37	1.32	1.66	1.57	1.50	1.41	0.73	1.43	2.16	0.01
20	Fluorene	0.22	0.28	0.22	4.28	2.80	5.44	3.36	4.20	2.68	0.28	0.30	0.26	5.45	5.25	5.67	5.36	5.05	4.74	2.95	5.12	8.07	0.04
21	Phenanthrene	0.27	0.32	0.26	5.32	3.49	6.30	3.89	5.20	3.32	0.31	0.37	0.32	6.18	5.95	7.26	6.87	6.26	5.88	3.57	6.23	9.80	0.05
22	Anthracene	0.11	0.13	0.11	1.63	1.07	1.93	1.19	1.57	1.00	0.13	0.14	0.12	1.95	1.88	2.01	1.91	1.74	1.63	1.09	1.81	2.89	0.01
23	Fluoranthene	0.25	0.23	0.25	4.18	2.74	3.85	2.37	4.29	2.74	0.33	0.34	0.30	5.62	5.41	5.73	5.43	5.12	4.81	2.62	5.22	7.83	0.04
24	Pyrene	0.27	0.31	0.31	2.58	1.69	2.93	1.81	2.93	1.87	0.39	0.42	0.37	3.76	3.62	3.98	3.77	3.54	3.33	1.79	3.57	5.36	0.03
25	Bens(a)anthracene																						
26	Chrysene																						
27	Benso(b)fluoranthene																						
28	Benso(k)fluoranthene																						
29	Benso(a)Pyrene																						
30	Indeno(1,2,3-cd)pyrene																						
31	Benso(g,h,i)perylene																						
32	Dibenso(a,h)anthracene																						

Table J.31. Signal count ratio and concentration of each tar compound at S/B ratio of 1.0 analysed with HTM.

No	Method	HTM																				
	Solvent	DCM						ρ_{DCM} = 1.32 g ml^{-1}		DCM-IPA						$\rho_{DCM-IPA}$ = 1.05 g ml^{-1}		Average tar mass		Tar amount	
	Category	Signal Count Ratio			Concentration					Signal Count Ratio			Concentration					DCM (G): (A+B+C) / 3	DCM-IPA (H): (D+E+F) / 3	in sample solution (I): (G+H)	in PC (I / 20
	Repeat	1	2	3	1		2		3		1	2	3	1		2		3				
	Mass of Tar Sample Solution (g)	NA	NA	NA	0.8650		0.8152		0.8427		NA	NA	NA	1.0104		0.9936		0.9862				
	Concentration unit	NA	NA	NA	ppm	µg (A)	ppm	µg (B)	ppm	µg (C)	NA	NA	NA	ppm	µg (D)	ppm	µg (E)	ppm	µg (F)	µg	µg	µg	µg ml
1	Benzene																					
2	Toluene																					
3	Pyridine																					
4	p-xylene + Ethylbenzene																					
5	m-xylene																					
6	o-xylene																					
7	Styrene																					
8	Phenol	1.36	1.46	1.50	56.99	37.34	61.22	37.81	62.90	40.16	13.49	13.78	11.74	564.63	543.34	576.65	545.67	491.25	461.40	38.44	516.80	555.24	2.78
9	Indene	3.88	4.23	4.50	119.27	78.16	130.11	80.35	138.34	88.32	0.43	0.54	0.16	13.38	12.87	16.61	15.72	4.93	4.63	82.28	11.07	93.35	0.47
10	o-cresol (2-methylphenol)	0.10	0.11	0.10	3.44	2.26	3.77	2.33	3.49	2.23	1.95	1.96	1.62	67.68	65.12	68.02	64.36	56.38	52.95	2.27	60.81	63.08	0.32
11	m+p-cresol (3+4-methylphenol)	0.06	0.06	0.05	1.14	0.75	1.21	0.74	1.07	0.68	4.65	4.83	3.96	95.07	91.49	98.86	93.55	80.89	75.97	0.73	87.00	87.73	0.44
12	Naphthalene	4.36	5.13	5.04	92.83	60.83	109.18	67.43	107.30	68.50	0.87	1.00	0.63	18.61	17.91	21.30	20.16	13.44	12.62	65.59	16.90	82.48	0.41
13	Quinoline	0.13	0.16	0.07	4.64	3.04	5.56	3.43	2.26	1.44	0.13	0.14	0.10	4.39	4.22	4.75	4.49	3.48	3.27	2.64	3.99	6.63	0.03
14	2-Methylnaphthalene	0.75	0.93	0.80	15.76	10.33	19.37	11.96	16.73	10.68	0.33	0.37	0.30	6.87	6.61	7.77	7.36	6.25	5.87	10.99	6.61	17.60	0.09
15	Isoquinoline	0.03	0.03	0.01	1.26	0.82	1.20	0.74	0.41	0.26	0.05	0.05	0.05	1.87	1.80	1.95	1.85	2.04	1.92	0.61	1.86	2.46	0.01
16	1-Methylnaphthalene	0.54	0.65	0.57	11.74	7.69	14.31	8.84	12.42	7.93	0.29	0.33	0.31	6.30	6.06	7.18	6.79	6.73	6.32	8.15	6.39	14.54	0.07
17	Biphenyl	0.19	0.24	0.20	5.03	3.29	6.21	3.84	5.23	3.34	0.12	0.15	0.14	3.18	3.06	3.81	3.61	3.70	3.47	3.49	3.38	6.87	0.03
18	Acenaphthylene	0.41	0.52	0.42	8.80	5.76	11.07	6.84	9.02	5.76	0.43	0.45	0.46	9.23	8.88	9.72	9.20	9.81	9.21	6.12	9.10	15.22	0.08
19	Acenapthene	0.05	0.07	0.05	1.15	0.75	1.42	0.87	1.05	0.67	0.07	0.07	0.06	1.41	1.36	1.48	1.40	1.34	1.26	0.77	1.34	2.11	0.01
20	Fluorene	0.21	0.26	0.20	5.12	3.36	6.34	3.91	4.73	3.02	0.25	0.26	0.22	6.08	5.86	6.20	5.87	5.42	5.09	3.43	5.60	9.03	0.05
21	Phenanthrene	0.23	0.27	0.19	5.79	3.79	6.87	4.24	4.89	3.12	0.25	0.25	0.22	6.42	6.18	6.41	6.07	5.72	5.37	3.72	5.87	9.59	0.05
22	Anthracene	0.11	0.12	0.09	2.75	1.80	3.18	1.97	2.33	1.49	0.10	0.09	0.08	2.50	2.40	2.45	2.32	2.19	2.05	1.75	2.26	4.01	0.02
23	Fluoranthene	0.12	0.14	0.08	3.32	2.18	3.79	2.34	2.12	1.36	0.13	0.13	0.11	3.50	3.37	3.47	3.29	3.00	2.82	1.96	3.16	5.12	0.03
24	Pyrene	0.10	0.11	0.08	2.38	1.56	2.58	1.59	1.87	1.19	0.11	0.11	0.09	2.75	2.65	2.72	2.58	2.26	2.13	1.45	2.45	3.90	0.02
25	Bens(a)anthracene	0.09	0.09	0.06	3.07	2.01	3.06	1.89	1.88	1.20	0.06	0.06	0.07	1.84	1.77	1.87	1.77	2.14	2.01	1.70	1.85	3.55	0.02
26	Chrysene	0.08	0.10	0.04	2.20	1.44	2.49	1.54	1.08	0.69	0.09	0.09	0.07	2.40	2.31	2.31	2.19	1.74	1.63	1.22	2.04	3.26	0.02
27	Benso(b)fluoranthene	0.05	0.05	0.03	1.55	1.02	1.64	1.02	0.94	0.60	0.06	0.06	0.06	2.00	1.93	2.05	1.94	1.92	1.80	0.88	1.89	2.77	0.01
28	Benso(k)fluoranthene	0.03	0.03	0.03	0.91	0.60	0.94	0.58	0.88	0.56	0.04	0.04	0.04	1.20	1.15	1.34	1.27	1.24	1.17	0.58	1.20	1.78	0.01
29	Benso(a)Pyrene	0.04	0.04	0.04	0.90	0.59	0.99	0.61	0.93	0.60	0.05	0.05	0.05	1.17	1.13	1.29	1.22	1.17	1.10	0.60	1.15	1.75	0.01
30	Indeno(1,2,3-cd)pyrene	0.02	0.02	0.02	0.76	0.50	0.90	0.56	0.76	0.48	0.02	0.02	0.02	0.76	0.73	1.02	0.97	0.70	0.66	0.51	0.79	1.30	0.01
31	Benso(g,h,i)perylene	0.01	0.01	0.00	0.33	0.22	0.20	0.12	0.14	0.09	0.03	0.02	0.01	0.96	0.92	0.52	0.49	0.50	0.47	0.14	0.63	0.77	0.00
32	Dibenso(a,h)anthracene	0.02	0.02	0.02	0.42	0.27	0.50	0.31	0.52	0.33	0.01	0.02	0.02	0.35	0.34	0.48	0.45	0.59	0.55	0.31	0.45	0.75	0.00

Table J.32. Total tar concentration for each tar compounds at S/B ratio of 1.0.

No	Tar component	Tar concentration (µg ml^{-1})		Average (µg ml^{-1})	Total tar (µg ml^{-1})
		LTM	HTM		
1	Benzene	2.43			2.43
2	Toluene	1.24			1.24
3	Pyridine	0.12			0.12
4	p-xylene + Ethylbenzene	0.08			0.08
5	m-xylene	0.09			0.09
6	o-xylene	0.07			0.07
7	Styrene	0.52			0.52
8	Phenol	2.66	2.78	2.72	2.72
9	Indene	0.41	0.47	0.44	0.44
10	o-cresol (2-methylphenol)	0.31	0.32	0.31	0.31
11	m+p-cresol (3+4-methylphenol)	0.42	0.44	0.43	0.43
12	Naphthalene	0.40	0.41	0.41	0.41
13	Quinoline	0.03	0.03	0.03	0.03
14	2-Methylnaphthalene	0.08	0.09	0.08	0.08
15	Isoquinoline	0.01	0.01	0.01	0.01
16	1-Methylnaphthalene	0.07	0.07	0.07	0.07
17	Biphenyl	0.03	0.03	0.03	0.03
18	Acenaphthylene	0.08	0.08	0.08	0.08
19	Acenapthene	0.01	0.01	0.01	0.01
20	Fluorene	0.04	0.05	0.04	0.04
21	Phenanthrene	0.05	0.05	0.05	0.05
22	Anthracene	0.01	0.02	0.02	0.02
23	Fluoranthene	0.04	0.03	0.03	0.03
24	Pyrene	0.03	0.02	0.02	0.02
25	Bens(a)anthracene		0.02		0.02
26	Chrysene		0.02		0.02
27	Benso(b)fluoranthene		0.01		0.01
28	Benso(k)fluoranthene		0.01		0.01
29	Benso(a)Pyrene		0.01		0.01
30	Indeno(1,2,3-cd)pyrene		0.01		0.01
31	Benso(g,h,i)perylene		0.00		0.00
32	Dibenso(a,h)anthracene		0.00		0.00

Table J.33. Signal count ratio and concentration of each tar compound at S/B ratio of 1.1 analysed with LTM.

No	Method	LTM																				
	Solvent	DCM					$\dot{\rho}_{DCM}$ = 1.32 g ml^{-1}				DCM-IPA					$\dot{\rho}_{DCM-IPA}$ = 1.05 g ml^{-1}				Average tar mass		Tar amount	
	Category	Signal Count Ratio			Concentration						Signal Count Ratio			Concentration						DCM (G): (A+B+C) / 3	DCM-IPA (H): (D+E+F) / 3	in sample solution (I): (G+H)	in PG (I / 200)
	Repeat	1	2	3	1		2		3		1	2	3	1		2		3					
	Mass of Tar Sample Solution (g)	NA	NA	NA	0.8810		0.8270		0.9249		NA	NA	NA	1.0248		1.0353		1.0674					
	Concentration unit	NA	NA	NA	ppm	µg (A)	ppm	µg (B)	ppm	µg (C)	NA	NA	NA	ppm	µg (D)	ppm	µg (E)	ppm	µg (F)	µg	µg	µg	µg ml^{-1}
1	Benzene	17.45	23.05	21.03	460.55	307.38	608.18	381.03	554.98	388.86	0.92	1.14	0.81	24.32	23.74	30.11	29.69	21.34	21.70	359.09	25.04	384.13	1.92
2	Toluene	11.29	12.13	11.59	278.88	186.13	299.51	187.65	286.26	200.58	0.69	0.76	0.57	16.98	16.57	18.81	18.55	13.99	14.22	191.45	16.45	207.90	1.04
3	Pyridine	0.56	1.16	1.03	20.16	13.46	42.08	26.37	37.49	26.27	0.07	0.14	0.14	2.42	2.36	5.07	5.00	5.09	5.17	22.03	4.18	26.21	0.13
4	p-xylene + Ethylbenzene	0.91	0.85	0.81	22.91	15.29	21.35	13.38	20.37	14.28	0.08	0.12	0.12	1.90	1.86	3.07	3.03	3.13	3.18	14.31	2.69	17.00	0.09
5	m-xylene	1.73	1.68	1.62	21.16	14.13	20.57	12.89	19.82	13.88	0.15	0.17	0.13	1.88	1.83	2.04	2.01	1.60	1.62	13.63	1.82	15.45	0.08
6	o-xylene	0.75	0.70	0.68	18.27	12.20	17.22	10.79	16.72	11.72	0.06	0.06	0.05	1.57	1.54	1.49	1.47	1.11	1.13	11.57	1.38	12.94	0.06
7	Styrene	5.16	5.28	5.03	125.28	83.61	128.13	80.28	122.19	85.62	0.33	0.35	0.29	8.04	7.84	8.50	8.39	6.96	7.07	83.17	7.77	90.94	0.45
8	Phenol	1.60	1.54	1.47	56.33	37.60	54.13	33.91	51.71	36.23	13.63	11.48	9.68	479.78	468.26	404.36	398.69	340.68	346.33	35.91	404.43	440.34	2.20
9	Indene	3.69	3.43	3.46	95.33	63.62	88.69	55.57	89.44	62.67	0.32	0.33	0.28	8.19	7.99	8.42	8.31	7.12	7.24	60.62	7.84	68.46	0.34
10	o-cresol (2-methylphenol)	1.16	0.00	0.05	37.97	25.34	0.00	0.00	1.62	1.13	1.91	1.54	1.41	62.50	61.00	50.33	49.63	46.29	47.05	8.82	52.56	61.38	0.31
11	m+p-cresol (3+4-methylphenol)	0.51	0.07	0.01	8.94	5.97	1.23	0.77	0.15	0.11	5.00	3.84	3.48	87.07	84.98	66.95	66.02	60.56	61.56	2.28	70.85	73.14	0.37
12	Naphthalene	4.75	4.34	4.25	92.72	61.88	84.70	53.06	83.08	58.21	0.71	0.76	0.58	13.91	13.57	14.75	14.55	11.39	11.58	57.72	13.23	70.95	0.35
13	Quinoline	0.18	0.11	0.08	5.40	3.60	3.19	2.00	2.25	1.57	0.08	0.09	0.07	2.39	2.33	2.65	2.62	2.14	2.18	2.39	2.38	4.77	0.02
14	2-Methylnaphthalene	0.27	0.73	0.70	4.81	3.21	13.19	8.26	12.55	8.79	0.27	0.28	0.23	4.92	4.81	5.00	4.93	4.06	4.13	6.76	4.62	11.38	0.06
15	Isoquinoline	0.98	0.02	0.00	31.37	20.93	0.66	0.41	0.00	0.00	0.06	0.04	0.03	1.83	1.78	1.29	1.27	1.07	1.09	7.12	1.38	8.50	0.04
16	1-Methylnaphthalene	0.71	0.47	0.51	13.45	8.98	8.96	5.61	9.56	6.70	0.34	0.28	0.23	6.49	6.33	5.22	5.15	4.43	4.51	7.10	5.33	12.43	0.06
17	Biphenyl	0.27	0.17	0.14	6.19	4.13	3.90	2.44	3.33	2.34	0.09	0.10	0.07	2.07	2.02	2.27	2.24	1.72	1.75	2.97	2.00	4.97	0.02
18	Acenaphthylene	0.71	0.37	0.32	13.63	9.10	7.05	4.42	6.19	4.33	0.43	0.36	0.28	8.28	8.08	6.85	6.76	5.29	5.38	5.95	6.74	12.69	0.06
19	Acenapthene	0.10	0.05	0.04	1.87	1.25	1.00	0.63	0.71	0.50	0.07	0.05	0.05	1.36	1.32	0.87	0.86	0.91	0.92	0.79	1.04	1.83	0.01
20	Fluorene	0.45	0.18	0.16	8.56	5.71	3.47	2.18	3.13	2.20	0.22	0.19	0.15	4.23	4.12	3.68	3.63	2.78	2.83	3.36	3.53	6.89	0.03
21	Phenanthrene	0.46	0.23	0.19	9.11	6.08	4.56	2.86	3.74	2.62	0.26	0.23	0.17	5.24	5.12	4.54	4.47	3.43	3.48	3.85	4.36	8.21	0.04
22	Anthracene	0.21	0.12	0.08	3.10	2.07	1.80	1.13	1.18	0.82	0.11	0.09	0.07	1.63	1.59	1.37	1.35	0.99	1.00	1.34	1.32	2.66	0.01
23	Fluoranthene	0.26	0.25	0.21	4.44	2.96	4.20	2.63	3.46	2.42	0.37	0.27	0.24	6.17	6.03	4.57	4.51	4.01	4.07	2.67	4.87	7.54	0.04
24	Pyrene	0.24	0.33	0.29	2.34	1.56	3.20	2.00	2.74	1.92	0.42	0.28	0.32	4.06	3.96	2.72	2.68	3.11	3.16	1.83	3.27	5.09	0.03
25	Bens(a)anthracene																						
26	Chrysene																						
27	Benso(b)fluoranthene																						
28	Benso(k)fluoranthene																						
29	Benso(a)Pyrene																						
30	Indeno(1,2,3-cd)pyrene																						
31	Benso(g,h,i)perylene																						
32	Dibenso(a,h)anthracene																						

Table J.34. Signal count ratio and concentration of each tar compound at S/B ratio of 1.1 analysed with HTM.

No	Method	HTM																			
	Solvent	DCM				ρ_{DCM} = 1.32 g ml^{-1}				DCM-IPA						$\rho_{DCM-IPA}$ = 1.05 g ml^{-1}		Average tar mass		Tar amount	
	Category	Signal Count Ratio			Concentration					Signal Count Ratio			Concentration							DCM (G): (A+B+C) / 3	DCM-IPA (H): (D+E+F) / 3	in sample solution (I): (G+H)	in PC (I / 20
	Repeat	1	2	3	1		2		3	1	2	3	1		2		3					
	Mass of Tar Sample Solution (g)	NA	NA	NA	0.8810		0.8270		0.9249	NA	NA	NA	1.0248		1.0353		1.0674					
	Concentration unit	NA	NA	NA	ppm	µg (A)	ppm	µg (B)	ppm	µg (C)	NA	NA	NA	ppm	µg (D)	ppm	µg (E)	ppm	µg (F)	µg	µg	µg	µg ml
1	Benzene																						
2	Toluene																						
3	Pyridine																						
4	p-xylene + Ethylbenzene																						
5	m-xylene																						
6	o-xylene																						
7	Styrene																						
8	Phenol	1.44	1.29	1.22	60.17	40.16	54.11	33.90	50.94	35.69	11.89	11.10	9.36	497.63	485.68	464.27	457.77	391.82	398.31	36.58	447.26	483.84	2.42
9	Indene	3.64	3.30	3.15	112.08	74.80	101.57	63.64	97.01	67.97	0.29	0.30	0.24	9.00	8.79	9.18	9.06	7.27	7.40	68.80	8.41	77.22	0.39
10	o-cresol (2-methylphenol)	0.12	0.09	0.09	4.04	2.70	3.27	2.05	3.11	2.18	1.74	1.56	1.40	60.41	58.96	54.30	53.54	48.60	49.41	2.31	53.97	56.28	0.28
11	m+p-cresol (3+4-methylphenol)	0.07	0.06	0.05	1.44	0.96	1.14	0.72	1.07	0.75	4.22	3.78	3.28	86.20	84.13	77.23	76.15	67.04	68.15	0.81	76.14	76.95	0.38
12	Naphthalene	4.88	4.23	3.83	103.73	69.23	89.97	56.37	81.53	57.13	0.63	0.74	0.58	13.38	13.06	15.64	15.42	12.33	12.53	60.91	13.67	74.58	0.37
13	Quinoline	0.16	0.12	0.10	5.45	3.64	4.14	2.59	3.52	2.47	0.11	0.11	0.07	3.80	3.71	3.92	3.87	2.42	2.46	2.90	3.35	6.24	0.03
14	2-Methylnaphthalene	0.93	0.70	0.63	19.49	13.01	14.63	9.17	13.20	9.25	0.25	0.29	0.23	5.19	5.06	5.99	5.90	4.89	4.97	10.47	5.31	15.79	0.08
15	Isoquinoline	0.03	0.02	0.02	1.18	0.79	0.74	0.46	0.64	0.45	0.04	0.05	0.04	1.60	1.56	1.75	1.72	1.46	1.49	0.57	1.59	2.16	0.01
16	1-Methylnaphthalene	0.68	0.50	0.45	14.88	9.93	10.86	6.80	9.94	6.96	0.24	0.25	0.25	5.18	5.06	5.54	5.46	5.37	5.46	7.90	5.33	13.23	0.07
17	Biphenyl	0.26	0.18	0.16	6.72	4.49	4.58	2.87	4.08	2.86	0.09	0.12	0.10	2.31	2.26	3.03	2.98	2.62	2.67	3.41	2.64	6.04	0.03
18	Acenaphthylene	0.54	0.34	0.31	11.66	7.78	7.38	4.62	6.63	4.65	0.32	0.34	0.31	6.92	6.75	7.33	7.23	6.56	6.67	5.68	6.88	12.57	0.06
19	Acenapthene	0.07	0.04	0.04	1.60	1.07	0.93	0.58	0.85	0.59	0.05	0.05	0.04	1.16	1.13	1.11	1.09	0.92	0.93	0.75	1.05	1.80	0.01
20	Fluorene	0.27	0.16	0.15	6.40	4.27	3.90	2.44	3.63	2.54	0.19	0.18	0.14	4.54	4.43	4.44	4.38	3.36	3.41	3.09	4.07	7.16	0.04
21	Phenanthrene	0.30	0.16	0.14	7.61	5.08	4.08	2.56	3.54	2.48	0.20	0.19	0.13	5.26	5.14	4.81	4.75	3.43	3.49	3.37	4.46	7.83	0.04
22	Anthracene	0.15	0.07	0.07	3.79	2.53	1.89	1.18	1.78	1.25	0.08	0.07	0.05	2.17	2.11	1.89	1.87	1.41	1.44	1.65	1.81	3.46	0.02
23	Fluoranthene	0.18	0.09	0.08	4.75	3.17	2.30	1.44	2.18	1.53	0.13	0.10	0.08	3.39	3.30	2.74	2.70	2.15	2.18	2.05	2.73	4.78	0.02
24	Pyrene	0.13	0.07	0.06	3.14	2.10	1.58	0.99	1.50	1.05	0.13	0.10	0.07	3.04	2.97	2.35	2.31	1.70	1.73	1.38	2.34	3.71	0.02
25	Bens(a)anthracene	0.11	0.05	0.04	3.51	2.34	1.75	1.09	1.31	0.92	0.06	0.06	0.06	1.89	1.85	2.10	2.07	1.82	1.85	1.45	1.92	3.37	0.02
26	Chrysene	0.12	0.06	0.05	3.05	2.04	1.48	0.93	1.34	0.94	0.11	0.06	0.05	2.96	2.88	1.68	1.65	1.30	1.32	1.30	1.95	3.25	0.02
27	Benso(b)fluoranthene	0.05	0.04	0.03	1.77	1.18	1.30	0.82	1.02	0.72	0.05	0.05	0.05	1.77	1.73	1.56	1.54	1.56	1.58	0.90	1.62	2.52	0.01
28	Benso(k)fluoranthene	0.03	0.03	0.03	1.01	0.68	0.82	0.51	0.88	0.61	0.03	0.04	0.04	1.05	1.03	1.23	1.21	1.31	1.33	0.60	1.19	1.79	0.01
29	Benso(a)Pyrene	0.04	0.03	0.03	0.98	0.65	0.77	0.48	0.81	0.57	0.04	0.04	0.05	1.03	1.01	1.10	1.09	1.13	1.15	0.57	1.08	1.65	0.01
30	Indeno(1,2,3-cd)pyrene	0.02	0.01	0.02	0.66	0.44	0.60	0.38	0.69	0.48	0.01	0.02	0.01	0.55	0.53	0.73	0.72	0.49	0.49	0.43	0.58	1.02	0.01
31	Benso(g,h,i)perylene	0.01	0.01	0.01	0.38	0.25	0.34	0.21	0.27	0.19	0.00	0.01	0.01	0.16	0.16	0.46	0.45	0.26	0.26	0.22	0.29	0.51	0.00
32	Dibenso(a,h)anthracene	0.02	0.02	0.02	0.49	0.33	0.57	0.35	0.58	0.41	0.02	0.03	0.02	0.53	0.51	0.74	0.73	0.49	0.50	0.36	0.58	0.94	0.00

Table J.35. Total tar concentration for each tar compounds at S/B ratio of 1.1.

No	Tar component	Tar concentration (µg ml^{-1})		Average (µg ml^{-1})	Total tar (µg ml^{-1})
		LTM	HTM		
1	Benzene	1.92			1.92
2	Toluene	1.04			1.04
3	Pyridine	0.13			0.13
4	p-xylene + Ethylbenzene	0.09			0.09
5	m-xylene	0.08			0.08
6	o-xylene	0.06			0.06
7	Styrene	0.45			0.45
8	Phenol	2.20	2.42	2.31	2.31
9	Indene	0.34	0.39	0.36	0.36
10	o-cresol (2-methylphenol)	0.31	0.28	0.29	0.29
11	m+p-cresol (3+4-methylphenol)	0.37	0.38	0.38	0.38
12	Naphthalene	0.35	0.37	0.36	0.36
13	Quinoline	0.02	0.03	0.03	0.03
14	2-Methylnaphthalene	0.06	0.08	0.07	0.07
15	Isoquinoline	0.04	0.01	0.03	0.03
16	1-Methylnaphthalene	0.06	0.07	0.06	0.06
17	Biphenyl	0.02	0.03	0.03	0.03
18	Acenaphthylene	0.06	0.06	0.06	0.06
19	Acenapthene	0.01	0.01	0.01	0.01
20	Fluorene	0.03	0.04	0.04	0.04
21	Phenanthrene	0.04	0.04	0.04	0.04
22	Anthracene	0.01	0.02	0.02	0.02
23	Fluoranthene	0.04	0.02	0.03	0.03
24	Pyrene	0.03	0.02	0.02	0.02
25	Bens(a)anthracene		0.02		0.02
26	Chrysene		0.02		0.02
27	Benso(b)fluoranthene		0.01		0.01
28	Benso(k)fluoranthene		0.01		0.01
29	Benso(a)Pyrene		0.01		0.01
30	Indeno(1,2,3-cd)pyrene		0.01		0.01
31	Benso(g,h,i)perylene		0.00		0.00
32	Dibenso(a,h)anthracene		0.00		0.00

Table J.36. Concentration of each tar compound from the investigated parameter 2: summary

Class	Compounds	0.7		0.8		0.9		1.0		1.1	
		µg ml^{-1}	g Nm^{-3}	µg ml^{-1}	g Nm^{-3}	µg ml^{-1}	g Nm^{-3}	µg ml^{-1}	g Nm^{-3}	µg ml^{-1}	g Nm^{-3}
2	Pyridine	0.17	0.15	0.12	0.10	0.20	0.18	0.12	0.11	0.15	0.14
	Phenol	1.43	1.29	3.25	2.92	2.46	2.22	2.68	2.42	2.28	2.05
	o-cresol (2-methylphenol)	0.29	0.26	0.29	0.26	0.24	0.22	0.24	0.22	0.21	0.19
	m+p-cresol (3+4-methylphenol)	0.73	0.66	0.72	0.65	0.51	0.46	0.58	0.52	0.50	0.45
	Quinoline	0.06	0.06	0.05	0.04	0.03	0.03	0.03	0.03	0.03	0.03
	Isoquinoline	0.08	0.07	0.02	0.01	0.01	0.01	0.01	0.01	0.01	0.01
	Subtotal class 2 tars concentration	***2.76***	***2.49***	***4.43***	***3.99***	***3.46***	***3.12***	***3.68***	***3.31***	***3.19***	***2.87***
3	Benzene	3.21	2.89	1.48	1.34	2.62	2.36	2.40	2.17	2.03	1.83
	Toluene	1.62	1.46	1.09	0.98	1.32	1.19	1.23	1.10	1.05	0.94
	p-xylene + Ethylbenzene	0.12	0.11	0.07	0.07	0.10	0.09	0.08	0.07	0.08	0.07
	m-xylene	0.13	0.11	0.09	0.08	0.10	0.09	0.09	0.08	0.08	0.07
	o-xylene	0.09	0.08	0.07	0.07	0.08	0.07	0.07	0.07	0.06	0.06
	Styrene	0.59	0.53	0.50	0.45	0.56	0.50	0.52	0.47	0.45	0.41
	Subtotal class 3 tars concentration	***5.75***	***5.18***	***3.31***	***2.99***	***4.77***	***4.30***	***4.40***	***3.96***	***3.75***	***3.37***
4	Indene	0.49	0.44	0.47	0.42	0.46	0.41	0.44	0.40	0.36	0.33
	Naphthalene	0.45	0.40	0.46	0.42	0.38	0.35	0.41	0.37	0.36	0.32
	2-Methylnaphthalene	0.09	0.08	0.11	0.10	0.08	0.07	0.09	0.08	0.07	0.07
	1-Methylnaphthalene	0.10	0.09	0.08	0.08	0.07	0.06	0.07	0.06	0.06	0.06
	Biphenyl	0.07	0.06	0.04	0.04	0.03	0.03	0.03	0.03	0.03	0.02
	Acenaphthylene	0.12	0.11	0.11	0.10	0.07	0.06	0.08	0.07	0.06	0.05
	Acenapthene	0.02	0.02	0.02	0.01	0.01	0.01	0.01	0.01	0.01	0.01
	Fluorene	0.08	0.07	0.07	0.06	0.04	0.04	0.04	0.04	0.03	0.03
	Phenanthrene	0.08	0.08	0.08	0.08	0.05	0.04	0.05	0.04	0.04	0.03
	Anthracene	0.03	0.03	0.03	0.03	0.02	0.01	0.02	0.02	0.01	0.01
	Subtotal class 4 tars concentration	***1.53***	***1.38***	***1.48***	***1.33***	***1.20***	***1.08***	***1.24***	***1.11***	***1.04***	***0.94***
5	Fluoranthene	0.05	0.05	0.05	0.04	0.03	0.03	0.03	0.03	0.03	0.03
	Pyrene	0.03	0.03	0.03	0.02	0.02	0.02	0.02	0.02	0.02	0.02
	Bens(a)anthracene	0.02	0.02	0.02	0.02	0.01	0.01	0.02	0.02	0.02	0.02
	Chrysene	0.08	0.07	0.03	0.02	0.01	0.01	0.02	0.01	0.02	0.01
	Benso(b)fluoranthene	0.02	0.02	0.02	0.01	0.01	0.01	0.01	0.01	0.01	0.01
	Benso(k)fluoranthene	0.01	0.01	0.01	0.01	0.01	0.00	0.01	0.01	0.01	0.01
	Benso(a)Pyrene	0.01	0.01	0.01	0.01	0.01	0.00	0.01	0.01	0.01	0.01
	Indeno(1,2,3-cd)pyrene	0.00	0.00	0.01	0.00	0.00	0.00	0.01	0.01	0.00	0.00
	Benso(g,h,i)perylene	0.01	0.01	0.01	0.00	0.00	0.00	0.00	0.00	0.00	0.00
	Dibenso(a,h)anthracene	0.01	0.01	0.00	0.00	0.00	0.00	0.00	0.00	0.00	0.00
	Subtotal class 5 tars concentration	***0.25***	***0.23***	***0.17***	***0.15***	***0.10***	***0.09***	***0.13***	***0.12***	***0.12***	***0.11***
Total tars concentration		**10.29**	**9.28**	**9.39**	**8.46**	**9.53**	**8.59**	**9.44**	**8.51**	**8.09**	**7.29**

Table J.37. Total concentration and yield of tars at each measured S/B ratio

Tar class	S/B ratio					Unit
	0.7	0.8	0.9	1.0	1.1	
Class 2	2.49	3.99	3.12	3.31	2.87	g Nm^{-3}
Class 3	5.18	2.99	4.30	3.96	3.37	
Class 4	1.38	1.33	1.08	1.11	0.94	
Class 5	0.23	0.15	0.09	0.12	0.11	
Tars concentration	*9.28*	*8.46*	*8.59*	*8.51*	*7.29*	
Gas Yield	*0.54*	*0.44*	*0.49*	*0.57*	*0.52*	Nm^3 kg$^{-1}_{od}$
Tars yield	*5.05*	*3.73*	*4.20*	*4.81*	*3.80*	g kg$^{-1}_{od}$

J.6.3. Investigated parameter 3 (Experiment performed on 27th September 2017)

Table 7.38. Signal count ratio and concentration of each tar compound from olivine-fluidized gasification analysed with LTM.

No	Method	LTM																					
	Solvent	DCM						ρ_{DCM} = 1.32 g ml^{-1}			DCM-IPA								$\rho_{DCM-IPA}$ = 1.05 g ml^{-1}		Average tar mass		Tar amount	
	Category	Signal Count Ratio			Concentration						Signal Count Ratio			Concentration							DCM (G): (A+B+C) / 3	DCM-IPA (H): (D+E+F) / 3	in sample solution (I): (G+H)	in PG (I / 200)
	Repeat	1	2	3	1		2		3		1	2	3	1		2		3					
	Mass of Tar Sample Solution (g)	NA	NA	NA	0.7759		0.7903		0.7172		NA	NA	NA	1.0392		0.9736		1.0715					
	Concentration unit	NA	NA	NA	ppm	µg (A)	ppm	µg (B)	ppm	µg (C)	NA	NA	NA	ppm	µg (D)	ppm	µg (E)	ppm	µg (F)		µg	µg	µg	µg ml^{-1}
1	Benzene	3.04	23.51	2.14	80.33	47.22	620.42	371.45	56.57	30.74	0.11	0.87	0.04	2.85	2.82	22.86	21.20	1.12	1.14		149.80	8.38	158.19	0.79
2	Toluene	3.23	15.62	2.06	79.79	46.90	385.77	230.97	50.95	27.68	0.26	0.60	0.11	6.49	6.42	14.72	13.65	2.68	2.74		101.85	7.60	109.45	0.55
3	Pyridine	1.55	1.43	1.63	55.99	32.91	51.86	31.05	59.09	32.11	0.53	0.39	0.36	19.04	18.85	14.01	12.99	13.07	13.34		32.02	15.06	47.08	0.24
4	p-xylene + Ethylbenzene	0.45	0.99	0.25	11.40	6.70	24.85	14.88	6.33	3.44	0.10	0.12	0.16	2.58	2.56	2.95	2.73	4.07	4.15		8.34	3.15	11.48	0.06
5	m-xylene	1.04	2.35	0.57	12.70	7.46	28.74	17.21	6.92	3.76	0.21	0.14	0.21	2.52	2.50	1.70	1.58	2.54	2.60		9.48	2.22	11.70	0.06
6	o-xylene	0.53	0.99	0.27	13.02	7.66	24.22	14.50	6.62	3.59	0.07	0.02	0.02	1.67	1.66	0.54	0.50	0.45	0.46		8.58	0.87	9.46	0.05
7	Styrene	4.05	6.73	2.00	98.38	57.83	163.26	97.75	48.44	26.32	0.40	0.12	0.08	9.62	9.53	2.84	2.64	1.82	1.86		60.63	4.67	65.31	0.33
8	Phenol	1.89	1.74	1.46	66.41	39.03	61.30	36.70	51.33	27.89	12.31	11.27	13.11	433.30	428.85	396.68	367.82	461.48	470.93		34.54	422.53	457.07	2.29
9	Indene	5.32	5.06	5.58	137.58	80.87	130.76	78.28	144.24	78.37	0.18	0.24	0.23	4.64	4.59	6.12	5.67	5.95	6.08		79.18	5.44	84.62	0.42
10	o-cresol (2-methylphenol)	0.12	0.08	0.11	3.81	2.24	2.77	1.66	3.58	1.94	1.73	1.51	1.77	56.74	56.15	49.62	46.01	58.13	59.32		1.95	53.83	55.78	0.28
11	m+p-cresol (3+4-methylphenol)	0.30	0.30	0.23	5.24	3.08	5.16	3.09	3.98	2.16	4.61	4.24	4.89	80.33	79.50	73.90	68.53	85.28	87.02		2.78	78.35	81.13	0.41
12	Naphthalene	6.01	6.10	7.97	117.29	68.94	119.15	71.33	155.76	84.63	0.72	0.76	0.69	14.12	13.97	14.92	13.83	13.56	13.83		74.97	13.88	88.85	0.44
13	Quinoline	0.12	0.12	0.18	3.48	2.04	3.63	2.17	5.32	2.89	0.10	0.11	0.14	3.08	3.05	3.19	2.96	4.27	4.36		2.37	3.45	5.82	0.03
14	2-Methylnaphthalene	0.52	0.40	0.63	9.35	5.49	7.30	4.37	11.42	6.20	0.32	0.26	0.30	5.69	5.63	4.73	4.38	5.39	5.51		5.35	5.17	10.53	0.05
15	Isoquinoline	1.33	1.43	1.77	42.73	25.12	45.88	27.47	56.67	30.79	0.34	0.33	0.35	11.04	10.93	10.60	9.83	11.29	11.52		27.79	10.76	38.55	0.19
16	1-Methylnaphthalene	0.87	0.97	1.26	16.42	9.65	18.38	11.00	23.83	12.95	0.28	0.27	0.31	5.33	5.28	5.15	4.78	5.86	5.98		11.20	5.35	16.55	0.08
17	Biphenyl	0.35	0.42	0.54	8.21	4.82	9.71	5.81	12.57	6.83	0.43	0.36	0.42	9.90	9.79	8.40	7.79	9.69	9.89		5.82	9.16	14.98	0.07
18	Acenaphthylene	1.00	1.27	1.58	19.18	11.28	24.35	14.58	30.12	16.37	0.40	0.39	0.47	7.71	7.63	7.53	6.98	9.07	9.26		14.07	7.96	22.03	0.11
19	Acenapthene	0.18	0.21	0.26	3.43	2.01	3.93	2.35	4.98	2.71	0.09	0.08	0.09	1.67	1.66	1.43	1.33	1.67	1.70		2.36	1.56	3.92	0.02
20	Fluorene	0.77	0.85	1.19	14.71	8.65	16.20	9.70	22.84	12.41	0.24	0.22	0.24	4.51	4.47	4.23	3.93	4.68	4.78		10.25	4.39	14.64	0.07
21	Phenanthrene	0.76	0.86	1.26	15.02	8.83	17.03	10.20	24.87	13.51	0.27	0.25	0.23	5.30	5.24	4.96	4.60	4.47	4.56		10.84	4.80	15.65	0.08
22	Anthracene	0.33	0.38	0.52	4.82	2.83	5.62	3.36	7.65	4.16	0.13	0.11	0.11	1.87	1.85	1.67	1.55	1.68	1.72		3.45	1.71	5.16	0.03
23	Fluoranthene	0.59	0.81	0.93	9.85	5.79	13.64	8.17	15.62	8.49	0.30	0.25	0.25	5.10	5.05	4.21	3.91	4.23	4.32		7.48	4.42	11.91	0.06
24	Pyrene	0.67	0.66	0.67	6.43	3.78	6.29	3.77	6.47	3.51	0.33	0.24	0.24	3.14	3.11	2.31	2.14	2.28	2.32		3.69	2.52	6.21	0.03
25	Bens(a)anthracene																							
26	Chrysene																							
27	Benso(b)fluoranthene																							
28	Benso(k)fluoranthene																							
29	Benso(a)Pyrene																							
30	Indeno(1,2,3-cd)pyrene																							
31	Benso(g,h,i)perylene																							
32	Dibenso(a,h)anthracene																							

Table J.39. Signal count ratio and concentration of each tar compound from olivine-fluidized gasification analysed with HTM.

No	Method	LTM																			
	Solvent	DCM					ρ_{DCM} = 1.32 g ml^{-1}				DCM-IPA						$\rho_{DCM-IPA}$ = 1.05 g ml^{-1}		Average tar mass		Tar amount	
	Category	Signal Count Rati			Concentration						Signal Count Ratio			Concentration								
	Repeat	1	2	3	1		2		3		1	2	3	1		2		3		DCM (G): (A+B+C) / 3	DCM-IPA (H): (D+E+F) / 3	in sample solution (I): (G+H)	in PG (I / 200)
	Mass of Tar Sample Solution (g)	NA	NA	NA	0.7759		0.7903		0.7172		NA	NA	NA	1.0392		0.9736		1.0715					
	Concentration unit	NA	NA	NA	ppm	µg (A)	ppm	µg (B)	ppm	µg (C)	NA	NA	NA	ppm	µg (D)	ppm	µg (E)	ppm	µg (F)	µg	µg	µg	µg ml^{-1}
1	Benzene																						
2	Toluene																						
3	Pyridine																						
4	p-xylene + Ethylbenzene																						
5	m-xylene																						
6	o-xylene																						
7	Styrene																						
8	Phenol	1.73	1.57	1.34	72.20	42.44	65.75	39.37	56.07	30.46	9.08	9.19	10.56	379.94	376.04	384.72	356.72	441.77	450.81	37.42	394.52	431.95	2.16
9	Indene	5.04	4.77	5.45	155.06	91.14	146.72	87.85	167.75	91.14	0.14	0.18	0.19	4.27	4.23	5.43	5.03	5.98	6.10	90.04	5.12	95.17	0.48
10	o-cresol (2-methylphenol)	0.14	0.11	0.14	4.77	2.80	3.81	2.28	4.87	2.65	1.32	1.26	1.44	45.87	45.40	43.61	40.44	49.91	50.94	2.58	45.59	48.17	0.24
11	m+p-cresol (3+4-methylphenol)	0.28	0.28	0.22	5.81	3.42	5.71	3.42	4.47	2.43	3.32	3.26	3.73	67.92	67.22	66.66	61.81	76.36	77.92	3.09	68.98	72.07	0.36
12	Naphthalene	5.35	5.22	7.12	113.77	66.87	111.08	66.51	151.40	82.26	0.56	0.65	0.56	11.95	11.83	13.82	12.82	11.96	12.20	71.88	12.28	84.16	0.42
13	Quinoline	0.47	0.37	0.55	16.29	9.57	12.73	7.62	18.88	10.26	0.24	0.22	0.24	8.18	8.10	7.59	7.04	8.24	8.41	9.15	7.85	17.00	0.09
14	2-Methylnaphthalene	1.03	1.08	1.49	21.57	12.68	22.65	13.56	31.14	16.92	0.22	0.23	0.24	4.57	4.53	4.88	4.53	5.09	5.19	14.39	4.75	19.14	0.10
15	Isoquinoline	0.01	0.02	0.02	0.30	0.18	0.59	0.35	0.89	0.48	0.06	0.06	0.07	2.12	2.10	2.17	2.01	2.72	2.77	0.34	2.29	2.63	0.01
16	1-Methylnaphthalene	0.78	0.82	1.11	17.01	10.00	17.88	10.71	24.31	13.21	0.27	0.26	0.27	5.87	5.81	5.60	5.19	5.95	6.07	11.30	5.69	17.00	0.08
17	Biphenyl	0.31	0.34	0.46	8.07	4.75	8.98	5.38	12.07	6.56	0.25	0.21	0.24	6.43	6.36	5.44	5.05	6.21	6.34	5.56	5.92	11.48	0.06
18	Acenaphthylene	0.80	0.91	1.22	17.26	10.15	19.44	11.64	26.26	14.27	0.27	0.27	0.31	5.85	5.79	5.81	5.39	6.68	6.82	12.02	6.00	18.02	0.09
19	Acenapthene	0.13	0.15	0.18	2.73	1.61	3.20	1.91	3.85	2.09	0.05	0.06	0.06	1.15	1.14	1.21	1.12	1.37	1.40	1.87	1.22	3.09	0.02
20	Fluorene	0.58	0.54	0.85	14.04	8.25	12.94	7.75	20.61	11.20	0.16	0.17	0.19	3.93	3.88	4.09	3.80	4.54	4.64	9.06	4.11	13.17	0.07
21	Phenanthrene	0.52	0.47	0.04	13.39	7.87	11.96	7.16	1.06	0.58	0.15	0.15	0.15	3.73	3.69	3.96	3.68	3.97	4.05	5.20	3.81	9.01	0.05
22	Anthracene	0.19	0.17	0.80	4.84	2.85	4.37	2.62	20.87	11.34	0.05	0.05	0.05	1.29	1.28	1.40	1.30	1.36	1.39	5.60	1.32	6.92	0.03
23	Fluoranthene	0.23	0.18	0.32	6.01	3.53	4.86	2.91	8.39	4.56	0.07	0.07	0.07	1.78	1.77	1.83	1.70	1.79	1.83	3.67	1.76	5.43	0.03
24	Pyrene	0.19	0.16	0.27	4.66	2.74	3.86	2.31	6.54	3.55	0.07	0.07	0.07	1.64	1.62	1.64	1.52	1.63	1.66	2.87	1.60	4.47	0.02
25	Bens(a)anthracene	0.15	0.15	0.18	4.81	2.83	4.91	2.94	6.07	3.30	2.04	0.68	0.69	67.26	66.57	22.39	20.76	22.60	23.07	3.02	36.80	39.82	0.20
26	Chrysene	0.10	0.08	0.11	2.52	1.48	1.98	1.19	2.81	1.53	0.01	0.03	0.03	0.26	0.25	0.90	0.84	0.83	0.85	1.40	0.65	2.04	0.01
27	Benso(b)fluoranthene	0.07	0.01	0.02	2.16	1.27	0.46	0.28	0.58	0.32	0.00	0.01	0.01	0.07	0.07	0.34	0.32	0.35	0.36	0.62	0.25	0.87	0.00
28	Benso(k)fluoranthene	0.04	0.03	0.05	1.22	0.71	0.92	0.55	1.39	0.76	0.01	0.02	0.02	0.16	0.16	0.62	0.58	0.74	0.76	0.67	0.50	1.17	0.01
29	Benso(a)Pyrene	0.05	0.04	0.06	1.22	0.72	1.06	0.64	1.61	0.87	0.01	0.02	0.02	0.21	0.21	0.60	0.55	0.62	0.63	0.74	0.47	1.21	0.01
30	Indeno(1,2,3-cd)pyrene	0.02	0.01	0.02	0.67	0.40	0.54	0.32	0.66	0.36	0.00	0.01	0.00	0.03	0.03	0.49	0.45	0.14	0.15	0.36	0.21	0.57	0.00
31	Benso(g,h,i)perylene	0.02	0.02	0.03	0.81	0.48	0.74	0.44	0.99	0.54	0.00	0.01	0.01	0.11	0.11	0.48	0.45	0.43	0.44	0.49	0.33	0.82	0.00
32	Dibenso(a,h)anthracene	0.03	0.02	0.03	0.79	0.47	0.48	0.29	0.74	0.40	0.00	0.02	0.01	0.06	0.06	0.48	0.44	0.26	0.27	0.39	0.26	0.64	0.00

Table J.40. Total concentration for each tar compounds generated using olivine.

No	Tar component	Tar concentration (µg ml^{-1})		Average (µg ml^{-1})	Total tar (µg ml^{-1})
		LTM	HTM		
1	Benzene	0.79			0.79
2	Toluene	0.55			0.55
3	Pyridine	0.24			0.24
4	p-xylene + Ethylbenzene	0.06			0.06
5	m-xylene	0.06			0.06
6	o-xylene	0.05			0.05
7	Styrene	0.33			0.33
8	Phenol	2.29	2.16	2.22	2.22
9	Indene	0.42	0.48	0.45	0.45
10	o-cresol (2-methylphenol)	0.28	0.24	0.26	0.26
11	m+p-cresol (3+4-methylphenol)	0.41	0.36	0.38	0.38
12	Naphthalene	0.44	0.42	0.43	0.43
13	Quinoline	0.03	0.09	0.06	0.06
14	2-Methylnaphthalene	0.05	0.10	0.07	0.07
15	Isoquinoline	0.19	0.01	0.10	0.10
16	1-Methylnaphthalene	0.08	0.08	0.08	0.08
17	Biphenyl	0.07	0.06	0.07	0.07
18	Acenaphthylene	0.11	0.09	0.10	0.10
19	Acenapthene	0.02	0.02	0.02	0.02
20	Fluorene	0.07	0.07	0.07	0.07
21	Phenanthrene	0.08	0.05	0.06	0.06
22	Anthracene	0.03	0.03	0.03	0.03
23	Fluoranthene	0.06	0.03	0.04	0.04
24	Pyrene	0.03	0.02	0.03	0.03
25	Bens(a)anthracene		0.20		0.20
26	Chrysene		0.01		0.01
27	Benso(b)fluoranthene		0.00		0.00
28	Benso(k)fluoranthene		0.01		0.01
29	Benso(a)Pyrene		0.01		0.01
30	Indeno(1,2,3-cd)pyrene		0.00		0.00
31	Benso(g,h,i)perylene		0.00		0.00
32	Dibenso(a,h)anthracene		0.00		0.00

Table J.41. Signal count ratio and concentration of each tar compound from silica-fluidized gasification analysed with LTM.

No	Method	LTM																					
	Solvent	DCM							ρ_{DCM} = 1.32 g ml^{-1}		DCM-IPA								$\rho_{DCM-IPA}$ = 1.05 g ml^{-1}		Average tar mass		Tar amount	
	Category	Signal Count Ratio			Concentration						Signal Count Ratio			Concentration							DCM (G): (A+B+C) / 3	DCM-IPA (H): (D+E+F) / 3	in sample solution (I): (G+H)	in PG (I / 200)
	Repeat	1	2	3	1		2		3		1	2	3	1		2		3						
	Mass of Tar Sample Solution (g)	NA	NA	NA	0.8320		0.8019		0.7916		NA	NA	NA	1.0194		1.0068		1.0357						
	Concentration unit	NA	NA	NA	ppm	µg (A)	ppm	µg (B)	ppm	µg (C)	NA	NA	NA	ppm	µg (D)	ppm	µg (E)	ppm	µg (F)		µg	µg	µg	µg ml^{-1}
1	Benzene	37.74	37.73	41.84	995.73	627.61	995.53	604.78	1103.88	661.99	0.66	0.59	0.81	17.40	16.90	15.68	15.04	21.27	20.98		631.46	17.64	649.10	3.25
2	Toluene	20.10	19.66	21.34	496.28	312.81	485.35	294.85	526.94	316.01	0.81	0.64	0.78	20.12	19.53	15.69	15.04	19.24	18.98		307.89	17.85	325.74	1.63
3	Pyridine	0.15	0.20	0.22	5.27	3.32	7.18	4.36	8.05	4.82	1.01	0.73	0.74	36.60	35.54	26.40	25.32	26.73	26.37		4.17	29.07	33.24	0.17
4	p-xylene + Ethylbenzene	1.37	1.17	1.30	34.36	21.66	29.45	17.89	32.55	19.52	0.22	0.19	0.10	5.57	5.41	4.75	4.56	2.56	2.52		19.69	4.16	23.85	0.12
5	m-xylene	2.71	2.61	2.83	33.19	20.92	31.93	19.40	34.62	20.76	0.34	0.26	0.61	4.15	4.03	3.17	3.04	7.50	7.40		20.36	4.82	25.18	0.13
6	o-xylene	1.15	1.09	1.19	28.28	17.82	26.81	16.29	29.23	17.53	0.02	0.02	0.03	0.59	0.57	0.55	0.52	0.70	0.69		17.21	0.60	17.81	0.09
7	Styrene	7.54	7.40	8.23	182.91	115.29	179.50	109.05	199.77	119.80	0.18	0.15	0.20	4.27	4.15	3.76	3.61	4.86	4.80		114.71	4.18	118.90	0.59
8	Phenol	0.01	0.00	0.01	0.23	0.15	0.16	0.10	0.18	0.11	16.52	16.48	17.59	581.55	564.60	580.30	556.43	619.45	611.01		0.12	577.35	577.46	2.89
9	Indene	4.90	5.03	5.60	126.54	79.76	129.98	78.96	144.73	86.79	0.38	0.32	0.45	9.72	9.43	8.28	7.94	11.56	11.41		81.84	9.59	91.43	0.46
10	o-cresol (2-methylphenol)	0.10	0.07	0.10	3.32	2.09	2.28	1.38	3.15	1.89	2.41	2.20	2.47	78.97	76.66	71.97	69.01	80.87	79.76		1.79	75.15	76.93	0.38
11	m+p-cresol (3+4-methylphenol)	0.22	0.12	0.17	3.87	2.44	2.00	1.22	2.94	1.76	6.12	6.17	6.86	106.53	103.43	107.47	103.05	119.59	117.96		1.81	108.15	109.95	0.55
12	Naphthalene	4.71	4.98	5.60	92.00	57.99	97.22	59.06	109.39	65.60	1.43	1.30	1.68	27.84	27.02	25.38	24.34	32.83	32.38		60.88	27.91	88.80	0.44
13	Quinoline	0.10	0.09	0.10	2.89	1.82	2.84	1.72	3.12	1.87	0.19	0.17	0.20	5.84	5.67	5.12	4.90	5.88	5.80		1.80	5.46	7.26	0.04
14	2-Methylnaphthalene	1.04	0.96	1.13	18.68	11.77	17.29	10.50	20.39	12.23	0.57	0.51	0.63	10.20	9.91	9.26	8.88	11.32	11.16		11.50	9.98	21.48	0.11
15	Isoquinoline	0.01	0.01	0.01	0.38	0.24	0.40	0.24	0.48	0.29	0.13	0.13	0.14	4.09	3.97	4.07	3.91	4.55	4.48		0.26	4.12	4.38	0.02
16	1-Methylnaphthalene	0.73	0.66	0.79	13.76	8.67	12.40	7.53	14.85	8.90	0.59	0.52	0.67	11.09	10.76	9.86	9.45	12.56	12.39		8.37	10.87	19.24	0.10
17	Biphenyl	0.30	0.28	0.33	6.90	4.35	6.59	4.00	7.71	4.62	0.71	0.41	0.69	16.43	15.95	9.64	9.25	15.97	15.75		4.32	13.65	17.97	0.09
18	Acenaphthylene	0.81	0.77	0.91	15.52	9.78	14.78	8.98	17.40	10.44	0.72	0.68	0.82	13.76	13.36	13.01	12.48	15.68	15.46		9.73	13.77	23.50	0.12
19	Acenapthene	0.12	0.11	0.17	2.36	1.49	2.02	1.23	3.15	1.89	0.10	0.12	0.12	1.91	1.85	2.22	2.12	2.20	2.17		1.53	2.05	3.58	0.02
20	Fluorene	0.60	0.50	0.64	11.52	7.26	9.67	5.88	12.19	7.31	0.43	0.39	0.47	8.21	7.97	7.53	7.22	9.05	8.93		6.81	8.04	14.85	0.07
21	Phenanthrene	0.59	0.50	0.67	11.68	7.36	9.93	6.03	13.35	8.01	0.43	0.42	0.53	8.54	8.29	8.37	8.02	10.50	10.35		7.13	8.89	16.02	0.08
22	Anthracene	0.22	0.19	0.29	3.21	2.02	2.82	1.71	4.31	2.58	0.14	0.14	0.18	2.13	2.07	2.11	2.02	2.59	2.55		2.11	2.21	4.32	0.02
23	Fluoranthene	0.44	0.38	0.51	7.46	4.70	6.45	3.92	8.55	5.13	0.45	0.48	0.55	7.52	7.30	8.03	7.70	9.20	9.07		4.58	8.02	12.61	0.06
24	Pyrene	0.43	0.51	0.54	4.12	2.60	4.92	2.99	5.21	3.13	0.39	0.37	0.59	3.74	3.63	3.56	3.42	5.62	5.55		2.90	4.20	7.10	0.04
25	Bens(a)anthracene																							
26	Chrysene																							
27	Benso(b)fluoranthene																							
28	Benso(k)fluoranthene																							
29	Benso(a)Pyrene																							
30	Indeno(1,2,3-cd)pyrene																							
31	Benso(g,h,i)perylene																							
32	Dibenso(a,h)anthracene																							

Table J.42. Signal count ratio and concentration of each tar compound from silica-fluidized gasification analysed with HTM.

No	Method	HTM																			
	Solvent	DCM						ρ_{DCM} = 1.32 g ml^{-1}		DCM-IPA						$\rho_{DCM-IPA}$ = 1.05 g ml^{-1}		Average tar mass		Tar amount	
	Category	Signal Count Ratio			Concentration					Signal Count Ratio			Concentration							DCM (G): (A+B+C) / 3	DCM-IPA (H): (D+E+F) / 3	in sample solution (I): (G+H)	in PG (I / 200)
	Repeat	1	2	3	1		2		3				1		2		3						
	Mass of Tar Sample Solution (g)	NA	NA	NA	0.8320		0.8019		0.7916		NA	NA	NA	1.0194		1.0068		1.0357					
	Concentration unit	NA	NA	NA	ppm	µg (A)	ppm	µg (B)	ppm	µg (C)	NA	NA	NA	ppm	µg (D)	ppm	µg (E)	ppm	µg (F)	µg	µg	µg	µg ml^{-1}
1	Benzene																						
2	Toluene																						
3	Pyridine																						
4	p-xylene + Ethylbenzene																						
5	m-xylene																						
6	o-xylene																						
7	Styrene																						
8	Phenol	0.02	0.05	0.02	0.96	0.60	2.09	1.27	1.02	0.61	0.05	0.05	0.06	2.26	2.20	2.25	2.16	2.33	2.30	0.83	2.22	3.05	0.02
9	Indene	4.89	4.85	5.53	150.34	94.76	149.25	90.67	170.07	101.99	0.33	0.27	0.38	10.13	9.83	8.40	8.06	11.64	11.48	95.81	9.79	105.60	0.53
10	o-cresol (2-methylphenol)	0.04	0.12	0.05	1.40	0.88	4.02	2.44	1.64	0.98	2.16	1.91	2.14	75.02	72.83	66.15	63.42	74.27	73.26	1.44	69.84	71.28	0.36
11	m+p-cresol (3+4-methylphenol)	0.19	0.09	0.12	3.79	2.39	1.92	1.17	2.55	1.53	5.42	5.02	5.49	110.75	107.52	102.68	98.45	112.18	110.65	1.70	105.54	107.24	0.54
12	Naphthalene	4.53	4.78	5.38	96.42	60.77	101.68	61.77	114.40	68.60	1.20	1.09	1.41	25.54	24.79	23.27	22.32	30.10	29.69	63.71	25.60	89.31	0.45
13	Quinoline	0.10	0.10	0.13	3.39	2.13	3.49	2.12	4.47	2.68	0.45	0.29	0.40	15.48	15.03	10.00	9.59	13.90	13.71	2.31	12.78	15.09	0.08
14	2-Methylnaphthalene	0.48	0.24	0.42	10.10	6.37	4.93	3.00	8.73	5.24	0.48	0.44	0.53	10.01	9.71	9.10	8.73	11.08	10.93	4.87	9.79	14.66	0.07
15	Isoquinoline	1.01	0.92	1.10	38.07	24.00	34.99	21.25	41.56	24.92	0.10	0.09	0.10	3.67	3.57	3.45	3.31	3.95	3.89	23.39	3.59	26.98	0.13
16	1-Methylnaphthalene	0.76	0.66	0.82	16.65	10.50	14.50	8.81	18.04	10.82	0.40	0.37	0.45	8.73	8.48	8.17	7.83	9.82	9.69	10.04	8.67	18.71	0.09
17	Biphenyl	0.40	0.29	0.33	10.50	6.62	7.49	4.55	8.68	5.21	0.16	0.17	0.20	4.10	3.98	4.44	4.26	5.13	5.06	5.46	4.43	9.89	0.05
18	Acenaphthylene	0.87	0.73	0.94	18.66	11.76	15.64	9.50	20.14	12.08	0.51	0.51	0.60	11.03	10.71	11.00	10.55	12.97	12.79	11.11	11.35	22.47	0.11
19	Acenapthene	0.13	0.10	0.13	2.84	1.79	2.24	1.36	2.80	1.68	0.09	0.08	0.10	1.87	1.81	1.73	1.66	2.08	2.06	1.61	1.84	3.45	0.02
20	Fluorene	0.59	0.47	0.62	14.22	8.96	11.46	6.96	14.87	8.92	0.34	0.31	0.39	8.27	8.03	7.60	7.29	9.32	9.20	8.28	8.17	16.45	0.08
21	Phenanthrene	0.50	0.46	0.59	12.93	8.15	11.72	7.12	15.25	9.14	0.31	0.32	0.38	7.92	7.69	8.14	7.81	9.66	9.53	8.14	8.34	16.48	0.08
22	Anthracene	0.38	0.18	0.26	9.86	6.22	4.80	2.92	6.68	4.01	0.10	0.11	0.13	2.71	2.63	2.80	2.69	3.37	3.32	4.38	2.88	7.26	0.04
23	Fluoranthene	0.33	0.22	0.29	8.65	5.45	5.75	3.50	7.67	4.60	0.17	0.16	0.19	4.54	4.41	4.36	4.18	5.04	4.97	4.52	4.52	9.04	0.05
24	Pyrene	0.36	0.17	0.22	8.66	5.46	4.05	2.46	5.39	3.24	0.19	0.13	0.15	4.56	4.43	3.12	2.99	3.62	3.57	3.72	3.66	7.38	0.04
25	Bens(a)anthracene	0.14	0.12	0.15	4.56	2.87	3.91	2.37	4.80	2.88	0.07	0.06	0.07	2.20	2.13	2.06	1.97	2.43	2.39	2.71	2.17	4.88	0.02
26	Chrysene	2.04	0.13	0.18	52.90	33.34	3.45	2.10	4.72	2.83	0.10	0.10	0.12	2.59	2.51	2.65	2.54	3.00	2.95	12.76	2.67	15.43	0.08
27	Benso(b)fluoranthene	0.04	0.09	0.10	1.13	0.71	2.83	1.72	3.34	2.00	0.08	0.08	0.08	2.49	2.41	2.52	2.42	2.69	2.65	1.48	2.49	3.97	0.02
28	Benso(k)fluoranthene	0.02	0.06	0.06	0.60	0.38	1.75	1.06	1.85	1.11	0.05	0.06	0.06	1.63	1.58	1.72	1.65	1.84	1.82	0.85	1.69	2.53	0.01
29	Benso(a)Pyrene	0.03	0.07	0.08	0.80	0.50	1.84	1.12	1.96	1.17	0.06	0.07	0.06	1.48	1.44	1.67	1.60	1.60	1.58	0.93	1.54	2.47	0.01
30	Indeno(1,2,3-cd)pyrene	0.00	0.02	0.02	0.20	0.13	0.87	0.53	0.77	0.46	0.02	0.02	0.01	0.99	0.96	0.65	0.63	0.58	0.57	0.37	0.72	1.09	0.01
31	Benso(g,h,i)perylene	0.01	0.04	0.04	0.38	0.24	1.51	0.92	1.28	0.77	0.03	0.04	0.03	1.07	1.04	1.32	1.26	1.15	1.13	0.64	1.14	1.79	0.01
32	Dibenso(a,h)anthracene	0.01	0.05	0.05	0.36	0.23	1.20	0.73	1.13	0.68	0.05	0.03	0.04	1.20	1.16	0.83	0.79	1.02	1.01	0.54	0.99	1.53	0.01

Table J.43. Total concentration for each tar compounds generated using silica.

No	Tar component	Tar concentration (µg ml^{-1})		Average (µg ml^{-1})	Total tar (µg ml^{-1})
		LTM	HTM		
1	Benzene	3.25			3.25
2	Toluene	1.63			1.63
3	Pyridine	0.17			0.17
4	p-xylene + Ethylbenzene	0.12			0.12
5	m-xylene	0.13			0.13
6	o-xylene	0.09			0.09
7	Styrene	0.59			0.59
8	Phenol	2.89	0.02	1.45	1.45
9	Indene	0.46	0.53	0.49	0.49
10	o-cresol (2-methylphenol)	0.38	0.36	0.37	0.37
11	m+p-cresol (3+4-methylphenol)	0.55	0.54	0.54	0.54
12	Naphthalene	0.44	0.45	0.45	0.45
13	Quinoline	0.04	0.08	0.06	0.06
14	2-Methylnaphthalene	0.11	0.07	0.09	0.09
15	Isoquinoline	0.02	0.13	0.08	0.08
16	1-Methylnaphthalene	0.10	0.09	0.09	0.09
17	Biphenyl	0.09	0.05	0.07	0.07
18	Acenaphthylene	0.12	0.11	0.11	0.11
19	Acenapthene	0.02	0.02	0.02	0.02
20	Fluorene	0.07	0.08	0.08	0.08
21	Phenanthrene	0.08	0.08	0.08	0.08
22	Anthracene	0.02	0.04	0.03	0.03
23	Fluoranthene	0.06	0.05	0.05	0.05
24	Pyrene	0.04	0.04	0.04	0.04
25	Bens(a)anthracene		0.02		0.02
26	Chrysene		0.08		0.08
27	Benso(b)fluoranthene		0.02		0.02
28	Benso(k)fluoranthene		0.01		0.01
29	Benso(a)Pyrene		0.01		0.01
30	Indeno(1,2,3-cd)pyrene		0.01		0.01
31	Benso(g,h,i)perylene		0.01		0.01
32	Dibenso(a,h)anthracene		0.01		0.01

Table J.44. Concentration of each tar compound from the investigated parameter 3: summary

Class	Compounds	SS		OS	
		µg ml^{-1}	g Nm^{-3}	µg ml^{-1}	g Nm^{-3}
2	Pyridine	0.17	0.15	0.23	0.21
	Phenol	1.43	1.29	2.19	1.98
	o-cresol (2-methylphenol)	0.29	0.26	0.21	0.19
	m+p-cresol (3+4-methylphenol)	0.73	0.66	0.51	0.46
	Quinoline	0.06	0.06	0.07	0.06
	Isoquinoline	0.08	0.07	0.10	0.09
	Subtotal class 2 tars concentration	***2.76***	***2.49***	***3.31***	***2.98***
3	Benzene	3.21	2.89	0.78	0.71
	Toluene	1.62	1.46	0.54	0.49
	p-xylene + Ethylbenzene	0.12	0.11	0.06	0.05
	m-xylene	0.13	0.11	0.06	0.05
	o-xylene	0.09	0.08	0.05	0.04
	Styrene	0.59	0.53	0.32	0.29
	Subtotal class 2 tars concentration	***5.75***	***5.18***	***1.81***	***1.63***
4	Indene	0.49	0.44	0.45	0.41
	Naphthalene	0.45	0.40	0.43	0.39
	2-Methylnaphthalene	0.09	0.08	0.08	0.07
	1-Methylnaphthalene	0.10	0.09	0.09	0.08
	Biphenyl	0.07	0.06	0.07	0.06
	Acenaphthylene	0.12	0.11	0.10	0.09
	Acenapthene	0.02	0.02	0.02	0.02
	Fluorene	0.08	0.07	0.07	0.06
	Phenanthrene	0.08	0.08	0.06	0.06
	Anthracene	0.03	0.03	0.03	0.03
	Subtotal class 2 tars concentration	***1.53***	***1.38***	***1.40***	***1.26***
5	Fluoranthene	0.05	0.05	0.04	0.04
	Pyrene	0.03	0.03	0.02	0.02
	Bens(a)anthracene	0.02	0.02	0.20	0.18
	Chrysene	0.08	0.07	0.01	0.01
	Benso(b)fluoranthene	0.02	0.02	0.00	0.00
	Benso(k)fluoranthene	0.01	0.01	0.01	0.01
	Benso(a)Pyrene	0.01	0.01	0.01	0.01
	Indeno(1,2,3-cd)pyrene	0.00	0.00	0.00	0.00
	Benso(g,h,i)perylene	0.01	0.01	0.00	0.00
	Dibenso(a,h)anthracene	0.01	0.01	0.00	0.00
	Subtotal class 2 tars concentration	***0.25***	***0.23***	***0.30***	***0.27***
Total tars concentration		**10.24**	**9.23**	**6.78**	**6.11**

Table J.45. Total concentration and yield of tars from each bed material.

Tar class	Bed material		**Unit**
	Silica	Olivine	
Class 2	2.49	2.98	g Nm^{-3}
Class 3	2.49	1.63	
Class 4	2.49	1.26	
Class 5	2.49	0.27	
Tars concentration	*9.96*	*6.15*	
Gas Yield	*0.54*	*0.60*	$Nm^3\ kg^{-1}_{od}$
Tars yield	*5.36*	*3.66*	$g\ kg^{-1}_{od}$